MICROGLIAL REACTIVITY AND FUNCTIONAL DEFICITS FOLLOWING TRAUMATIC BRAIN INJURY IN THE NEONATE RAT

A Dissertation

Submitted to the Faculty

of

Drexel University College of Medicine

by

Lauren A. Hanlon

in partial fulfillment of the

requirements for the degree

of

Doctor of Philosophy

February 2017

DEDICATION

This dissertation is dedicated to:

Robert and Emma Turner

Thank you for paving this road for me.

ACKNOWLEDGMENTS

I would like to thank my mentor, Dr. Ramesh Raghupathi, for taking a chance on a student with no prior research experience. Thank you for creating an atmosphere in which I could learn, laugh, and love science.

Thank you to my committee for their support and guidance: Dr. Cunningham for being the chair and answering all of my various neuroinflammation questions. Dr. Gao for pushing me to a better scientist and being my go-to resource for all things electrophysiology. Dr. Bethea for making the time to review my research and lend his immense expertise to my project. Finally, Dr. Phillips for attending every meeting over video conference despite various technical difficulties and providing supportive and constructive suggestions.

Thank you to Jimmy Huh for all of your guidance. You have been a wonderful mentor, friend, and constant source of support.

Thank you to my lab mate, Laura Krafjack. Your calming presence in the lab made long, frustrating days just a little bit easier. Thank you for your support and friendship.

Thank you to Dr. Ann Mae DiLeonardi for being a role model and friend.

Thank you to all of the students and technicians that lent their time and effort to this project, especially Rupal Prasad, Doug Fox, Cameron Trueblood and Joanne Simien.

Thank you to Dr. Jessica Barson and Preeti Badve for their assistance in conducting preliminary QPCR experiments.

To the friends that I consider family: your endless understanding, encouragement, and love have gotten me through the tough times. You all made sure that I took time for myself to relax and have fun and that helped me stay sane.

To the Hanlon/Reimer family: Thank you for your support, for loving me like one of your own, and for always being proud of my accomplishments.

To my siblings: You are all part of me and your friendships are irreplaceable.

To my sister, Kristina: Thank you for being my person. You make me a better person, sister, and friend. I couldn't have done this without you.

To my brother, Danny: Thank you for always making me laugh.

To my sister, Brooke and my niece, Evey: Thank you for being so awesome.

To my incredible parents for encouraging their children to dream big and for doing whatever is necessary to help them live those dreams. You are both true inspirations and I wouldn't be the person I am today without your unwavering love and support.

To Toby: You sat next to me the entire time I wrote this document. Thank you for your loyalty and unconditional love.

And finally, to my husband Andrew: You have the patience of a saint. You didn't sign up to marry a graduate student, but you never complained. Thank you for being my safe place in all of this chaos. Your love and support mean the world to me.

Table of Contents

ABSTRACT

Microglial Reactivity and Functional Deficits Following Traumatic Brain Injury in the Neonate Rat

Lauren Hanlon

Advisor: Ramesh Raghupathi, Ph.D.

Traumatic brain injury (TBI) is a leading cause of disability in young children as survivors face life-long physical and cognitive impairments. Inflammation, specifically microglia/macrophage activation, has been identified as a target for acute therapeutic intervention for the traumatically-injured adult brain, but it is unclear whether this strategy will be effective in the immature injured brain. Closed head injury in the 11-day-old rat induced robust microglia/macrophage reactivity in multiple brain regions and was associated with neurodegeneration and axonal injury. Additionally, brain-injured animals demonstrated cognitive deficits and motor function impairments at 4 weeks post-injury, mirroring the sustained functional deficits observed in humans. Immediately after injury, intracerebral depletion of microglia/macrophages with clodronate or inhibition of active microglia/macrophages systemically with minocycline decreased the number of total and activated microglia/macrophages in the injured brain. This effect was accompanied by an increase in neurodegeneration at 3 days post-injury, suggestive of a lack of clearance of degenerating cells. Both of these acute manipulations, however, were associated with an increase in microglia/macrophage reactivity and neurodegeneration at 4 weeks post-injury that coincided with hyperactivity (clodronate)

or hypoactivity (minocycline) within the injury site. In addition, systemic minocycline administration reversed alterations in cortical activity, deficits in working memory, and impairment of forelimb function that were not associated with neurodegeneration or microglia/macrophage activation. These results are not only suggestive of off-target effects of minocycline, but also emphasize the importance of acute post-injury microglia/macrophage reactivity and the need for a more target-specific anti-inflammatory therapeutic strategy in the developing brain.

CHAPTER 1: GENERAL INTRODUCTION

1.1 CLINICAL REVIEW OF PEDIATRIC TBI: EPIDEMIOLOGY, CHARACTERIZATION, PATHOLOGY, FUNCTIONAL OUTCOMES, AND MANAGEMENT.

1.1.1 Epidemiology

In the United States, an estimated 1.7 million people sustain a traumatic brain injury (TBI) each year and while 80% of these people are acutely treated and released from the hospital, approximately 52,000 people die after incurring a TBI (Faul et al., 2010). Older adults over the age of 75 have the highest rates of hospitalization (339/100,000) and death (57/100,000) due to TBI, but children ages 0-14 account for 35% of TBI-related emergency room visits making them the age group with the highest incidence of TBI. Within this age group, the youngest children (ages 0-4) have the highest incidence of emergency room visits due to TBI with a rate of over 1200 visits per every 100,000 people (Faul et al., 2010). The incidence of TBI in this age group consists of both accidental and inflicted abusive trauma (Ewing-Cobbs et al., 1998, Keenan and Bratton, 2006) as 29% and 43% of TBI-related deaths in children 0-4 are due to motor vehicle accidents and abuse, respectively (CDC Website). Abusive head trauma (AHT) in infants is not just restricted to what has been conventionally defined as “shaken baby syndrome” and now encompasses impact-driven traumas and while it has been historically very difficult to diagnose AHT, the incidence of diagnosis has increased in the last decade (Jenny et al., 1999, Kelly et al., 2015, Narang et al., 2016).

In a population-based study of severe or fatal pediatric TBI, children under the age of 1 had a higher rate of inflicted TBI (29.7/100,000) compared to accidental TBI (20.1/100,000). Male children of non-European descent were more likely to be the victims of inflicted trauma and that while children with young, first-time mothers (less

than 21 years of age) were more likely to be abused, the abuser was often a male adult (Keenan et al., 2003) (Parks et al., 2012). The rate of severe and fatal inflicted TBIs, however, drastically decreased after the age of 1 (3.8/100,000) (Keenan et al., 2003). The most common cause of TBI in children over the age of 1 is falls as the children are learning to walk and have trouble avoiding obstacles (Keenan and Bratton, 2006). As the children age, motor vehicle accidents and sports accidents become more common causes of injury (Faul et al., 2010).

1.1.2 Classification of pediatric TBI

Injury Severity

Over 40 years ago, the need for a universal brain injury severity scale was recognized and thus the Glasgow Coma Scale (GCS) was born (Teasdale and Jennett, 1974). This scale assesses eye opening, verbal responses, and motor responses in order to give the patient a score ranging from 3 to 15 that denotes injury severity (Table 1.1).

Table 1.1. Standard Glasgow Coma Scale (GCS)

Eye Opening	Verbal Response	Motor Response
		6: Obeys commands
	5: Oriented (to self and environment)	5: Localizes to stimulus
4: Spontaneous	4: Confused	4: Withdraws to pain

3: To Speech	3: Inappropriate words	3: Abnormal flexion
2: To Pain	2: Incomprehensible sounds (moaning/groaning)	2: Extension
1: No Response	1: No Response	1: No Response

Table recreated from: (Teasdale and Jennett, 1974, Matis and Birbilis, 2008)

In an attempt to classify brain injury severity, assigned GCS scores correspond to either a mild injury (13-15), a moderate injury (9-12), or a severe injury (3-8) (Sternbach, 2000). It is believed that taking loss of consciousness (LOC) into consideration when characterizing the severity of injury is beneficial in terms of treatment and predicting outcomes. The Head Injury Severity Scale (HISS) uses GCS scores and LOC to separate severities into 5 different intervals that better characterize the differences in mild and moderate injuries: minimal (score of 15 with no LOC), mild (score of 14-15 with LOC of less than 5 minutes or impaired alertness/memory), moderate (score of 9-13 with LOC greater than 5 minutes or a focal neurological deficit), severe (score of 5-8), or critical (score of 3-4) (Stein and Spettell, 1995).

Due to the nonverbal nature of infants, it can be difficult to accurately diagnose the severity of a head injury (both inflicted and accidental) as these children often present with symptoms that are similar to a range of different ailments- lethargy, crying, vomiting, irritability (Jenny et al., 1999, Keenan and Bratton, 2006). An infant GCS has been adapted with a better characterization of responses in very young children (Reilly et

al., 1988) (Table 1.2). The verbal response column was modified to cater to the verbal abilities of infants.

Table 1.2 Infant Glasgow Coma Scale

Eye Opening	Verbal Response	Motor Response
		6: Obeys commands
	5: Cooing and babbling	5: Withdraws from touch
4: Spontaneous	4: Irritable cries	4: Withdraws from pain
3: To speech	3: Crying in reaction to pain	3: Flexion to pain
2: To pain	2: Moaning to pain	2: Extension to pain
1: No response	1: No response	1: No response

Table recreated from: Reilly et al., 1988; Matis and Birbilis, 2008

Concerns were still raised, however, about an infant's ability to follow commands in assessment of the motor response and the ease at which verbal responses could be misinterpreted (i.e. the criteria for an irritable cry or the distinction between moaning and babbling) (Martens, 1993, Matis and Birbilis, 2008). In 2000, the Children's Hospital of Philadelphia released a novel coma scale for use in children under the age of 2 called the Infant Face Scale (Durham et al., 2000, Table 1.3).

Table 1.3 The Infant Face Scale (IFS)

Eye Opening	Verbal/Facial Response	Motor Response
		6: Spontaneous normal movements
	5: Crying spontaneously (with grimacing and tears), with handling, or to minor pain; alternating sleep with periods of quiet wakefulness	5: Spontaneous normal movements reduced in frequency, hypoactivity
4: Spontaneous	4: Crying spontaneously (with grimacing and tears), with handling, or to minor pain; no periods of quiet wakefulness maintained	4: Nonspecific movement to deep pain only
3: To verbal stimulation or touch	3: Crying only in reaction to deep pain	3: Abnormal rhythmic spontaneous movements, seizure activity
2: To pain	2: Grimaces only to pain with no sounds or tears	2: Spontaneous extension or to painful stimuli
1: No response	1: No facial response to pain	1: Flaccid

Table recreated from: Durham et al., 2000.

This scale addresses concerns over the subjective nature of the infant GCS and the child's verbal and motor abilities by basing the measures on objective behaviors that are appropriate for the age group. When this scale was tested, the interrater reliability was substantially increased in assessment of infants that sustained a TBI or suffered a hypoxic-ischemic insult when compared to the interrater reliability of the GCS (Durham et al., 2000). The adaptation of the GCS and the utilization of the IFS emphasize the need for consideration of age-dependency in characterizing injury severity in young children and further demonstrate a common theme in pediatric brain injury research- what works for the adult brain may not work for the immature brain.

Biomechanics of Injury

Traumatic brain injuries are often placed in one of two biomechanical categories: focal injuries and diffuse injuries. Focal injuries are associated with impact-driven trauma and involve skull fractures, evidence of contusion, and hematomas whereas diffuse injuries are associated with trauma caused by rapid acceleration/deceleration forces and tend to result in tearing injuries that often affect the white matter (Andriessen et al., 2010). Injuries to the developing brain, however, may result in pathologies associated with both of these broad injury categories as both impact and rotational forces are common mechanisms of injury in both accidental and inflicted trauma. The characteristics of shaken baby syndrome, for example, have been expanded to include impact-based pathology and may now be referred to as "shaken impact syndrome." Using doll models of 1-month old infants, Duhaime et al. (1987) demonstrated that

impact was necessary to break the injury threshold associated with subdural hematoma and diffuse axonal injury. Additionally, the properties of the infant skull differ from the adult and may further facilitate the melding of these two types of injury (Duhaime et al., 1987). Margulies and Thibault (2000) demonstrated that the decreased thickness and overall pliancy of the infant skull resulted in a decreased ability of the skull to absorb energy during the application of an external force. They also demonstrated that, due to these parameters, an external force would cause much greater deformations therefore affecting more than just the area of direct application and causing a more diffuse pattern of injury (Margulies and Thibault, 2000). These findings emphasize the complexity of pediatric TBI and indicate that the pathology may reflect aspects of both focal and diffuse injuries.

1.1.3 Tissue pathology of pediatric TBI

Skull Fractures

Skull fractures are a common pathologic occurrence following TBI in the infant, are indicative of impact-based trauma, and are often identified through X-ray imaging or computed tomography (CT) (Ewing-Cobbs et al., 1998, Ewing-Cobbs et al., 2000, Keenan et al., 2004, Alhelali et al., 2015, Culotta et al., 2017). The presence of skull fractures has been reported in both inflicted and accidental TBI. In an early prospective study, children that sustained a TBI due to either accidental or non-accidental causes did not differ in the frequency or types (multiple, linear, depressed, diastatic) of skull fracture (Ewing-Cobbs et al., 1998). Further studies, however, indicated that skull fractures were more common in children that sustained a TBI from accidental causes (motor vehicle

accident, fall, drop, etc.) (Ewing-Cobbs et al., 2000, Keenan et al., 2004). While the number of fractures was higher in the non-inflicted group, the distribution of the types of fractures (linear, depressed, diastatic) was similar between the non-inflicted and inflicted groups (Ewing-Cobbs et al., 2000). In a separate study, 59% of children that sustained an accidental TBI had skull fractures whereas only 17.5% of the children that sustained an inflicted injury group had a skull fracture (Keenan et al., 2004). In a histopathologic study of severe inflicted injury in infants and young children, however, 85% of subjects showed evidence of impact to the head at the time of autopsy with 42% of these children sustaining skull fractures and 58% showing evidence of sub-scalp bruising (Geddes et al., 2001b). With the expansion of the criteria for abusive head trauma to include impact-based injuries, skull fracture alone may not be enough to separate accidental and inflicted injuries.

Extra-axial Collections

Extra-axial collections encompass any fluid collection outside of the brain parenchyma and include epidural, subdural, and subarachnoid hematomas and hemorrhages. These bleeds occur in both inflicted and non-inflicted cases, but may differ in frequency and severity between the different external causes (Ewing-Cobbs et al., 1998, Ewing-Cobbs et al., 2000, Tung et al., 2006). In a prospective review, subdural hematomas occurred more frequently in children who sustained TBIs due to non-accidental (80%) rather than accidental causes (45%), but epidural hematomas were 4 times more likely in children with accidental TBI. Collections in the subarachnoid space, however, did not show any differences between accidental and non-accidental injury

mechanisms (Ewing-Cobbs et al., 1998). Further analysis of subdural hematomas revealed that inflicted TBI in infants resulted in mixed-density subdural hematomas that may be suggestive of repetitive brain trauma where accidental trauma resulted in hyperdense subdural hematomas (Tung et al., 2006).

Retinal hemorrhage

Retinal hemorrhage (RH) has been used as a marker of an inflicted TBI diagnosis as the rapid acceleration and deceleration forces often associated with "shaken baby/shaken impact syndrome" can cause ocular damage (Duhaime et al., 1998). In a small prospective study of 20 infants with inflicted TBI and 20 infants that sustained a TBI due to accidental causes, 70% of the inflicted TBI victims presented with RH. Of these 70%, all but one of the children presented with hemorrhages in both retinae while there was no evidence of RH in the accidental injury group (Ewing-Cobbs et al., 1998). In a larger study, a large proportion of children that sustained inflicted TBI had RH (76%), but there was a proportion of non-inflicted cases that presented with RH (8%) indicating that RH is not just a characteristic of inflicted TBI (Keenan et al., 2004).

Atrophy and Ventriculomegaly

Evidence of cerebral atrophy in the acute period post injury may be indicative of previous unreported injuries. A proportion of children that sustained an inflicted TBI demonstrated evidence of cerebral atrophy and ex vacuo ventriculomegaly (enlarged ventricular space) on their entry scans while those that were treated for an accidental injury did not (Ewing-Cobbs et al., 2000). There is evidence, however, that a moderate to

severe accidental injury can result in chronic atrophy and ventricular alterations (Wilde et al., 2005, Ghosh et al., 2009). In a study that used MRI to investigate volumetric changes in children (ages 3-13 at the time of injury) a year after an accidental moderate to severe traumatic brain injury, whole brain volume and grey matter volume were decreased in injured subjects compared to age-matched uninjured controls and injury resulted in an increased ventricular volume, CSF volume, and an increased ventricle-to-brain ratio (Wilde et al., 2005). In a separate study that investigated the correlation between ventricular abnormalities and GCS score, children with lower original GCS scores were more likely at 4 months post-injury to develop an abnormal ventricle-to-brain ratio (Ghosh et al., 2009). These studies indicate that with time, a single moderate to severe injury will result in atrophy and ventricular enlargement irrespective of whether the injury was accidental or inflicted.

White Matter Injury

The sampling for neuropathologic studies in post-mortem tissue comes primarily from severe inflicted injuries, but these studies have made interesting discoveries about the nature of axonal injury following these types of injuries (Vowles et al., 1987, Shannon et al., 1998, Gleckman et al., 1999, Geddes et al., 2001a, Geddes et al., 2001b). Using the silver stain method, Vowles et al. (1987) observed axonal swellings in the subcortical white matter and corpus callosum in infants that had sustained TBIs and determined that DAI (diffuse axonal injury) was more common in infants that sustained skull fractures and contusional tears (Vowles et al., 1987). Over a decade later, beta-amyloid precursor protein (β-APP) immunohistochemistry was used to visualize axonal

injury and the idea that shaking alone was sufficient to cause axonal damage or whether axonal injury was a consequence of hypoxic damage following injury was tested. Shannon et al. (1998) reported that, in a group of infants whose primary injury mechanism was shaking (all subjects lacked skull fractures), there was evidence of β-APP labeling in the cerebral white matter- specifically the corpus callosum and internal capsule. They also reported, however, that 86% of control brains from infants that died from hypoxic-ischemic injury demonstrated similar evidence of axonal injury indicating that respiratory distress (apnea following injury) and brain swelling may be contributing factors to DAI. Shaking produced evidence of axonal injury in the cervical spinal cord that distinguished the victims of inflicted injury from those that incurred a hypoxic-ischemic insult (Shannon et al., 1998). A similar study found evidence of β-APP labeling indicative of DAI in both infants that were shaken and infants that were struck, but did not find evidence of labeling in the control brains, one of which sustained a hypoxic-ischemic injury (Gleckman et al., 1999). Geddes et al. (2001a, 2001b) identified a pattern of DAI in the midbrain and brainstem of infants that sustained inflicted injuries that they believed was related to the increase in intracranial pressure and hypoxic damage due to the geographic relation to affected vasculature. Additionally, infants that demonstrated severe traumatic damage also exhibited evidence of TAI (traumatic axonal injury) within the hemispheric white matter, corpus callosum, and internal capsule. These studies suggest that both non-impact and impact-based trauma can result in axonal injury that may also be related to acute hypoxia and increased intracranial pressure.

Imaging studies have given us insight into the white matter damage sustained in children that survive their injuries. MRI analysis revealed acute evidence of shearing in

the corpus callosum of infants that sustained accidental TBIs and evidence of impaired myelination, indicative of previous injury, in infants that sustained inflicted injury (Ewing-Cobbs et al., 2000). Imaging studies allow for investigation into the long-term integrity of the white matter tract after pediatric brain injury (Suskauer and Huisman, 2009). A relationship between atrophy of the white matter and GCS score was identified as children with lower GCS scores at the time of injury were more likely to have higher percentages of white matter loss at least a year after injury (Ghosh et al., 2009). In a study that investigated the integrity of white matter tracts at least one year after injury in early childhood (approximately 3 years old) using diffusion tensor imaging (DTI), reduced fractional anisotropy (FA) was observed in several white matter regions including the corpus callosum, internal capsule, and longitudinal fasciculus. These reductions were also associated with lower GCS scores at the time of injury indicating that moderate to severe injuries are more likely to result in long-term alterations in white matter integrity (Yuan et al., 2007). In a more recent study, brain-injured young children (ages 6-10) showed a greater decrease in FA compared to brain-injured adolescents (ages 11-15) indicating age-dependency in white matter damage, but both age groups demonstrated similar degrees of change in FA between the 3-month and 24-month scans (Ewing-Cobbs et al., 2016). These, and the results from post-mortem studies, indicate that axonal injury may result in axotomy and long-term white matter atrophy.

1.1.4 Functional Outcomes

Young children and infants that sustain traumatic brain injuries demonstrate a wide range of neurobehavioral deficits in the months to years following the injury that

include deficits in different areas of cognition, the development of psychiatric disorders, deficits in social interaction, locomotor difficulties, and the appearance of seizure activity and development of seizure disorders.

Cognition

Sustaining an injury in infancy or early childhood has strong implications for the development of cognitive skills. Very young children (up to 42 months of age) are typically evaluated using the Bayley Scale of Infant Development (BSID) that takes into account age-appropriate behavior and levels of arousal/responsiveness through a series of play activities. As the child ages, the tests within the BSID begin to encompass language and emotional development as well (Nellis & Gridley, 1994). Using the BSID, Ewing-Cobbs et al. (1999) demonstrated that infants and young children that sustained moderate to severe TBIs had significantly decreased Bayley Behavior Rating Scores for mental development at both baseline and at the 3-month follow-up when compared to control subjects (Ewing-Cobbs et al., 1999). In a separate study, approximately 4 years after sustaining a moderate to severe TBI, children demonstrated cognitive development scores that were below average with over 50% of the subjects falling in the "extremely abnormal" range (Barlow et al., 2005). Furthermore, children aged 4 months to 7 years that sustained severe inflicted TBIs showed no improvement in a variety of different IQ measures (composite, verbal, perceptual-performance) between 6 months and 24 months post-injury indicating a lack of improvement and developmental arrest (Ewing-Cobbs et al., 1997). Anderson et al. (2005) even indicated that children that sustained their injury

when they were younger than 3 years of age showed evidence of continued cognitive impairment at the 12 and 30 month follow-up assessments (Anderson et al., 2005).

In addition to this general lack of cognitive development, children that sustain TBIs also exhibit deficits in specific areas of cognition such as verbal working memory, visuo-spatial memory, and attention that may contribute to difficulties in a school setting. Researchers administered two working memory assessments to children that sustained TBIs (aged 0-15 years at the time of injury) and age-matched controls: the category listening span dual-task (CLS-DT) as a measure of verbal working memory that dealt with correct responses regarding the content and order of word strings and the visuospatial span dual-task (VSS-DT) as a measure of visuospatial working memory that dealt with correct responses regarding the content and order of strings of 4x4 block sets. Children that sustained injuries demonstrated significant decreases in correct responses in the VSS-DT and a mild, but insignificant decrease in correct responses in the CLS-DT (Treble et al., 2013). Similarly children that incurred TBIs in early childhood showed deficits in verbal working memory when they were simultaneously asked to decide if sentences were true or false and remember the last word of these sentences in order (sentence span task) (Ewing-Cobbs et al., 2008). In addition to deficits in memory, children that sustain TBIs demonstrate difficulties in different areas of attention. Children that sustained severe injuries had greater deficits in sustained attention, reaction time, and shifting attention compared to children that sustained mild injuries and healthy controls (Catroppa and Anderson, 2005). Brain-injured children are also at high risk for developing attention-deficit hyperactivity disorder (referred to as secondary ADHD or s-ADHD). Children with TBI and children with diagnosed ADHD had similar deficits in

response inhibition in a task that required the children to respond to a stop signal (Ornstein et al., 2013). Additionally, 12% of children that sustained a TBI were diagnosed with s-ADHD and exhibited increased deficits in working memory and attention compared to uninjured children diagnosed with ADHD (Ornstein et al., 2014).

Many cognitive outcomes do not manifest in childhood TBI survivors until they reach school-age and heavily involve deficient language processes (Ewing-Cobbs and Barnes, 2002). Children that sustained early TBIs, for example, demonstrated deficits in both expressive and receptive language (Ewing-Cobbs et al., 1989) and in word fluency (Levin et al., 2001). Brain-injured children also demonstrated deficits in several different areas of reading ability such as word reading accuracy, fluency, and reading comprehension (Johnson et al., 2015). Cognitive deficits may also contribute to deficits in mathematical skills based on the observation that brain-injured children exhibit deficits in standardized math skills such as simple calculations and applied word problems (Raghubar et al., 2013). Due to an increase in cognitive deficits affecting basic school subjects such as reading and math, brain-injured children utilized more specialized support services and have lower academic competency scores compared to their normally-developing peers (Prasad et al., 2016).

Social and Behavioral Outcomes

Children that sustain brain injuries in early childhood demonstrate decreased social competencies and are at risk of developing psychiatric disorders. Parents of children that sustained severe accidental TBIs between the ages of 3 and 7 years reported scores on two separate social skills assessments that were significantly decreased

compared to controls and children that sustained moderate injuries (Ganesalingam et al., 2011). Additionally, children with severe TBIs demonstrated increased gesturing during the initiation of social communication indicating a lack of proper verbalization compared to age matched children that sustained mild injuries (Ewing-Cobbs et al., 2012). When children were separated by mechanism of injury (accidental vs. inflicted injury), social abilities did not differ between the two groups, but social responsiveness and caregiver sociability ratings were significantly decreased in children with severe TBI irrespective of mechanism (Ewing-Cobbs et al., 2013).

Max et al. (2001) characterized personality changes in brain-injured children that encompassed five different alterations: labile, aggressive, disinhibited, apathetic, and paranoid. Brain-injured children demonstrated evidence of personality changes over a series of follow-up psychiatric assessments and children with severe injuries were more likely to exhibit personality changes compared to those with mild injuries (59% vs. 5%). These personality changes were most commonly characterized as an increase in irritability or an increase in aggression associated with disinhibited verbalizations (Max et al., 2001). The development of psychiatric mood disorders has only recently been a point of focus in pediatric TBI research. It has been reported that 11% of children in a sample of pediatric TBI survivors develop novel depressive disorders in the years following injury, but that the development of depression may be more common in children that are slightly older at the time of injury (average of 12 years old) (Max et al., 2012). Interestingly, the incidence of novel anxiety disorder following injury was similar (10%), but was associated with a younger age at injury (average of 8 years old) and documented changes in personality (Max et al., 2015). These studies indicate that brain-

injured children that survive their injuries go on to deal with severe psychiatric and psychosocial alterations that could negatively impact their overall development.

Locomotor Outcomes

While cognitive outcomes are widely considered and studied, brain-injured children may also demonstrate motor difficulties as areas of the brain dealing with motor planning and control may be affected directly by the injury and secondarily by alterations in neural development caused by the injury. In assessments using the motor component of the Bayley Infant Development Scale (children 4-42 months) and the McCarthy Motor Scale (children 42-72 months), children with severe injuries had significantly decreased motor scores at both initial testing and 6 month follow-up compared to the mild/moderate injury group (Ewing-Cobbs et al., 1989). In a separate study, severely injured children only improved in motor score in the first 6 months following injury and did not show any further improvement at the 12- or 24-month follow-up assessments (Ewing-Cobbs et al., 1997). In a more in-depth measure of timed motor dexterity where children were asked to place pegs in a pegboard (the grooved pegboard test), severely injured children exhibited decreased accuracy in this task compared to age-matched controls (Ewing-Cobbs et al., 2008).

Post Traumatic Seizures

Abnormalities in neural network activity can manifest as seizure activity following a traumatic brain injury. Injuries in children can disrupt the development of optimal connectivity in the brain as the immature brain may still be forming the correct

synaptic connections. Children under the age of 5 that sustain severe injuries demonstrate an increased incidence of seizures in the early stages following injury (Annegers et al., 1998). In a study where 11% of severely injured children demonstrated seizure activity, 68% of these children had seizures in the first 12 hours post-injury (as evidenced by physician report or EEG (electroencephalogram) activity) (Liesemer et al., 2011). In addition to severity of injury (severely-injured children demonstrate a higher rate of seizure activity compared to more mild injuries), the age at injury has been identified as a significant risk factor for the development of seizure activity as 62% of children under the age of 1 developed seizures compared to only 30% of children over the age of 1 (Arndt et al., 2013). In 20% of children where the injury was so severe that they needed decompressive craniectomies, a diagnosis of epilepsy was made and anti-epileptic medications were prescribed in the chronic post-injury period (Kan et al., 2006).

1.1.5 Management of Pediatric TBI

Acute Management

There are guidelines in place to aid emergency department physicians in initiating the best course of treatment for children presenting with a traumatic brain injury (Hardcastle et al., 2014). Very acute management following TBI in children is primarily focused on establishing a clear airway and monitoring intracranial pressure (ICP). It is common for children to be intubated and rely on a respirator to combat any episodes of post-injury apnea. Physicians may administer sedatives or other pharmacologic interventions to try to slow cerebral metabolism and decrease intracranial pressure to combat further secondary injury mechanisms. If children are unresponsive to

pharmacologic intervention and ICP continues to increase, physicians may turn to more drastic measures such as craniectomies or cerebrospinal fluid drainage. There has also been evidence that acute hypothermia may aid in lowering ICP (Adelson et al., 2005).

Long-Term Management

Long-term management following pediatric TBI is focused on two aspects: treating comorbid developments such as psychiatric illnesses or epilepsy and providing rehabilitative support such as physical rehabilitation, cognitive therapy, or specialized educational support. Anti-convulsant and anti-psychotic medications are common after pediatric TBI to manage epilepsy and common psychiatric changes such as increased aggression or depression (Ylvisaker et al., 2005). Physical rehabilitation in children may focus on repetitive exercises to strengthen synaptic connectivity of the desired circuit and improve long-term function. Cognitive rehabilitation has shifted focus in the recent past from cognitive exercises in clinical settings to community-based therapy focused on the individual's needs, every day routine, and education of the child's parents and teachers. Home-based therapy directly involving the child's caregivers has shown positive effects on neurodevelopmental outcomes in very young children (Prasad et al., 2008). There has also been a push for teachers to receive training in TBI-specific educational methods so as to facilitate educational success in the pediatric TBI population (Ylvisaker et al., 2001, Glang et al., 2004).

A main focus in both clinical and pre-clinical pediatric TBI research is to acutely combat the initiation of secondary injury processes that increase the likelihood that the

children will develop comorbid pathologies and long-term functional impairments thus hoping to decrease the burden associated with long-term management following injury. Identified therapeutic targets, however, must undergo rigorous preclinical testing in relevant animal models of pediatric TBI.

1.2 ANIMAL MODELS OF PEDIATRIC TBI

Several pre-clinical animal models for pediatric TBI have been developed that use different species such as mice, rats, rabbits, and pigs. These models span several different age groups to encompass different developmental time points and utilize a number of various injury mechanisms including fluid-percussion injury, rotational-acceleration injury, weight-drop injury, and controlled cortical impact. Additionally, various injury severities are used to simulate different injury pathologies associated with pediatric TBI such as atrophy, inflammation, ventriculomegaly, white matter injury, and behavioral impairment.

1.2.1 Fluid-Percussion Brain Injury

Fluid-percussion brain injury (FPI) is induced by delivering a rapid pulse of saline through a craniotomy onto the intact dura to create a deformation of the brain. This pulse can be delivered at different atmospheric pressures to create varying levels of injury severity and the craniotomy can be conducted in different areas of the skull (i.e. midline vs. lateral) to affect different brain regions. This technique, however, is technically taxing as the device requires a large amount of space and cannot be readily moved.

While this technique is commonly used in adult animals (Sullivan et al., 1976, Dixon et al., 1987, McIntosh et al., 1989, Carbonell et al., 1998, Spain et al., 2010), a few groups utilize this injury technique in the developing animal. Prins et al. (1996) compared lateral (left parietal cortex) fluid-percussion injuries of increasing severities (mild: 1.35-1.45 atm, moderate: 2.65-2.75 atm, severe: 3.65-3.75 atm) in 3 different age groups: adult rats, PND 28 rats, and PND17 rats. The immature rats demonstrated increased hypotension and increased mortality at every injury severity compared to the adult rats. Additionally, moderately injured (2.65-2.75 atm) adult rats and PND28 rats demonstrated deficits in spatial learning that corresponded to decreased glucose metabolism in the hippocampus whereas moderately injured PND17 rats did not demonstrate any cognitive deficit or alteration in metabolism (Prins and Hovda, 1998, 2001). They also demonstrated that this injury could inhibit enrichment-induced neuroplasticity by reducing dendritic arborization (Fineman et al., 2000, Ip et al., 2002). Fluid-percussion has also been used to induce TBI in a model using neonatal and juvenile piglets. Armstead and Kurth (1994) compared a moderate (1.9-2.3 atm) lateral FPI in newborn (PND1-5) and juvenile (3-4 weeks) pigs and found that the newborn pigs had pronounced acute increases in hemoglobin oxygen saturation response that then severely decreased and this swing was not as severe in the juvenile pigs. Additionally, newborn pigs demonstrated a more prolonged reduction of cerebral blood flow following the injury (Armstead and Kurth, 1994).

1.2.2 Rotational-Acceleration Brain Injury

The rotational-acceleration injury model is a non-impact model of diffuse brain injury that seeks to replicate the rotational forces involved in motor vehicle accidents and sports collisions. Because this injury device is uniquely constructed, it has not been reproduced. The model was developed for use in adult minipigs and injury resulted in transient coma, astrogliosis, and diffuse axonal injury (Ross et al., 1994, Smith et al., 1997). The model has since been adapted for use in both newborn (3-5 days old) and juvenile piglets (4 weeks old). Following axial (horizontal) rotation of moderate intensity, 4-week old piglets demonstrate increased apnea and suppressed EEG activity in the minutes to hours following the injury compared to sham-injured and piglets that received a mild severity (Ibrahim et al., 2010). Additionally, moderately-injured animals demonstrated increased subarachnoid hemorrhage and more pronounced axonal injury compared to the mild injury group. In newborn pigs, rotational injury in the axial (horizontal) plane resulted in apnea and transient coma immediately following the injury. Evidence of subdural bleeding and diffuse axonal injury was observed histologically at 6 hours post-injury (Raghupathi and Margulies, 2002). Further study determined that the direction of rotation mattered as animals that underwent rotational accelerations in the sagittal and axial (horizontal) planes showed exacerbated pathology (subarachnoid hemorrhage, brainstem injury, and diffuse axonal injury) at 6 hours post-injury compared to animals that underwent rotational acceleration in the coronal direction (Eucker et al., 2011). Additionally, piglets injured in the sagittal plane demonstrated exacerbated acute injury responses as evidenced by increased incidence of apnea and duration of unconsciousness and a reduction in cerebral blood flow compared to the coronal and horizontal groups. Behaviorally, piglets that were subjected to a moderate injury

demonstrated decreased exploratory behavior and deficits in visual problem solving out to 4 days post-injury (Friess et al., 2007).

Recently, this model has been expanded to incorporate repetitive cyclic rotations such as those sustained by children that incur repetitive abusive shaking episodes. Newborn piglets that underwent cyclic rotations did not demonstrate any axonal injury 6 hours post-injury, but showed an increased presence of axonal injury at 24 hours and 6 days post-injury (Coats et al., 2017). Also, cyclic injuries produced more pronounced decreases in cerebral blood flow and increased the incidence of extra-axial hemorrhage compared to non-cyclic injuries.

1.2.3 Weight-Drop Brain Injury

The weight-drop model of TBI is popular because it can be used to induce both diffuse and focal injuries at different severities and can incorporate various aspects of injury biomechanics. For example, this injury is most-often conducted on a pliable surface (i.e. anything from foam padding to a suspended kim wipe) to allow the head some degree of free movement with the impact (Marmarou et al., 1994, Meehan et al., 2012). To induce injury, a weight is dropped down a tube and connects with the footplate that is directly against the intact dura for a more focal injury (Feeney et al., 1981) or the intact skull for a more diffuse injury (Marmarou et al., 1994). Additionally, this technique is technically favorable due to the ease at which the device is constructed and the portability of the apparatus. In a weight-drop model that utilizes open injury directly to the dura (10g weight), the cerebrovascular responses of juvenile (PND25-32) and adult (2-3 months) rats were compared (Grundl et al., 1994). While there were no differences

in infarct area in either age group, the immature animals had increased brain water content compared to the mature group out to 48 hours post-injury, but the mature rats demonstrated decreased local cerebral blood flow in more regions than the immature rats at 2 hours post-injury.

The use of closed head weight-drop injury has been well-characterized in a model using PND17 rats (Adelson et al., 1996). Different weights were utilized to induce a gradation of injury severity (75g, 100g, or 125g) and acute injury responses were characterized. The 100g weight produced a severe injury that exacerbated acute post-injury responses (increased apnea time, longer time to reflexive responses, decreased weight gain) and resulted in increased edema and enlarged ventricles. When the severe injury (100g) was compared to an ultra-severe injury (150g), both injuries produced alterations in motor function post-injury, but only the ultra-severe injury produced a spatial learning impairment in the second post-injury week (Adelson et al., 1997) that was sustained out to 3 months post-injury (Adelson et al., 2000). These behavioral alterations were accompanied by histopathologic evidence of edema and ventriculomegaly, as well as axonal injury and astrocytic reactivity but no overt evidence of neuronal cell death (Adelson et al., 2001).

Injury-induced cell death was investigated in this injury model in different age groups using an array of biochemical techniques and revealed severe age-dependent effects in the presence and severity of neuronal damage after injury (Bittigau et al., 1999). In two different protocols (one in which the same force was applied and one in which the force was altered to take brain weight into account) in PND3, PND7, PND 10, PND14 and PND30 rats, apoptotic cell death was detected via TUNEL and silver stains

at 24 hours post-injury in the PND3, PND7, PND10, and PND14 rats, but not those injured on PND30. The severity of apoptotic damage was greatest in the rats injured on PND3 and PND7 and only these two age groups still showed cellular evidence of apoptosis at 5 days post-injury. The presence of apoptotic cell death in the PND7 animals was confirmed by increased c-jun and decreased bcl-2 mRNA expression in the injured cortex as well as increased detection of histone-associated DNA fragments and caspase 3-like activity in the injured cingulum, cortex, thalamus, and hippocampus at 24 hours post-injury. When put together with the previously cited studies, irrespective of potential differences in injury severity, there seems to be age-dependent effects in the acute response to injury and the cellular neuropathology resulting from weight-drop injury.

1.2.4 Controlled Cortical Impact Injury

Controlled cortical impact (CCI) is a modification of the weight-drop injury and was first characterized in the adult ferret using a pneumatically-driven piston that allowed for control of the velocity and depth of deformation associated with the impact (Lighthall, 1988). The model was soon adapted for use in the rat (Dixon et al., 1991) and is now also available as an electrically-powered device. This model is extremely popular due to its ability to control for injury biomechanics (i.e. velocity and depth of deformation), its ability to simulate both focal and diffuse injuries depending on craniotomy, injury biomechanics, and impactor tip (i.e. metal vs. silicone tips, flat vs. protruding tips), and because the device itself is not overly large or cumbersome. Pediatric CCI models utilize a wide range of animals, age groups, and injury severities to simulate the pathologies associated with human pediatric TBI.

In the juvenile mouse (PND21), lateral impact to the intact dura resulted in the formation of a cavity under the impact site at 1 day post-injury indicative of a focal injury (Tong et al., 2002). This lesion continued to worsen as the size of the cavity increased between 2 weeks and 3 months post-injury indicating prolonged neurodegenerative processes (Pullela et al., 2006). The injured mice demonstrated neurodegeneration in the cortex surrounding the impact site and the hippocampus at 1 and 3 days post-injury and in the thalamus at 3 days post-injury. This neurodegeneration corresponded with loss of Neu-N labeled cells and the presence of activated microglia in these regions at 7 days post-injury. Similarly, brain-injured mice demonstrated evidence of degeneration in the subcortical white matter (Tong et al., 2002). These mice also demonstrated prolonged hyperactivity, decreased general anxiety-like behavior, deficits in spatial learning, and deficits in social behavior weeks to months after the injury (Pullela et al., 2006, Semple et al., 2012).

Adelson et al. (2013) compared mild, moderate, and severe focal CCI injuries to the intact dura of PND7 (1.5mm, 1.75mm, 2.0mm) and PND17 (1.5mm, 2.0mm, 2.5mm) rats. Four weeks after injury, rats that were injured on PND7 demonstrated severe cortical atrophy at the mild deformation and exhibited large lesions at the moderate and severe depths that affected the cortex, underlying white matter, and the hippocampus. The moderate and severe injuries also resulted in spatial learning and memory deficits in the second week post-injury. Rats that were injured on PND17 had cortical lesions that increased in size with the increasing severity, but did not involve the hippocampus although there appeared to be hippocampal atrophy. Brain-injured animals showed spatial learning deficits at all injury severities, but animals in the moderate and severe

groups demonstrated visual impairment. These results indicated that these two age groups responded to injury differently as evidenced by the differences in lesion formation and spatial learning deficits.

The Raghupathi lab has also conducted age-at-injury experiments as well as comparisons between injury severities and injury types (focal vs. diffuse, lateral vs. midline). The injury model that we utilize in our immature rats (PND11 or PND17) involves an impact to the intact skull rather than the intact dura and this allows for consideration of the role that the skull plays in pediatric TBI. In PND17 rats, midline injury with a metal impactor tip did not result in cavitation or overt tissue atrophy, but demonstrated a diffuse pattern of degeneration present in the cortex, white matter, hippocampus, and thalamus, as well as traumatic axonal injury in the corpus callosum, cingulum, and lateral white matter in the form of amyloid precursor protein accumulation, neurofilament compaction, and neurofilament dephosphorylation (Huh et al., 2008, DiLeonardi et al., 2009, 2012). Injury to the white matter also manifested as compound action potential impairment as injured animals showed decreased signal amplitudes in both the myelinated and unmyelinated components of the signal across 14 days post-injury with the myelinated axons showing a greater impairment than the unmyelinated axons (Dileonardi et al., 2012). Additionally, these animals exhibited spatial learning impairment out to the third week post-injury (Huh et al., 2008).

In a study comparing lateral focal injury PND11 and PND17 rats, both age groups demonstrated evidence of cortical lesion and calpain activation in the cortex and white matter at 6 hours, 24 hours, and 3 days (Huh et al., 2006). Injury at PND17 resulted in the formation of a cavity by 4 weeks post-injury whereas injury at PND11 resulted in

cortical atrophy and enlargement of the lateral ventricle (Huh and Raghupathi, 2007). Both age groups exhibit evidence of traumatic axonal injury in the form of amyloid precursor protein accumulation (Huh et al., 2006, Huh et al., 2011). While both age groups demonstrated deficits in spatial learning at 28 days post-injury, the extent of the deficit was significantly larger in the animals injured on PND11 and only PND11 animals showed spatial memory deficits in the probe trial (Huh and Raghupathi, 2007), indicating an age-dependent vulnerability in terms of the extent of cognitive impairment following injury.

This age dependency was also shown in a model of lateral diffuse injury using a silicone impactor tip. This injury produced gross tissue alterations in the P11 animal in the form of cortical, white matter, and subcortical atrophy as well as ventriculomegaly while this injury in the PND17 animals did not produce any overt tissue damage (Raghupathi and Huh, 2007). Both age groups showed evidence of axonal injury in the white matter tracts and the thalamus, but PND11 animals showed increased astroglial reactivity and only PND11 animals demonstrated a spatial learning impairment at 28 days post-injury. This model of diffuse injury also produces a robust microglia/macrophage response accompanied by degeneration in the cortex, white matter, hippocampus, and thalamus (Hanlon et al., 2016b) (Chapters 3 & 4).

Impact to the intact dura in neonatal rabbits (PND5-7) produced similar results to those produced in the mouse and rat. The injury resulted in severe lesion at the impact site that, over time, affected the white matter and subcortical structures. Microglial reactivity was significantly increased in the white matter at 7 days post-injury. The animals also showed decreased neurobehavioral function and a deficit in novel object

recognition memory (Zhang et al., 2015). Impact to the intact dura in piglets of different ages (5 days, 1 month, 4 months) showed that injury to the older animal produced a greater extent of cell loss (Duhaime et al., 2000).

Despite vast differences in the brains of rodents and larger mammals such as pigs, pediatric injury models in both types of animals have successfully modeled the pathology associated with different types and severities of human pediatric traumatic brain injury such as tissue atrophy, ventriculomegaly, white matter injury, and inflammation. Using models such as these to elucidate secondary mechanisms involved in these pathologies may provide relevant therapeutic targets to ameliorate further brain damage and functional impairment.

1.3 MECHANISMS OF PEDIATRIC TRAUMATIC BRAIN INJURY

1.3.1 Cell Death

Cell loss is apparent in children following TBI through volumetric analysis revealing evidence of tissue atrophy (Verger et al., 2001, Wilde et al., 2005, Suskauer and Huisman, 2009). In preclinical models of injury to the immature brain, evidence of cell death is apparent through the formation of lesions/cavitations, the presence of tissue atrophy, and through detection of markers associated with necrosis, apoptosis, and excitotoxicity (Bittigau et al., 1999, Tong et al., 2002, Huh et al., 2006, Huh and Raghupathi, 2007). After injury, dysregulation of excitatory neurotransmission and calcium influx can result in cellular damage referred to as excitotoxicity (Choi, 1987) and

there is evidence that excitotoxicity can lead the cell down either apoptotic or necrotic cell death pathways (Portera-Cailliau et al., 1997, Huh and Raghupathi, 2009). Evidence of excitoxicity has been confirmed in the human population through the discovery of high amounts of glutamate in the cerebrospinal fluid of children that sustained a severe TBI (Ruppel et al., 2001). Because calpain is activated by rises in intracellular calcium concentrations, this cysteine protease has conventionally been associated with necrotic cell death and has been implicated in post-injury degeneration (Kampfl et al., 1997). Our lab has demonstrated an increase in calpain-mediated spectrin breakdown products in the cortex, thalamus, and white matter out to 3 days following injury to the PND11 rat indicating a role for excitotoxicity and necrotic damage in the pathophysiology of injury to the immature brain (Huh et al., 2006). There is some evidence, however, that calpain is also associated with apoptotic cell death and can affect aspects of the intrinsic apoptotic pathway through its ability to inactivate anti-apoptotic protein bcl-2 and activate caspase-3 (Harwood et al., 2005). Apoptotic cell death may also play a role in neurodegeneration following injury to the developing brain as researchers observed increased DNA fragmentation, increased caspase 3 activity, and down-regulation of bcl-2 after injury and discovered that these apoptotic markers were most severe in young PND3 and PND7 brain-injured rats (Bittigau et al., 1999). Directly targeting the dysregulation of excitatory neurotransmission with NMDA or AMPA receptor antagonists following traumatic brain injury in the adult have produced very promising positive results that range from neuroprotection to the amelioration of cognitive impairment (Hamm et al., 1993, Belayev et al., 2001, Rao et al., 2001). The immature brain, however, responds differently to changes in excitatory neurotransmission because the circuitry depends on

activity for proper development (Giza et al., 2007). This was further demonstrated by the observation that NMDA receptor antagonism increased delayed apoptosis in the developing brain following TBI (Pohl et al., 1999). These results suggest that targeting alterations in excitatory neurotransmission following insult to the immature brain may exacerbate injury pathology.

While alterations in excitatory neurotransmission can cause cell death, neuronal damage can also be mediated by external forces such as alterations in the glial response following injury. Microglia, specifically, can release pro-inflammatory cytokines and harmful mediators such as nitric oxide that will cause cellular injury and may result in cell death (Loane and Byrnes, 2010). Microglial involvement following traumatic brain injury will be discussed in more depth in section 1.4.

1.3.2 Axonal Injury

Traumatic axonal injury is a hallmark pathology of pediatric TBI and is readily reproduced in pre-clinical models. In the year following injury, children demonstrated a decreased percentage of white matter on follow-up MRI scans compared to uninjured age-matched controls (Ghosh et al., 2009). In our model of closed head injury in the PND11 rat, we recently showed that there is severe atrophy in the white matter over time indicating the loss of damaged axons (Hanlon et al., 2016b). Proposed secondary mechanisms behind axotomy following traumatic brain injury include ionic dysregulation, calpain-mediated proteolysis, impaired axonal transport, microtubule degradation, and neurofilament compaction (Pettus et al., 1994, Pettus and Povlishock, 1996, Saatman et al., 1996, Okonkwo et al., 1998, Buki et al., 1999, Stone et al., 2001).

Impaired axonal transport can be visualized through the accumulation of amyloid precursor protein leading to axonal swelling and eventual disconnection and has been observed in models of contusive and diffuse injury in the immature brain (Raghupathi and Huh, 2007, DiLeonardi et al., 2009, Eucker et al., 2011, Huh et al., 2011). In addition to structural alterations in the axon, there is also evidence that brain injury in the immature animal impairs signal conduction throughout white matter fiber bundles (Dileonardi et al., 2012). So far, a viable treatment strategy for ameliorating white matter histopathology and functional deficits has not been identified (DiLeonardi et al., 2009, 2012).

1.4 MICROGLIA/MACROPHAGES AND THEIR ROLE IN TRAUMATIC BRAIN INJURY

1.4.1 Microglia Biology

Origin

Sources indicate that microglia make up approximately 10-15% of all the cells in the brain, but this number may vary across brain regions and species (Lawson et al., 1990, Azevedo et al., 2009). They are known as the resident macrophages of the CNS because they were once believed to originate from hematopoietic stem cells much like monocytes and peripheral macrophages due to their structural and functional similarities (Hickey and Kimura, 1988, Eglitis and Mezey, 1997). With scientific advances in cellular fate mapping and genetic manipulations, however, recent studies have indicated that microglia originate from a special population of macrophages from the yolk sac prior to the vascularization of the brain (Ginhoux et al., 2010, Schulz et al., 2012). It is evident

that in times of distress, however, peripheral cells can infiltrate the brain and assume microglial phenotype and function indicating that yolk sac-derived microglia and hematopoietically-derived peripheral macrophages share some similarities (London et al., 2013).

Activation

Microglia exist in three morphologically distinct phenotypes: resting, ramified, and activated. Resting microglia are characterized by their thin cell bodies and long, complex processes. The term "resting" may be misleading, however, as it implies that these microglia are inactive, but these cells are constantly scanning their environment and releasing mediators to aid in maintaining the integrity of the surrounding neuronal circuitry (Hanisch and Kettenmann, 2007). Using two-photon microscopy and genetically modified mice with fluorescently tagged microglia, microglia were visualized in vivo and it was observed that the processes of resting microglia were extremely motile and exhibited cycles of extension and withdrawal (Nimmerjahn et al., 2005). Furthermore, the processes of resting microglia make direct connections with synapses suggestive of a role in synapse maintenance (Wake et al., 2009). It has become evident that neuronal signaling in the healthy brain assists in keeping microglia in a surveilling or "resting" state (Kierdorf and Prinz, 2013). Such signals include the interaction between neuronal membrane-bound CD200 and the CD200 receptor on microglia as CD200 knockout mice exhibited increases in microglial number and activated morphology (Hoek et al., 2000). Additionally, neurons express cell surface proteins that signal to the microglia that they are healthy and do not need to be phagocytosed such as signal

regulatory protein alpha (SIRPα) (van Beek et al., 2005). As microglia detect perturbations in the environment, they undergo a morphological change. A cell that seems to be in the middle of this change and could go on to become fully activated or return to resting, depending on the signals in the microenvironment, is sometimes referred to as an "intermediately active" or "ramified" cell (Gomes-Leal, 2012). These cells exhibit enlarged cell bodies that are still elongated with a visible shortening of the processes. Recently, cells that meet these criteria have been identified after injury as "rod" microglia, but it is unclear what function these types of cells have in the pathophysiology of injury (Taylor et al., 2014). When a microglia becomes fully "activated" the processes retract and the cell soma becomes enlarged and rounded taking on an amoeboid morphology more similar to that of peripheral macrophages. It is through this morphological change that the cells are believed to become highly mobile and phagocytic (Nimmerjahn et al., 2005). Microglia can become activated in response to neuronal damage through the detection of cell membrane fragments, purines, and glutamate indicating that the neuron is releasing its cytosolic contents into the extracellular space. These can activate the triggering receptor expressed on myeloid cells 2 (TREM2) thus signaling for the microglia to become active and phagocytose the dying cell (Neumann and Takahashi, 2007, Kierdorf and Prinz, 2013). In addition to a change in morphology, these activating signals can also trigger the release of soluble mediators such as pro- and anti-inflammatory cytokines, chemokines, and nitric oxide that can have beneficial or deleterious effects on the surrounding cells (Biber et al., 2007).

Synthesis and Release of Soluble Mediators

While microglia are not the only cells in the brain that can synthesize and release pro- and anti-inflammatory mediators, the use of these mediators to maintain homeostasis and respond to CNS insult is well-characterized in microglia (Hanisch, 2002, Kettenmann et al., 2011, Smith et al., 2012, Nayak et al., 2014). Microglia not only synthesize and release cytokines and chemokines, they also contain receptors for some of these molecules to act as regulatory mechanisms and, in the specific case of chemokine receptors, to aid in chemotactic migration (Kettenmann et al., 2011). Some of the well-characterized pro-inflammatory cytokines associated with microglial reactivity are interleukin-1β (IL-1β), tumor necrosis factor α (TNFα), interleukin-6 (IL-6) and interferon gamma (IFN-γ) (Ramesh et al., 2013). Microglia utilize chemokines such as macrophage inflammatory proteins (MIPs: MIP-1α, MIP-1β, MIP-2, Mip-3β), Interleukin-8 (IL-8), macrophage colony stimulating factor (M-CSF), and monocyte chemoattractant protein-1 (MCP-1) to attract other microglia and migratory peripheral cells (including peripheral macrophages) to the site of damage (Hanisch, 2002). Microglia can also synthesize and release nitric oxide (NO) and the excitotoxic tryptophan metabolite quinolinic acid (QA) that can be extremely detrimental to cell survival (Boje and Arora, 1992, Bal-Price and Brown, 2001, Guillemin, 2012). These pro-inflammatory, chemotactic, and potentially neurotoxic characteristics are associated with an M1 microglial phenotype that has emerged in the study of detrimental microglial contributions to CNS pathology (Heneka et al., 2014, Tang and Le, 2016). Microglia can also release mediators that are considered beneficial or anti-inflammatory in order to dampen the spread of neuroinflammation within the brain and modulate neuronal circuitry. For example, in response to neuronal damage and upregulation of pro-

inflammatory mediators, microglia will also release the endogenous interleukin-1 receptor antagonist (IL-1ra) and the anti-inflammatory cytokine IL-10 (Hanisch, 2002). Similarly, microglia can release growth factors such as transforming growth factor beta (TGFβ) that has been shown to aid in neurogenesis (Battista et al., 2006). This beneficial anti-inflammatory profile has been associated with the alternative activation state M2 in which the most popular marker is Arginase-1, an enzyme expressed by microglia that is associated with wound repair (Cherry et al., 2014). While investigations into the M1/M2 microglial polarization have seen a rise in recent years, some evidence has been put forth that indicates that microglia don't exist in perfectly polarized activated states, but that they can express markers associated with either phenotype at the same time (Morganti et al., 2016). However, some researchers don't believe this M1/M2 polarization exists in microglia in the healthy or damaged brain (Ransohoff, 2016).

Role in Development

Microglia play crucial roles in brain development and this may be a factor in the pathophysiology of TBI in the immature brain. Microglia have been implicated in developmental cell death, vascularization, synapse formation, and neurogenesis (Pont-Lezica et al., 2011). While microglia have been shown to congregate to areas of apoptosis, they may do more than just arrive to engulf the dying cell. When the microglial CD11b integrin was deleted in mice, there was a decrease in developmental cell death indicating that microglia may play an active role in mediating cell death in the hippocampus (Wakselman et al., 2008). One of the biggest responsibilities that microglia have in the developing brain is synaptic pruning- a process by which unnecessary

synaptic connections are removed in order to strengthen and enhance necessary circuitry. This process was confirmed in the developing mouse brain as labeled post synaptic density proteins were observed within labeled microglia. Additionally, when the fractalkine receptor was knocked down in developing mice, there was an increase in total post-synaptic density proteins and synaptic spine density, and a decrease in the frequency of spontaneous excitatory post synaptic currents (sEPSCs), indicating that fractalkine serves as an important mediator in microglial-neuronal interaction and without it, microglia do not properly execute their synaptic pruning responsibilities, resulting in immature connectivity (Paolicelli et al., 2011). The confirmation of microglial involvement in synaptic pruning may have important implications for neurodevelopmental disorders in which aberrant connectivity results in behavioral dysfunction (i.e. autism or schizophrenia). Finally, microglial-associated mediators that have been identified as harmful pro-inflammatory molecules in the injured brain act as powerful neuromodulators that allow for the development of functional neuronal circuitry (McAfoose and Baune, 2009). For example, IL-1 activity in the healthy brain seems to be necessary for hippocampal-dependent memory processes as blockade of this signaling resulted in memory impairment (Goshen et al., 2007).

Role in ischemic brain injury in the neonate

Hypoxic-ischemic (HI) injuries in the neonate produced microglial responses that were evident 4 hours after injury and peaked around 4 days, but evidence of activation still remained out to 14 days post-insult (McRae et al., 1995, Ivacko et al., 1996). Similarly, HI in 7-day-old rats resulted in acute increases in inflammatory mediators such

as IL-1β and TNFα and prolonged expression of microglial/macrophage marker MHC1 out to 42 days post-injury (Bona et al., 1999). This injury also induced increases in chemokine expression indicating that hypoxic-ischemic injury was sufficient to mount an inflammatory response involving chemotactic migration of immune cells (Cowell et al., 2002). The use of anti-inflammatory therapeutics in HI have produced mixed results with some studies citing significant rescue of injury-induced damage and others claiming that these therapies exacerbate damage in the developing brain. Similar to results in adult TBI, blockade of IL-1 signaling reduced gliosis, myelin loss, and improved motor outcomes such as impairments in overall locomotion and limb dexterity following HI injury and inflammatory insult initiated by administration of lipopolysaccharide (LPS) (Girard et al., 2012). Antibiotics with anti-microglial properties such as doxycycline and minocycline have been shown to alleviate injury-induced damage to neurons and oligodendrocytes as well as alleviate neurological dysfunction following HI injury (Arvin et al., 2002, Jantzie et al., 2005, Cai et al., 2006). However, in a model of HI injury in the neonate mouse, minocycline administration significantly increased lesion volume (Tsuji et al., 2004). In a model of neonatal stroke, cellular depletion of microglia also exacerbated lesion area (Faustino et al., 2011). Finally, in contrast to results in the adult, progesterone treatment in neonatal rats following HI exacerbated injury-induced hemispheric damage. Interestingly this exacerbation was only observed in rats injured on PND7 and PND14, but not those injured on PND21 emphasizing that treatments may not function through the same mechanisms in young animals compared to older animals (Tsuji et al., 2012).

Age-dependent effects of microglial priming prior to brain injury

The endotoxin lipopolysaccharide (LPS) activates microglia in both neonate and adult animals (Hoogland et al., 2015). In the adult brain, LPS-induced microglial activation prior to cryogenic injury resulted in neuronal protection as LPS-treated brain-injured mice demonstrated fewer TUNEL-labeled cells in the injured cortex (Chen et al., 2012). Interestingly, even when mice were exposed to LPS in utero, neuroprotection was conferred when they sustained a hypoxic-ischemic injury on PND70 (Wang et al., 2007). LPS preconditioning in adult mice also protected neurons from TNFα-induced damage following stroke (Rosenzweig et al., 2007) and reduced contusion volume and motor deficits following TBI (Longhi et al., 2011). Preconditioning prior to weight-drop brain injury reduced gliosis and axonal injury in the corpus callosum in adult rats (Turner et al., 2017). These results indicate a neuroprotective role for LPS preconditioning and microglial priming in the context of injury to the adult brain. In the immature brain, however, LPS preconditioning has had mixed results in models of hypoxic-ischemic (HI) injury and these conflicts appear to be dependent on the timing of LPS delivery and the length of HI exposure. When LPS (0.3 mg/kg) was delivered 24 hours prior to a 50-minute HI insult, it reduced brain injury as measured by regional morphologic analysis. When this same dose of LPS was delivered 6 hours or 72 hours before either a 20-minute or 50-minute HI insult, however, brain injury was significantly increased (Eklind et al., 2005). In a different study, 0.3 mg/kg LPS 24 hours prior to a 2-hour insult resulted in a high mortality rate, but 0.05 mg/kg LPS 24 hours prior decreased acute post-insult microglia/macrophage activation and NOS production as well as reducing long-term brain damage and ameliorating learning and memory deficits in adulthood (Lin et al.,

2009). When LPS was administered in utero and HI was induced at PND5 or 9, treated pups demonstrated exacerbated brain injury, reduced myelin, and increased caspase-3 activity (Wang et al., 2007). These inconsistent results emphasize the complexity of microglial/macrophage activity during development, especially in the context of injury.

1.4.2 Clinical Evidence for Microglial Involvement in Pediatric TBI

The microglial response in children following traumatic brain injury is often monitored via serum biomarker analysis. As previously mentioned, microglia release a host of different pro- and anti-inflammatory mediators, growth factors, and neurotoxic chemicals that can be monitored post-injury (Woodcock and Morganti-Kossmann, 2013). In assessments of cytokines concentrations in the CSF following severe TBI in children, cytokines IL-1β, IL-6, and IL-10 were elevated indicating an increase in pro-inflammatory signaling but also an endogenous increase in anti-inflammatory signaling to combat the injury (Bell et al., 1997, Buttram et al., 2007). Additionally, there seemed to be an age-dependency in the observed levels of IL-10 with children under the age of 4 producing significantly higher levels of IL-10 irrespective of injury severity (Bell et al., 1997). Additionally, chemokines IL-8 and MIP-1α were also increased indicating migratory signaling to other immune cells (Buttram et al., 2007). Children that sustain severe traumatic brain injury also have significantly higher concentrations of quinolinic acid in their CSF indicating high levels of microglia/macrophage activation in the brain following injury (Berger et al., 2004). While children that sustain severe injuries seemed to be more likely to mount a measurable immune response, there was evidence that children that sustained mild TBIs had significantly higher concentrations of IL-6 in their

CSF indicating a role for inflammation in a range of different injury severities (Berger et al., 2009).

1.4.3 Microglial Reactivity Following TBI

Adult TBI

In models of TBI in the adult, cellular microglial activation has been detected in both grey and white matter following different severities of injury (Csuka et al., 2000, Raghavendra Rao et al., 2000, Igarashi et al., 2007, Venkatesan et al., 2010, Wang et al., 2014) and increases in the production of inflammatory mediators have been observed (Shohami et al., 1994, Fan et al., 1995, 1996, Stover et al., 2000, Song et al., 2002, Natale et al., 2003, Israelsson et al., 2008). Treatments targeting this immune response in the adult brain following TBI have been rather successful in mediating injury-induced cell death and functional impairment indicating a role for microglial activation and inflammation in the neurodegenerative mechanisms following injury. Progesterone treatment following traumatic brain injury in the adult rat decreased IL-1β and TNFα expression and has been associated with a decrease in apoptotic markers and improvement on a spatial learning and memory task (He et al., 2004, Djebaili et al., 2005). Minocycline administration has been shown to decrease microglial reactivity and was associated with similar reductions in apoptosis and functional impairments following TBI (Sanchez Mejia et al., 2001, Kovesdi et al., 2012, Siopi et al., 2012). Finally, blockade of harmful pro-inflammatory IL-1 signaling can significantly reduce neuronal damage and ameliorate cognitive dysfunction (Toulmond and Rothwell, 1995, Sanderson

et al., 1999). In the immature brain, the microglial response has been thoroughly investigated following non-impact hypoxic-ischemic brain injury.

Neonate TBI

Very few studies have been conducted investigating microglial reactivity and the role of inflammation following impact to the developing brain. In adolescent mice (PND35), a mild impact resulted in an increase in microglial reactivity in only the corpus callosum at 24 hours, but there were no differences in labeling between brain-injured animals and sham-injured controls at 3 months post-injury and this initial increase was not associated with volumetric changes or increases in cell death (Semple et al., 2016). In a model of moderate contusive injury in the PND21 mouse, microglial activation was apparent in the ipsilateral cortex around the lesion, the CA2 region, CA3 region and dentate gyrus of the hippocampus, and the thalamus out to 7 days post-injury. All of these regions also demonstrated evidence of fluoro-jade B-positive (FJB+) degenerating cells in the same time frame (Tong et al., 2002). This injury also resulted in enhanced infiltration of leukocytes and neutrophils as these cell types were elevated in the brains of animals injured on PND21 compared to brain-injured adult animals (Claus et al., 2010). After injury to the neonatal rabbit (PND5-7), researchers characterized a robust microglial response in the white matter of brain-injured animals that was associated with both an increase in microglial cell number and a morphologic activation that was heaviest at 3 days post-injury, but persisted to 21 days and may be associated with persistent cognitive deficits (Zhang et al., 2015). While neuroinflammation has been identified as a target for pediatric TBI, there are still only a few studies targeting this cascade or the

microglial response following impact-based trauma to the immature brain (Potts et al., 2006). Brain-injured neonatal mice that were deficient in neutrophil elastase (released by activated neutrophils recruited from the periphery) demonstrated a decrease in cell death and markers of oxidative stress as well as functional recovery in spatial learning and memory assessment. Acutely targeting neutrophil elastase with an inhibitor, however, only reduced acute cell death and had no effect on long-term behavioral outcomes emphasizing the complexity of targeting aspects of the neuroinflammatory cascade following injury to the immature brain (Semple et al., 2015). Because neutrophils can be recruited by chemotactic signals released by microglia (specifically IL-8 and MIP-2), these results also still indicate that microglial reactivity is pivotally involved in this process (Hanisch, 2002, Kobayashi, 2008). Finally, our lab has demonstrated that repetitive trauma to the PND11 rat induces dense microglia/macrophage reactivity in the cortex, corpus callosum, and thalamus that is associated with neurodegeneration, axonal injury, and spatial learning and memory deficits. Acute treatment with minocycline in this model only resulted in a decrease in activated microglia/macrophages in the corpus callosum at 3 days post-injury and had no effect on neurodegeneration or axonal injury, but exacerbated spatial memory deficits in the second post-injury week (Hanlon et al., 2016a).

The microglial response following impact injury to the immature brain is not simply a replica of the response that occurs in adults or in models of non-impact brain injury. The role of microglial activation following injury to the developing brain needs further investigation, especially if anti-inflammatory treatments are going to be used in

brain-injured children. This thesis aims to characterize the cellular microglia/macrophage response in a model of neonatal traumatic brain injury and to investigate its role in neuropathological alterations and long-term functional impairments through the use of post-injury microglia/macrophage manipulations.

CHAPTER 2: STATEMENT OF SPECIFIC AIMS

Traumatic brain injury (TBI) is a leading cause of death and disability in children with those aged 0-4 having the highest incidence of emergency room visits due to TBI (Faul et al., 2010). Children that survive their injuries exhibit long-term pathologic changes such as atrophy and ventriculomegaly and demonstrate a wide array of functional impairments (Wilde et al., 2005, Ghosh et al., 2009). Evidence of neuroinflammation in brain-injured children has been documented and may play a pivotal role in the perpetuation of injury-induced neuronal damage and behavioral impairments (Berger et al., 2004, Buttram et al., 2007, Berger et al., 2009). Our lab has demonstrated that closed head injury in the PND11 rat resulted in atrophy, indicative of cell loss/degeneration, ventricle enlargement, axonal injury, and spatial learning and memory deficits thus reproducing the pathology observed in human pediatric TBI (Raghupathi and Huh, 2007). We have preliminary evidence that this injury produces a microglia/macrophage response, but the characterization of this response and its effects on pathology and behavioral alterations has yet to be elucidated. Inflammation following pediatric TBI has also been identified as a potential target for therapeutic intervention (Potts et al., 2006) as anti-inflammatory treatments have been successful in ameliorating cell death and behavioral dysfunction in models of TBI in the adult (Sanchez Mejia et al., 2001, He et al., 2004, Siopi et al., 2012). The evidence for the success of anti-inflammatory interventions in the developing brain following non-impact injury is conflicting as some report neuroprotection and others report exacerbation of injury-induced pathology (Arvin et al., 2002, Tsuji et al., 2004, Cai et al., 2006, Carty et al., 2008, Faustino et al., 2011, Tsuji et al., 2012). Investigating the microglia/macrophage response and using different manipulations targeting either the entire cell or the activation

state will not only illuminate its role in post-injury pathology and behavioral alterations, but it will also shed light on the efficacy of targeting post-injury microglia/macrophage activation in the immature brain.

SPECIFIC AIM 1:

Part A: Characterize the post-injury microglia/macrophage response and investigate novel functional deficits in axonal conduction and cortical electrophysiology. Hypothesis: The microglia/macrophage response will overlap regionally and temporally with neurodegeneration, axonal injury, and axonal degeneration suggesting a role for microglia/macrophages in these post-injury pathologies. Brain-injured animals will exhibit deficits in cortical activity and axonal conduction in regions where degeneration and microglia/macrophage reactivity are present.

Part B: Elucidate the role of microglia/macrophages in post-injury pathology and functional deficits using clodronate-mediated microglia/macrophage depletion. Hypothesis: Clodronate-treated brain-injured animals will demonstrate a decrease in degeneration and axonal injury that will ameliorate deficits in cortical field potential, axonal conduction, and spatial learning and memory.

SPECIFIC AIM 2:

Investigate the role of microglia/macrophage activation in post-injury pathology and functional deficits by using minocycline to reduce activated (amoeboid) microglia/macrophages. Hypothesis: Minocycline treatment will decrease microglia/macrophage activation while simultaneously decreasing neurodegeneration and axonal injury. Minocycline-treated animals will also demonstrate improvements in cortical activity and spatial learning and memory.

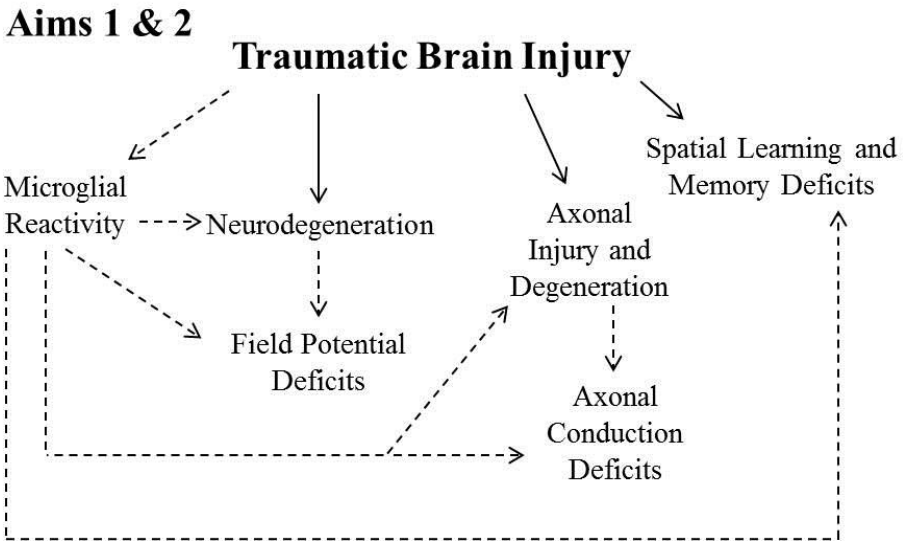

SPECIFIC AIM 3:

Part A: Expand the functional profile of our injured animals beyond that of spatial learning and memory and neuronal activity within the impact site to include relevant behavioral assessments in the chronic post-injury period (anxiety, working memory, seizures, motor) and a characterization of neuronal activity a region that does not demonstrate post-injury cellular pathology. Hypothesis: Brain-injured will demonstrate increased anxiety, working memory impairment, an increased susceptibility to seize, and deficits in locomotion. Animals will not exhibit alterations in neuronal activity in the frontal cortex, indicating a role for degeneration and microglia/macrophage reactivity in post-injury neuronal activity.

Part B: Investigate the role of acute microglia/macrophage manipulations on behavioral impairment in the chronic post-injury period. Hypothesis: The acute neuroprotection afforded by clodronate-mediated depletion and minocycline-mediated decreased

reactivity hypothesized in Aims 1 and 2 will aid in attenuating chronic post-injury behavioral impairment.

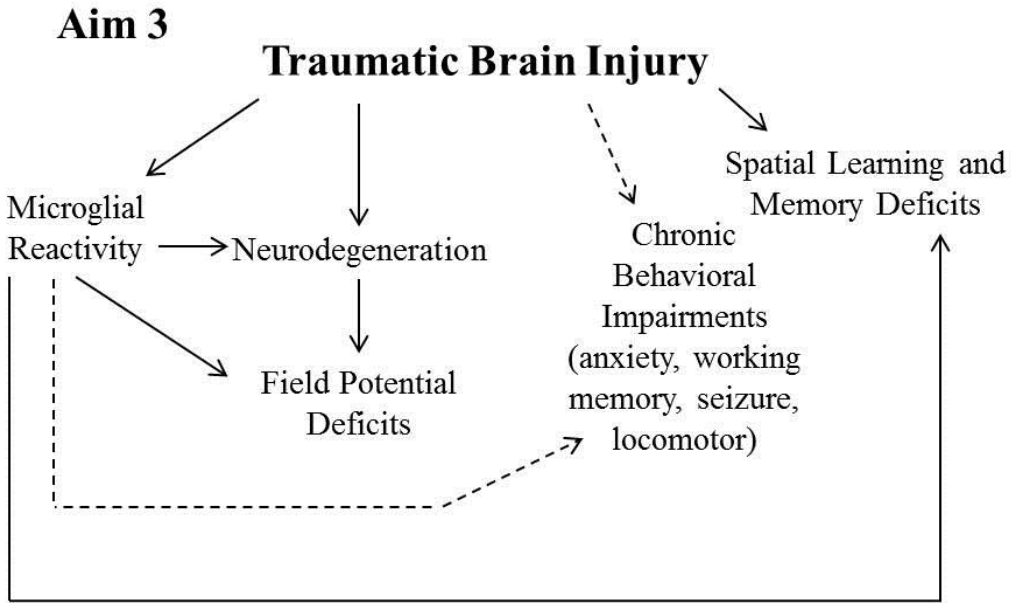

CHAPTER 3: CHARACTERIZATION OF THE MICROGLIA/MACROPHAGE RESPONSE FOLLOWING TBI IN THE NEONATE RAT AND THE EFFECTS OF LOCAL MICROGLIA/MACROPHAGE DEPLETION

3.1 ABSTRACT

Neuroinflammatory mediators and markers of microglia/macrophage activation have been identified in the cerebrospinal fluid of children that have sustained traumatic brain injuries indicating that these immune cells may play a significant role in the pathophysiology of the injury. In this study, microglia/macrophage reactivity was assessed following injury to the PND 11 rat. Injury produced a robust microglia/macrophage response in the cortex, thalamus, and subiculum at 3 days post-injury that was sustained out to 4 weeks. This microglia/macrophage reactivity was associated with the sustained presence of FJB(+) profiles in all of these regions. Interestingly, cortical activity was only altered at 3 days post-injury despite the sustained presence of FJB-labeled cells. Microglia/macrophage reactivity was also observed in the corpus callosum and lateral white matter tracts out to 4 weeks post-injury and was associated with evidence of axonal degeneration (FJB) and axonal injury (APP). Similarly, axons in the white matter of brain-injured animals showed both conduction and transport deficits. Peri-injury microglia/macrophage depletion was conducted via clodronate injection to investigate the role of microglia/macrophages in these various post-injury pathologies. At 15 days post-injury, microglia/macrophages showed evidence of repopulation but exhibited a strange rod-like phenotype in brain-injured animals that progressed to an increase in activated amoeboid cells by 35 days post-injury. This coincided with an increase in FJB labeling in all regions. In the cortex, this increase in FJB labeling was also associated with hyperactivity. Clodronate, which has largely been identified as selectively targeting microglia/macrophages, also decreased astrocytic reactivity indicating non-specific targeting. Interestingly, despite an increase in FJB(+)

profiles in the white matter, axonal injury and axonal conduction deficits were unaffected by microglia/macrophage depletion. Finally, brain-injured animals treated with clodronate did not show attenuation or exacerbation of injury-induced spatial learning and memory deficits at 2 or 4 weeks post-injury. Sham-injured animals treated with clodronate, however, showed a mild, but transient spatial learning deficit indicating a role for glia in physiological cognitive development. While these results support the notion that post-injury microglia/macrophage activation is needed for the maintenance of neuropathology, the depletion may have been too severe of an intervention and further investigation is warranted.

3.2 INTRODUCTION

Pediatric traumatic brain injury (TBIs) is a devastating health problem that can result in long-term pathologic and functional alterations that can significantly affect quality of life (Annegers et al., 1998, Ewing-Cobbs et al., 2000, Schwartz et al., 2003, Keenan et al., 2004, Anderson et al., 2005, Ewing-Cobbs et al., 2008, Max et al., 2015). While advocating for injury prevention in children is admirable, it is essential that targets are identified and therapeutics are developed aimed at halting the secondary damage associated with biochemical cascades following injury (Greve and Zink, 2009). Neuroinflammation has been identified as a potential therapeutic target following pediatric TBI as evidence has emerged that the increased presence of pro-inflammatory mediators in the cerebrospinal fluid of brain-injured children may correlate with injury severity and may be exacerbated in young children (≤ 4 years of age) (Amick et al., 2001, Potts et al., 2006, Buttram et al., 2007, Berger et al., 2009). These inflammatory mediators are associated with a cascade that involves microglia/macrophage activation post-injury and specific evidence for this reactivity has also been observed in the CSF of traumatically injured children (Berger et al., 2004, Loane and Kumar, 2016).

Microglia/macrophage reactivity has been identified in pediatric traumatic brain injury models using rodents and rabbits, but their role in the pathophysiology of pediatric trauma remains unclear (Zhang et al., 2015, Chhor et al., 2016). Additionally, microglia play a large role in proper brain development indicating that their role in injury to the developing brain may be more complex than their role following injury to the fully-developed adult brain (Graeber and Streit, 2010, Loane and Byrnes, 2010). Targeting the microglia/macrophage response following hypoxic-ischemic (HI) injury to the

developing brain, however, has produced results that are very similar to the success reported in the use of anti-microglia/macrophage treatments following TBI in the adult indicating that an anti-microglia/macrophage therapeutic may provide neuroprotection in an impact-based model of pediatric brain injury (Sanchez Mejia et al., 2001, Arvin et al., 2002, He et al., 2004, Djebaili et al., 2005, Cai et al., 2006, Plane et al., 2010).

In our model of TBI to the PND11 rat, injury results in tissue atrophy, axonal injury, and prolonged spatial learning and memory deficits (Raghupathi and Huh, 2007). We have limited preliminary evidence that indicates that this injury also results in microglia/macrophage reactivity. One of the goals of this study to characterize the cellular microglial response following injury as it relates to neurodegeneration, axonal pathology, and alterations in neuronal activity. The second goal of this study is to investigate how these pathologies are altered in the absence of an acute microglia/macrophage response through the use of clodronate-mediated microglia/macrophage depletion. Clodronate (dichloromethylene-bisphosphonate, Cl_2MBP) can be packaged in liposomes to specifically target and induce the apoptosis of phagocytic cells and is commonly used to target peripheral macrophages (Lehenkari et al., 2002, van Rooijen and van Kesteren-Hendrikx, 2003). It has shown efficacy in depleting microglia from mixed cultures and in the limited use of this compound in the brain, it has been successful in significantly decreasing the total number of microglia (Faustino et al., 2011, Drabek et al., 2012, Kumamaru et al., 2012, Asai et al., 2015). Based on the previous work targeting the microglia/macrophage response in both adults (TBI) and neonates (HI), it is our hypothesis that by removing the

microglia/macrophages, we will block their detrimental contribution to secondary injury and observe an amelioration of injury-induced neuropathology and functional deficits.

3.3 MATERIALS AND METHODS

3.3.1 Brain Injuries

All surgical procedures were done in accordance with the rules and regulations of the Institutional Animal Care and Use Committee at Drexel University College of Medicine. On postnatal day 11, male and female Sprague Dawley rat pups (Charles River Laboratories, Wilmington, MA) were randomly assigned to injury conditions (Sham-Injured, N=; Brain-Injured, N=). Animals were placed in a nose cone and anesthetized using 5% isoflurane and a 2cm incision slightly left of the midline was made to expose the skull. Once exposed, the periosteum was cleared away and a small mark was made on the skull over the left parietal cortex midway between the bregma and lambda sutures to indicate the impact site. Four minutes after the start of anesthesia exposure, animals were removed from the nose cone, placed in plastic rodent restrainer (Braintree Scientific, Braintree, MA), and moved to the stage of the controlled cortical impact device (CCI, Custom Design and Fabrication, Richmond, VA, Fig. 3.1). The piston tip (5mm silicone impactor tip) was zeroed over the previously made mark and then electrically driven into the intact skull at velocity of 5m/s with an injury depth of 3mm and a dwell time of 100ms. Sham-injured animals were treated exactly the same as brain-injured animals but did not undergo impact. Animals were allowed to right themselves before being placed back under anesthesia to be sutured. Surgical procedure and recovery occurred on heating pads to maintain the animals' body temperatures. Post-surgery, animals recovered in a separate cage for at least 30 minutes before being placed back with the mother.

3.3.2 Fluoro-Gold Injections

Fluoro-Gold (2%, Fluorochrome) was injected into the left cortex of both sham-injured and brain-injured animals 14 days post-injury. Animals were initially placed under 5% isoflurane anesthetic for the incision and situating the animal in blunt-tipped stereotactic jaw bars. The anesthetic was tapered down to 2-3% for the duration of the surgery. A 10-µl glass syringe (Hamilton, Franklin, MA) and a microsyringe injection pump (Micro-4, World Precision Instruments, Sarasota, FL) were used to withdraw 5µl of the working Fluoro-Gold solution into the syringe. After zeroing the tip at bregma and moving the tip to the desired coordinates, the spot was marked and a burr hole was drilled into the skull. The dura was punctured using a 26 1/2 gauge needle, the needle was zeroed at the dura, and was lowered into the brain. The needle was left stationary in the brain for 2 minutes prior to the beginning of infusion. The compound was delivered at a rate of 1µl/minute for a total of 2µl in 2 minutes. The syringe was left stationary in the brain for 5 minutes after the completion of infusion before being raised slowly from the brain to minimize draw back. Animals were removed from the jaw bars, sutured, and moved to the recovery cage. All surgical procedures and recovery occurred on circulating heating pads to maintain body temperature and the animals were allowed to recover for 30 minutes before being returned to their home cages.

3.3.3 Clodronate Administration

Liposome-encapsulated clodronate or empty control liposomes were administered to both sham-injured and brain-injured animals 24 hours after injury on

postnatal day 12. Animals were initially placed under 5% isoflurane anesthetic for suture removal, cleaning and reopening of the incision site, and situating the animal in blunt-tipped stereotactic jaw bars. The anesthetic was tapered down to 1-2% for the duration of the injection surgery. Separate 100-µl glass syringes (Hamilton, Franklin, MA) and a microsyringe injection pump (Micro-4, World Precision Instruments, Sarasota, FL) were used to withdraw 30µl of Clodrosome® (liposome-encapsulated clodronate) or Encapsome® (empty liposomes, Encapsula NanoSciences, Brentwood, TN). The syringe was zeroed at the intersection of the bregma and midline sutures and moved into position for burr hole markings (cortical injection: 1.5mm posterior to bregma and 1.7mm lateral to the midline; thalamic injection: 3.5mm posterior to bregma and 1.7mm lateral to the midline). Two burr holes were made in the skull in the targeted areas and the dura was punctured with a 26 1/2 gauge needle. Once zeroed in the burr hole, the needle was lowered 1.7mm into the cortex and left still for 2 minutes before the pump was switched on. The compound was delivered at a rate of 1µl/minute for a total of 10µl in 10 minutes. The syringe was left stationary in the brain for 5 minutes after the completion of infusion before raised slowly from the brain to minimize draw back. The syringe was then moved and zeroed over the burr hole for the thalamic injection and lowered 3.7mm into the brain. The same procedure was repeated as described for the cortical injection. Once the syringe was removed from the brain, the animal was taken out of the jaw bars and sutured. All surgical procedures and recovery occurred on circulating heating pads to maintain body temperature and the animals were allowed to recover for at least an hour before being returned to the mother.

3.3.4 Histology and Immunohistochemistry

At the appropriate time points, animals were anesthetized (sodium pentobarbital, 60mg/kg, i.p.) and perfused transcardially with 4% paraformaldehyde. Brains were left in the skull in paraformaldehyde for 24 hours before being extracted from the skull, post-fixed for an additional 24 hours, and placed in 30% sucrose at 4°C until the time of slicing. Brains were sliced on a freezing-stage sliding microtome after being flash frozen in 2-methyl butane at -40°C. Twelve sets of coronal sections (40-45μm thick) were taken starting approximately at the bregma suture to 5-6mm posterior to bregma. Depending on the age of the animal, each set of sections contained 12-16 sections and were stored in 5ml vials filled with cryoprotectant (30% ethylene glycol, 30% glycerol) at -20°C until use. Adjacent sets of sections were mounted on gelatin-coated slides and stained for Fluoro-Jade B (FJB) or Nissl-myelin (2% Cresyl Violet and 0.2% Cyanine R) (Hanlon et al., 2016). Sections from FG brains were mounted and allowed to dry in the dark before being coverslipped with DPX mounting media. Using free-floating immunohistochemistry protocols, additional separate sets of sections (full or half vials) were evaluated for microglia/macrophages using antibodies for anti-ionized calcium-binding adaptor molecule 1 (Iba1, Wako, Richmond, VA, 1:20,000) and CD68 (Clone ED1, BioRad, formerly AbD Serotech, Hercules, CA, 1:500), astrocytes using glial fibrillary acidic protein (GFAP, Sigma, St. Louis, MO: 1:5,000) and traumatic axonal injury using a polyclonal antibody to the C-terminal end of amyloid precursor protein (APP, Zymed, San Francisco, CA, 1:2,000). For anti-APP immunohistochemistry, antigen retrieval was executed by incubation with 10mM sodium citrate (pH 6.5) in a 60ºC water bath for 20 minutes. Primary antibody binding was detected using

biotinylated donkey anti-rabbit IgG (Jackson ImmunoResearch, West Grove, PA, 1:1000 for APP and 1:500 for Iba1) or biotinylated donkey anti-mouse IgG (Jackson ImmunoResearch, West Grove, PA, 1:500 for ED-1 and GFAP). Antibody binding was visualized using the ABC Elite System with diaminobenzidine (Vector Laboratories, Burlingame, CA).

3.3.5 Quantification Methods for Histology and Immunohistochemistry

The areas of the cortex (from midline to rhinal fissure) of the injured hemisphere and white matter (corpus callosum, cingulum and lateral aspects up to the rhinal fissure) were measured in Nissl-myelin-labeled sections via manual tracing using Image J software (NIH) (Hanlon et al., 2016). Quantification in the cortex (layers 2 through 5 of the retrosplenial, motor and somatosensory cortices), hippocampus (dorsal subiculum) and thalamus (dorsolateral and lateral geniculate nuclei), and was conducted by counting labeled profiles (Iba1, ED-1, FJB) in 3-5 high power field (HPF) images (20x magnification) per section across 3-5 non-adjacent sections; Iba1(+) profiles that exhibited an activated morphology were counted and presented as a percent of total Iba1(+) profiles in that region. ED-1(+) profiles were counted as separate phenotypes: amoeboid morphology (enlarged, rounded cells with few to no visible processes) and rod morphology (elongated cells with thick cell bodies and few to no visible processes). Fluoro-Jade B(+) profiles (regardless of size) and amoeboid/rod ED-1(+) profiles were counted in 3 HPF images (20x magnification) per section that covered the area between the corpus callosum, cingulum and the lateral aspects of the white matter up to the rhinal fissure across 3-5 sections. Because of the density of Iba1 labeling in the white matter,

clear cellular bodies could not be distinguished in order to conduct reliable cell counting. For this reason, we used a thresholding approach from digitized images (Image J, NIH) and the labeled area was divided by the corresponding total area measured in the Nissl-myelin stained sections to address severe atrophy in the white matter (Hanlon et al., 2016). GFAP labeling was quantified in the cortex using this same measured thresholding technique except the labeled area was not measured as a function of the nissl-myelin-stained cortical area due increased confidence in the cortical boundaries in GFAP-labeled sections as opposed to white matter boundaries in Iba1-labeled sections. APP-labeled profiles were quantified in the white matter and thalamus using a modified grid analysis method (DiLeonardi et al., 2009) where the presence of APP(+) profiles were marked in a 6x5 grid overlaid onto 20x images (Photoshop). In the white matter, 3 images across 5 sections (15 images) where analyzed and in the thalamus, 3 images across 3 sections (9 images) were analyzed.

3.3.6 Compound Action Potential Electrophysiology

Compound action potential (CAP) electrophysiology was conducted as previously described (Reeves et al., 2005, DiLeonardi et al., 2009). Briefly, animals were anesthetized with 5% isoflurane, decapitated, and the brain was rapidly removed and placed in oxygenated (95% O_2/5% CO_2) ice-cold artificial cerebrospinal fluid (aCSF) (130 mM NaCl, 24 mM $NaHCO_3$, 10 mM glucose, 3.5mM KCl, 1.25 mM $Na_2H_2PO_4$, 1.5 mM $MgSO_4$ .7H_2O, 2mM $CaCl_2$.2H_2O). The brain was adhered to the vibratome block using superglue and the block was placed with the ventral surface of the brain facing the blade in the vibratome bath chamber. The bath chamber was filled with ice-cold aCSF

and was continuously oxygenated. Coronal slices were cut at a thickness of 450μm starting at bregma and ending at approximately 4mm posterior to bregma. After 1 hour of incubation at room temperature, slices were moved to the aCSF-filled recording chamber where they were continuously bathed with fresh aCSF for the duration of recording. A bipolar, tungsten stimulating electrode (with an inter-tip distance of approximately 350μm) was placed in the injured (left hemisphere) corpus callosum and a pulled glass recording pipette filled with aCSF was placed in the corpus callosum approximately 1mm away from the stimulating electrode. Potentials were evoked using constant current pulses (200μs duration) from a Master-8 pulse stimulator (A.M.P.I, Jerusalem, Israel) at increasing intensities (manual current stepping) and recorded using an Axoclamp 2B amplifier. A maximum current was found for each slice and input/output curves were constructed using decreasing 200μA current steps from the maximum. The amplitude of the N1 (myelinated) component was measured as the difference (in millivolts) between the top of first positive peak and the trough of the first negative peak. The amplitude of the N2 component (unmyelinated) was measured as the difference (in mV) between the trough of the second negative peak and baseline. The conduction velocity was measured as the difference in time between the stimulating artifact and the first negative peak (N1) or second negative peak (N2) at max stimulus amplitude. All quantitative analysis was made on representative waveforms that were the average of 4 sweeps at that particular stimulus intensity and presented as an input/output curve. Data in the clodronate study was presented as bar graphs at the max stimulus amplitude.

3.3.7 Cortical Evoked Field Potential Electrophysiology

Animals were anesthetized with 5% isoflurane, decapitated, and the brain was rapidly removed and placed in oxygenated (95% O_2/5% CO_2) ice-cold artificial cerebrospinal fluid (aCSF) (130 mM NaCl, 24 mM $NaHCO_3$, 10 mM glucose, 3.5mM KCl, 1.25 mM $Na_2H_2PO_4$, 1.5 mM $MgSO_4$ .7H_2O, 2mM $CaCl_2$.2H_2O). The brain was adhered to the vibratome block using superglue and the block was placed with the ventral surface of the brain facing the blade in the vibratome bath chamber. The bath chamber was filled with ice-cold aCSF and was continuously oxygenated. Coronal slices were cut at a thickness of 450μm starting at 1.5 mm anterior to bregma and ending at approximately 4mm posterior to bregma. After a 1 hour incubation (30 minutes at 37°C and 30 minutes at room temperature), slices were moved to the aCSF-filled recording chamber where they were continuously bathed with fresh aCSF for the duration of recording. A bipolar, tungsten stimulating electrode (World Precision Instruments, Sarasota, FL) was placed in layer 2 of the injured cortex and a pulled glass recording pipette filled with aCSF was placed in layer 5 of the same cortex (not directly underneath- offset by approximately 300μm). Potentials were evoked using constant current pulses (200μs duration) from a Master-8 pulse stimulator (A.M.P.I, Jerusalem, Israel) at increasing intensities (manual current stepping from 0-1000μA) and recorded using an Axoclamp 2B amplifier. Slices reacted similarly to current input and demonstrated a plateau around 800μA therefore all data is presented at this current intensity. The amplitude of the signal was measured as the difference (in millivolts) between baseline and the middle of the primary peak, the latency of the signal was measured as the difference in time (ms) between the beginning of the stimulus artifact and the middle of the primary peak, and the duration of the signal was measured as the

duration/width (ms) of the peak at 50% of the measured amplitude. All quantitative analysis was made on representative waveforms that were the average of 5 sweeps at that particular stimulus intensity (800μA for representation of data).

3.3.8 Spatial Learning and Memory Morris Water Maze Assessment

Spatial learning was assessed on days 10-13 and 28-31 in separate groups of animals in the clodronate study (Fig. 3.2B). Animals were trained over 4 days to find the location of the hidden platform submerged approximately 1cm below the surface of the water as previously described (Hanlon et al., 2016a, Hanlon et al., 2016b). On each day, animals completed 4 different trials (60s each) being released from 4 different points 90° apart around the edge of the maze (i.e. north, south, east, west). The water was kept relatively cool at 18-20°C to motivate the animals to find the platform in order to escape the swimming task. The latency to find the hidden platform was averaged across trials for each day and presented as a learning curve across 4 days. On the 5^{th} day of assessment (day 14 or day 32), the platform was removed from the pool and animals were tracked using an overhead camera and Accutrak software (AccuScan Instruments Inc, Columbus, OH) for two 60-second trials to assess time spent in zones closest (platform) or furthest (peripheral) away from the former location of the platform. Following the probe trials, animals were subjected to a visible platform trial in which the platform was placed back in the water, the water level was lowered so that the top inch of the platform was exposed, and a flag was adhered to the top of the platform. These data were analyzed in terms of latency to the platform in order to detect if the animals had any type of visual deficits.

3.3.9 Statistical Analysis

All statistics were performed using Statistica 7 (StatSoft, Tulsa OK). All data are presented as mean ± standard error of the mean. Outcome measures were compared across groups (sham-injured empty-lip, brain-injured empty-lip, sham-injured clod-lip, brain-injured clod-lip) as a function of time (when applicable) and sex (when there were adequate numbers of each sex per group) using appropriate analyses of variance (ANOVA). Outcomes only involving two groups (i.e. sham vs. injured at one time point) were analyzed using independent samples t-tests. For spatial learning and memory, injury (sham vs. injured) and treatment (empty-lip vs. clod-lip) were used as separate independent factors. When necessary, post-hoc analyses were performed using the Newman-Keuls test and a value of $p \leq 0.05$ was considered significant.

3.4 RESULTS

3.4.1 Microglia/macrophage reactivity and associated neuropathology in grey matter regions

Traumatic brain-injury in the neonate rat resulted in sustained microglia/macrophage reactivity

Iba1 labeling in the cortex of sham-injured animals (Fig. 3.3A-C) revealed microglia that demonstrated a resting phenotype (Fig. 3.3G). These cells had small cell bodies (Fig. 3.3H, black arrow) and long, elaborate processes (Fig. 3.3H, white arrows). Over time from 3 days (Fig. 3.3A) to 28 days (Fig. 3.3C), it seemed that the processes associated with these cells became longer and more complex which may suggest a developmental maturation of the microglia between post-natal day 14 (3 days post-surgery) and post-natal day 39 (28 days post-surgery). Iba1 labeling in the injured cortex of brain-injured animals (Fig. 3.3D-F) was dense and contained cells that demonstrated an activated phenotype (Fig. 3.3H). These cells had enlarged, rounded cell bodies (Fig. 3.3H, dashed outline) and very few short, thick processes (Fig. 3.3H, white arrows). These morphologic changes were observed in microglia/macrophages beginning around the anterior edge of the impact site (approximately in line with the bregma suture, Fig. 3.1B) and extending through the impact site. Reactivity in the cortex was observed in the retrosplenial cortex and in layers 2-5 of the motor and somatosensory cortices. Although the labeling was most intense at 3 days post-injury (Fig. 3.3D), evidence of cellular reactivity was still present 4 weeks after the injury (Fig. 3.3F).

Using an ED-1 antibody (CD68), we were able to specifically label activated microglia/macrophages. This antibody recognizes a lysosomal glycoprotein and its

expression levels may correlate with phagocytic activity (Damoiseaux et al., 1994). ED-1 labeling was scarcely observed in the cortex of sham-injured animals (Fig. 3.4A-C) and overlapped regionally and temporally with the observed Iba1 labeling in brain-injured animals (Fig. 3.4D-F). The activated ED-1(+) microglia exhibited two distinct phenotypes: amoeboid-shaped cells (Fig. 3.4G) and rod-shaped cells (Fig. 3.4H). The amoeboid cells were intensely labeled, rounded, and had few, if any, visible processes (Fig. 3.4G). The rod-shaped cells had an elongated, thick cell body with short, thick processes (Fig. 3.4H). Because both of these phenotypes were identified as active through ED-1 labeling, our quantitative analyses of ED-1(+) labeling will account for these morphologies separately. Microglia/macrophage reactivity (as assessed by both Iba1 and ED-1 labeling) was also present in the thalamus and hippocampus in the hemisphere ipsilateral to the injury (not shown). In the thalamus, activated cells were present in the lateral nuclei, specifically the dorsolateral thalamus and the lateral geniculate nucleus. Labeling in the hippocampus was restricted to the dorsal subiculum. Obvious increases in cellularity or morphologic activation was not observed in the hemisphere contralateral to the injury.

Microglia/macrophage reactivity was associated with Fluoro-jade B (FJB) labeling

FJB(+) cells were observed in grey matter regions (cortex, thalamus, subiculum) that also exhibited increases in microglia/macrophage reactivity indicating an association between neuronal damage and microglia/macrophage reactivity. Sham-injured animals do not exhibit any FJB(+) labeling in any region at any time post-injury (Fig. 3.5A). Labeled cells in the cortex were large and exhibited layered distribution indicative of

neurons (Fig. 3.5B-D). Evidence of neuronal degeneration was still observed out to 28 days post-injury (Fig. 3.5D). FJB labeling in the subiculum also demonstrated neuronal morphology while labeling in the thalamus was more varied and contained a mix between neuronal morphology and small, punctate profiles indicative of axonal degeneration (not shown).

Neuronal activity in the cortex within the impact site is altered at 3 days post-injury

Evoked field potential recordings were taken from layer 5 of the motor cortex at the level of bregma at 3, 7, and 21 days post-injury (Fig. 3.6). From our histologic analyses, we know that this is the approximate beginning of the rostral-caudal distribution of cellular microglia/macrophage reactivity and neurodegeneration. At 3 days post-injury, signals from brain-injured animals were visibly smaller than those from sham-injured animals (Fig. 3.6A). Quantification of the size of the signal revealed a significant effect of injury ($F_{1,28}$=18.54, $p<0.001$), time ($F_{2,28}$=12.19, $p<0.001$), and an interaction between injury and time ($F_{2,28}$=11.82, $p<0.001$, Fig. 3.6B). There was no significant interaction between injury, time, and sex ($F_{2,28}$=2.47, $p=0.10$). Post-hoc analysis of the interaction between injury and time revealed a developmental decrease in amplitude between 3, 7, and 21 days in sham-injured animals ($p<0.001$). At 3 days post-injury, brain-injured animals had significantly smaller signals compared to sham-injured animals ($p<0.001$), but this effect was transient and the signals were recovered to sham level at 7 ($p=0.32$) and 21 ($p=0.85$) days post-injury. In quantification of the latency of the signal, there was no significant interaction between injury and time ($F_{2,28}$=1.88, $p=0.17$) despite an apparent increase in the latency of the signals from brain-injured

animals at 3 days (Fig. 3.6C). There was also no significant interaction between injury, time, and sex of the animal ($F_{2,28}$=0.13, p=0.87). The duration or width of the signal was also assessed and quantification revealed a significant effect of time ($F_{2,28}$=5.91, p<0.01) that indicated that the signals were wider at 7 days compared to 3 (p<0.01) and 21 days (p<0.05) irrespective of injury status (Fig. 3.6D). There was no significant interaction between injury and time ($F_{2,28}$=1.84, p=0.18) or between injury, time, and sex ($F_{2,28}$=1.86, p=0.17).

Further within the impact site, approximately 3mm behind bregma, evoked field potentials were recorded from the motor cortex (Fig. 3.7). This area demonstrated heavy microglia/macrophage reactivity and neurodegeneration. Interestingly, signals from brain-injured animals did not appear to differ from sham-injured animals (Fig. 3.7A). Quantification of the amplitude of the signals revealed a significant effect of time ($F_{2,24}$=5.24, p<0.05) that indicated a developmental decrease in the size of the signals between 3 and 21 days (p<0.05) irrespective of injury status (Fig. 3.7B). There was no significant interaction between injury and time ($F_{2,24}$=0.23, p=0.80) or between injury, time, and sex ($F_{2,24}$=0.37, p=0.70). Assessment of the latency of the signal also demonstrated no significant interactions ($F_{2,24}$=0.91, p=0.42, Fig 3.7C). Quantification of the duration of the signal revealed a significant interaction between injury, time, and sex ($F_{2,24}$=4.41, p<0.02), but post hoc analysis revealed no significant effects (Fig. 3.7D).

3.4.2 Microglia/macrophage reactivity and white matter pathology

Microglia/macrophage reactivity was sustained in the white matter up to 28 days post-injury

ED-1(+) microglia/macrophages were observed in the white matter in both sham-injured (Fig. 3.8A-C) and brain-injured animals (Fig. 3.8D-F). ED-1(+) microglia/macrophages were distributed throughout the white matter in both hemispheres in sham-injured animals at 3 days post-surgery (PND14, Fig. 3.8A), but their presence was minimal by 28 days post-surgery (PND39, Fig. 3.8C). In brain-injured animals, activated microglia/macrophages were present in the corpus callosum, cingulum, and lateral white matter tracts at 3 (Fig. 3.8D), 15 (Fig. 3.8E), and 28 (Fig. 3.8F) days post-injury. Both amoeboid and rod phenotypes were observed.

Microglia/macrophage reactivity in the white matter was associated with axonal degeneration and axonal injury

Sham-injured animals demonstrated no evidence of FJB labeling in the white matter (Fig. 3.9A), but FJB(+) profiles were observed in the white matter of brain-injured animals (Fig. 3.9B-D). Labeling in the white matter was diffuse and the labeled profiles were small and punctate indicative of axonal segments (Tong et al., 2002, Huh et al., 2008). FJB(+) profiles were heavily evident at 3 (Fig. 3.9B) and 15 (Fig. 3.9C) days post-injury, but were not as apparent 4 weeks post-injury (Fig. 3.9D) despite the fact that microglia/macrophage activation is still observed at this time point (Fig. 3.8F). Accumulation of amyloid precursor protein (APP) was apparent at 3 days post-injury in the corpus callosum, cingulum, and lateral white matter tracts where there was also evidence of axonal degeneration and microglia/macrophage reactivity (Fig. 3.9F). Sham-injured animals do not exhibit any evidence of APP labeling (Fig. 3.9E).

Axonal conduction deficits were observed in the corpus callosum of brain-injured animals

In addition to the observed axonal degeneration and axonal injury, we have previously reported that injury to the PND11 rat results in progressive atrophy of the white matter tracts (Raghupathi and Huh, 2007). Axonal conduction was assessed in the injured corpus callosum at 1 day (prior to white matter atrophy) and 14 days post-injury (Fig. 3.10). At 1 day post-surgery (PND12) sham-injured animals demonstrated large deflections indicative of strong signaling from both the myelinated (N1) and unmyelinated (N2) axons in the fiber tract (Fig. 3.10A). Signals from brain-injured animals at 1 day post-injury were obviously smaller than those from sham-injured animals (Fig. 3.10A). Separate repeated measures ANOVAs analyzing the amplitudes of the myelinated (N1) and unmyelinated components over 5 current steps revealed significant effects of injury (N1: $F_{1,32}=14.77$, $p<0.01$; N2: $F_{1,32}=9.65$, $p<0.05$), current step (N1: $F_{4,32}=28.95$, $p<0.001$, N2: $F_{4,32}=29.34$, $p<0.001$), and an interaction between injury and current step (N1: $F_{4,32}=5.99$, $p<0.01$; N2: $F_{4,32}=4.56$, $p<0.01$, Fig. 3.10B,C). Post hoc analysis revealed that both the myelinated (Fig. 3.10B) and unmyelinated (Fig. 3.10C) portions of the signal from brain-injured animals was significantly smaller than sham-injured animals irrespective of current injection ($p<0.05$). At 14 days post-injury, brain-injured animals demonstrated smaller signaling from myelinated fibers (N1), but did not seem to be deficient in signaling from the unmyelinated fibers (N2) (Fig. 3.10D). Assessment of the amplitude of the signals from the myelinated component revealed significant effects of injury ($F_{1,28}=8.85$, $p<0.05$), current step ($F_{4,28}=25.54$, $p<0.001$), and an interaction between injury and current step ($F_{4,28}=4.04$, $p<0.05$) that indicated that

brain-injured animals were still deficient in signaling from myelinated fibers at 14 days post-injury ($p<0.05$, Fig. 3.10E). The deficit in the signaling from the unmyelinated fibers observed at 24 hours post-injury, however, was recovered by 14 days (injury: $F_{1,28}=0.22$, $p=0.66$; current step: $F_{4,28}=18.79$, $p<0.001$; injury x current step: $F_{4,28}=0.99$, $p=0.43$, Fig. 3.10F). There were no differences in conduction velocity for either component at either time point (24 hours: N1, $t(9)=0.77$; $p=0.46$, N2, $t(9)=0.78$; $p=0.45$; 14 days: N1, $t(7)=-0.01$; $p=0.99$, N2, $t(7)=-0.04$; $p=0.97$; Fig. 3.10G).

Brain-injured animals demonstrated deficits in axonal transport 2 weeks after injury

Axonal transport was assessed by injecting a retrograde tracer (Fluoro-Gold) into the left hemisphere of sham-injured and brain-injured animals at 14 days post-injury (Fig. 3.11). Despite the fact that there is evidence of FJB(+) cells in the cortex at this time, uptake of the tracer was similar in the injected cortex between brain-injured (Fig. 3.11B) and sham-injured animals (Fig. 3.11A). Labeled cells were present in the cortex contralateral to the injection 5 days post-injection (Fig. 3.11C,D). Sham-injured animals demonstrated heavy labeling indicating strong transport of the tracer (Fig. 3.11C). While there were labeled cells in the contralateral cortex of brain-injured animals, the transport did not seem to be as efficient compared to the sham-injured animals (Fig. 3.11D) This observation was confirmed by quantification as brain-injured animals had significantly fewer labeled cells in the contralateral cortex compared to sham-injured animals ($t(5)=-4.73$; $p<0.01$).

3.4.3 Clodronate-mediated microglia/macrophage depletion in the cortex

Depletion and repopulation of Iba1(+) and ED-1(+) microglia/macrophages in the cortex

Sham-injured (Fig. 3.12A-C) and brain-injured (Fig. 3.12D-F) animals that received the empty liposomes demonstrated typical labeling and reactivity. At 3 days post-injury, sham-injured animals (Fig. 3.12G) and brain-injured animals (Fig. 3.12J) that received the clodronate liposomes demonstrated very few labeled microglia/macrophages in the cortex around the site of injection. By 15 days post-injury, however, labeling in sham-injured animals appeared normal. While microglia/macrophages were appearing in the cortex of brain-injured clod-lip animals at 15 days post-injury, the total number still seemed decreased compared to brain-injured animals that received the empty liposomes and the microglia/macrophages demonstrated an interesting rod-like phenotype (Fig. 3.12K). By 35 days, the brain-injured animals that were injected with clodronate seemed to demonstrate a higher level of morphologically "active" microglia/macrophages (Fig. 3.12L). Assessment of total Iba1(+) microglia/macrophages in the cortex at 15 and 35 days revealed significant effects of status ($F_{3,26}$=33.02, $p<0.001$), time ($F_{1,26}$=87.73, $p<0.001$), and an interaction between status and time ($F_{3,26}$=7.61, $p<0.001$, Fig. 3.12M). Post hoc analysis revealed that brain-injured animals that received the empty liposomes had significantly more Iba1(+) microglia/macrophages in the cortex compared to their corresponding sham-injured group and the brain-injured animals that received the clodronate at both 15 and 35 days ($p<0.05$). Sham-injured animals that received the clodronate did not differ from those that received the empty liposomes at either 15 ($p=0.73$) or 35 days ($p=0.56$). Similarly, the total number of microglia/macrophages in the cortex of brain-injured animals that received clodronate did not differ from the total

number in the corresponding sham group at either time point (15d, p=0.93; 35d, p=0.06). There was no significant interaction between status, time, and sex ($F_{3,26}$=0.34, p=0.80).

With the appearance of the rod-shaped microglia/macrophages in brain-injured animals that received the clodronate at 15 days post-injury (Fig. 3.12K) and the apparent increase in activated cells at 35 days post-injury (Fig. 3.12L), we evaluated microglia/macrophage activation following clodronate depletion using ED-1 labeling (Fig. 3.13). Sham-injured animals that received the empty liposomes demonstrated activated microglia/macrophages in the cortex, but this was restricted to the area of injection at 3 days post-injury (Fig. 3.13A) and dissipated over time (Fig. 3.13B,C). Brain-injured animals that received the empty liposomes demonstrated typical cortical labeling (Fig. 3.13D-F). Sham-injured animals injected with the clodronate demonstrated very little labeling across all three time points (Fig. 3.13G-I). Brain-injured animals that received the clodronate had few labeled cells in the cortex at 3 days post-injury (Fig. 3.13J), demonstrated an increase in rod-shaped microglia/macrophages at 15 days post-injury (Fig. 3.13K), and seemed to have an increase in total labeling at 35 days post-injury (Fig. 3.13L). Quantification of amoeboid-shaped microglia/macrophages revealed a significant effect of status ($F_{3,34}$=18.89, p<0.001), time ($F_{2,34}$=4.53, p<0.05), and an interaction effect between status and time ($F_{6,34}$=7.81, p<0.001, Fig. 3.13M). Brain-injured animals treated with the empty liposomes had significantly higher numbers of amoeboid microglia/macrophages at 3 days compared to the corresponding sham-injured group (p<0.001) and the brain-injured animals that received the clodronate (p<0.001). These effects were not sustained to 15 and 35 days post-injury. There was no difference in the numbers of amoeboid microglia/macrophages in the cortex of sham-injured

animals at any time point. Interestingly, at 35 days post-injury, brain-injured animals that had sustained acute microglia/macrophage depletion demonstrated a significant increase in the number of activated amoeboid-shaped microglia/macrophages in the cortex compared to the corresponding sham-injured group ($p<0.01$) and brain-injured animals that received the empty liposomes ($p<0.05$) indicating a rebound effect in microglia/macrophage activation following acute depletion. Quantification of rod-shaped microglia/macrophages showed a significant effect of status ($F_{3,34}=6.70$, $p<0.01$) and an interaction between status and time ($F_{6,34}=4.71$, $p<0.01$, Fig. 3.13M). Post hoc analysis revealed mild effects with brain-injured animals that received the empty liposomes demonstrating a significant increase in rod-shaped microglia/macrophages at 3 days post-injury compared to sham-injured animals ($p<0.01$), but this effect was not sustained to 15 or 35 days post-injury. Additionally, starting at 15 days post-injury, there seemed to be an increase in rod-shaped cells in brain-injured animals that received the clodronate, but these counts did not reach significance compared to the corresponding sham-injured group ($p=0.10$) or the brain-injured animals that received the vehicle ($p=0.13$). There was no significant interaction between status, time, and sex for either amoeboid ($F_{6,34}=0.16$, $p=0.98$) or rod ($F_{6,34}=0.80$, $p=0.57$) microglia/macrophages.

Effect of clodronate administration on GFAP(+) astrocytic reactivity in the cortex

Brain-injured animals that received the empty liposomes showed a visible increase in GFAP immunoreactivity in cortex at 3 days post-injury (Fig. 3.14B). Animals treated with clodronate, however, seemed to show a decrease in the density of astrocytes in the cortex regardless of injury status (Fig. 3.14C,D). This was confirmed by a

thresholding analysis to assess the percentage of the cortex that exhibited GFAP(+) immunoreactivity. A one-way ANOVA revealed a significant effect of status ($F_{3,12}$=28.89, p<0.001, Fig. 3.14E) that indicated that brain-injured animals that received the empty liposomes had increased astrocytic reactivity compared to the corresponding sham-injured animals (p<0.01). Sham-injured animals that received the clodronate showed a significant decrease in GFAP immunoreactivity compared to sham-injured animals that received the empty liposomes (p<0.05). Similarly, brain-injured animals treated with clodronate had a significantly decreased percent area of labeling compared to brain-injured empty-lip animals (p<0.001) and there was no difference in reactivity between sham-injured and brain-injured clod-lip animals (p=0.72).

Effect of microglia/macrophage depletion on neurodegeneration in the cortex

Sham-injured animals were assessed for FJB(+) reactivity as they demonstrated evidence of labeling around the sites of injection at 3 days post-injury (Fig. 3.15A,G) but the appearance of FJB(+) profiles in sham-injured animals dissipated over time (Fig. 3.15B,C,H,I). Brain-injured animals treated with clodronate (Fig. 3.15J-L) demonstrated visible increases in FJB(+) labeling in the cortex at all time points compared to sham-injured animals and those that received the empty liposomes (Fig. 3.15D-F). Quantification revealed a significant effect of status ($F_{3,35}$=61.91, p<0.001, Fig. 3.15M) that indicated that brain-injured animals treated with clodronate had significantly increased numbers of FJB(+) profiles in the cortex compared to the corresponding sham-injured animals (p<0.001) and brain-injured empty-lip animals (p<0.01) regardless of time post-injury. Importantly, there was no difference in FJB labeling between sham-

injured animals (p=0.30). There was no interaction between status, time, and sex ($F_{3,35}$=0.56, p=0.76).

Effect of acute microglia/macrophage depletion on neuronal activity in the chronic post-injury period

Cortical activity at the bregma level did not show any differences between sham- and brain-injured animals at 21 days post-injury (Fig. 3.6) and this lack of difference was confirmed at 4 weeks post-injury (Fig. 3.16). Additionally, acute clodronate administration did not affect activity in this region as there were no significant effects of status for measurement of amplitude ($F_{3,24}$=0.41, p=0.75, Fig. 3.16A), latency ($F_{3,24}$=0.84, p=0.49, Fig. 3.16B), or duration ($F_{3,24}$=0.25, p=0.86, Fig. 3.16C) of the signals. Additionally, there were no interactions between status and sex for any measure (amplitude: $F_{3,24}$=0.76, p=0.53; latency: $F_{3,24}$=0.89, p=0.46; duration: $F_{3,24}$=1.55, p=0.23). Further into the impact site, at -3mm behind bregma, signals from brain-injured animals that received clodronate appeared much larger than those from sham-injured animals or brain-injured animals that received the empty liposomes (Fig. 3.17A). Quantification of the amplitude of signal revealed a significant effect of status ($F_{3,24}$=3.45, p<0.05, Fig. 3.17B) that confirmed this observation as the signals from brain-injured clod-lip animals were significantly larger than those from sham-injured clod-lip animals (p<0.05) and brain-injured clod-lip animals (p<0.05). There were no differences in the amplitude of the signals from sham-injured animals (p=0.90) or between sham-injured empty-lip and brain-injured empty-lip animals (p=0.53). Analysis of the amplitude of signal showed a significant effect of status ($F_{3,24}$=4.71, p<0.05, Fig. 3.17C) that interestingly indicated

that signals from brain-injured animals treated with the empty liposomes were faster than the signals from the corresponding sham-injured animals ($p<0.05$). This observation was not extended to sham- and brain-injured animals that received the clodronate ($p=0.12$). There were no differences in the duration of the signals ($F_{3,24}=1.41$, $p=0.27$, Fig. 3.17D) and no interactions between status and sex for any measure (amplitude: $F_{3,24}=0.39$, $p=0.76$; latency: $F_{3,24}=1.23$, $p=0.32$; duration: $F_{3,24}=0.69$, $p=0.56$).

3.4.4 Clodronate-mediated microglia/macrophage depletion in the white matter

Clodronate was injected into the deeper layers of the cortex so that diffusion of the substance would also target the subcortical white matter. Both sham-injured and brain-injured animals injected with clodronate demonstrated severe depletion in the corpus callosum, cingulum, and lateral white matter at 3 days post-injury (Fig. 3.18C,D). Quantification of Iba1 immunoreactivity in the white matter at 15 and 35 days revealed a significant interaction between status and time ($F_{3,26}=15.10$, $p<0.001$, Fig. 3.18E) that indicated that brain-injured empty-lip animals had a significantly higher percentage of labeled white matter compared to sham-injured empty lip animals at 15 ($p<0.001$) and still demonstrated a mild increase at 35 days ($p=0.06$). Brain-injured empty lip animals also demonstrated significantly higher levels of Iba1 immunoreactivity in the white matter compared to brain-injured clod-lip animals at 15 days ($p<0.001$) but this effect was not sustained out to 35 days ($p=0.53$). There was no interaction between status and sex ($F_{3,26}=0.87$, $p=0.47$).

Sham-injured animals demonstrated a small amount of APP immunoreactivity in the white matter at 3 days post-injury due to the intracerebral injection (Fig. 3.18F,H).

Brain-injured animals demonstrated robust APP labeling in the white matter irrespective of microglia/macrophage depletion (Fig. 3.18G,I). Grid analysis quantification of APP labeling revealed a significant effect of status ($F_{3,14}$=59.64, p<0.001, Fig. 3.18J) that indicated that brain-injured animals had more APP labeling compared to sham-injured animals regardless of treatment (p<0.001), but that there were no differences between sham-injured (p=0.15) and brain-injured groups (p=0.57). While depletion of microglia/macrophages in the white matter did not affect axonal injury, it had a significant effect on FJB(+) labeling in the white matter (Fig. 3.18K). Quantification of the number of FJB(+) profiles in the white matter revealed a significant effect of status ($F_{3,25}$=14.70, p<0.001, Fig. 3.18K) that indicated that brain-injured animals treated with clodronate had significantly more FJB(+) profiles compared to sham-injured clod-lip animals (p<0.001) and brain-injured empty-lip animals (p<0.001). There was no significant interaction between status, time, and sex ($F_{3,25}$=0.60, p=0.62). Additionally, there was no difference compound action potential electrophysiology between brain-injured empty-lip and brain-injured clod-lip animals at 7 days post-injury (Fig. 3.18L). Analysis of the signals revealed no significant difference in the size of the myelinated (N1) and unmyelinated (N2) components of the signal (N1: t(5)=1.48, p=0.20; N2: t(5)=1.43, p=0.21).

3.4.5 Clodronate-mediated microglia/macrophage depletion in the thalamus

Similar to the cortex, Iba1(+) and ED-1(+) microglia/macrophages were effectively depleted in the thalamus of both sham-injured and brain-injured animals at 3 days post-injury (images not shown). Analysis of total Iba1(+) microglia/macrophages at

15 and 35 days revealed a significant interaction between status and time ($F_{3,26}$=2.94, p≤0.05, Fig. 3.19A) that indicated that brain-injured empty-lip animals had significantly more microglia/macrophages in the thalamus compared to sham-injured empty lip and brain-injured clod-lip animals at both 15 (p<0.001) and 35 days (p<0.05) post-injury. There was no difference between sham-groups and either time point (15d: p=0.82, 35d: p=0.64) and the number of microglia/macrophages in the thalamus of brain-injured clod-lip animals was back to sham level at 15 days post-injury (p=0.89). Quantification of ED-1-labeled amoeboid microglia/macrophages in the thalamus also revealed a significant interaction effect between status and time ($F_{6,34}$=11.94, p<0.001, Fig. 3.19B). Post-hoc revealed a significant effect of injury on amoeboid microglia/macrophages as brain-injured empty-lip animals had significantly more amoeboid microglia/macrophages compared to sham-injured empty-lip animals at 3 and 15 days post-injury (p<0.001). This effect, however, was lost by 35 days (p=0.73). Brain-injured clod-lip animals had significantly fewer amoeboid microglia/macrophages than brain-injured empty-lip animals at 3 days post-injury (p<0.001) but this effect was not present at 15 days (p=0.10) and was reversed at 35 days with brain-injured clod-lip animals having significantly more amoeboid microglia/macrophages in the thalamus compared to both sham-injured clod-lip animals (p<0.01) and brain-injured empty-lip (p<0.05). Quantification of rod microglia/macrophages also revealed a significant interaction between status and time ($F_{6,34}$=7.06, p<0.001, 3.19B), but this effect only indicated that brain-injured animals that received the empty liposomes had significantly more rod microglia/macrophages compared to sham-injured animals and did not show a significant increase in rod microglia/macrophages in the brain-injured clod-lip animals over time.

Additionally there was no effect of sex on Iba1 labeling ($F_{3,26}$=0.80, p=0.51), ED-1(+) amoeboid microglia/macrophages ($F_{6,34}$=0.45, p=0.84) or ED-1(+) rod microglia/macrophages ($F_{6,34}$=0.16, p=0.99).

Fluoro-jade B labeling in the thalamus was significantly increased in brain-injured animals that sustained acute microglia/macrophage depletion. A significant interaction between status and time ($F_{6,35}$=5.54, p<0.001, Fig. 3.19C) revealed that brain-injured animals that received clodronate had significantly more FJB(+) profiles in the thalamus than both the corresponding sham group and brain-injured empty-lip animals at all times post-injury (p<0.05). There were no differences between sham-injured animals at any time point and brain-injured empty lip animals demonstrated a significant increase in FJB(+) profiles compared to the corresponding sham group at 3 and 15 days post-injury (p<0.001) that was reduced to only a mild increase at 35 days (p=0.06). There was no effect of sex on FJB labeling in the thalamus ($F_{6,35}$=1.47, p=0.22). Despite a decrease in activated microglia/macrophages and an increase in FJB labeling in the thalamus of brain-injured clod-lip animals at 3 days post-injury, there was no difference in axonal injury present in the thalamus. A significant effect of status ($F_{3,14}$=35.44, p<0.001, Fig. 3.19D) revealed that both brain-injured groups had significantly more APP(+) labeling in the thalamus compared to sham-injured animals (p<0.001), but there was no effect of clodronate administration (p=0.88).

3.4.6 Clodronate-mediated microglia/macrophage depletion in the subiculum

Through diffusion of the compound from the thalamic injection, we were able to also decrease microglia/macrophages in the subiculum of the hippocampus (Fig.

3.20A,C). Quantification of Iba1(+) microglia/macrophages in the subiculum at 15 and 35 days post-injury revealed a significant interaction effect between status and time ($F_{3,26}$=14.00, p<0.001, Fig. 3.20A) that indicated that brain-injured animals that received the empty lip had significantly more Iba1(+) microglia/macrophages than both sham-injured animals and brain-injured clod-lip animals at 15 days post-injury, but there was no differences between any groups at 35 days post-injury. Like in the cortex and thalamus, the total number of microglia/macrophages in the subiculum was back to sham level in brain-injured animals that received the clodronate by 15 days post-injury. Significant interactions between status and time were observed for amoeboid ($F_{6,33}$=8.48, p<0.001) and rod ($F_{6,33}$=4.97, p<0.01, Fig. 3.20C) microglia/macrophages in the subiculum. Post hoc analysis revealed that, similar to the cortex and thalamus, amoeboid microglia/macrophages were significantly increased in the subiculum at 35 days post-injury compared to sham-injured and brain-injured empty-lip animals (p<0.001). This effect, however, may be due to sex as an interaction between status, time, and sex ($F_{6,33}$=3.71, p<0.01) revealed that brain-injured clod-lip females had significantly more amoeboid microglia/macrophages in the subiculum than all other groups at 35 days post-injury. The only significant effect on rod microglia/macrophages in the subiculum occurred at 3 days post-injury as brain-injured animals that received the empty liposomes had significantly more rod microglia/macrophages in the subiculum compared to both sham-injured and brain-injured animals that received the clodronate (p<0.05). There was no effect of sex on Iba1 immunoreactivity ($F_{3.26}$=0.98, p=0.42) or ED-1(+) rod microglia/macrophages ($F_{6,33}$=0.31, p=0.93) in the subiculum.

Like in the cortex and thalamus, FJB reactivity was increased in the subiculum of brain-injured animals that received the clodronate at 3, 15, and 35 days post-injury (Fig 3.20B). This was confirmed by a significant effect of status ($F_{3.36}$=29.13, p<0.001) that indicated that brain-injured animals that received the empty liposomes had significantly more FJB(+) profiles in the subiculum compared to the corresponding empty-lip sham-injured group (p<0.01), but that brain-injured animals that received the clodronate had significantly more FJB(+) profiles than both the corresponding clod-lip sham-injured group (p<0.001) and the empty-lip brain-injured group (p<0.001) irrespective of time post-injury. There was no effect of sex on FJB reactivity in the subiculum ($F_{3.36}$=0.95, p=0.47).

3.4.7 Effect of microglia/macrophage depletion on injury-induced spatial learning and memory impairment

Spatial learning and memory was assessed in separate groups of animals on post-injury days 10-14 (Fig. 3.21A,B) and 28-32 (Fig. 3.21C,D). On days 10-14 sham-injured animals that received the empty liposomes performed much like what we've observed in the previous use of this test (Raghupathi & Huh, 2007). Sham-injured animals that received the clodronate, however, seemed to be performing similarly to the brain-injured empty-lip animals and brain-injured animals that received the clodronate seemed to be performing slightly worse than both the clod-lip shams-injured animals and the brain-injured empty-lip animals. These differences, however, were subtle and there was no significant effect of injury or treatment on spatial learning ($F_{1,51}$=2.22, p=0.15; $F_{1,51}$=2.67, p=0.12 , Fig. 3.21A). In the probe trial, brain-injured animals spent more time in the

peripheral zone furthest away from the platform compared to sham-injured animals irrespective of treatment, but this effect did not reach full significance ($F_{1,17}$=4.01, p=0.06, Fig. 3.21B). Brain-injured animals did, however, spend significantly less time in the platform zone compared to sham-injured animals ($F_{1,17}$=4.67, p<0.05) and there was no significant effect of injury or treatment on performance in the visible platform trial ($F_{1,17}$=0.002, p=0.97). When animals were assessed on post-injury days 28-32, brain-injured animals were significantly impaired in their ability to locate the hidden platform compared to sham-injured animals irrespective of treatment ($F_{1,45}$=8.59, p<0.05, Fig. 3.21C). There was no effect of clodronate administration on spatial learning at this time point. In the probe trial, there was no effect of injury or treatment on the amount of time spent in the peripheral zones ($F_{1,15}$=0.09, p=0.76, Fig. 3.21D), but brain-injured animals spent less time in the platform zone than sham-injured animals ($F_{1,15}$=4.67, p<0.05) indicating a retention deficit irrespective of clodronate administration. There was no effect of injury or treatment on the visible platform trial ($F_{1,15}$=2.02, p=0.18).

3.5 DISCUSSION

Following closed head injury to the neonate rat, microglia/macrophage reactivity was observed as a function of increased cellularity and morphologic transformation in the cortex, thalamus, subiculum, and white matter of brain-injured rats. Microglia/macrophage reactivity closely associated with neurodegeneration, axonal degeneration, and evidence of axonal injury. While we hypothesized that microglia/macrophage depletion would ameliorate neuropathology and functional deficits, we discovered that the loss of microglia/macrophages around the time of injury actually caused a sustained exacerbation of neuropathology that included increased microglia/macrophage activation in the chronic post-injury period. This increase in neuropathology altered neuronal activity, but did not affect spatial learning and memory ability.

The temporal and regional similarities between microglia/macrophage reactivity and neurodegeneration and axonal injury suggest that microglia/macrophages are involved in these processes. Microglia have been shown to associate with apoptotic cells during development and closely associate with fluoro-jade B labeling in a model of contusive injury to the PND21 mouse (Pont-Lezica, et al., 2001; Tong et al., 2002). It is unclear, however, whether microglia/macrophages actively perpetuate cell death and axonal injury or whether they are simply activated in those regions in order to clear out the damaged cells. There is evidence to suggest that microglia initially become activated in response to neuronal damage, but can then remain activated and perpetuate further damage through the release of toxic mediators (Loane and Kumar, 2016).

In the white matter, microglia play a role in providing trophic support to oligodendrocyte precursor cells to aid them through differentiation into a mature myelinating oligodendrocyte and therefore these cells share a very close spatial relationship (Domingues et al., 2016). When activated by an insult, both microglia and astrocytes can inhibit this maturation thus causing oligodendrocyte damage and myelination deficits (Peferoen et al., 2014, Domingues et al., 2016). Oligodendrocyte death has been observed following TBI in the adult rat and HI injury in the neonate rat (Liu et al., 2002, Lotocki et al., 2011). It is possible that the fluoro-jade B labeling we observed in the white matter may be indicative of both axonal fragments and dying oligodendrocytes. Labeling specifically for oligodendrocytes, oligodendrocyte precursor cells, and myelin basic protein will allow us to elucidate a stronger spatial and temporal relationship between microglial activation and oligodendrocyte damage.

This study suggests that removal of microglia/macrophages around the time of the injury is actually deleterious to the immature brain as clodronate administration resulted in a severe and sustained increase in neurodegeneration. The increase in FJB(+) profiles observed at 3 days post-injury following microglia/macrophage depletion may be indicative of a lack of phagocytosis of damaged cells following injury. In the chronic post-injury period, however, brain-injured animals that received clodronate exhibited increased microglia/macrophage activation associated with increased degeneration in several brain regions suggesting this secondary wave of activation may play an active role in the observed degeneration. This is supported by the fact that neuronal activity was altered in brain-injured animals that received the clodronate. In brain-injured animals that did not undergo microglia/macrophage depletion, neuronal activity was not altered in

the hindlimb region of the motor cortex at 4 weeks post-injury despite the sustained presence of injury-induced neurodegeneration. When neurodegeneration and microglia/macrophage reactivity were increased in this region, the signals showed evidence of hyperactivity indicating dysfunction of neuronal circuitry and deleterious effects of acute microglia/macrophage depletion in the developing brain.

While the number of total Iba1(+) microglia/macrophages returned to sham-injury level by 2 weeks post-injury, the repopulated microglia/macrophages in brain-injured animals demonstrated a rod-like phenotype. Rod-like microglia/macrophages have been observed following TBI in the adult rat and our current study has identified that these microglia/macrophages are an activated phenotype as evident by ED-1 immunoreactivity, but it is unclear whether or not they play a specific role in post-injury pathology (Taylor et al., 2014). There is some evidence to suggest that rod-like microglia are highly proliferative and can rapidly transformation to amoeboid shape (Tam and Ma, 2014). It is possible that the increase in rod-like microglia/macrophages in clodronate-treated brain-injured animals is indicative of microglia/macrophage proliferation and some of these rod-like cells go on to become amoeboid-shaped microglia/macrophages at 35 days post-injury.

While acute microglia/macrophage depletion did increase FJB(+) labeling in the white matter at 15 and 35 days post-injury, this was not associated with a simultaneous increase in microglia/macrophage reactivity suggesting a different mechanism. As indicated with the original time course, more study into the specific effect of microglial depletion on oligodendrocytes is necessary, especially with the increase in FJB(+) profiles observed in the white matter in the chronic post-injury period. Axonal injury and

axonal conduction were unaffected by treatment with clodronate. These results support published observations using inducible microglial depletion in a model of repetitive TBI in adult mice. Brain-injured animals in which microglia were genetically depleted did not show any alterations in silver staining, APP accumulation, or neurofilament labeling in the white matter compared to brain-injured animals containing intact microglia (Bennett and Brody, 2014).

There are two published studies that detail the use of clodronate-mediated microglial depletion in the brain following an insult (Faustino et al., 2011, Drabek et al., 2012). In a model of hypothermic cardiac arrest in adult rats, clodronate administration effectively decreased the number of microglia in the hippocampus of injured rats, but did not result in amelioration of cell death (Drabek et al., 2012). Clodronate-mediated depletion exacerbated lesion size following stroke in the neonatal rat (Faustino et al., 2011) emphasizing the importance of microglia in response to injury to the developing brain. In the present study, we also demonstrated that clodronate is not specific to microglia/macrophages in the brain. Clodronate administration resulted in a decrease in the density of astrocytes in the cortex in both sham- and brain-injured animals. In culture, liposomal clodronate was effective in removing microglia without affecting astrocytes (Kumamaru et al., 2012). Additionally, GFAP-labeled astrocytes in the brain did not take up fluorescently-tagged empty liposomes (Faustino et al., 2011). The fact that clodronate affected astrocytes in our study makes separating the role of microglia/macrophages and astrocytes in post-injury pathology difficult as it has been shown that depletion of astrocytes can also result in neuronal damage (Lima et al., 2014). Also, the whole-cell depletion of microglia/macrophages may be too harsh of a

manipulation in the developing brain and a more targeted approach (such as utilizing anti-inflammatory drugs) may be more effective in ameliorating post-injury pathology.

3.6 FIGURE LEGENDS

Figure 3.1 Controlled cortical impact injury device. Image of the controlled cortical impact device (A) depicting the convex-shaped silicone impactor tip (inset). Photo of a 14-day-old rat brain overlaid with a 5mm circle depicting the region of direct impact (B).

Figure 3.2 Experimental Timeline. Timeline for the time course **(A)** and clodronate studies **(B)**.

Figure 3.3 Iba1-labeled microglia/macrophages in the cortex. Representative photomicrographs of Iba1(+) microglia/macrophages in the cortex of sham-injured **(A-C)** and brain-injured **(D-F)** animals at 3 **(A,D)**, 15 **(B,E)**, and 28 **(C,F)** days post-injury. Representative photomicrograph s of a resting microglia/macrophage characterized by a thin cell body and long, elaborate processes **(G)** and an activated microglia/macrophage characterized by an enlarged cell body with few short, thick processes **(H)**. Scale bar **(F)** = 100 μm, scale bar **(H)** = 10 μm,

Figure 3.4 ED-1-labeled microglia/macrophages in the cortex. Representative photomicrographs of activated ED-1(+) microglia/macrophages in the cortex of sham-injured **(A-C)** and brain-injured **(D-F)** animals at 3 **(A,D)**, 15 **(B,E)**, and 28 **(C,F)** days post-injury. Representative photomicrographs of an amoeboid microglia/macrophage characterized by a round cell body and few, if any, visible processes **(G)** and a rod microglia/macrophage characterized by an elongated, thick cell body and short processes **(H)**. Scale bar **(F)** = 100 μm, scale bar **(H)** = 10 μm,

Figure 3.5 Time course of neurodegeneration in the cortex. Representative photomicrograph depicting no positive labeling in the cortex of sham-injured animals **(A)**. Representative photomicrographs of FJB(+) profiles in the cortex of brain-injured animals at 3 **(B)**, 15 **(C)**, and 28 **(D)** days post-injury. Scale bar **(F)** = 100 μm.

Figure 3.6 Evoked field potential recordings from the injured cortex at bregma. Representative traces from the bregma-level cortex of sham-injured and brain-injured animals at 3 days post-injury **(A)**. Quantification of signal amplitude **(B)**, signal latency **(C)**, and signal duration **(D)** in the bregma-level cortex at 3, 7, and 21 days post-injury. Error bars represent the standard error of the mean. *$p \leq 0.05$ compared to corresponding sham-injured group.

Figure 3.7 Evoked field potential recordings from the injured cortex 3mm posterior to bregma. Representative traces from the -3mm cortex of sham-injured and brain-injured animals at 3 days post-injury **(A)**. Quantification of signal amplitude **(B)**, signal latency **(C)**, and signal duration **(D)** in the bregma-level cortex at 3, 7, and 21 days post-injury. Error bars represent the standard error of the mean.

Figure 3.8 ED-1-labeled microglia/macrophages in the white matter. Representative photomicrographs of activated ED-1(+) microglia/macrophages in the white matter of sham-injured **(A-C)** and brain-injured **(D-F)** animals at 3 **(A,D)**, 15 **(B,E)**, and 28 **(C,F)** days post-injury. **(F)** = 100 μm, scale bar.

Figure 3.9 Time course of neurodegeneration in the white matter. Representative photomicrograph depicting no positive labeling in the white matter of sham-injured animals **(A)**. Representative photomicrographs of FJB(+) profiles in the white matter of brain-injured animals at 3 **(B)**, 15 **(C)**, and 28 **(D)** days post-injury. Representative photomicrographs of APP labeling in the white matter of sham-injured **(E)** and brain-injured **(F)** animals at 3 days post-injury. Scale bar **(D,F)** = 100 μm.

Figure 3.10 Compound action potential electrophysiology in the corpus callosum. Representative traces from the corpus callosum of sham-injured and brain-injured animals 24 hours post-injury **(A)**. Quantification of the amplitude of the myelinated (N1) portion of the signal **(B)** and the unmyelinated portion (N2) of the signal **(C)** at 24 hours post-injury across five 200 μA current steps. Representative traces from the corpus callosum of sham-injured and brain-injured animals 14 days post-injury **(D)**. Quantification of the amplitude of the myelinated (N1) portion of the signal **(E)** and the unmyelinated portion (N2) of the signal **(F)** at 14 days post-injury across five 200 μA current steps. Quantification of the conduction velocity for signals from the myelinated and unmyelinated axons in the fiber track at 24 hours and 14 days post-injury **(G)**. Error bars represent the standard error of the mean. *$p \leq 0.05$ compared to corresponding sham-injured group.

Figure 3.11 Transport of Fluoro-Gold across the corpus callosum at 14 days post-injury. Representative photomicrographs of the injection site in the left cortex of sham-

injured **(A)** and brain-injured **(B)** animals and FG(+) profiles in the cortex contralateral to the injection (right cortex) of sham-injured **(C)** and brain-injured **(D)** animals. Quantification of FG(+) profiles in the right cortex **(E)**. *p≤0.05 compared to corresponding sham-injured group. Error bars represent the standard error of the mean. Scale bar **(B)** = 200 μm, scale bar **(D)** = 100 μm.

Figure 3.12 Iba1(+) microglia/macrophages in the cortex following clodronate-mediated depletion.

Representative photomicrographs of sham-injured **(A-C)** and brain-injured **(D-F)** animals injected with the empty liposomes and sham-injured **(G-I)** and brain-injured **(J-L)** animals treated with the clodronate liposomes at 3 **(A,D,G,J)**, 15 **(B,E,H,K)**, and 35 **(C,F,I,L)** days post-injury. Quantification of total Iba1(+) microglia/macrophages in the cortex at 15 and 35 days **(M)**. Error bars represent the standard error of the mean . *p≤0.05 compared to corresponding (time-matched) sham-injured group, #p≤0.05 compared to corresponding (time-matched) brain-injured empty-lip animals. Scale bar **(L)** = 100 μm.

Figure 3.13 ED-1(+) microglia/macrophages in the cortex following clodronate-mediated depletion. Representative photomicrographs of sham-injured **(A-C)** and brain-injured **(D-F)** animals injected with the empty liposomes and sham-injured **(G-I)** and brain-injured **(J-L)** animals treated with the clodronate liposomes at 3 **(A,D,G,J)**, 15 **(B,E,H,K)**, and 35 **(C,F,I,L)** days post-injury. Quantification of ED-1(+) microglia/macrophages exhibiting amoeboid and rod morphologies at 3, 15 and 35 days

(M). Error bars represent the standard error of the mean. *p≤0.05 compared to corresponding (time-matched) sham-injured group, #p≤0.05 compared to corresponding (time-matched) brain-injured empty-lip animals. Scale bar **(L)** = 100 μm.

Figure 3.14 GFAP(+) astrocytes in the cortex following clodronate-mediated microglia/macrophage depletion. Representative photomicrographs of sham-injured **(A)** and brain-injured **(B)** animals injected with the empty liposomes and sham-injured **(C)** and brain-injured **(D)** animals treated with the clodronate liposomes at 3 days post-injury. Quantification of the percent area of GFAP labeling in the cortex at 3 days post-injury **(E)**. Error bars represent the standard error of the mean . *p≤0.05 compared to corresponding sham-injured group, #p≤0.05 compared to brain-injured empty-lip animals. @p≤0.05 difference between sham-injured groups. Scale bar **(L)** = 100 μm.

Figure 3.15 FJB(+) profiles in the cortex following clodronate-mediated microglia/macrophage depletion. Representative photomicrographs of sham-injured **(A-C)** and brain-injured **(D-F)** animals injected with the empty liposomes and sham-injured **(G-I)** and brain-injured **(J-L)** animals treated with the clodronate liposomes at 3 **(A,D,G,J)**, 15 **(B,E,H,K)**, and 35 **(C,F,I,L)** days post-injury. Quantification of total FJB(+) profiles in the cortex at 3, 15, and 35 days **(M)**. Error bars represent the standard error of the mean. Scale bar **(L)** = 100 μm.

Figure 3.16 Cortical activity in the chronic post-injury period following acute clodronate-mediated microglia/macrophage depletion. Quantification of the amplitude

(A), latency **(B)**, and duration **(C)** of signals taken from layer 5 of the motor cortex at bregma level 4 weeks post-injury. Error bars represent the standard error of the mean.

Figure 3.17 Cortical activity within the impact site at 4 weeks post-injury following acute clodronate-mediated microglia/macrophage depletion.

Representative traces from the -3mm motor cortex of sham-injured and brain-injured animals that received the empty liposomes and sham-injured and brain-injured animals that received the clodronate 4 weeks post-injury **(A)**. Quantification of signal amplitude **(B)**, signal latency **(C)**, and signal duration **(D).** Error bars represent the standard error of the mean. *p≤0.05 compared to corresponding sham-injured group, #p≤0.05 compared to brain-injured empty-lip animals.

Figure 3.18 White matter pathology following clodronate-mediated microglia/macrophage depletion. Representative photomicrographs of Iba1(+) microglia/macrophages in the lateral white matter of sham-injured **(A)** and brain-injured **(B)** animals injected with the empty liposomes and sham-injured **(C)** and brain-injured **(D)** animals treated with the clodronate liposomes at 3 days post-injury. Quantification of the percent area of Iba1 labeling in the white matter at 15 and 35 days post-injury **(E)**. Representative photomicrographs of APP(+) profiles in the lateral white matter of sham-injured **(F)** and brain-injured **(G)** animals injected with the empty liposomes and sham-injured **(H)** and brain-injured **(I)** animals treated with the clodronate liposomes at 3 days post-injury. Quantification of the percent positive boxes labeled with APP in the white matter at 3 days post-injury via grid analysis **(J)**. Quantification of FJB(+) profiles in the

white matter at 15 and 35 days post-injury **(K)**. Quantification of the size of the signals from the myelinated (N1) and unmyelinated (N2) components of the white matter fiber bundle at 7 days post-injury. Data presented from the max stimulus amplitude **(L)**. Error bars represent the standard error of the mean. *p≤0.05 compared to corresponding sham-injured group, #p≤0.05 compared to brain-injured empty-lip animals. Scale bar **(I)** = 100 μm.

3.19 Effects of acute clodronate-mediated microglia/macrophage depletion on thalamic pathology. Quantification of total Iba1(+) microglia/macrophages in the thalamus of sham-injured and brain-injured animals that received either the empty or clodronate liposomes at 15 and 35 days post-injury **(A)**. Quantification of ED-1(+) microglia/macrophages in the thalamus that exhibit amoeboid or rod morphologies at 3, 15, and 35 days post-injury **(B)**. Quantification of FJB(+) profiles in the thalamus at 3, 15, and 35 days post-injury **(C)**. Quantification of APP(+) profiles in the thalamus at 3 days post-injury presented as the percent positive boxes that were positively labeled in the grid analysis **(D)**. Error bars represent the standard error of the mean. *p≤0.05 compared to corresponding sham-injured group, #p≤0.05 compared to brain-injured empty-lip animals.

3.20 Effects of acute clodronate-mediated microglia/macrophage depletion on pathology in the subiculum of the hippocampus. Quantification of total Iba1(+) microglia/macrophages in the subiculum of sham-injured and brain-injured animals that received either the empty or clodronate liposomes at 15 and 35 days post-injury **(A)**.

Quantification of FJB(+) profiles in the subiculum at 3, 15, and 35 days post-injury **(B)**. Quantification of ED-1(+) microglia/macrophages in the thalamus that exhibit either the amoeboid or rod morphologies at 3, 15, and 35 days post-injury **(C)**. Error bars represent the standard error of the mean. *p≤0.05 compared to corresponding sham-injured group, #p≤0.05 compared to brain-injured empty-lip animals.

3.21 Spatial learning and memory assessment at 2 different time points following acute clodronate-mediated microglia/macrophage depletion. Assessment of spatial learning on days 10-13 post-injury in the Morris water maze presented as latency to find the hidden platform over 4 training days **(A)**. Times spent in the peripheral and platform zones, and latency to the visible platform during the probe day on day 14 post-injury **(B)**. Spatial learning assessment on days 28-31 post-injury **(C)** and probe trial assessments on day 32 post-injury **(D)**. Error bars represent the standard error of the mean. *p≤0.05 compared to corresponding sham-injured group.

3.7 TABLES AND FIGURES

Figure 3.1 Controlled cortical impact injury device.

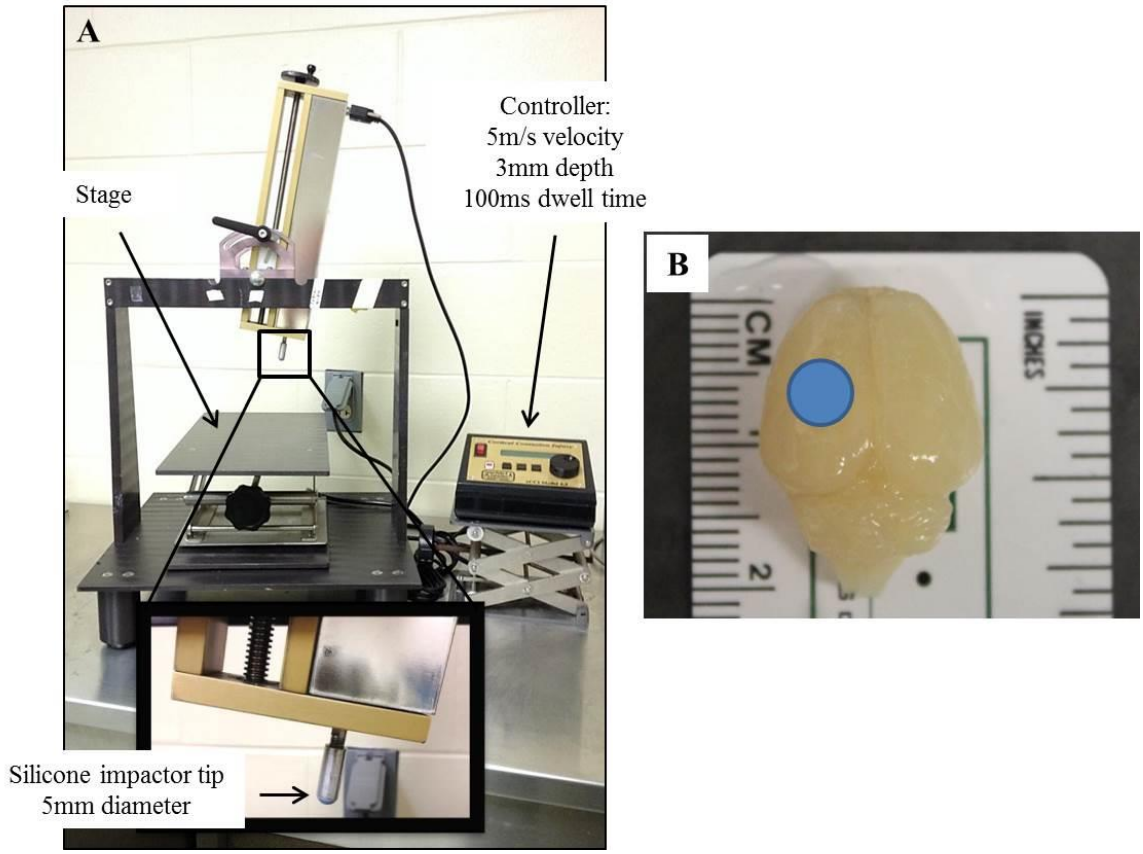

Figure 3.2 Experimental Timeline.

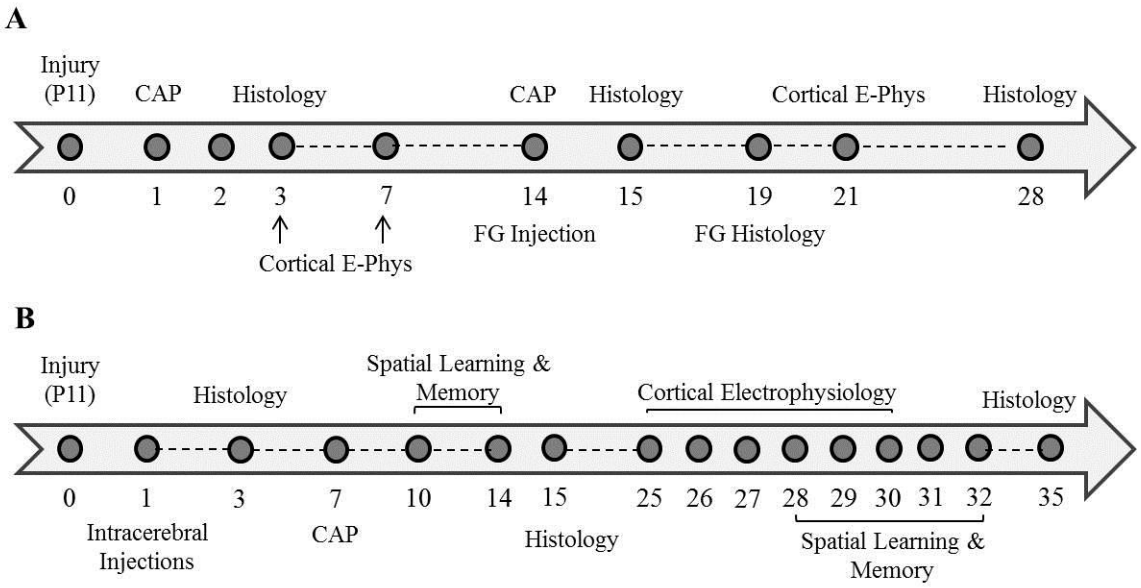

Figure 3.3 Iba1-labeled microglia/macrophages in the cortex.

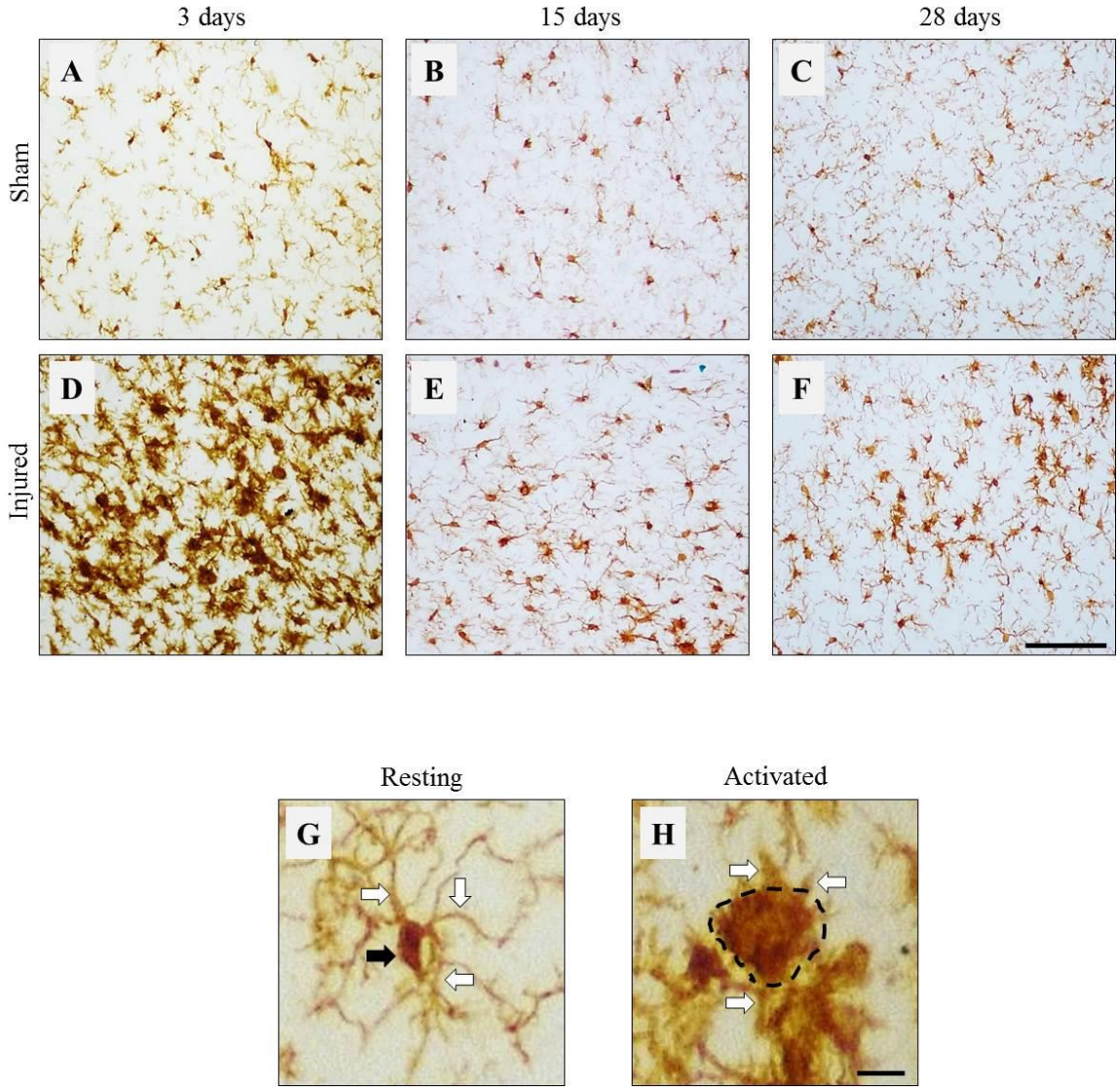

Figure 3.4 ED-1-labeled microglia/macrophages in the cortex.

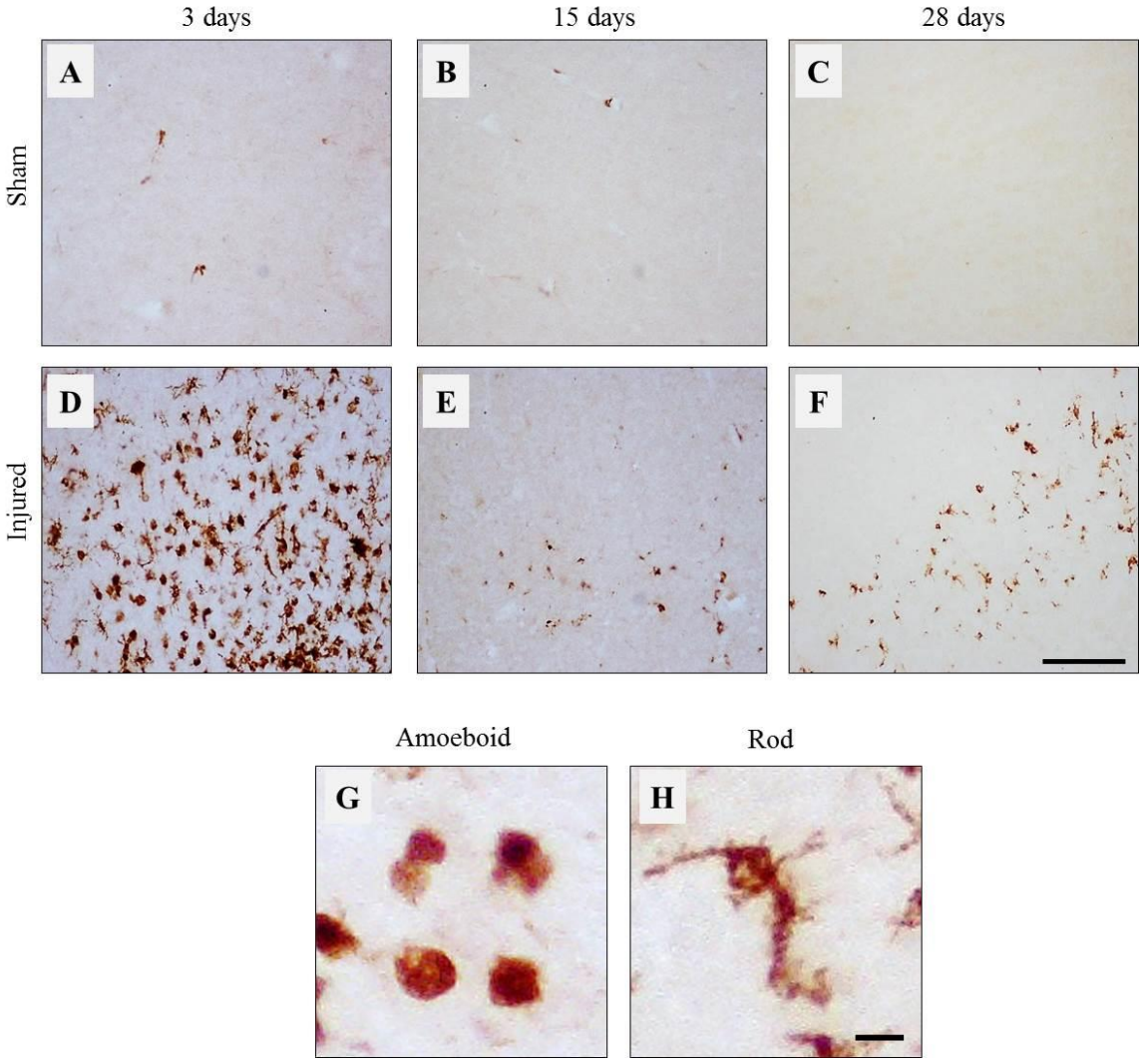

Figure 3.5 Time course of neurodegeneration in the cortex.

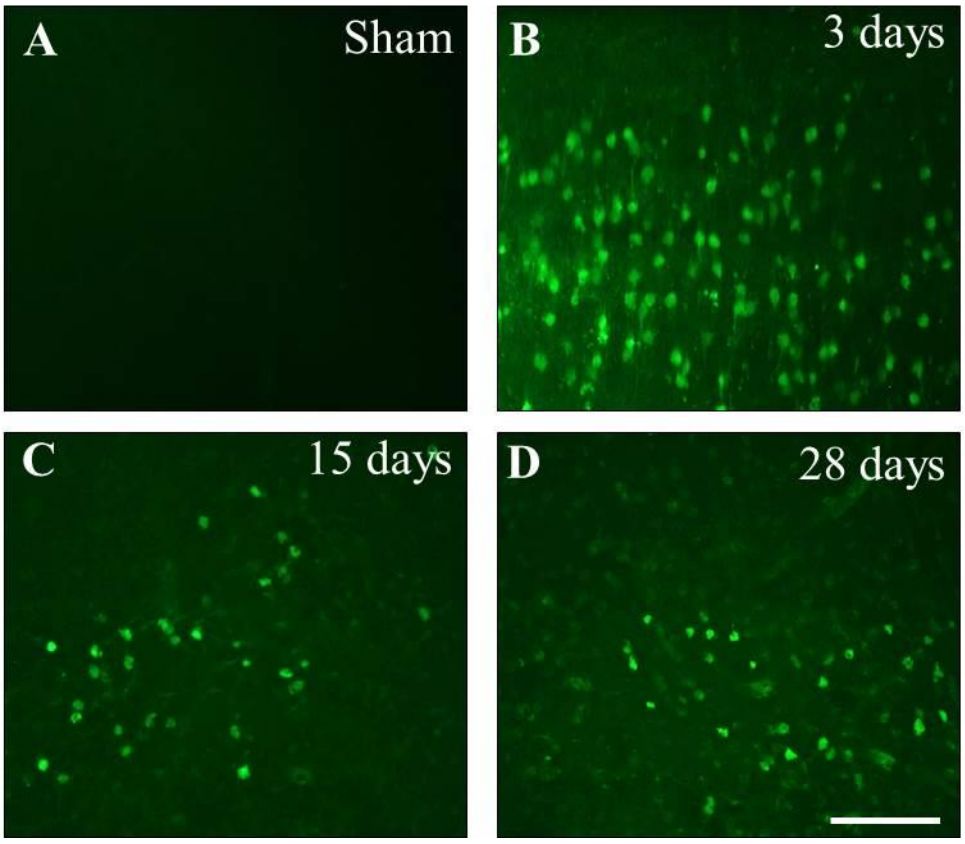

Figure 3.6 Evoked field potential recordings from the injured cortex at bregma.

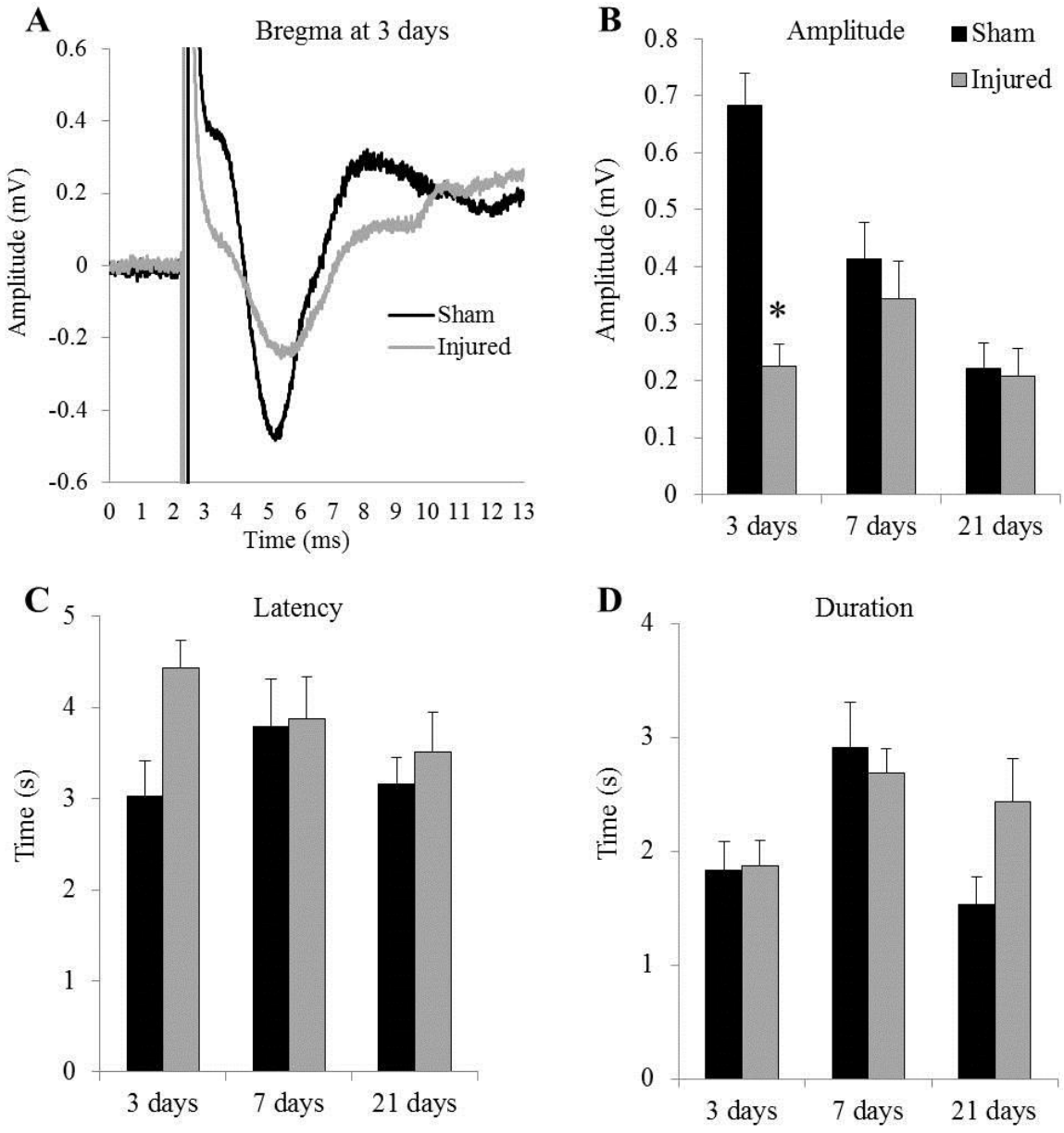

Figure 3.7 Evoked field potential recordings from the injured cortex 3mm posterior to bregma.

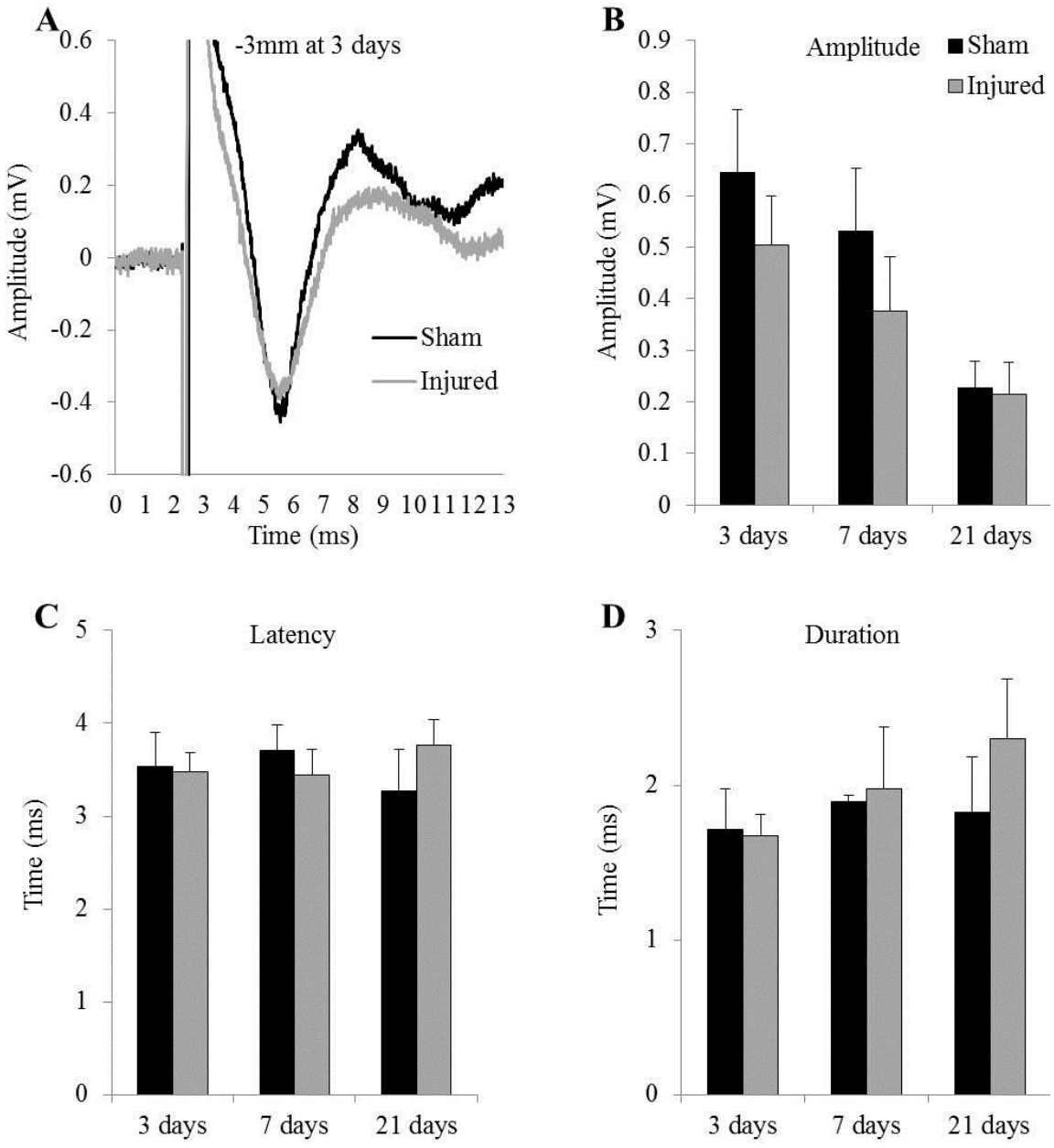

Figure 3.8 ED-1-labeled microglia/macrophages in the white matter.

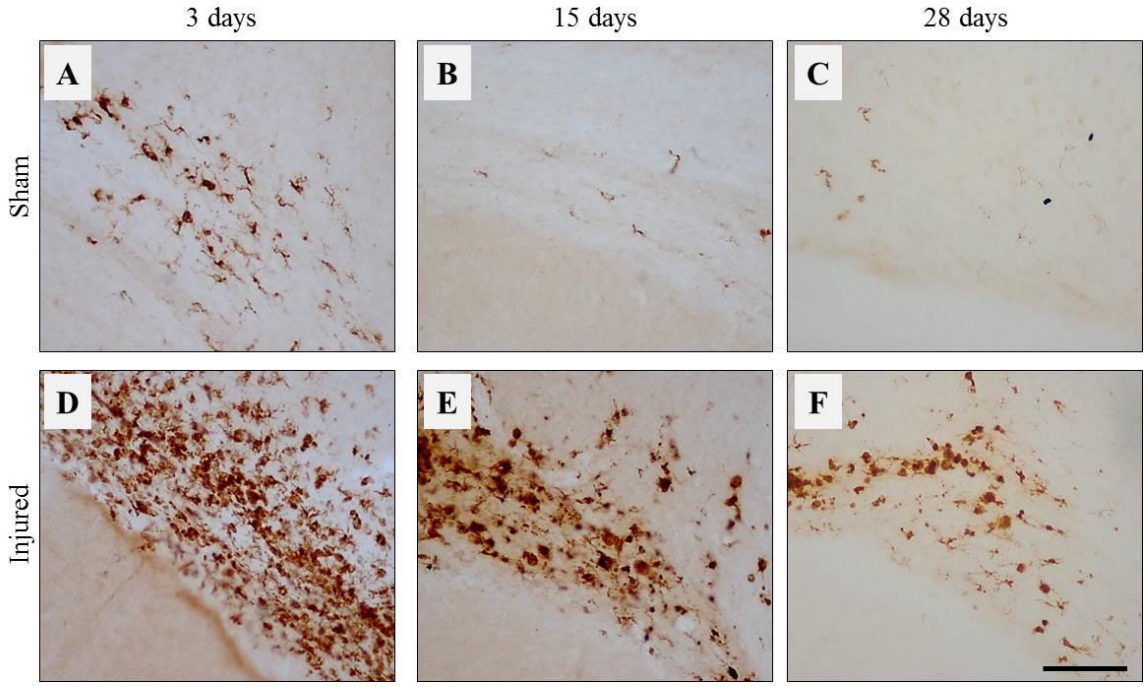

Figure 3.9 Time course of neurodegeneration in the white matter.

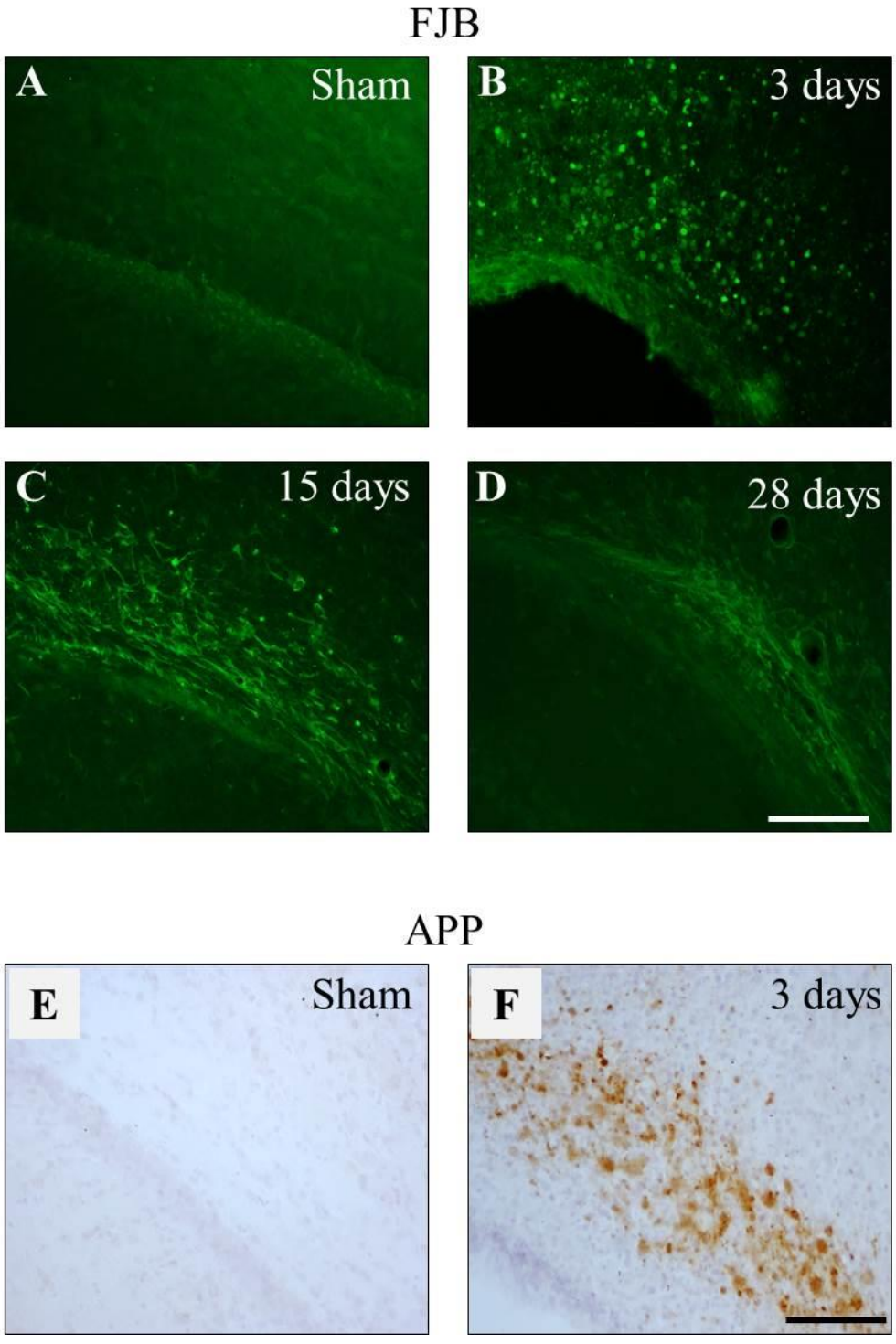

Figure 3.10 Compound action potential electrophysiology in the corpus callosum.

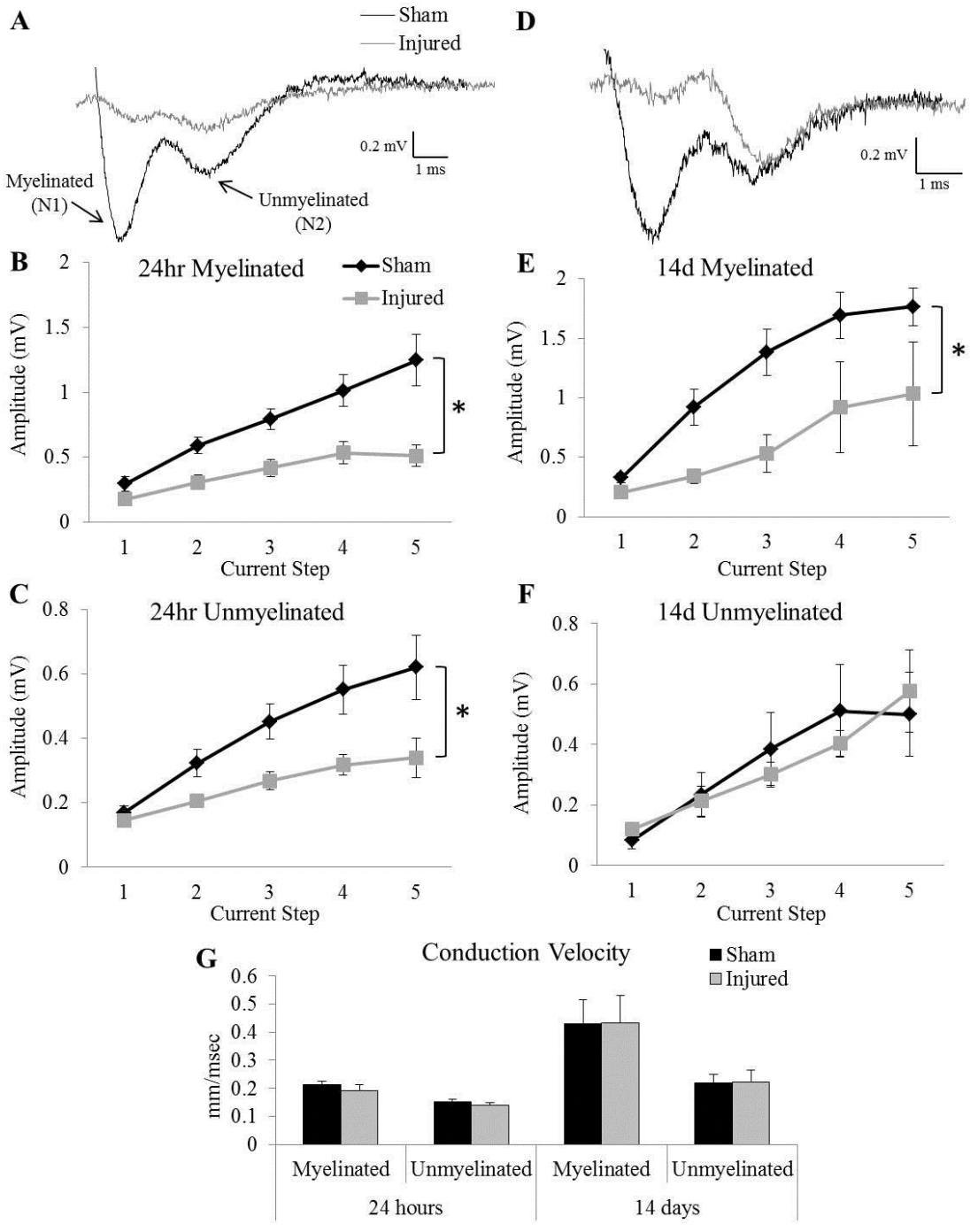

Figure 3.11 Transport of Fluoro-Gold across the corpus callosum at 14 days post-injury.

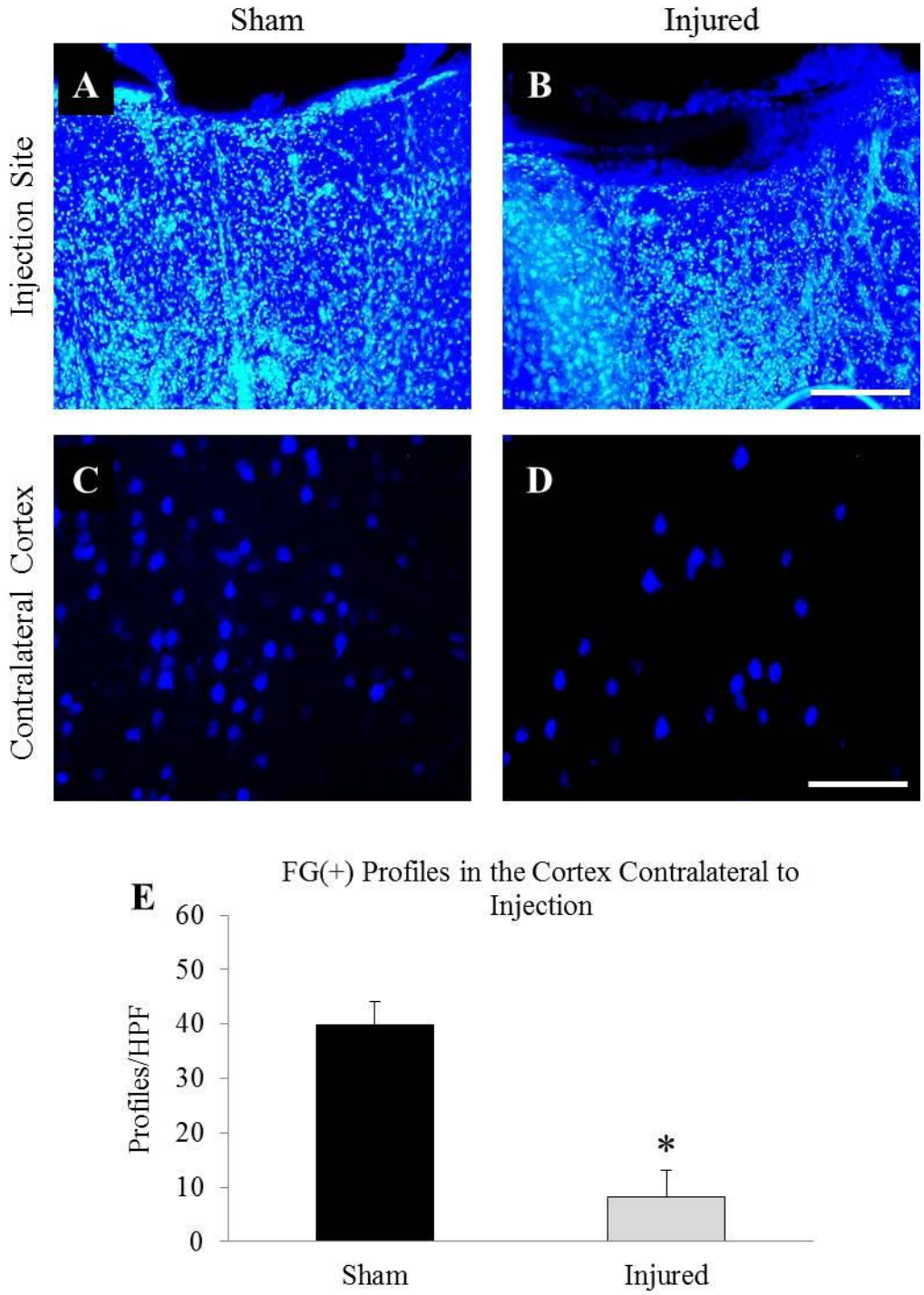

Figure 3.12 Iba1(+) microglia/macrophages in the cortex following clodronate-mediated depletion.

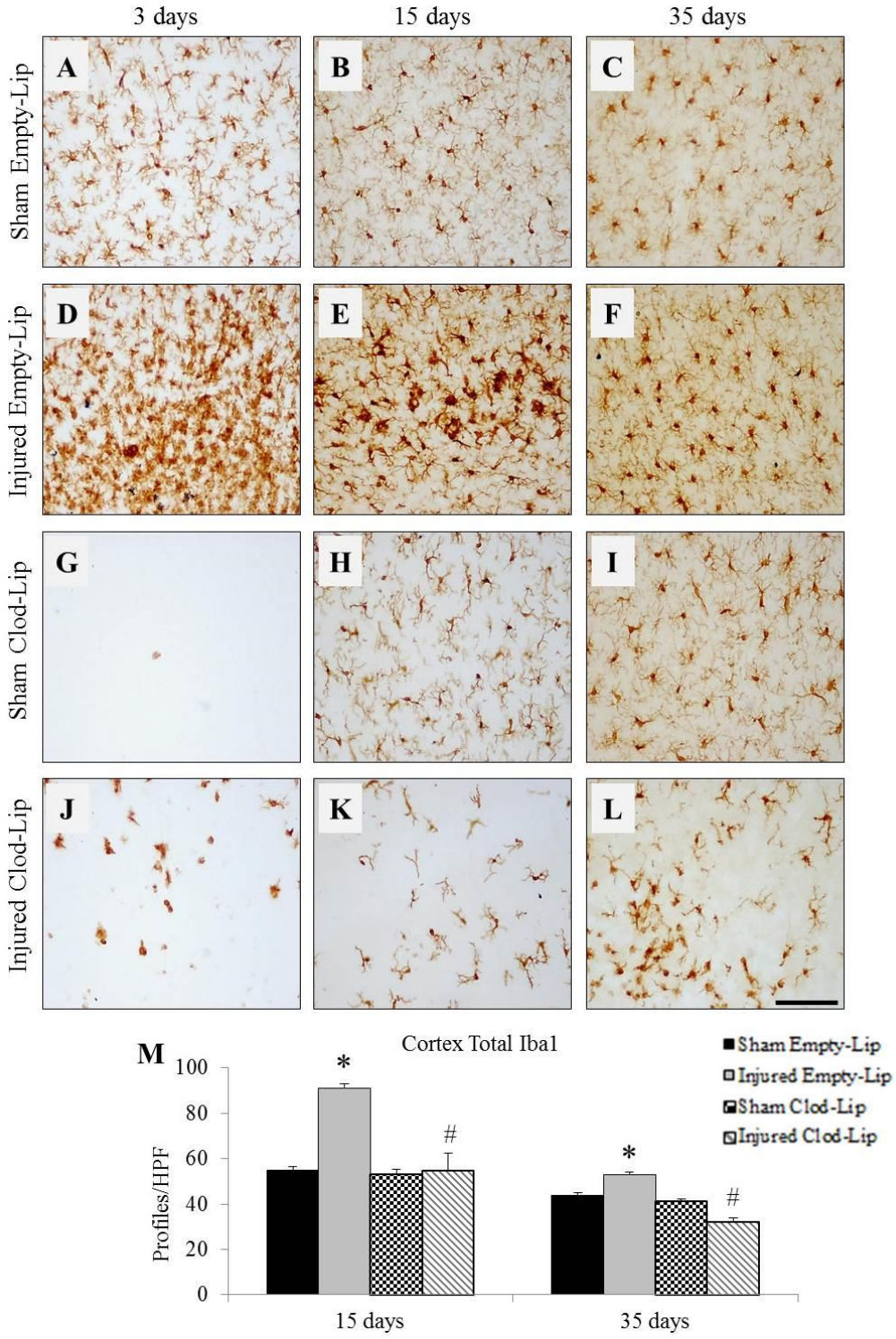

Figure 3.13 ED-1(+) microglia/macrophages in the cortex following clodronate-mediated depletion.

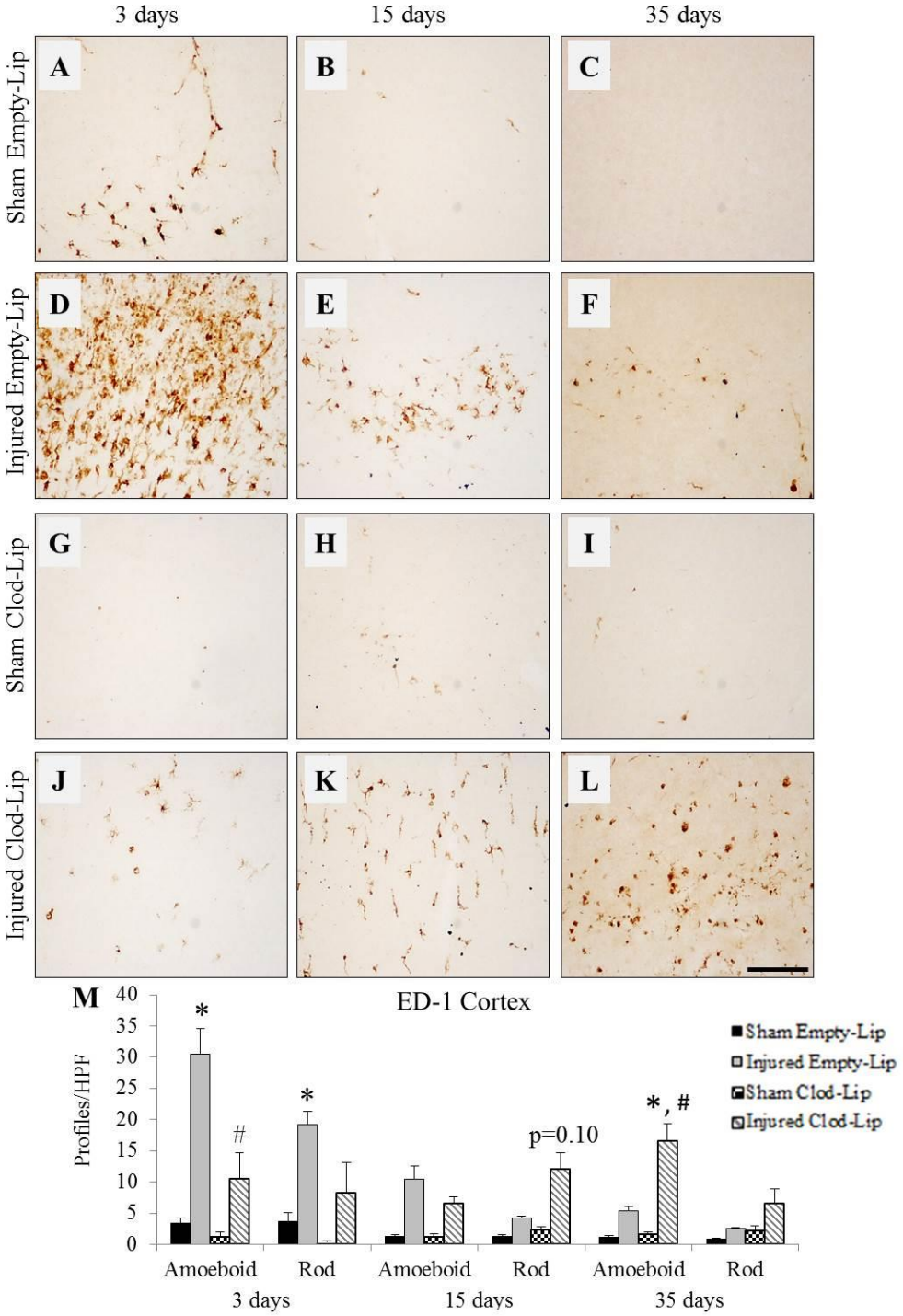

Figure 3.14 GFAP(+) astrocytes in the cortex following clodronate-mediated microglia/macrophage depletion.

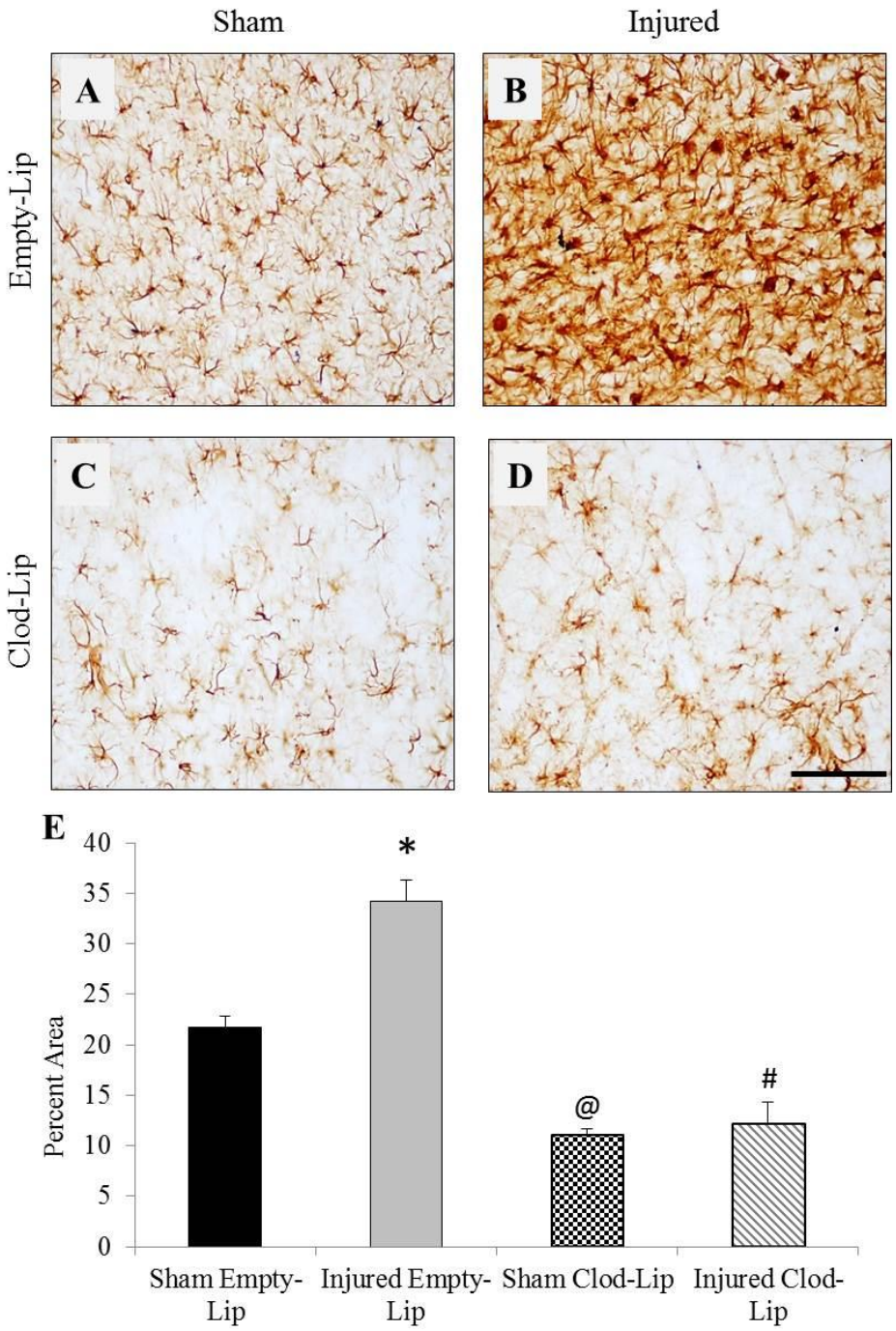

Figure 3.15 FJB(+) profiles in the cortex following clodronate-mediated depletion.

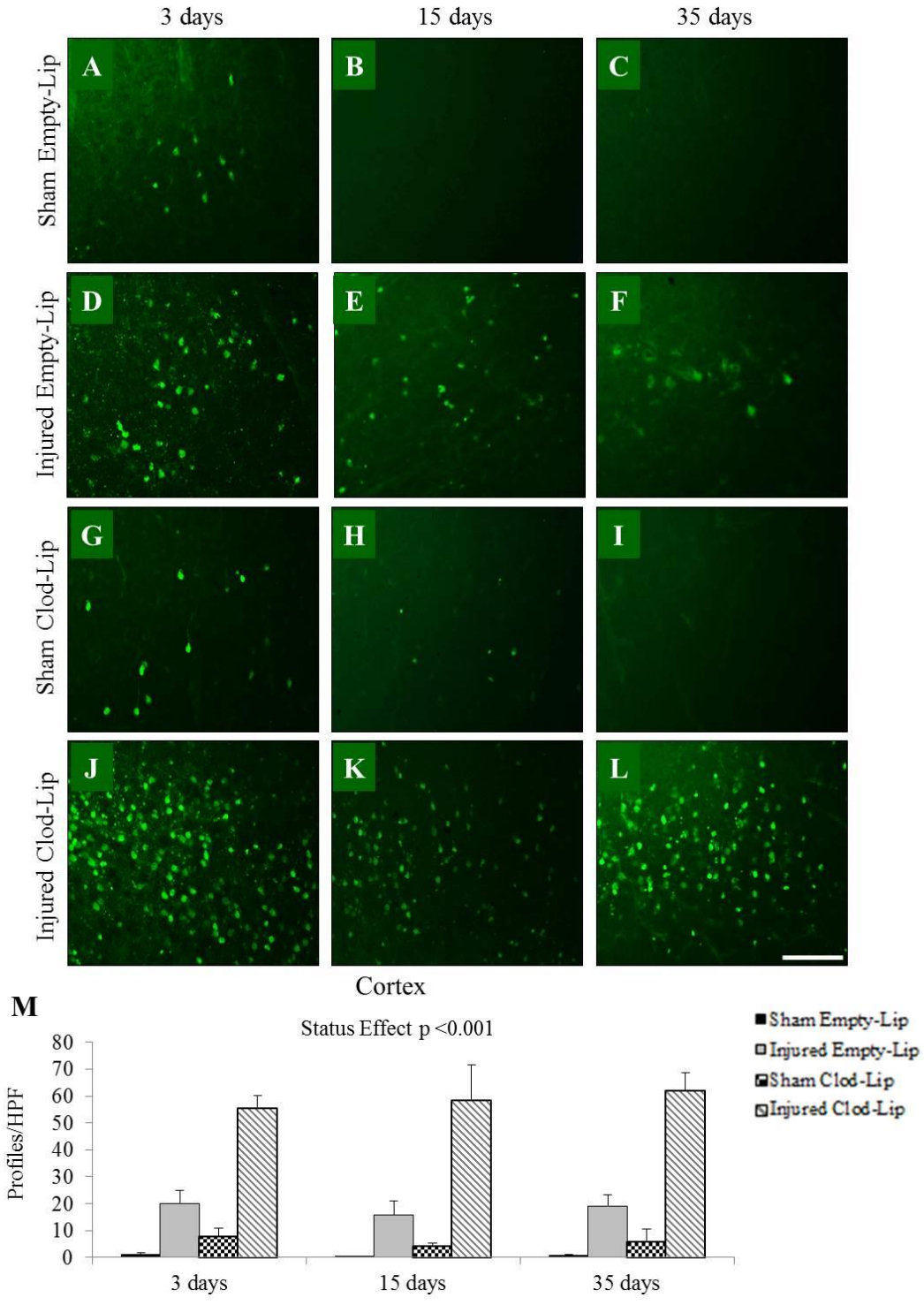

Figure 3.16 Cortical activity in the chronic post-injury period following acute clodronate-mediated microglia/macrophage depletion.

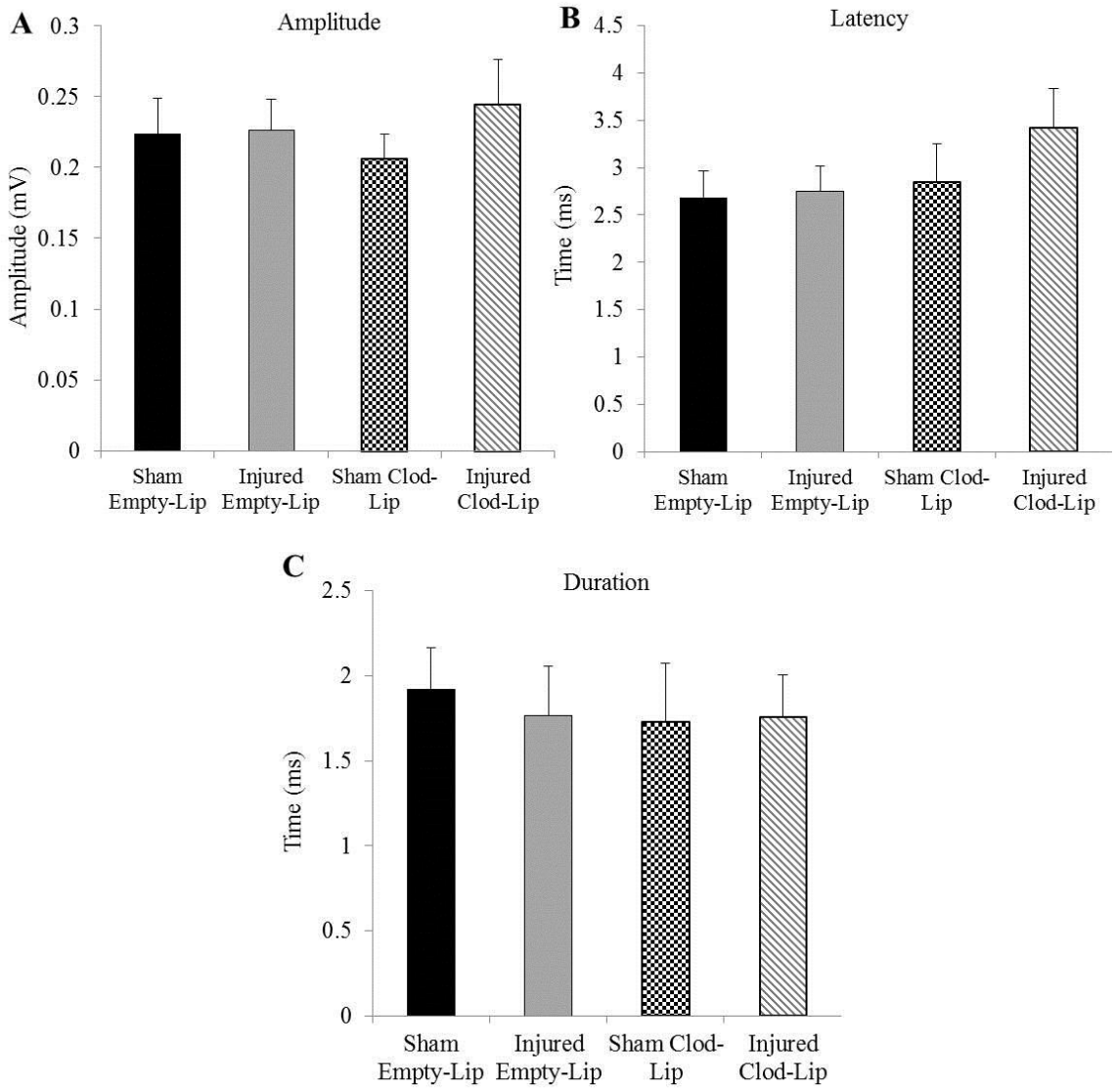

Figure 3.17 Cortical activity within the impact site at 4 weeks post-injury following acute clodronate-mediated microglia/macrophage depletion.

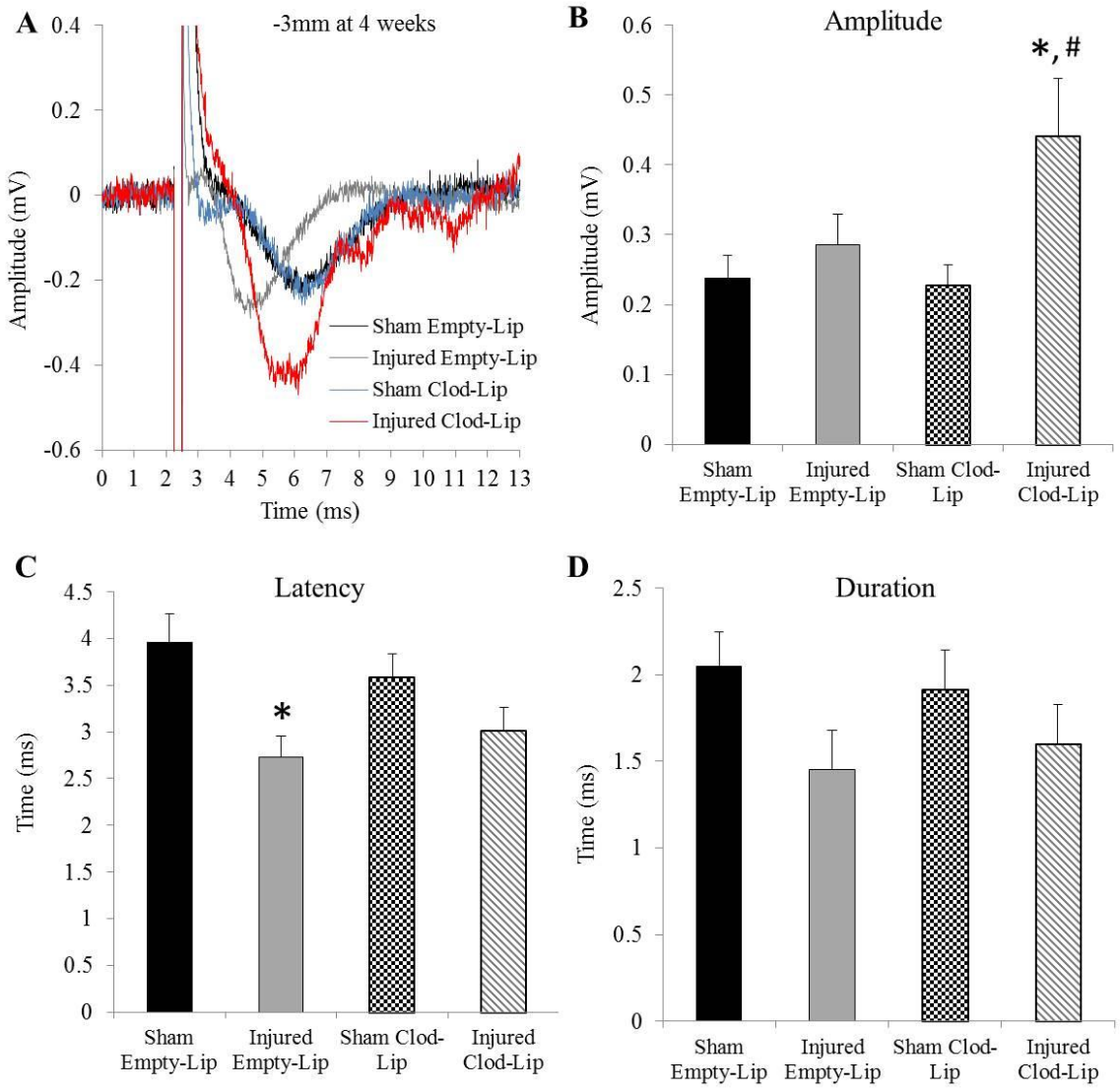

Figure 3.18 White matter pathology following clodronate-mediated microglia/macrophage depletion.

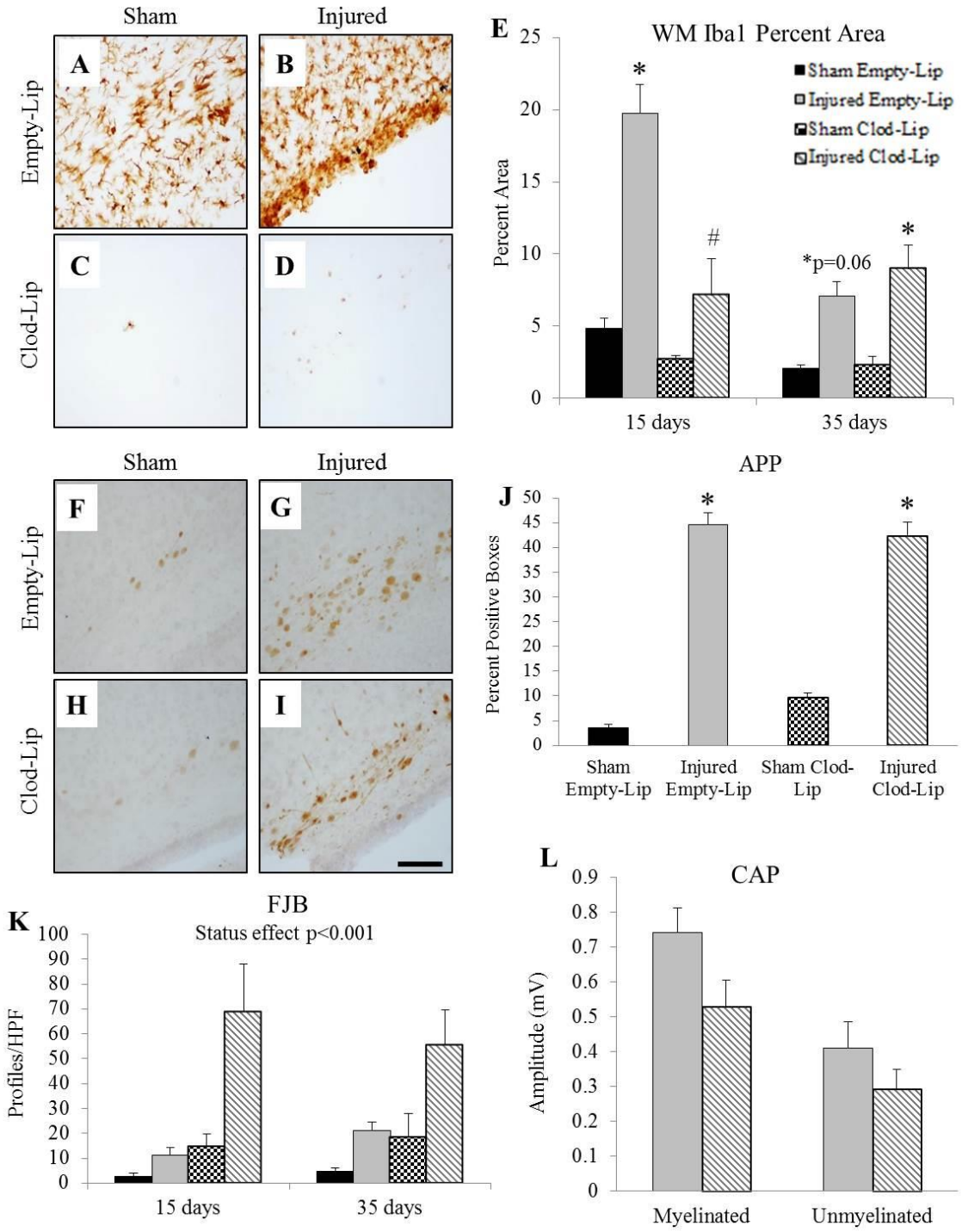

3.19 Effects of acute clodronate-mediated microglia/macrophage depletion on thalamic pathology.

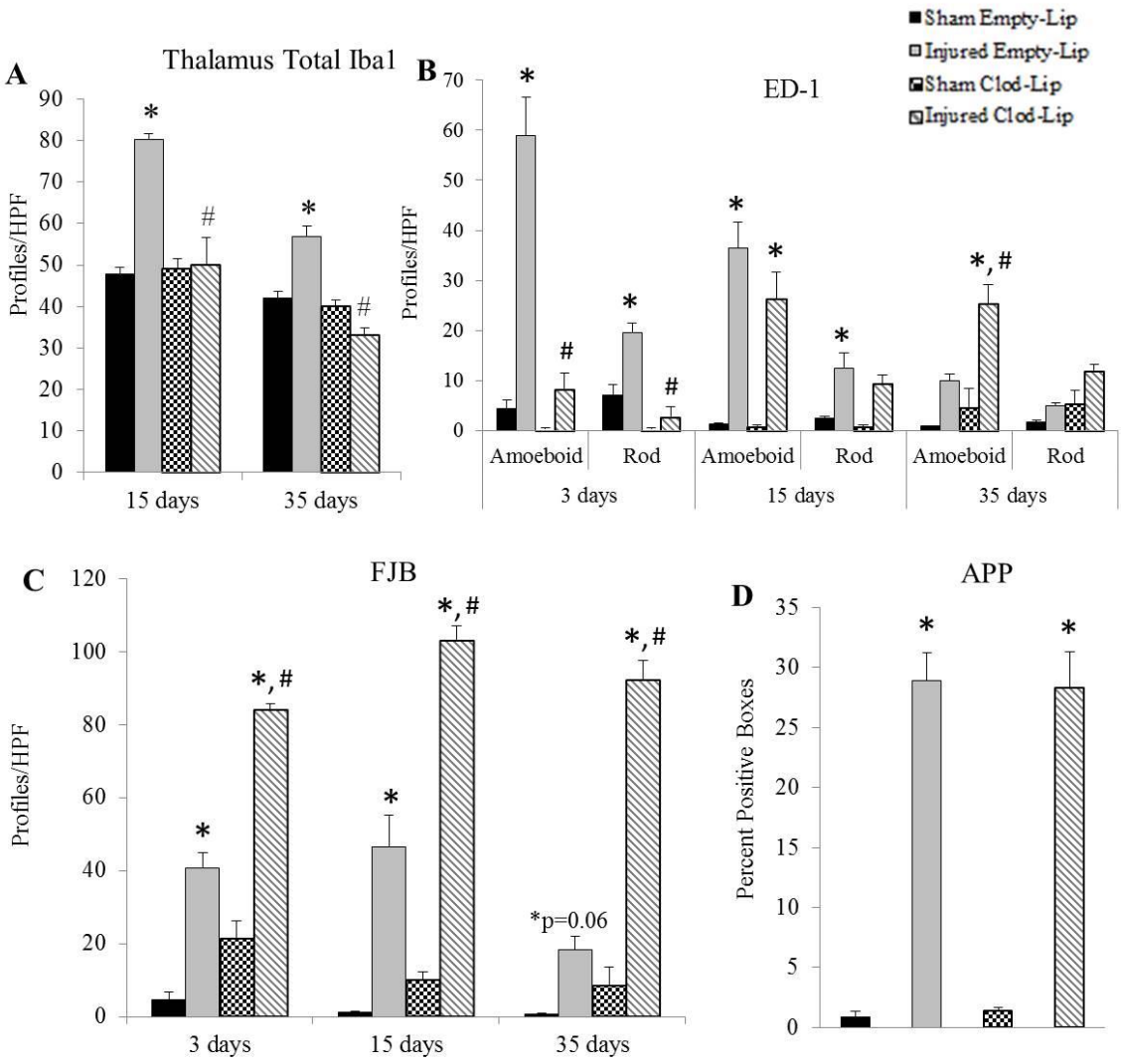

3.20 Effects of acute clodronate-mediated microglia/macrophage depletion on pathology in the subiculum of the hippocampus.

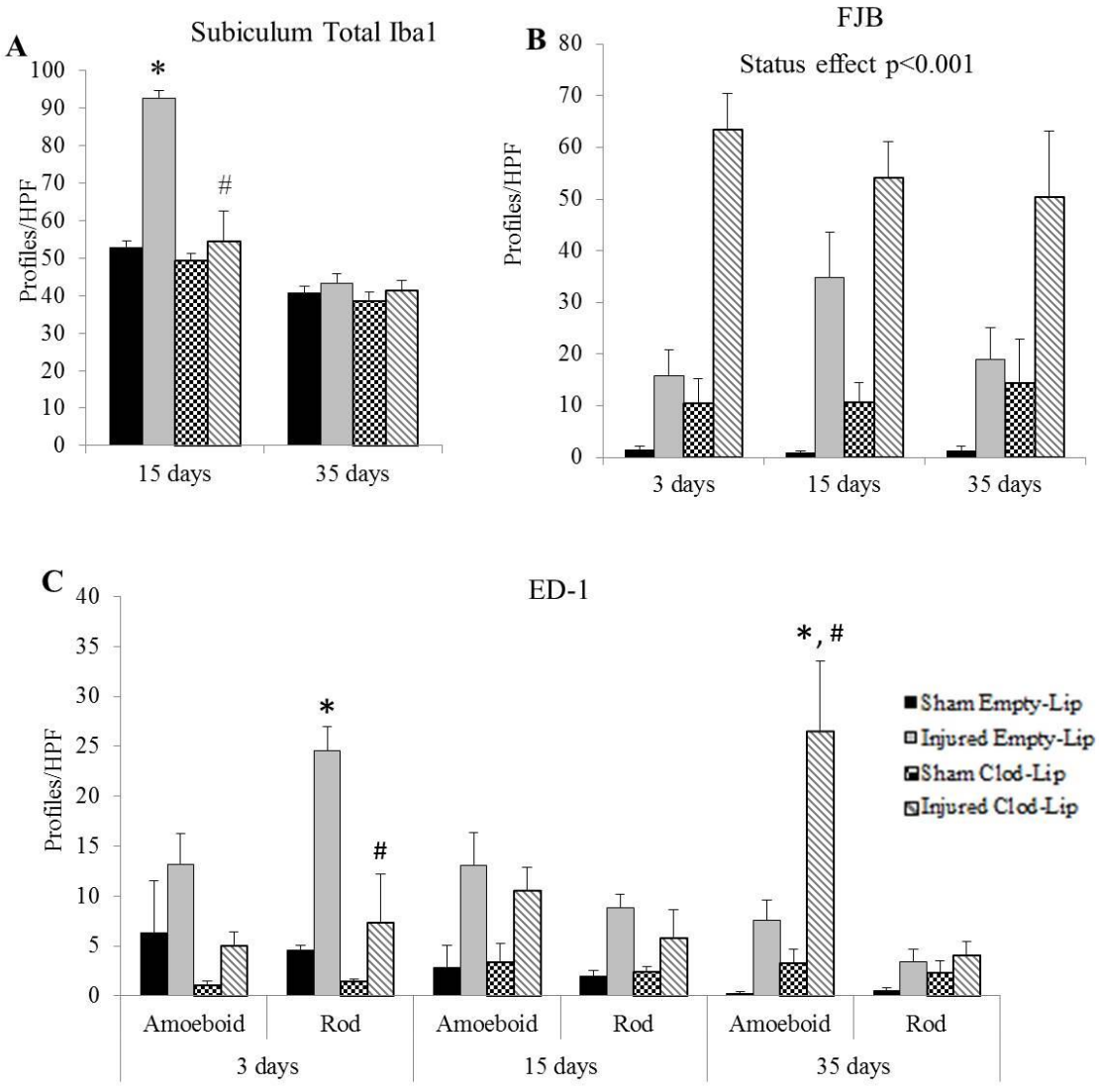

3.21 Spatial learning and memory assessment at 2 different time points following acute clodronate-mediated microglia/macrophage depletion.

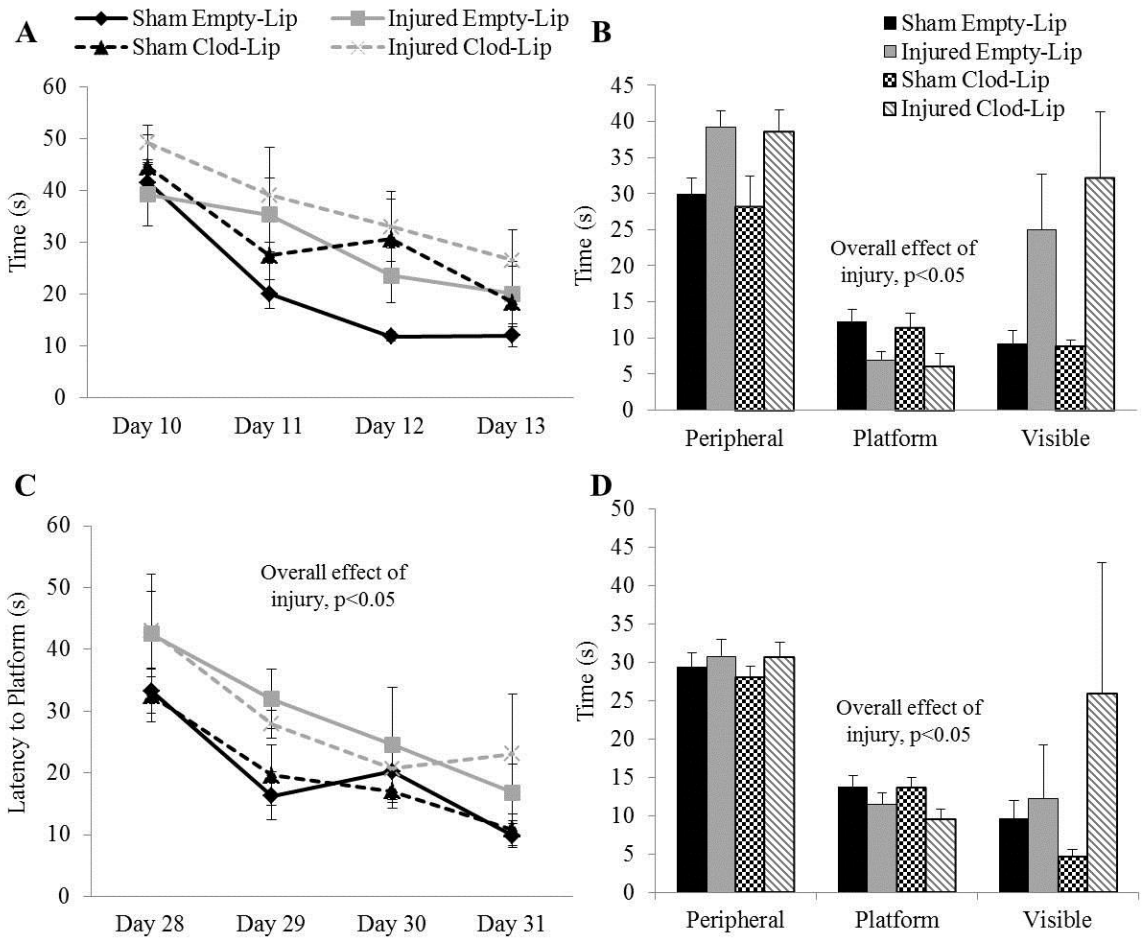

CHAPTER 4: ACUTE MINOCYCLINE TREATMENT FOLLOWING TRAUMATIC BRAIN INJURY IN THE NEONATE RAT

4.1 ABSTRACT

The role of microglia/macrophages in the pathophysiology of injury to the developing brain has been extensively studied. In children under the age of 4 who have sustained a traumatic brain injury (TBI), markers of microglial/macrophage activation were increased in the cerebrospinal fluid and were associated with worse neurologic outcome. Minocycline is an antibiotic that decreases microglial/macrophage activation following hypoxic-ischemia in neonatal rodents and TBI in adult rodents thereby reducing neurodegeneration and behavioral deficits. In this study, 11-day-old rats received an impact to the intact skull and were treated for 3 days with minocycline. Immediately following termination of minocycline administration, microglial/macrophage reactivity was reduced in the cortex and hippocampus and was accompanied by an increase in the number of fluoro-Jade B profiles suggestive of a reduced clearance of degenerating cells. This effect was not sustained at 7 days post-injury, but weeks (15 days and 4 weeks) after the injury minocycline treatment resulted in an increase in activated microglia/macrophages that coincided with an increase in neurodegeneration in the cortex and hippocampus of brain-injured animals. This was also associated with hypoactivity as measured through evoked field potential in the cortex of brain-injured minocycline-treated animals. Although microglial/macrophage reactivity was reduced in the white matter tracts and the thalamus at 3 days post-injury and subsequently increased in these regions in the weeks following injury, minocycline treatment did not affect axonal injury, axonal degeneration, or neurodegeneration. Injury-induced spatial learning and memory deficits were also not affected by minocycline and sex had minimal effects on either injury-induced alterations or the

efficacy of minocycline treatment. Collectively, these data demonstrate the differential effects of minocycline in the immature brain following impact trauma and suggest that minocycline may not be an effective therapeutic strategy for TBI in the immature brain.

4.2 INTRODUCTION

With close to half a million children affected annually, traumatic brain injury (TBI) remains one of the most common causes of disability and death in infants and children (Langlois et al., 2005, Faul, 2010, Coronado et al., 2011). The youngest age group (≤ 4 years old) exhibit worse outcome following moderate to severe TBI compared to older children (Anderson et al., 2005, Coronado et al., 2011). Pediatric TBI patients commonly exhibit traumatic axonal injury (TAI) and brain atrophy which are associated with prolonged cognitive deficits such as impairments of learning and memory, attention, and executive function (Duhaime and Raghupathi, 1999, Ewing-Cobbs et al., 2004, Tong et al., 2004, Anderson et al., 2005, Ewing-Cobbs et al., 2006, Catroppa et al., 2007, Catroppa et al., 2008, Anderson et al., 2009). Injury to the immature brain may also have adverse effects on the development of cognitive abilities (Babikian et al., 2015). Unfortunately, no specific therapies exist, with supportive care in the acute post-traumatic period being the only current treatment option.

While the mechanisms underlying neuropathologic alterations following TBI in the immature brain are not completely understood, inflammation may play an important role in the sequelae of secondary injury. Activation of microglia, the resident immuno-competent cells in the brain, and peripheral macrophage infiltration are thought to play an important role in the acute and chronic neurodegeneration observed following brain injury (Kreutzberg, 1996, Nimmerjahn et al., 2005, Hanisch and Kettenmann, 2007, Ransohoff and Perry, 2009, Graeber and Streit, 2010, Beynon and Walker, 2012). Markers of microglial/macrophage activation such as sCD163, ferritin, and interleukins-6,-8 and -10 were increased in cerebrospinal fluid (CSF) from children after TBI with

more prominent increases observed in the youngest age group (≤ 4 years of age), suggesting that these patients may be at higher risk for worse neurologic outcome (Bell et al., 1997, Whalen et al., 2000, Newell et al., 2015). In neonatal rodents, hypoxic-ischemia (HI) or ischemia resulted in robust microglial/macrophage activation (McRae et al., 1995, Ivacko et al., 1996, Denker et al., 2007, Vexler and Yenari, 2009, Ferrazzano et al., 2013). Increased microglial reactivity in the injured hemisphere following TBI in the immature mouse brain corresponded to areas containing degenerating neurons and was associated with an expansion of the cortical lesion and spatial learning deficits (Tong et al., 2002, Pullela et al., 2006). In addition, microglial reactivity has also been observed in the white matter tracts that was associated with an increase in tissue loss of the injured hemisphere and working and recognition memory deficits in a rabbit model of pediatric TBI (Zhang et al., 2015). These data suggest that microglial/macrophage activity may be involved in ongoing pathogenesis following TBI in the immature brain and may potentially serve as a therapeutic target.

Minocycline is a second generation tetracycline derivative antibiotic with anti-inflammatory properties, effectively crosses the blood-brain barrier after systemic administration and has demonstrated neuroprotection in many models of brain injury and neurodegenerative diseases (Elewa et al., 2006, Kim and Suh, 2009, Plane et al., 2010, Garrido-Mesa et al., 2013). Following neonatal rodent models of HI, minocycline decreased microglial activation which was associated with a reduction in injury-induced neuronal damage, oligodendroglial cell death, hypomyelination, white matter atrophy and locomotor deficits (Cai et al., 2006, Fan et al., 2006, Carty et al., 2008, Cikla et al., 2016). In a model of pediatric cardiac arrest, acute treatment with minocycline reduced

microglial activation along with neurodegeneration and apoptosis (Tang et al., 2010). Treatment with minocycline following TBI in the adult mouse resulted in a reduction of microglial activation and proliferation which was associated with a decrease in pro-inflammatory cytokine response, cerebral edema, lesion volume and attenuation of locomotor and spatial memory deficits (Homsi et al., 2009, Homsi et al., 2010, Siopi et al., 2011, Siopi et al., 2012). Similarly, minocycline administration following moderate-severe contusive trauma to the adult rat brain reduced microglial activation and improved behavioral function (Abdel Baki et al., 2010, Lam et al., 2013). In contrast, minocycline did not attenuate cell death, axonal injury or tissue loss despite reducing active microglia following either diffuse brain trauma in the adult mouse (Bye et al., 2007) or repetitive brain trauma in the neonate rat (Hanlon et al., 2016a). Depleting the brain of its resident microglia exacerbates cell death following neonatal stroke (Faustino et al., 2011) but appears to not affect the extent of white matter injury following TBI (Bennett and Brody, 2014). It must be noted that not all effects of minocycline can be attributed to its effects on reducing microglial/macrophage activation following brain injury. Fox et al., (2005) observed that minocycline administration following focal ischemia in the neonate rat did not reduce the extent of microglial activation but did reduce the volume of injury. Although microglial activation was not evaluated, minocycline treatment reduced both apoptotic and excitotoxic cell death following HI in the neonatal rat (Arvin et al., 2002), reduced caspase activation following contusive brain trauma in the adult mouse (Sanchez Mejia et al., 2001) and attenuated inflammatory protein expression in a rat model of mild blast TBI (Kovesdi et al., 2012). By contrast, minocycline worsened injury-induced infarction and tissue atrophy in a mouse model of HI (Tsuji et al., 2004). Collectively,

these data underscore the complicated relationship between injury-induced microglial/macrophage activation and ensuing brain damage.

With the goal of understanding the role of microglial/macrophage activation in neonatal brain trauma, the present study sought to test the hypothesis that minocycline treatment following TBI will attenuate microglial/macrophage reactivity along with neuronal and axonal degeneration leading to decreases in brain atrophy and a reversal of spatial learning and memory deficits. The effects of both short-term (3 days) administration of minocycline (45mg/Kg/dose) were tested in a well characterized model of single TBI in the 11-day-old rat. This injury results in neuronal and axonal degeneration, TAI, microglial/macrophage reactivity, tissue atrophy and cognitive deficits that last up to 4 weeks post-injury (Raghupathi and Huh, 2007).

4.3 MATERIALS AND METHODS

4.3.1 Brain Injury and Minocycline Administration

Animals were injured as described in chapter 3.3.1. Immediately following the injury, animals were randomly assigned to receive a 45mg/Kg dose of minocycline hydrochloride (Sigma, St. Louis MO) dissolved in phosphate-buffered saline (PBS), or vehicle (PBS, 0.2mL/Kg) via an intraperitoneal (i.p.) injection. Sham-injured animals were also randomly assigned to receive either vehicle or minocycline. Minocycline or vehicle was injected every 12 hours for 3 days for a total of 6 injections (45 mg/Kg/injection or 0.2 mL/Kg/injection). This dose and dosing paradigm was successful in reducing acute microglial/macrophage activation in neonate repetitive TBI (Hanlon et al., 2016a) and other models of neonate HI (Buller et al., 2009). Animal numbers for each outcome are listed in Table 4.1.

4.3.2 Intra-Cortical Fluoro-Gold Injections

Animals were injected with the retrograde tracer FluoroGold (2%, FluoroChrome) as previously described (Chapter 3.3.2). For this study, however, the tracer was injected into the uninjured (right) cortex to address the potential confound that cells in the injured cortex were deficient in their uptake of the tracer.

4.3.3 Histology and Immunohistochemistry

Animals were sacrificed at the appropriate time points according to methods described in chapter 3.3.4. Coronal sections were assessed for immunohistochemistry as previously described (Hanlon et al., 2016b) (Chapter 3.3.4). Briefly, coronal sections

were mounted on gelatin-subbed slides and subsequently stained with Nissl-Myelin or Fluoro-Jade B (FJB) for detection of gross tissue alterations and degeneration (Hanlon et al., 2016b). Sections from FG brains were mounted and allowed to dry in the dark before being coverslipped with DPX mounting media. Microglia/macrophages were evaluated with free-floating immunohistochemistry using anti-ionized calcium-binding adaptor molecule 1 (Iba1, Wako, Richmond, VA, 1:20,000) and CD68 (Clone ED1, BioRad, formerly AbD Serotech, Hercules, CA, 1:500), astrocytes were visualized using glial fibrillary acidic protein (GFAP, Sigma, St. Louis, MO, 1:5,000), and traumatic axonal injury using a polyclonal antibody to the C-terminal end of amyloid precursor protein (APP, Zymed, San Francisco, CA, 1:2,000).

4.3.4 Quantification of histology

Quantification of histology was performed as previously described (Chapter 3.3.5). Exceptions include that APP(+) profiles in the white matter and thalamus were counted in 20x images instead of being analyzed with an overlaid grid analysis (15 images in the WM and 9 images in the thalamus). Also, Iba1 labeling in the white matter was counted in 20x images when the density of labeling allowed (15 days post-injury).

4.3.5 Cortical Evoked Field Potential Recordings

Evoked field potential recordings were taken from layer 5 of the motor cortex at bregma and 3mm posterior to bregma at 3 days and 4 weeks post-injury and quantified as previously described (Chapter 3.3.7).

4.3.6 Spatial Learning and Memory Assessment

Spatial learning and memory was assessed on post-injury days 10-14 as previously described (Chapter 3.3.8).

4.3.7 Statistical Analysis

All statistics were performed using Statistica 7 (StatSoft, Tulsa OK). All data are presented as mean ± standard error of the mean. Sham-injured animals that received vehicle injections were not statistically different from those that were treated with minocycline in any of the various histologic and behavioral outcome measures and were therefore combined for statistical purposes. Outcome measures were compared across groups (sham, injured + vehicle, injured + minocycline) as a function of time (when applicable) and sex (when there were adequate numbers of each sex per group) using appropriate analyses of variance (ANOVA). When necessary, post-hoc analyses were performed using the Newman-Keuls test and a value of $p \leq 0.05$ was considered significant. Animal numbers for each outcome are listed in Table 4.1.

4.4 RESULTS

4.4.1 Effects of acute minocycline treatment on histopathology and neuronal activity in the injured cortex.

Minocycline treatment decreased microglial/macrophage reactivity while simultaneously increasing neurodegeneration in the cortex at 3 days post-injury.

In sham-injured animals and in brain-injured minocycline-treated animals, Iba1-positive microglia/macrophages displayed processes suggestive of a "resting" phenotype (Fig. 4.2A and 4.2C, white arrows). Brain-injured animals that received either vehicle or minocycline injections contained "activated" microglia/macrophages, in which processes were fewer and/or shorter and cell bodies were larger (Fig. 4.2B and 4.2C, black arrows), in the retrosplenial cortex and through all layers of the motor and somatosensory cortices. Quantification of the number of Iba1(+) microglia/macrophages in the cortex at both 3 and 7 days post-injury revealed an interaction effect between group and time ($F_{2,20}$=13.73, $p<0.001$; Fig. 4.2G) with a post-hoc analysis indicating that both brain-injured groups contained more microglia/macrophages compared to the time-matched sham-injured animals, and that minocycline-treated, brain-injured animals had significantly fewer total microglia/macrophages than brain-injured animals that received vehicle; the latter effect was only noted at 3 days post-injury ($p<0.001$), but not at 7 days post-injury ($p=0.39$; Fig. 4.2G). Sex, when used as an independent variable, demonstrated no interaction with group or time ($F_{2,20}$=0.06, $p=0.94$). Similarly, quantitative analyses of activated microglia/macrophages revealed an interaction effect between group and time ($F_{2,20}$=4.88, $p<0.05$; Fig. 4.2H) with the post-hoc analysis indicating that minocycline treatment was only effective in decreasing the proportion of activated

microglia/macrophages in brain-injured animals at 3 days post-injury ($p<0.01$); sex of the animals did not influence the interaction between group and time ($F_{2,20}=0.01$, $p=0.99$).

Activated microglia/macrophages were additionally labeled using an antibody to CD68/ED-1 at 3 days post-injury (Fig. 4.2D-F). The activated microglia/macrophages took on two types of morphologies: amoeboid cells that were enlarged and rounded and rod cells that exhibited thick, elongated cell bodies. Both types of cells had few if any visible processes (Fig. 4.2F Insets). Qualitative analysis revealed that minocycline-treated brain-injured animals (Fig. 4.2F) appeared to have fewer ED-1-labeled cells in the cortex compared to brain-injured animals that received the vehicle (Fig. 4.2E). One-way ANOVA of the number of amoeboid cells revealed a significant effect of status ($F_{2,6}=12.08$, $p<0.01$, Fig. 4.2L) and post hoc assessment revealed that brain-injured animals had significantly more amoeboid cells than sham-injured animals irrespective of treatment ($p<0.01$). Despite observed qualitative differences, there was no significant difference in the number of amoeboid cells between brain-injured minocycline-treated animals and those that received the vehicle ($p=0.41$). Analysis of rod microglia/macrophages also revealed a significant effect of status ($F_{2,6}=17.27$, $p<0.01$, Fig. 4.2L) that showed that brain-injured animals had significantly more rod microglia/macrophages compared to sham-injured animals ($p<0.05$). The number of rod microglia/macrophages showed a trending decrease between brain-injured minocycline-treated animals and those that received the vehicle ($p=0.06$).

Astrocytic reactivity was visualized in the cortex using an antibody to glial fibrillary acidic protein (GFAP). Low power area thresholding analysis was conducted due to the diffuse nature of the labeling (Fig. 4.2G-I). Analysis revealed a significant

effect of status ($F_{2,8}$=53.27, p<0.001, Fig. 4.2M) that indicated a severe increase in the area of labeling in the cortex of brain-injured animals compared to sham-injured animals (p<0.001). Minocycline treatment had no effect on astrocytic reactivity in the cortex (p=0.17).

In cortical areas that contained reactive microglia/macrophages and astrocytes, FJB-labeled degenerating neurons were observed (Fig. 4.3B and 4.3C); there were no FJB(+) profiles in the sham-injured animals (Fig. 4.3A). A three-way ANOVA revealed an interaction effect between treatment status and time ($F_{1,17}$=14.47, p<0.01; Fig. 4.2I) and minocycline-treated, brain-injured animals had significantly more FJB+ profiles than brain-injured animals (p<0.001) at 3 days post-injury but not at 7 days post-injury (p=0.61); sex of the animals did not affect FJB reactivity in the cortex ($F_{1,17}$=0.79, p=0.39). Impact to the intact skull of either the neonate male or the female rat did not result in an overt lesion or cavitation of the underlying cortex (Fig. 4.3E and 4.3F). Cortical layers in sham-injured (Fig. 4.3D) and in brain-injured animals that received vehicle (Fig. 4.3E) or minocycline (Fig. 4.3F) demonstrated typical cellular labeling.

Acute minocycline treatment was associated with an increase in microglial/macrophage reactivity and an increase in neurodegeneration in the cortex at 15 days post-injury.

At 15 days post-injury, microglial/macrophage reactivity was still present in the cortex of brain-injured animals as evidenced by an increase in Iba1-labeled microglia/macrophages (Fig. 4.4A-C) and the presence of ED-1 labeled cells (Fig. 4.4D-F). Analysis of the total number of microglia/macrophages revealed a significant effect of injury status ($F_{2,9}$=16.19, p<0.01; Fig. 4.4J) and post hoc assessment demonstrated that

brain-injured animals had significantly more Iba1-labeled cells in the cortex compared to sham-injured animals ($p<0.01$). The number of total microglia/macrophages did not differ between minocycline-treated brain-injured animals and those that received the vehicle ($p=0.21$). Analysis of amoeboid ED-1-labeled cells in the cortex also revealed a status effect ($F_{2,9}=22.54$, $p<0.001$; Fig. 4.4K). Post hoc analysis showed that, while brain-injured animals that received the vehicle appeared to have more labeled cells compared to sham-injured animals, the difference was not significant ($p=0.08$). Brain-injured minocycline-treated animals, however, had significantly more amoeboid ED-1-labeled cells compared to both sham-injured ($p<0.001$) and brain-injured vehicle animals ($p<0.01$). Similarly, there was a significant effect of status in the analysis of the number of rod-shaped ED-1-labeled cells ($F_{2,9}=39.86$, $p<0.001$; Fig. 4.4K). There was no significant difference between sham-injured and brain-injured animals that received the vehicle ($p=0.26$), but minocycline-treated brain-injured animals had significantly more rod-shaped cells than both sham-injured ($p<0.001$) and brain-injured animals that received the vehicle ($p<0.001$). These results indicate that the acute treatment that initially decreased reactivity altered the microglial/macrophage response almost two weeks after the cessation of treatment. Similar to the 3-day time point, FJB-labeled profiles were observed in brain-injured animals in the same areas of cortex as the microglial/macrophage reactivity (Fig. 4.4H,I) and there was no evidence of FJB labeling in the sham-injured animals (Fig. 4.4G). When the total number of FJB-labeled profiles were analyzed, there was a significant effect of status ($F_{1,6}=37.01$, $p<0.01$; Fig. 4.4L) that indicated that brain-injured minocycline-treated animals had significantly more FJB-labeled profiles in the cortex than brain-injured animals that received the vehicle

($p<0.01$). These results indicate that the increase in neurodegeneration may be connected to the increase in microglial/macrophage reactivity.

Increased microglial/macrophage reactivity and neurodegeneration in brain-injured minocycline-treated animals was sustained in the cortex out to 4 weeks post-injury.

At 4 weeks post-injury, there were very few ED-1-labeled cells in the cortex of sham-injured animals (Fig. 4.5A), but brain-injured animals demonstrated visible labeling irrespective of treatment (Fig. 4.5B,C). Analysis of the amoeboid ED-1-labeled cells revealed a significant effect of status ($F_{2,11}=17.64$, $p<0.001$; Fig. 4.5G) and post hoc assessment indicated that brain-injured animals had significantly more amoeboid cells than sham-injured animals ($p<0.01$), but that minocycline treatment had no effect on the number of amoeboid cells in the cortex ($p=0.10$). There was no interaction between sex and injury status in the quantification of amoeboid microglia ($F_{2,11}=2.21$, $p=0.16$) There was also a significant status effect in the rod-like ED-1(+) cells ($F_{2,11}=10.23$, $p<0.01$; Fig. 4.5G) that indicated that both brain-injured animals that received the vehicle did not differ from sham-injured animals ($p=0.11$). Minocycline-treated brain-injured animals, however, had significantly more rod-like ED-1-labeled cells than both sham-injured ($p<0.01$) and brain-injured animals that received the vehicle ($p<0.05$). Again, there was no interaction between injury status and sex of the animal in this measure ($F_{2,11}=0.18$, $p=0.84$). Similar to previous time points, both brain injured groups displayed FJB(+) profiles in the cortex (Fig. 4.5E,F) while there was no visible labeling in the cortex of sham-injured animals (Fig. 4.5D). In quantifying the FJB-labeled profiles in the cortex, there was a significant effect of status ($F_{1,7}=18.08$, $p<0.01$; Fig. 4.5H) indicating that

brain-injured minocycline-treated animals had significantly more FJB-labeled profiles in the cortex than brain-injured animals that received the vehicle. Interestingly, there was a mild interaction between sex and status ($F_{1,7}$=5.92, p=0.05) that indicated that brain-injured males treated with minocycline had significantly more FJB(+) profiles in the cortex than any other group (p<0.05).

Minocycline treatment reversed hypoactivity in the cortex at bregma level at 3 days post-injury.

The motor cortex at the bregma level marks the anterior portion of the impact site and contains FJB-labeled profiles and activated microglia. At 3 days post-injury, brain-injured animals that received the vehicle demonstrated visibly smaller evoked field potentials compared to sham-injured and brain-injured minocycline-treated animals (Figure 4.6A). Quantitative analysis of the size of the signals from this region revealed a significant effect of status ($F_{2,13}$=4.33, p<0.05; Fig. 4.6B). Brain-injured animals treated with vehicle had significantly smaller signals than sham-injured animals (p<0.05). This deficit was rescued by treatment with minocycline as the signals from minocycline-treated brain-injured animals were similar in size to those from sham-injured animals (p=0.49). There was no interaction between sex and status ($F_{2,13}$=0.20, p=0.82). There was no significant effect of status for the latency of signal ($F_{2,13}$=0.75, p=0.49, Fig. 4.6C) or the duration of signal ($F_{2,13}$=0.61, p=0.56, Fig. 4.6D). Also, there was no interaction between status and sex for either variable (latency: $F_{2,13}$=0.37, p=0.70; duration: $F_{2,13}$=0.67, p=0.53).

Acute minocycline treatment resulted in hypoactivity in the impact site at 4 weeks post-injury.

Well within the impact site, 3mm posterior to the bregma suture, there was no effect of injury or sex on the amplitude ($F_{2,12}$=0.26, p=0.26, Fig. 4.7B) or latency ($F_{2,12}$=0.13, p=0.88, Fig. 4.7C) of the signals at 3 days post-injury. Interestingly, there was a significant status effect in the quantification of the duration of the signals ($F_{2,12}$=10.68, p<0.01, Fig. 4.7D) that indicated that the signals from brain-injured animals had a longer duration than those from sham-injured animals (p<0.05). There was also an interaction between sex and status at 3 days post-injury ($F_{2,12}$=9.81, p<0.01) and post hoc analysis revealed that brain-injured females that were treated with the vehicle had significantly longer durations than brain-injured males that were treated with the vehicles (p<0.05). Oppositely, the duration of signal from brain-injured minocycline-treated females was significantly smaller than the duration of signal from brain-injured minocycline-treated males (p<0.01). There were no differences between sham-injured males and females at 3 days post-injury (p=0.65). At 4 weeks post-injury, however, brain-injured minocycline-treated animals demonstrated visibly weaker signals than those from sham-injured and brain-injured animals that received the vehicle (Fig. 4.7A). Quantitative analysis of the signal amplitude revealed a significant effect of status ($F_{2,10}$=11.25, p<0.01, Fig. 4.7B), but no significant interaction between status and sex (($F_{2,10}$=1.77, p=0.22). Further analysis showed that the signals from sham-injured animals did not differ from those from brain-injured animals that received the vehicle (p=0.29). Brain-injured minocycline-treated animals, however, exhibited significantly smaller signals than those from sham-injured (p<0.01) and brain-injured vehicle animals

($p<0.05$, Fig. 4.7A,B). There was no significant effect of status or sex for the latency of the signal ($F_{2,10}=1.32$, $p=0.31$, Fig. 4.7C), but there was an interaction effect between sex and status for the duration of the signals ($F_{2,10}=10.30$, $p<0.01$, Fig. 4.7D). Post hoc analysis, however, revealed that there were no significant differences between male and female animals within each group or across groups. These results indicate that acute minocycline treatment can have detrimental effects on neuronal activity even 4 weeks after the injury.

4.4.2 Effects of minocycline treatment on microglial/macrophage reactivity and degeneration in the hippocampus.

Minocycline treatment decreased in microglial/macrophage reactivity while simultaneously increasing neurodegeneration in the subiculum at 3 days post-injury.

Closed head impact in the neonate rat resulted in neurodegeneration and microglial/macrophage reactivity in the hippocampus and was restricted to the dorsal aspect of the subiculum. As observed in the cortex, most Iba1(+) microglia/macrophages in the sham-injured animals exhibited the typical "resting" morphology (Fig. 4.8A), whereas in the brain-injured animals activated microglia/macrophages were also observed (Fig.4.8B,C). Quantification of Iba1(+) microglia/macrophages only revealed a group effect ($F_{2,20}=8.44$, $p<0.01$; Fig. 4.8J), with more microglia/macrophages in brain-injured animals compared to sham-injured animals ($p<0.001$); however there was no difference between the two brain-injured groups ($p=0.77$). By contrast, analysis of the proportion of activated microglia/macrophages indicated an interaction effect between group and time ($F_{2,20}=9.45$, $p<0.01$; Fig. 4.8K). Brain-injured animals had a significantly

higher proportion of activated Iba1-labeled microglia/macrophages than sham-injured animals ($p<0.001$) and minocycline-treated brain-injured animals had a lower percent of activated microglia/macrophages than brain-injured animals that were injected with vehicle ($p<0.001$). As was observed in the cortex, minocycline treatment only decreased the proportion of activated microglia/macrophages in brain-injured animals at 3 days post-injury ($p<0.001$) and not at 7 days post-injury ($p=0.47$). The sex of the animals did not affect either the total amount of Iba1 (+) microglia/macrophages ($F_{2,20}=0.30$, $p=0.74$) or the proportion of activated microglia/macrophages ($F_{2,20}=0.34$, $p=0.72$) in the subiculum.

Sham-injured animals demonstrated very little ED-1 labeling in the subiculum (Fig. 4.8D) whereas brain-injured animals demonstrated both amoeboid and rod-shaped ED-1-labeled cells in the subiculum at 3 days post-injury (Fig. 4.8E,F). While both brain-injured groups appeared to have more amoeboid cells than sham-injured animals and minocycline-treated brain-injured animals appeared to have significantly fewer amoeboid cells than brain-injured animals that received the vehicle, the status effect did not reach significance ($F_{2,4}=6.48$, $p=0.06$, Fig. 4.8L). This could, however, be due to the small sample sizes used for the ED-1 study at 3 days post-injury (N=4 animals/group). There was, however, a significant status effect when analyzing the number of rod-shaped ED-1-labeled cells in the subiculum at 3 days post-injury ($F_{2,4}=41.63$, $p<0.01$). Post hoc analysis revealed that both brain-injured groups had significantly more rod-shaped cells compared to sham-injured animals ($p<0.05$) and that brain-injured minocycline-treated animals had fewer rod-shaped cells than those treated with the vehicle ($p<0.01$) indicating an effect of treatment on this cellular subtype.

Similar to the cortex, brain-injured animals exhibited FJB-positive labeling in the subiculum (Fig. 4.8H,I) whereas sham-injured animals showed no visible labeling (Fig. 4.8G). Quantification of FJB(+) profiles revealed an effect between treatment status and time ($F_{1,17}$=44.45, p<0.001; Fig. 4.8M) with minocycline treatment increasing the number of FJB(+) cells at 3 days (p<0.001) but not at 7 days post-injury (p=0.48; Fig. 4.8M). Sex of the animals did not influence FJB reactivity in the subiculum ($F_{1,17}$=1.43, p=0.25).

Minocycline treatment resulted in increased microglial/macrophage reactivity and increased neurodegeneration in the subiculum at 15 days post-injury.

At 15 days post-injury, brain-injured animals still demonstrated visible increases in Iba1-labeled cells and contained labeled cells that displayed activated morphology whereas the labeled cells in sham-injured animals mostly exhibited resting morphologies (Fig. 4.9A). Quantification of total Iba1-labeled microglia/macrophages showed a status effect ($F_{2,9}$=22.82, p<0.001, Fig. 4.9J) in which brain-injured animals had significantly more labeled cells than sham-injured animals (p<0.001), but brain-injured minocycline-treated animals had similar numbers of total Iba1-labeled cells compared to brain-injured animals that received the vehicle (p=0.26) indicating that there was no effect of treatment on total cellularity. When slices were stained for activated microglia/macrophages using ED-1, sham-injured animals demonstrated very little labeling (Fig. 4.9D) while rod- and amoeboid-shaped cells were observed in the subiculum of brain-injured animals (Fig. 4.9E,F). Significant effects of status were observed for the counts of both amoeboid ($F_{2,9}$=20.02, p<0.001) and rod cells ($F_{2,9}$=11.84, p<0.01, Fig. 4.9K). Brain-injured animals demonstrated more ED-1 labeling in the subiculum than sham-injured animals

for measures of both amoeboid and rod phenotypes ($p<0.05$). Brain-injured animals treated with minocycline, however, had significantly more amoeboid cells in the subiculum compared to brain-injured animals that were injected with the vehicle ($p<0.01$), but there was no difference in the number of rod-like ED-1-labeled cells between brain-injured groups ($p=0.12$). This increase in amoeboid microglia/macrophages in the subiculum appeared to coincide with an increase in FJB-labeled profiles (Fig.4.9G-I,L). Quantification of FJB-positive profiles in the subiculum revealed a significant effect of status ($F_{1,6}=16.69$, $p<0.01$, Fig. 4.9L) indicating that minocycline treatment was associated with an increase in FJB labeling in the subiculum of brain-injured animals.

4.4.3 Effects of minocycline treatment on microglial/macrophage reactivity, degeneration, and axonal injury in the thalamus.

Minocycline administration reduced microglial/macrophage reactivity, but exacerbated degeneration and had no effect on axonal amyloid precursor protein accumulation at 3 days post-injury.

In the thalamus of brain-injured animals, Iba-1 and ED-1-positive reactive microglia/macrophages were observed within the dorsolateral and lateral geniculate nuclei (Fig. 4.10B,C,E,F). Microglia/macrophages in the thalamus of sham-injured animals demonstrated a resting phenotype visible through Iba1 labeling and very few ED-1-labeled cells (Figure 4.10A,D). Brain-injured animals, irrespective of treatment condition, had significantly more Iba(+) microglia/macrophages ($F_{2,20}=5.55$, $p<0.05$; Fig. 4.10G) and a significantly greater proportion of activated Iba1(+) microglia/macrophages

($F_{2,20}$=18.44, p<0.001; Fig. 4.10H) than sham-injured animals. Brain-injured animals treated with minocycline had similar numbers of microglia/macrophages and a similar proportion of activated microglia/macrophages compared with brain-injured animals that received vehicle at both 3 and 7 days post-injury (total: 3 days, p=0.80; 7 days, p=0.79; proportion: 3 days, p=0.47; 7 days, p=0.35; Fig. 4.10G and 4.10H). Neither the total Iba1(+) microglia/macrophages ($F_{2,20}$=0.10, p=0.90) nor the proportion of activated Iba1(+) microglia/macrophages ($F_{2,20}$=0.79, p=0.47) was affected by the sex of the brain-injured animals. Quantification of ED-1 labeling at 3 days post-injury revealed significant effects of status for both amoeboid ($F_{2,6}$=121.47, p<0.001, Fig. 4.10I) and rod ($F_{2,6}$=37.34, p<0.001) microglia/macrophages. Brain-injured animals had significantly more amoeboid (p<0.001) and rod (p<0.01) cells compared to sham-injured animals irrespective of treatment. Brain-injured animals treated with minocycline, however, had fewer ED-1-labeled amoeboid and rod cells compared to brain-injured animals that received the vehicle (p<0.01) indicating that minocycline was specifically affecting activated microglia/macrophages and that using ED-1 staining may be more sensitive to detect these changes.

Fluoro-Jade B(+) profiles were observed in the same thalamic nuclei as the activated microglia/macrophages in brain-injured animals (Fig. 4.11B,C). FJB(+) profiles in the thalamus of brain-injured animals exhibited both large cellular morphologies and showed evidence of smaller, fragmented profiles indicative of axonal degeneration. Sham-injured animals did not demonstrate any FJB(+) profiles (Fig. 4.11A). Quantification of FJB+ profiles revealed a significant effect of treatment status ($F_{1,17}$=4.45, p<0.05) that indicated that minocycline-treated brain-injured animals had

significantly more FJB+ profiles compared to brain-injured animals that received vehicle irrespective of sex or time ($p<0.05$; Fig. 4.11G). There was, however, an interaction effect between sex and treatment status ($F_{1,17}=6.143$, $p<0.05$) that demonstrated that female brain-injured animals that received the vehicle had fewer FJB+ reactivity than male animals that received the vehicle and female minocycline-treated animals ($p<0.05$). Evidence of traumatic axonal injury (TAI) as revealed by the presence of amyloid precursor protein (APP) accumulation within axons was observed only at 3 days post-injury (Fig. 4.11E,F) and not in sham-injured animals (Fig. 4.11D). Analysis of the number of APP(+) profiles indicated no effect of treatment status ($F_{1,7}=0.12$, $p=0.74$, Fig. 4.11H).

Minocycline treatment does not significantly affect microglial/macrophage reactivity and neurodegeneration in the thalamus at 15 days post-injury.

At 15 days post-injury, microglial/macrophage reactivity was evident in the thalamus of brain-injured animals using both Iba1 (Fig. 4.12B,C) and ED-1 (Fig. 4.12E,F) labeling. Much like the cortex and subiculum, Iba1-labeled microglia/macrophages in the thalamus of sham-injured animals displayed resting phenotype (Fig. 4.12A) and there were very few ED-1-labeled cells (Fig. 4.12D). Quantification of total Iba1-labeled microglia/macrophages showed a significant effect of injury status ($F_{2,9}=27.72$, $p<0.001$, Fig. 4.12J) where brain-injured animals had significantly more microglia/macrophages than sham-injured animals ($p<0.01$). The difference between brain-injured minocycline-treated animals and brain-injured animals that were injected with vehicle was trending on significant with the minocycline group

having slightly more microglia/macrophages than the vehicle group ($p=0.06$). Significant effects of injury status were observed for both ED-1-labeled amoeboid ($F_{2,9}=11.62$, $p<0.01$) and rod ($F_{2,9}=12.11$, $p<0.01$, Fig. 4.12K) microglia/macrophages, but post hoc analysis indicated that there were no differences between brain-injured groups (amoeboid: $p=0.28$; rod: $p=0.20$). There was no effect of status in the quantification of FJB(+) profiles in the thalamus indicating no difference between brain-injured groups ($F_{1,6}=0.05$, $p=0.83$, Fig. 4.12L).

Minocycline treatment was associated with increased microglial/macrophage reactivity but no corresponding increase in neurodegeneration at 4 weeks post-injury.

At 4 weeks post-injury, brain-injured animals still showed dense ED-1 (Fig. 4.13B,C) and FJB (Fig. 4.13E,F) labeling in the thalamus. Sham-injured animals showed no FJB labeling (Fig. 4.13D) and very little ED-1 labeling (Fig. 4.13A). Analysis of ED-1 labeling revealed significant effects of injury status for both amoeboid ($F_{2,11}=22.76$, $p<0.001$) and rod microglia/macrophages ($F_{2,11}=23.74$, $p<0.001$, Fig. 4.13G), but no interaction between status and sex for either measure (amoeboid: $F_{2,11}=0.39$, $p=0.69$; rod: $F_{2,11}=2.40$, $p=0.14$). Brain-injured animals had significantly more amoeboid and rod microglia/macrophages compared to sham-injured animals ($p<0.01$). There was a significant effect of minocycline treatment as brain-injured animals treated with minocycline had significantly more amoeboid and rod microglia/macrophages compared to brain-injured animals that received the vehicle ($p<0.05$). While brain-injured animals treated with minocycline appeared to have more FJB(+) profiles in the thalamus than those treated with vehicle, there was no significant effect of injury status ($F_{1,7}=3.78$,

p=0.09) and no significant interaction between injury status and sex of the animal ($F_{1,7}$=2.09, p=0.19).

4.4.4 Effects of acute minocycline treatment on white matter pathology

Minocycline-mediated reduction in microglial/macrophage reactivity had no effect on neurodegeneration and axonal injury in the white matter at 3 days post-injury.

In sham-injured animals, Iba1-labeled microglia/macrophages in the corpus callosum, cingulum and white matter tracts below the site of impact were sparse and displayed a large number of processes (Fig. 4.14A). At 3 days post-injury, reactive microglia/macrophages (Fig. 4.14B and 4.14C) were observed as extremely dense labeling. Quantitative analysis of Iba1(+) immunoreactivity revealed an interaction effect between group and time ($F_{2,20}$=86.23, p<0.001), wherein a post-hoc analysis indicated that both brain-injured groups had a significantly larger Iba1 immunoreactive area than that in sham-injured animals (p<0.001) and that minocycline-treated brain-injured animals had significantly smaller labeled areas at 3 days post-injury (p<0.001) but not at 7 days post-injury (p=0.45) compared to brain-injured animals injected with vehicle (Fig. 4.14G). Brain-injured animals also exhibited ED-1(+) profiles in the white matter tracts (Fig. 4.14E,F). At this time, sham-injured animals also exhibited visible ED-1 labeling in the white matter (Fig. 4.14D) although not to the degree of the brain-injured animals. There was a significant effect of status when quantifying amoeboid ($F_{2,6}$=202.98, p<0.001), but not rod ($F_{2,6}$=1.07, p=0.40, Fig. 4.14H) microglia/macrophages in the white matter at 3 days post-injury. Post hoc analysis of the amoeboid cell count revealed that both groups of brain-injured animals had significantly more amoeboid cells compared to

sham-injured animals ($p<0.001$), but minocycline-treated brain-injured animals had significantly fewer amoeboid cells compared to those that received the vehicle ($p<0.01$).

Fluoro-Jade B(+) profiles were observed at both 3 (Fig. 4.15B and 4.15C) and 7 days post-injury (not shown) in a diffuse and punctate pattern suggestive of axonal degeneration; no FJB+ labeling was observed in sham-injured animals (Fig. 4.15A). Regions containing reactive microglia/macrophages and FJB labeling also demonstrated injured axons exhibiting intra-axonal accumulation of APP (Fig. 4.15E and 4.15F) whereas sham-injured animals did not exhibit APP immunoreactivity (Fig. 4.15D). Despite the effect on Iba1 and ED-1 immunoreactivity, there was no effect of minocycline treatment on FJB reactivity ($F_{1,17}=0.007$, $p=0.93$; Fig. 4.15G) or the number of APP+ profiles in the white matter of brain-injured animals ($F_{1,5}=0.74$, $p=0.43$; Fig. 4.15H). The sex of the animals failed to demonstrate any interaction effects with group or time with regards to Iba1 ($F_{2,20}=0.82$, $p=0.46$), FJB reactivity ($F_{1,17}=0.01$, $p=0.93$), or APP ($F_{1,5}=0.74$, $p=0.43$) in the white matter tracts. The area of the white matter below the impact site in brain-injured animals was significantly smaller compared to that in sham-injured animals at both 3 and 7 days post-injury ($F_{2,20}=10.90$, $p<0.001$) and was unaffected by treatment with minocycline at either 3 days ($p=0.47$) or 7 days post-injury ($p=0.77$; Fig. 4.15H) and sex ($F_{2,20}=0.09$, $p=0.91$).

Axonal degeneration was unaffected by a minocycline-mediated increase in amoeboid microglia/macrophages in the white matter at 15 days post-injury.

At 15 days post-injury, Iba1(+) and ED-1(+) cells were counted in the white matter of sham-injured (Fig. 4.16A,D), brain-injured vehicle (Fig. 4.16B,E), and brain-

injured minocycline (Fig. 4.16C,F) animals. No effect of injury status was observed in the total Iba1 counts ($F_{2,9}$=2,02, p=0.17, Fig. 4.16J) indicating that there were no differences in the total number of Iba1(+) microglia/macrophages between sham-injured and brain-injured animals or between treatment conditions in the brain-injured group. Quantification of amoeboid and rod microglia/macrophages in ED-1-labeled sections, however, did reveal significant effects of injury status (amoeboid: $F_{2,9}$=37.23, p<0.001; rod: $F_{2,9}$=15.48, p<0.01; Fig. 4.16K). Significantly more ED-1(+) microglia/macrophages were observed in brain-injured animals compared to sham-injured animals irrespective of morphology (p<0.01), but minocycline treatment resulted in an increase in only amoeboid morphology when compared to brain-injured animals that received the vehicle (p<0.05; rod: p=0.37, Fig. 4.16K). Very few FJB(+) profiles were observed in the white matter of brain-injured animals (Fig. 4.16H,I) at 15 days post-injury and there were no positive profiles in the sham-injured animals (Fig. 4.16G). Despite observing corresponding increases in microglial/macrophage reactivity and FJB(+) profiles in the cortex and subiculum at this time point, the increase in amoeboid microglia/macrophages was not associated with an increase in FJB(+) profiles in the white matter of brain-injured minocycline-treated animals ($F_{1,6}$=2.46, p=0.17, Fig. 4.16L).

Minocycline administration did not affect axonal transport in the third week post-injury

Both sham-injured and brain-injured animals demonstrated uptake of the tracer as evident by robust fluorescence in the injected cortex (Fig. 4.17A-C). Fluoro-Gold (FG) was also present as diffuse labeling in the white matter (not shown). In the cortex

contralateral to the injection (the left cortex), the morphology associated with FG(+) profiles appeared neuronal. There was a visible increase in the number of FG(+) profiles in the cortex of sham-injured animals (Fig. 4.17D) compared to both brain-injured groups (Fig. 4.17E,F). There did not, however, appear to be a difference between the brain-injured groups. Quantification revealed that sham-injured animals did have more FG(+) labeling in the cortex (69 ± 12 profiles) than brain-injured animals that received the vehicle (25 ± 12 profiles) and brain-injured minocycline-treated animals (26 ± 8 profiles), but this effect was only trending on significance perhaps due to the small sample size ($F_{2,7}$=3.67, p=0.08, Fig. 4.17G).

Axonal degeneration was not associated with alterations in microglial/macrophage reactivity out to 4 weeks post-injury.

ED-1(+) microglia/macrophages were still observed in the white matter of brain-injured animals (Fig. 4.18B,C) at 4 weeks post-injury whereas there were very few labeled cells in the white matter of sham-injured animals (Fig. 4.18A). Similar to the 15-day quantification, there was a significant effect of injury status on ED-1(+) amoeboid microglia/macrophages in the white matter ($F_{2,11}$=104.37, p<0.001). At 4 weeks, however, there was also a significant effect of injury status on rod microglia/macrophages ($F_{2,11}$=16.75, p<0.001). Post hoc analysis revealed that brain-injured animals had significantly more ED-1(+) microglia/macrophages than sham-injured animals irrespective of morphology (p<0.001) and that brain-injured minocycline-treated animals had significantly more amoeboid (p<0.001) and rod (p<0.05) microglia/macrophages than brain-injured animals that were injected with the vehicle.

Also similar to the 15-day time point, there were very few FJB(+) profiles in the white matter of brain-injured animals (Fig. 4.18E,F) and no visible labeling in the sham-injured animals (Fig. 4.18D). There were no differences in the number of FJB(+) profiles in the white matter between minocycline-treated brain-injured animals and those that received the vehicle ($F_{1,7}$=0.30, p=0.60). Additionally, sex of the animal did not affect microglial/macrophage reactivity or neurodegeneration in the white matter (amoeboid: $F_{2,11}$=2.60, p=0.12; rod: $F_{2,11}$=0.34, p=0.72; FJB: $F_{1,7}$=0.22, p=0.65).

4.4.5 Effect of minocycline on injury-induced spatial learning and memory deficits.

Minocycline administration does not affect spatial learning and memory impairments in the second post-injury week.

Brain injury resulted in a spatial learning deficit based on the observation that brain-injured animals exhibited an increased latency to locate the hidden platform compared to sham-injured animals (Fig. 4.19A). A repeated measures ANOVA revealed main effects of injury status ($F_{2,84}$=3.14, p=0.05) and training day ($F_{3,84}$=35.51, p<0.001), but no interaction effect between status and training day ($F_{6,84}$=0.97, p=0.45) or between group, training day, and sex ($F_{6,84}$=1.02, p=0.42; Fig. 4.19A). Post-hoc analysis indicated that sham-injured animals took a shorter amount of time to locate the hidden platform compared to brain-injured animals that received vehicle (p<0.05), but not those that received minocycline (p=0.06). However, both groups of brain-injured animals had similar latencies to the hidden platform across treatment days (p=0.42) indicating that minocycline treatment had no effect on injury-induced spatial learning deficits. The decreased efficiency in learning the location of the platform was associated with a

retention deficit based on the observation that brain-injured animals spent less time in the platform zone ($F_{2,28}$=3.41 $p<0.05$; Fig. 4.19B) that was not affected by treatment or sex ($F_{2,28}$=0.31, p=0.73). There was no difference in the amount of time spent in the peripheral zone between brain- and sham-injured animals ($F_{2,28}$=2.61, p=0.09) possibly because female rats, irrespective of injury/treatment status, spent significantly more time in the peripheral zone compared to male rats ($F_{1,28}$=4.21, $p<0.05$, Fig. 4.19B). Importantly, the learning and memory deficits appeared not to be due to problems in vision based on the lack of either a group or sex effect in the visible platform trial ($F_{2,28}$=1.67, p=0.21; Fig. 4.19B) or problems in motor function based on similar swim speeds in sham- and brain-injured male and female rats (sham-injured: 23 ± 0.84 cm/s; brain-injured vehicle: 24 ± 1.39 cm/s; brain-injured minocycline: 21 ± 0.88 cm/s; $F_{2,28}$=0.49, p=0.62).

4.5 DISCUSSION

The present study demonstrates that short-term minocycline administration initiated immediately following closed head injury in the neonate rat reduced the total number of microglia/macrophages and microglial/macrophage activation when evaluated upon termination of treatment. This reduction was accompanied by an increase in the extent of neurodegeneration and was not sustained to 4 days after treatment ended. In the weeks post-injury, however, acute minocycline treatment was associated with an increase in both neurodegeneration and microglial/macrophage reactivity and resulted in hypoactivity in a region of the injured motor cortex. Moreover, there was no attenuation of spatial learning and memory deficits that were tested in the second week post-injury. Collectively, these data suggest that acute minocycline treatment may not be a viable strategy for TBI in the neonate.

Short-term administration of minocycline (similar to the paradigm used in this study) has been found effective in decreasing microglial/macrophage activation following neonatal hypoxic ischemia (Cai et al., 2006, Fan et al., 2006, Lechpammer et al., 2008, Cikla et al., 2016), pediatric cardiac arrest (Tang et al., 2010), neonatal repetitive TBI (Hanlon et al., 2016a), and adult TBI (Bye et al., 2007, Homsi et al., 2010, Siopi et al., 2011). The reduction in activated microglia/macrophages was accompanied by an attenuation of neuronal damage (Cikla et al., 2016), a decrease in asphyxia-induced neurodegeneration (Tang et al., 2010), and a reduction of lesion volume following TBI (Homsi et al., 2010). However, the association between microglial/macrophage activation and attendant neurodegeneration in brain injury is not quite clear-cut: minocycline treatment following TBI in the adult mouse decreased F4/80-labeled microglia that

exhibited the activated phenotype without affecting lesion volume or TUNEL labeling (Bye et al., 2007) whereas in a model of neonatal stroke minocycline failed to reduce microglial activation, but still had a beneficial effect on lesion volume (Fox et al., 2005). In contrast to all the above studies, the decrease in acute microglial activation observed in the present study was in fact, associated with an increase in the number of FJB+ neurons suggestive of either a lack of clearance of degenerating neurons or that microglia may play a more active role in neuronal survival following injury to the immature brain (Potter et al., 2009). This latter possibility is supported by the fact that depletion of microglia following stroke in neonatal rats causes an increase in lesion size (Faustino et al., 2011). Microglial/macrophage activation also occurs in white matter tracts following injury to either the neonate or the adult brain. In the neonate, HI-induced microglial activation and the concomitant oligodendrocyte cell death, myelin loss and decrease in white matter volume were attenuated by minocycline (Cai et al., 2006, Fan et al., 2006, Lechpammer et al., 2008). In the adult mouse, TBI-induced loss of corpus callosum volume was attenuated by minocycline treatment (Siopi et al., 2011). In contrast, short-term administration of minocycline in the present study did not affect axonal injury, degeneration, or transport, an observation that was similar to those in a model of repetitive brain trauma in the neonate rat (Hanlon et al., 2016a) and closed head injury in the adult mouse (Homsi et al., 2010). In this regard, genetic ablation of microglia in the white matter did not reduce trauma-induced axonal injury (Bennett and Brody, 2014).

A sustained effect on microglial/macrophage activation and neurodegeneration was not observed at 7 days post-injury after the treatment was terminated, but because we administered minocycline to the developing brain, it was worthwhile to assess if this

acute manipulation had any effect on neuropathology in the weeks after ending treatment. When we looked at microglial/macrophage reactivity and neurodegeneration out to 4 weeks post-injury, we found that minocycline-treated brain-injured animals exhibited increases in both of these measures, specifically in the cortex and subiculum, and this may suggest that the microglia/macrophages are playing an active role in the observed neurodegeneration. This increase in neurodegeneration and microglial/macrophage reactivity was associated with hypoactivity as measured by evoked field potential recordings at 4 weeks post-injury. In contrast to our results, Fan et al. (2006) observed beneficial effects of minocycline 2 weeks after ending an acute treatment paradigm. Minocycline-treated brain-injured animals demonstrated a sustained decrease in microglial reactivity that was associated with decreased white matter damage and behavioral improvements. These differential effects could be due to either dosing (Fan et al. used a pre-injury loading dose and only administered the drug once a day for 3 days) or the type of injury (HI vs TBI). There are a few studies, however, that indicate that minocycline administration may cause deleterious effects when used in the immature brain. For example, an increase in lesion severity was observed in HI rats treated with minocycline (Tsuji et al., 2004). Similarly, minocycline treatment exacerbated apoptosis caused by NMDA receptor antagonism (Inta et al., 2016).

Minocycline, however, did not cause an attenuation or exacerbation of injury-induced spatial learning and retention deficits in the second week post-injury. Consistent with these observations, minocycline did not affect motor deficits in brain-injured adult mice (Bye et al., 2007) or spatial learning and memory following HI in neonatal mice (Cikla et al., 2016) and TBI in adult rats (Kelso et al., 2011). This lack of sustained

effect may be due to the fact that the half-life of minocycline in rodents is rather short (2-3 hours) (Andes and Craig, 2002) or the fact that in the second week post-injury, minocycline administration resulted in an exacerbation of cellular neuropathology. In contrast, a number of studies have demonstrated that minocycline reduced behavioral impairments days and weeks after treatment termination in HI-injured neonatal rats (Fan et al., 2006) and in adult mice following TBI (Homsi et al., 2010, Siopi et al., 2012). Again, it is possible that these differences may relate to the variability in dose and dosing paradigms, the type of injury and the age of the animal employed in the various studies.

When appropriate, our statistical analyses included sex as an independent variable and led to the observation that sex did not consistently influence injury-induced microglial/macrophage reactivity, neurodegeneration or cognitive function. In this regard, a recent study reported that injury-induced increases in microglial numbers were not dependent on the sex of the injured neonate animal (Chhor, et al. 2016). However, injury-induced mitochondrial dysfunction (Robertson and Saraswati, 2015), changes in neuronal structure (Semple, et al., 2016) and social recognition (Semple et al., 2016) were more apparent in male rats, whereas injury-induced deficits in play behavior was predominantly observed in female rats (Mychasiuk, et al., 2014). In our study, sex did not influence the effects of minocycline in the various outcomes, an observation that is in contrast to the effect of progesterone which was effective in reversing mitochondrial dysfunction only in male rat pups (Robertson and Saraswati, 2015). These observations underscore the importance of utilizing sex as a variable in histologic and behavioral analyses when treatment injury-induced alterations and efficacy of neuroprotective strategies are tested.

The results described here have several limitations. First, while the efficacy of this dose has been well-documented (Buller et al., 2009), only a single dose (45 mg/kg/injection) and dosing paradigm was utilized. Adjusting the dose or extending the dosing paradigm may alter the chronic effects of minocycline. For example, neonatal mice that received a lower daily dose (22.5 mg/kg) of minocycline for 6 days showed improvement in white matter pathology following hypoxia-ischemia (Carty et al., 2008), raising the possibility that 45 mg/kg may be too high in the neonates. And while no other study has shown the exacerbated chronic cellular pathology that we observed, it is possible that this is a consequence of the dose/dosing paradigm and further dose response studies are needed.

Secondly, while minocycline was an effective tool in decreasing microglial/macrophage reactivity following injury, this compound has several off-target effects. Minocycline deposits in the bones and teeth of treated patients causing discoloration (Douglas, 1963, Poliak et al., 1985, McCleskey et al., 2004, Sanchez et al., 2004), and we routinely observe a bright yellow discoloration in the skulls of our minocycline-treated sham- and brain-injured rats (not shown). Due to its ability to chelate calcium and deposit in teeth and bones, the drug is not typically recommended for use in pregnant women or young children (Buller et al.,2009). Another common side effect of minocycline treatment is gastrointestinal disturbances due to its antibiotic properties (Goulden et al., 1996, Smith and Leyden, 2005) and alteration of the gut microbiome has been shown to influence neuroinflammation and behavioral processes such as cognition (Rea et al., 2016, Galland, 2014). Additionally, minocycline treatment can cause a lupus-like autoimmune disorder referred to as minocycline-induced lupus

(MIL) that can have a wide array of detrimental effects including hepatitis, systemic inflammation resulting in arthritis, weight loss, and fatigue (Schlienger et al., 2000). While these side effects are commonly associated with chronic minocycline treatment in humans, it is still possible that the results we observed are confounded by systemic influences. Minocycline administration has also caused neurological side effects as many chronic users complain of vertigo, ataxia, and headaches (Williams et al., 1974, Smith and Leyden, 2005). Minocycline has also been shown to influence astrocytic reactivity and neuronal activity. While we did not observe a treatment effect on injury-induced astrocytic reactivity at 3 days, administering minocycline prior to exposing mixed neuron-astrocyte cultures to Aβ significantly reduced astrocytic morphologic changes and Aβ-induced increases in pro-inflammatory cytokine release (Garwood et al., 2011). In a model using LPS challenge in adult rats, however, minocycline administration decreased both Iba1 and ED-1 expression without affecting GFAP expression (Yoon et al., 2012) indicating conflicting evidence for minocycline's effects on astrocytic reactivity and may once again be attributable to differences in dosing. Minocycline has also been shown to directly alter neuronal activity through modulation of glutamatergic neurotransmission thus making interpretation of minocycline's effects on evoked field potential recordings difficult (Gonzalez et al., 2007). For these reasons, the utilization of minocycline as both a tool for microglial/macrophage inhibition and a potential therapeutic should be carefully considered.

Thirdly, only spatial learning and memory in the Morris water maze was used to test cognitive function, although minocycline has been effective in reducing deficits in this measure of cognition (Fan et al., 2006, Lam et al., 2013). Nevertheless, future studies

warrant the use of a wider range of functional outcomes that may allow researchers to better understand the differential effects of minocycline treatment following injury to the developing brain. Additional future investigations should investigate the effect of minocycline on microglial/macrophage phenotype as it has been documented that minocycline can selectively target the pro-inflammatory M1 phenotype (Kobayashi et al., 2013) and similarly decrease harmful mediators associated with an M1 phenotype such as IL-1β and TNFα (Yrjanheikki et al., 1999, Wang et al., 2005, Bye et al., 2007, Wasserman and Schlichter, 2007).

4.6 FIGURE LEGENDS

Figure 4.1 Experimental Timelines. (A) Schematic representing the treatment paradigm and histological/behavioral time points. **(B)** Schematic representing the treatment paradigm and electrophysiological time points.

Figure 4.2 Glial reactivity in the injured cortex at 3 and 7 days post-injury following acute minocycline treatment. Representative photomicrographs of Iba1 **(A-C)**, ED-1 **(D-F)**, and GFAP **(G-I)** labeling in the cortex of sham-injured **(A,D,G)**, brain-injured animals that received the vehicle **(B,E,H)** and minocycline-treated brain-injured animals **(C,F,I)** at 3 days post-injury. **Insets in panel F** represent examples of ED-1 labeled microglia/macrophages in amoeboid or rod form. Quantification of total Iba1-labeled microglia/macrophages **(G)** and the percent activated microglia/macrophages **(H)** at 3 and 7 days post-injury. Quantification of ED-1-labeled microglia/macrophages displaying amoeboid or rod morphology **(L)** and the percent area labeled with GFAP staining in the injured cortex **(M)** at 3 days post-injury. *$p \leq 0.05$ compared to corresponding sham-injured group. #$p \leq 0.05$ compared to the brain-injured vehicle group. Error bars represent the standard error of the mean. Scale bar **(F)**= 100μm; Scale bar **(F Insets)** = 10μm; Scale bar **(I)** = 500μm.

Figure 4.3 Degeneration and gross tissue pathology in the injured cortex at 3 and 7 days post-injury following minocycline treatment. Representative photomicrographs of FJB labeling in the cortex **(A-C)** and Nissl-Myelin-stained sections **(D-F)** of sham-injured **(A,D)**, brain-injured vehicle **(B,E)** and minocycline-treated brain-injured animals

(C,F) at 3 days post-injury. Quantification of total FJB-labeled profiles in the cortex at 3 and 7 days post-injury **(G)**. #p≤0.05 compared to the brain-injured vehicle group. Error bars represent the standard error of the mean. Scale bar **(C)**= 100μm; Scale bar **(F)** = 500μm μm.

Figure 4.4 Histological outcomes in the injured cortex at 15 days post-injury following acute minocycline treatment. Representative photomicrographs of Iba1 **(A-C)**, ED-1 **(D-F)** and FJB (**G-I**) labeling in the cortex of sham-injured **(A,D,G)**, brain-injured vehicle **(B,E,H)** and brain-injured minocycline-treated animals **(C,F,I)** at 15 days post-injury. Quantification of total Iba1-labeled microglia/macrophages **(J)**, ED-1 labeled microglia/macrophages displaying amoeboid or rod morphology **(K, insets)**, and total FJB-labeled profiles **(L)** in the cortex at 15 days post-injury. *p≤0.05 compared to corresponding sham-injured group. #p≤0.05 compared to the brain-injured vehicle group. Error bars represent the standard error of the mean. Scale bar **(I)**= 100μm.

Figure 4.5 Histological outcomes in the injured cortex at 4 weeks post-injury following acute minocycline treatment. Representative photomicrographs of ED-1 **(A-C)** and FJB (**D-F**) labeling in the cortex of sham-injured **(A,D)**, brain-injured vehicle **(B,E)** and brain-injured minocycline-treated animals **(C,F)** at 4 weeks post-injury. Quantification of ED-1-labeled microglia/macrophages displaying amoeboid or rod morphology **(G)**, and total FJB-labeled profiles **(H)** in the cortex at 4 weeks post-injury. *p≤0.05 compared to corresponding sham-injured group. #p≤0.05 compared to the brain-

injured vehicle group. Error bars represent the standard error of the mean. Scale bar **(F)**= 100μm.

Figure 4.6 Evoked field potential recordings from the injured cortex at bregma following acute minocycline treatment. **(A)** Representative traces from the bregma-level cortex of sham-injured, brain-injured vehicle, and brain-injured minocycline-treated animals at 3 days post-injury. Quantification of signal amplitude **(B)**, signal latency **(C)**, and signal duration **(D)** in the bregma-level cortex at 3 days post-injury. *p≤0.05 compared to corresponding sham-injured group.

Figure 4.7 Evoked field potential recordings from the injured cortex at -3mm at 3 days and 4 weeks following acute minocycline treatment. **(A)** Representative traces from the -3mm level cortex of sham-injured, brain-injured vehicle, and brain-injured minocycline-treated animals at 4 weeks post-injury. Quantification of signal amplitude **(B)**, signal latency **(C)**, and signal duration **(D)** in the -3mm-level cortex at 3 daysand 4 weeks post-injury. *p≤0.05 compared to corresponding sham-injured group.

Figure 4.8 Acute histological outcomes in the injured subiculum following minocycline treatment. Representative photomicrographs of Iba1 **(A-C)**, ED-1 **(D-F)**, and FJB **(G-I)** labeling in the cortex of sham-injured **(A,D,G)**, brain-injured vehicle **(B,E,H)** and minocycline-treated brain-injured animals **(C,F,I)** at 3 days post-injury. Quantification of total Iba1-labeled microglia/macrophages at 3 and 7 days post-injury **(J)**, the percent activated Iba1-labeled microglia/macrophages at 3 and 7 days post-injury

(K), ED-1-labeled microglia/macrophages displaying amoeboid or rod morphology at 3 days post-injury **(L)**, and total FJB-labeled profiles in the cortex at 3 and 7 days post-injury **(M)** . *p≤0.05 compared to corresponding sham-injured group. #p≤0.05 compared to the brain-injured vehicle group. Error bars represent the standard error of the mean. Scale bar **(F)**= 100μm.

Figure 4.9 Histological outcomes in the injured subiculum at 15 days post-injury following acute minocycline treatment. Representative photomicrographs of Iba1 **(A-C)**, ED-1 **(D-F)** and FJB (**G-I**) labeling in the subiculum of sham-injured **(A,D,G)**, brain-injured vehicle **(B,E,H)** and brain-injured minocycline-treated animals **(C,F,I)** at 15 days post-injury. Quantification of total Iba1-labeled microglia/macrophages **(J)**, ED-1 labeled microglia/macrophages displaying amoeboid or rod morphology **(K)**, and total FJB-labeled profiles **(L)** in the subiculum at 15 days post-injury. *p≤0.05 compared to corresponding sham-injured group. #p≤0.05 compared to the brain-injured vehicle group. Error bars represent the standard error of the mean. Scale bar **(I)**= 100μm.

Figure 4.10 Microglial/macrophage reactivity in the injured thalamus following minocycline treatment at 3 and 7 days post-injury. Representative photomicrographs of Iba1 **(A-C)** and ED-1 **(D-F)** labeling in the thalamus of sham-injured **(A,D)**, brain-injured vehicle **(B,E)** and minocycline-treated brain-injured animals **(C,F)** at 3 days post-injury. Quantification of total Iba1-labeled microglia/macrophages **(G)** and the percent activated microglia/macrophages **(H)** at 3 and 7 days post-injury, and ED-1 labeled microglia/macrophages displaying amoeboid or rod morphology **(I)** in the thalamus at 3

days post-injury *p≤0.05 compared to corresponding sham-injured group. #p≤0.05 compared to the brain-injured vehicle group Scale bar **(F)**= 100μm.

Figure 4.11 Degeneration and axonal injury in the injured thalamus at 3 and 7 days post-injury following acute minocycline treatment. Representative photomicrographs of FJB **(A-C)** and APP **(D-F)** labeling in the thalamus of sham-injured **(A,D)**, brain-injured vehicle **(B,E)** and minocycline-treated brain-injured animals **(C,F)** at 3 days post-injury. Quantification of total FJB-labeled profiles at 3 and 7 days post-injury **(G)** and the total APP-labeled profiles at 3 days post-injury **(H)**. Scale bar **(F)**= 100μm.

Figure 4.12 Microglial/macrophage reactivity and degeneration in the injured thalamus at 15 days post-injury following acute minocycline treatment. Representative photomicrographs of Iba1 **(A-C)**, ED-1 **(D-F)** and FJB (**G-I**) labeling in the thalamus of sham-injured **(A,D,G)**, brain-injured vehicle **(B,E,H)** and brain-injured minocycline-treated animals **(C,F,I)** at 15 days post-injury. Quantification of total Iba1-labeled microglia/macrophages **(J)**, ED-1 labeled microglia/macrophages displaying amoeboid or rod morphology **(K)**, and total FJB-labeled profiles **(L)** in the thalamus at 15 days post-injury. *p≤0.05 compared to corresponding sham-injured group. #p≤0.05 compared to the brain-injured vehicle group. Error bars represent the standard error of the mean. Scale bar **(I)**= 100μm.

Figure 4.13 Microglial/macrophage reactivity and degeneration in the injured thalamus at 4 weeks post-injury following acute minocycline treatment.

Representative photomicrographs of ED-1 **(A-C)** and FJB (**D-F**) labeling in the thalamus of sham-injured **(A,D)**, brain-injured vehicle **(B,E)** and brain-injured minocycline-treated animals **(C,F)** at 4 weeks post-injury. Quantification of ED-1-labeled microglia/macrophages displaying amoeboid or rod morphology **(G)**, and total FJB-labeled profiles **(H)** in the thalamus at 4 weeks post-injury. *p≤0.05 compared to corresponding sham-injured group. #p≤0.05 compared to the brain-injured vehicle group. Error bars represent the standard error of the mean. Scale bar **(F)**= 100μm.

Figure 4.14 Effect of acute minocycline treatment on microglial/macrophage reactivity in the white matter at 3 and 7 days post-injury. Representative photomicrographs of Iba1 **(A-C)** and ED-1 **(D-F)** labeling in the white matter of sham-injured **(A,D)**, brain-injured vehicle **(B,E)** and minocycline-treated brain-injured animals **(C,F)** at 3 days post-injury. Quantification the percent area of Iba-1 labeling at 3 and 7 days post-injury **(G)** and ED-1-labeled microglia/macrophages displaying amoeboid or rod morphology at 3 days post-injury **(H)**. *p≤0.05 compared to corresponding sham-injured group. #p≤0.05 compared to the brain-injured vehicle group. Error bars represent the standard error of the mean. Scale bar **(F)**= 100μm.

Figure 4.15 Effect of acute minocycline treatment on degeneration and axonal injury in the white matter at 3 and 7 days post-injury. Representative photomicrographs of FJB **(A-C)** and APP **(D-F)** labeling in the white matter of sham-injured **(A,D)**, brain-injured vehicle **(B,E)** and minocycline-treated brain-injured animals **(C,F)** at 3 days post-injury. Quantification of total FJB-labeled profiles at 3 and 7 days

post-injury **(G)**, total APP-labeled profiles at 3 days post-injury **(H)**, and white matter area at 3 and 7 days post-injury **(I)**. Error bars represent the standard error of the mean. Scale bar **(F)**= 100μm.

Figure 4.16 Microglial/macrophage reactivity and degeneration in the injured white matter at 15 days post-injury following acute minocycline treatment. Representative photomicrographs of Iba1 **(A-C)**, ED-1 **(D-F)** and FJB (**G-I**) labeling in the white matter of sham-injured **(A,D,G)**, brain-injured vehicle **(B,E,H)** and brain-injured minocycline-treated animals **(C,F,I)** at 15 days post-injury. Quantification of total Iba1-labeled microglia/macrophages **(J)**, ED-1 labeled microglia/macrophages displaying amoeboid or rod morphology **(K)**, and total FJB-labeled profiles **(L)** in the white matter at 15 days post-injury. *p≤0.05 compared to corresponding sham-injured group. #p≤0.05 compared to the brain-injured vehicle group. Error bars represent the standard error of the mean. Scale bar **(I)**= 100μm.

Figure 4.17 Effect of minocycline on axonal transport of retrograde tracer Fluoro-Gold in the third week post-injury.

Representative photomicrographs of the injection site in the right cortex **(A-C)** and FG(+) profiles in the cortex contralateral to the injection **(D-F)** in sham-injured **(A,D)**, brain-injured vehicle **(B,E)**, and brain-injured minocycline **(C,F)** animals. Quantification of the number of FG(+) profiles in the cortex contralateral to injection **(G)**. Scale bar **(C)** = 200μm, Scale bar **(F)** = 100μm.

Figure 4.18 Microglial/macrophage reactivity and degeneration in the injured white matter at 4 weeks post-injury following acute minocycline treatment.

Representative photomicrographs of ED-1 **(A-C)** and FJB (**D-F**) labeling in the thalamus of sham-injured **(A,D)**, brain-injured vehicle **(B,E)** and brain-injured minocycline-treated animals **(C,F)** at 4 weeks post-injury. Quantification of ED-1-labeled microglia/macrophages displaying amoeboid or rod morphology **(G)**, and total FJB-labeled profiles **(H)** in the white matter at 4 weeks post-injury. *p≤0.05 compared to corresponding sham-injured group. #p≤0.05 compared to the brain-injured vehicle group. Error bars represent the standard error of the mean. Scale bar **(F)**= 100μm.

Figure 4.19 Spatial learning and memory assessment following acute minocycline treatment. (A) Latency to the hidden platform in sham-injured, brain-injured vehicle, and brain-injured minocycline animals over 4 days (post-injury days 10-13). **(B)** Probe trial assessment on post-injury day 14 with the platform removed from the maze. Quantification of time spent in the zones closest (platform) and furthest away (peripheral) from the former platform location and time it took to locate the platform when it was put back in the maze and made visible. *p≤0.05 compared to corresponding sham-injured group. Error bars represent the standard error of the mean.

4.7 TABLES & FIGURES

Table 4.1 Listing of animals used in statistical analysis for each outcome

		Time point			
		3d	**7d**	**15d**	**28d**
Outcome	**Group**	**N**	**N**	**N**	**N**
Iba1	Sham	4	3	4	N/A
	Injured Vehicle	7	4	4	
	Injured Minocycline	9	5	4	
ED-1	Sham	3	N/A	4	6
	Injured Vehicle	3		4	5
	Injured Minocycline	3		4	6
GFAP	Sham	4	N/A	N/A	N/A
	Injured Vehicle	3			
	Injured Minocycline	4			
NM (white matter area)	Sham	4	3	N/A	N/A
	Injured Vehicle	7	4		
	Injured Minocycline	9	5		
FJB	Sham	N/A	N/A	N/A	N/A
	Injured Vehicle	7	4	4	5
	Injured Minocycline	9	5	4	6
APP	Sham	N/A	N/A	N/A	N/A
	Injured Vehicle	4			
	Injured Minocycline	5			
Bregma E-phys	Sham	7	N/A	N/A	N/A
	Injured Vehicle	6			
	Injured Minocycline	6			
-3mm E-phys	Sham	7	N/A	N/A	4
	Injured Vehicle	6			4
	Injured Minocycline	5			8
Spatial Learning	Sham	11			
	Injured Vehicle	11			
	Injured Minocycline	12			
Fluoro-Gold	Sham	2			
	Injured Vehicle	4			
	Injured Minocycline	4			
Total	**Sham**	**37**			
	Injured Vehicle	**41**			
	Injured Minocycline	**50**			

*Overlap in histology outcomes and spatial learning/15d histology

Figure 4.1 Experimental Timelines.

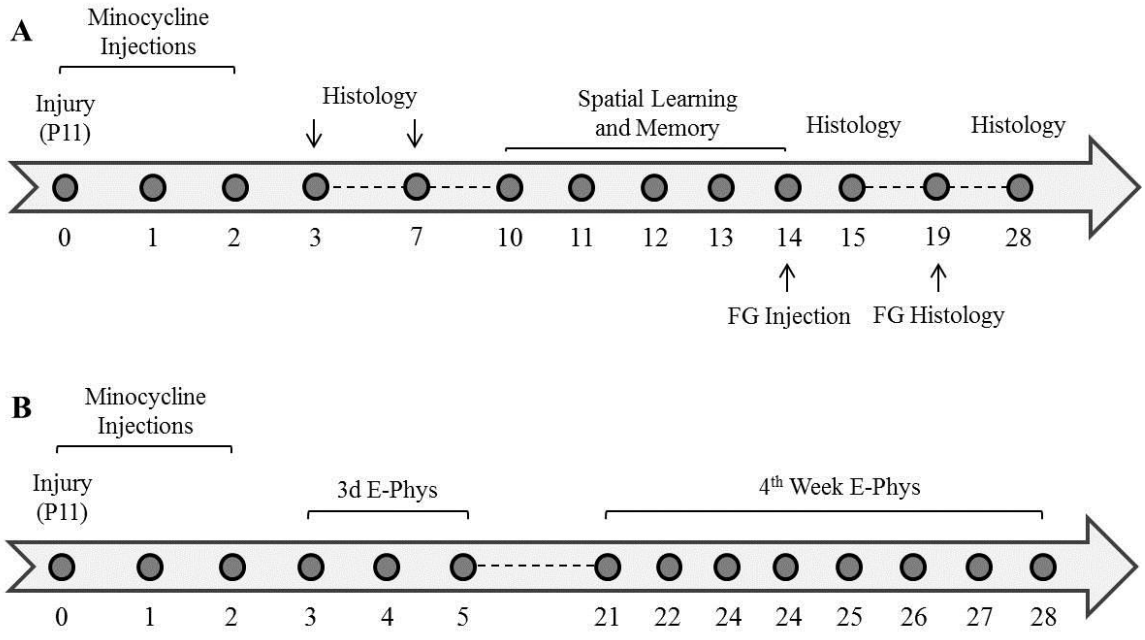

Figure 4.2 Glial reactivity in the injured cortex at 3 and 7 days post-injury following acute minocycline treatment.

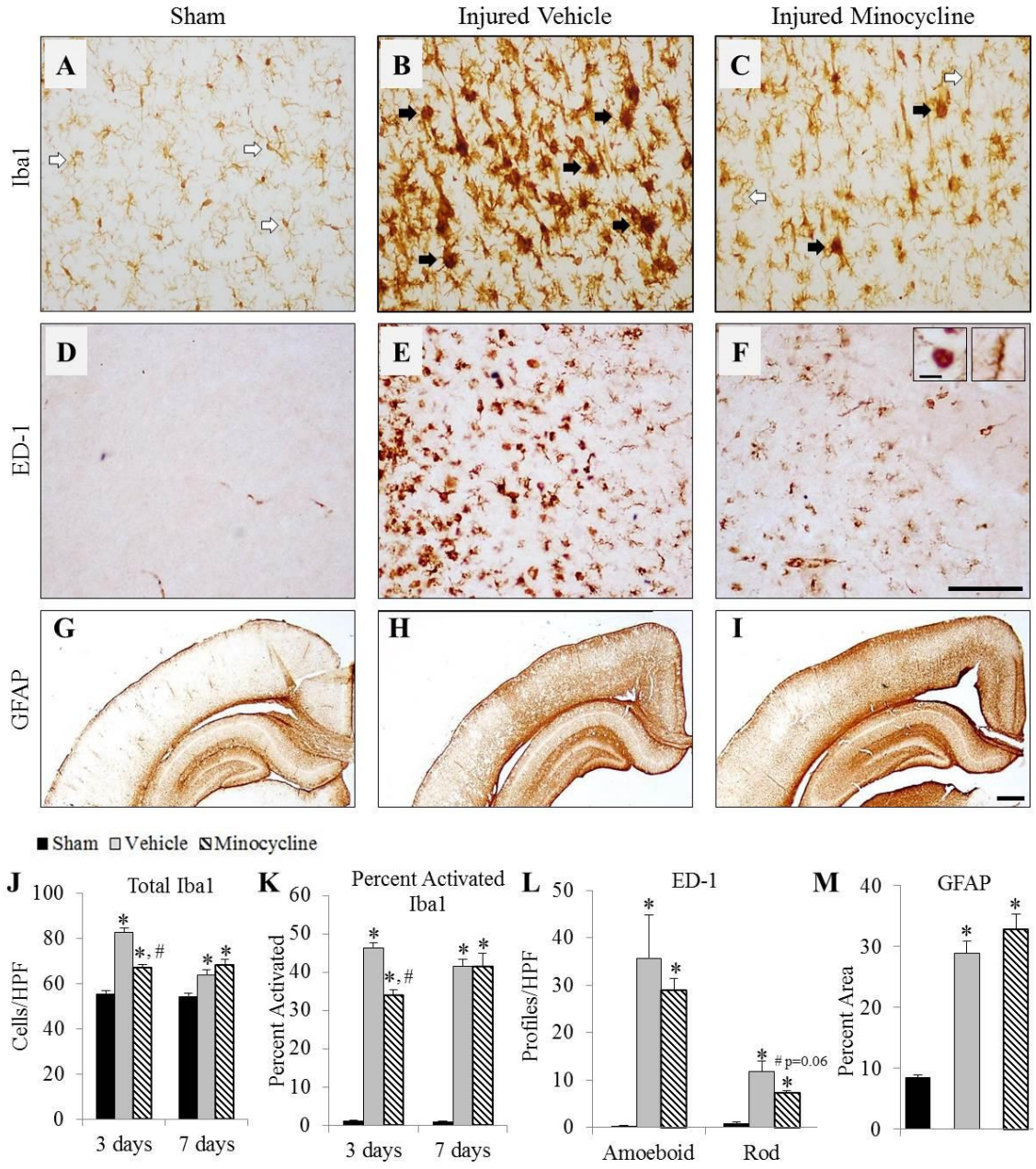

Figure 4.3 Degeneration and gross tissue pathology in the injured cortex at 3 and 7 days post-injury following minocycline treatment.

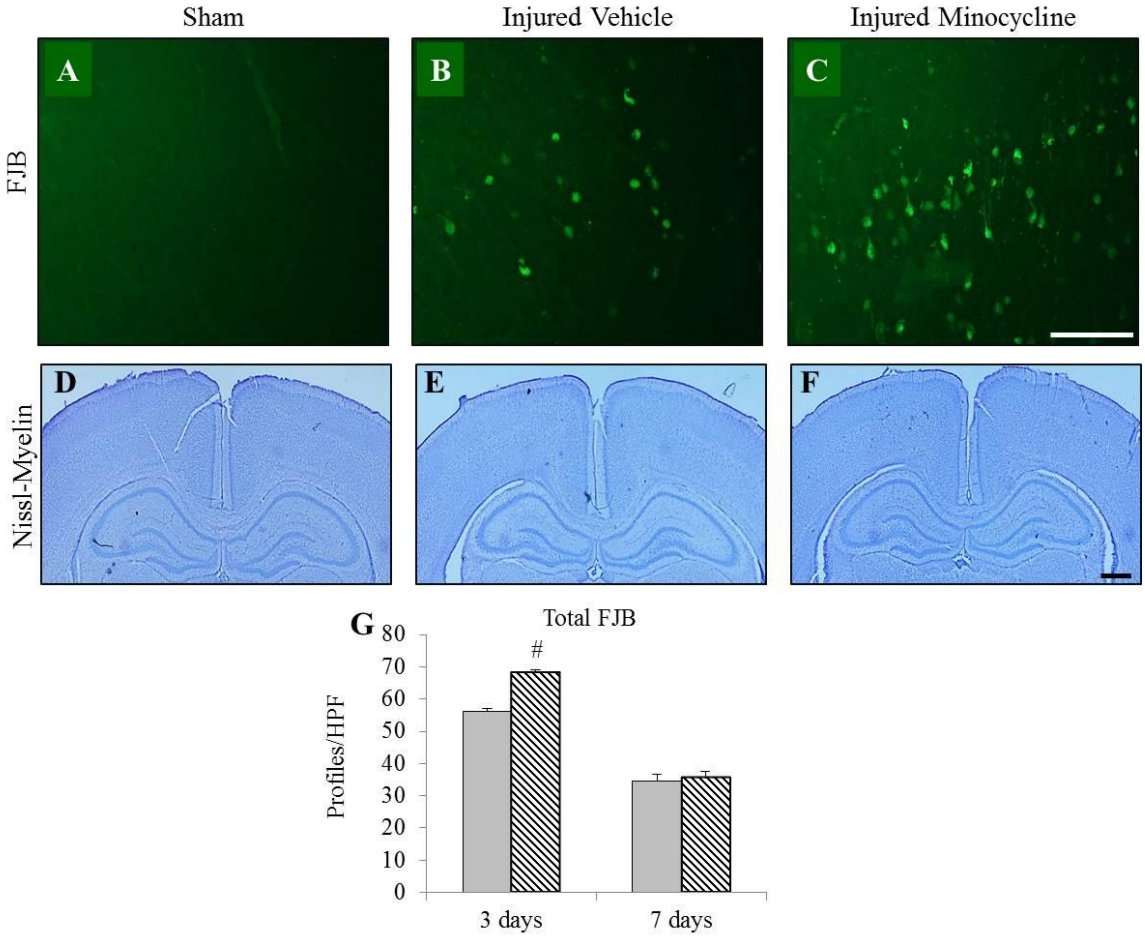

Figure 4.4 Microglial/macrophage reactivity and neurodegeneration in the injured cortex at 15 days post-injury following acute minocycline treatment.

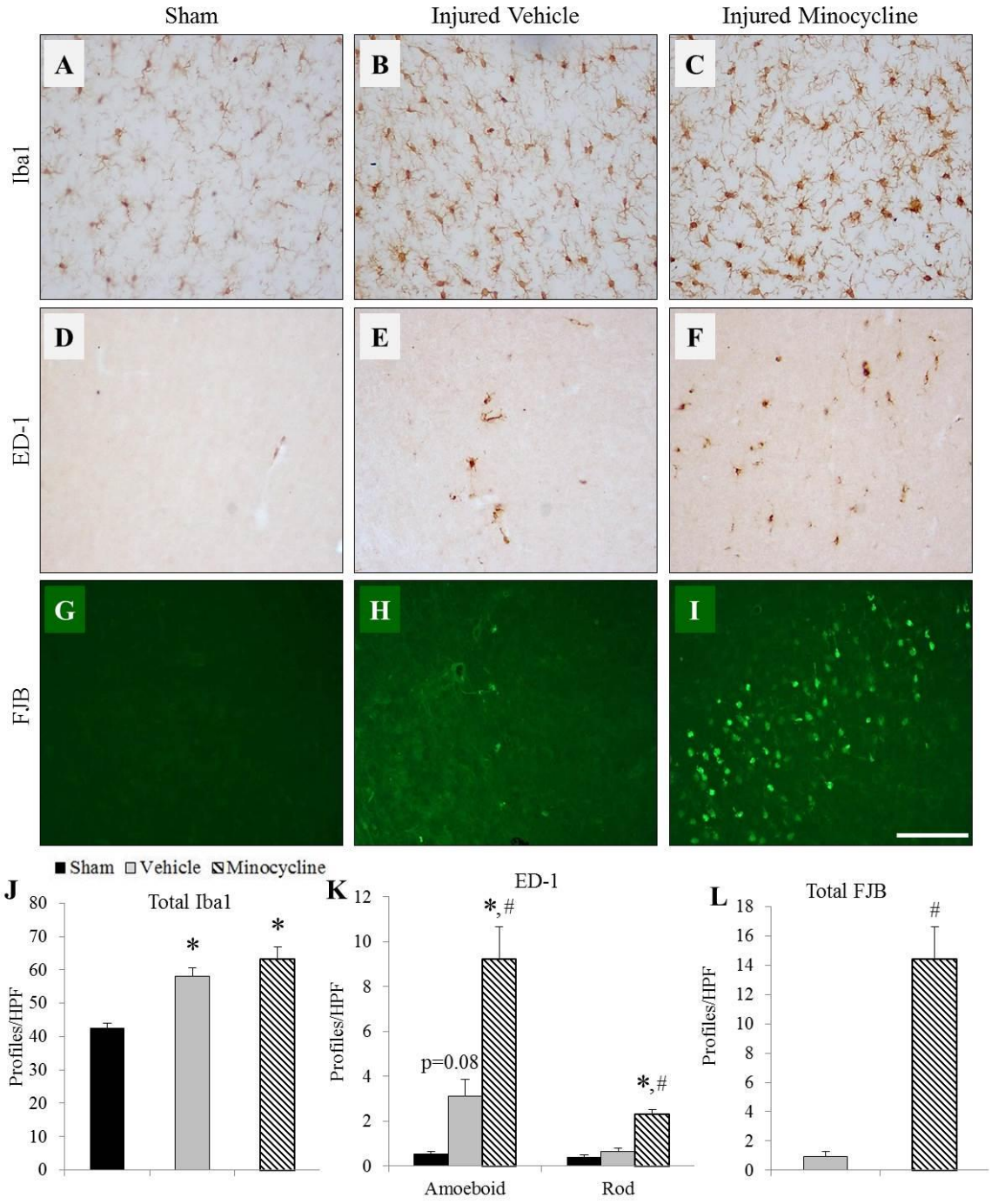

Figure 4.5 Microglial/macrophage reactivity and neurodegeneration in the injured cortex 4 weeks post-injury following acute minocycline treatment.

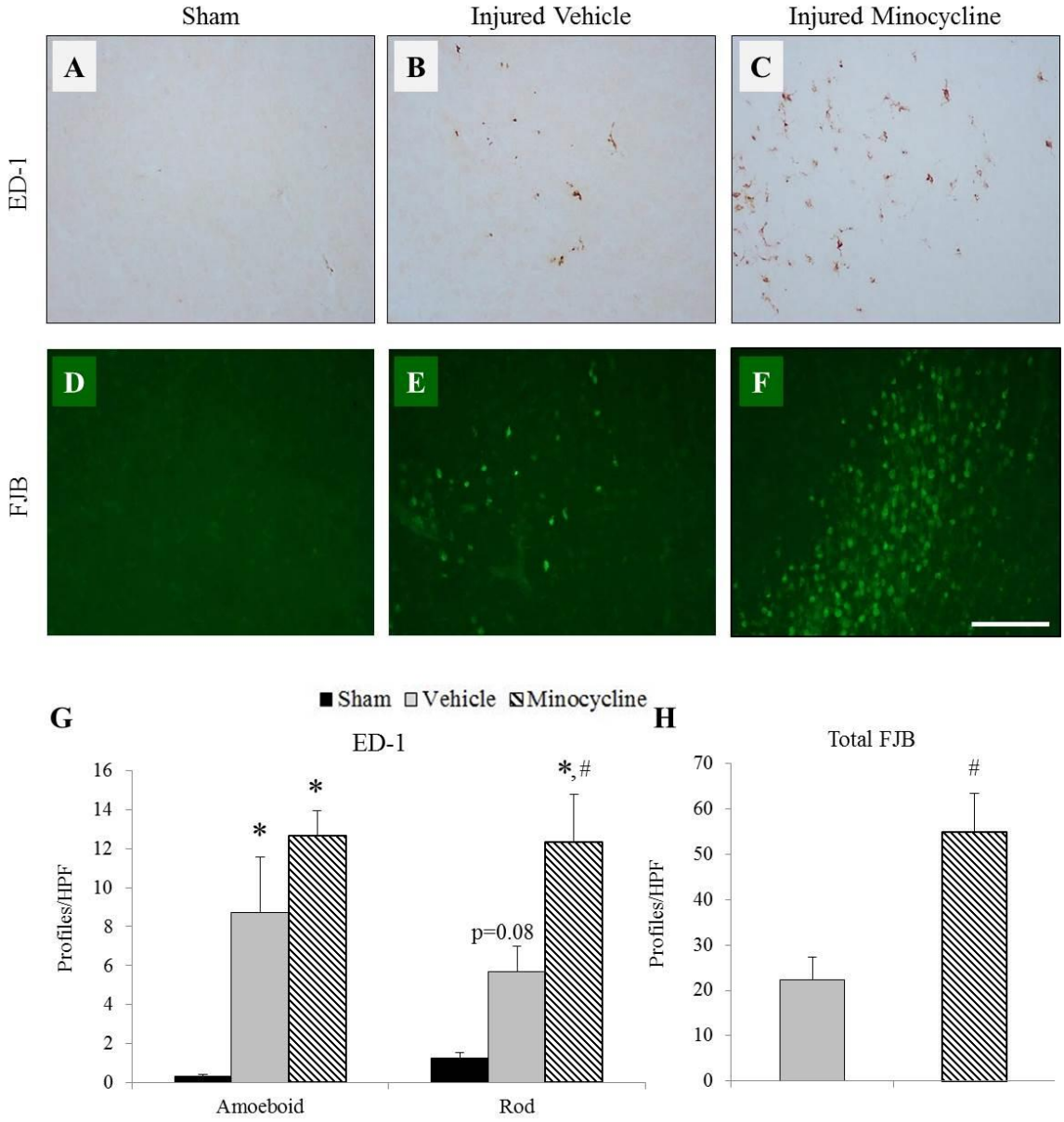

Figure 4.6 Evoked field potential (EFP) recordings from the injured cortex at bregma following acute minocycline treatment.

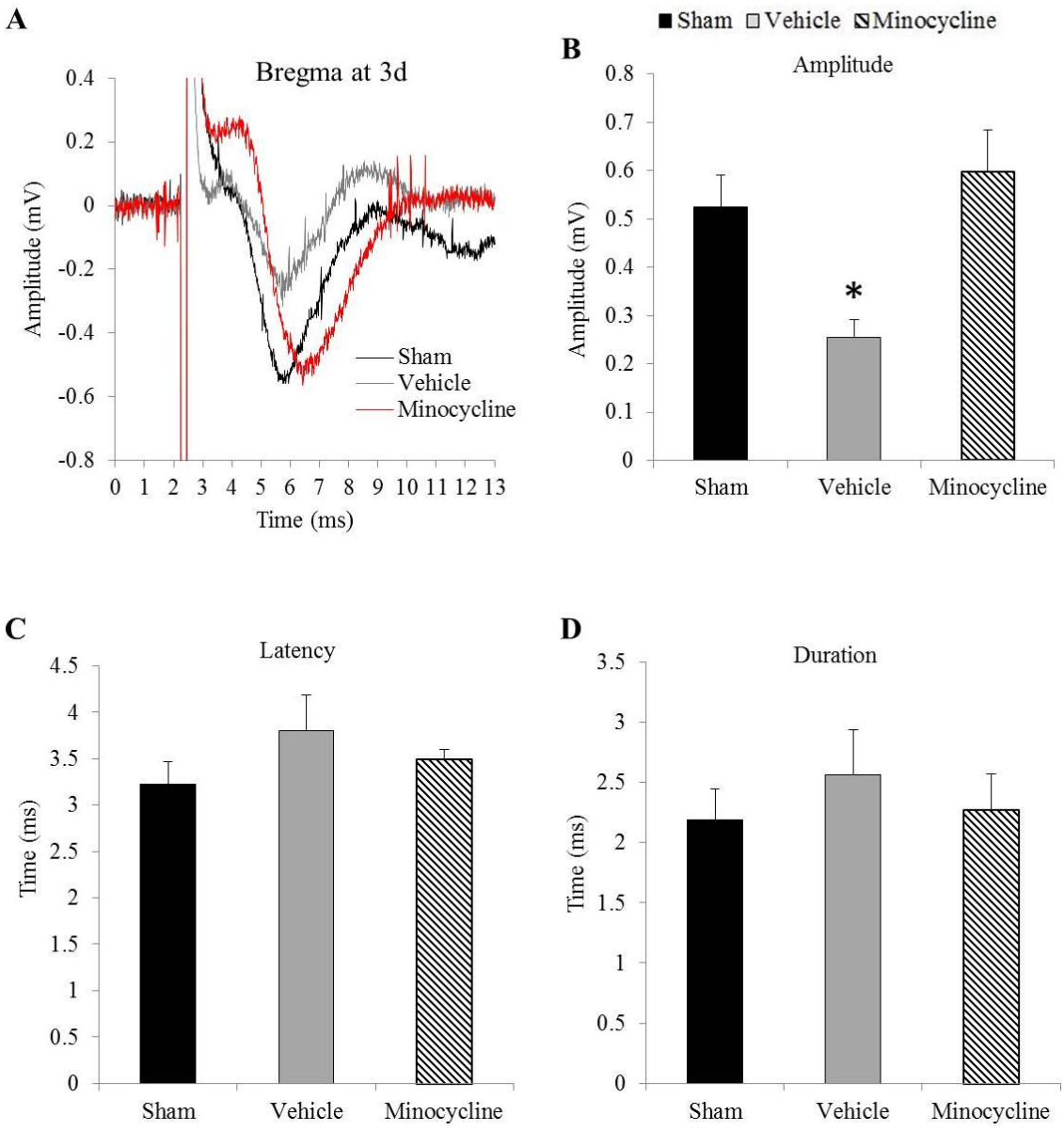

Figure 4.7 EFP recordings from the injured cortex at -3mm at 3 days and 4 weeks following acute minocycline treatment.

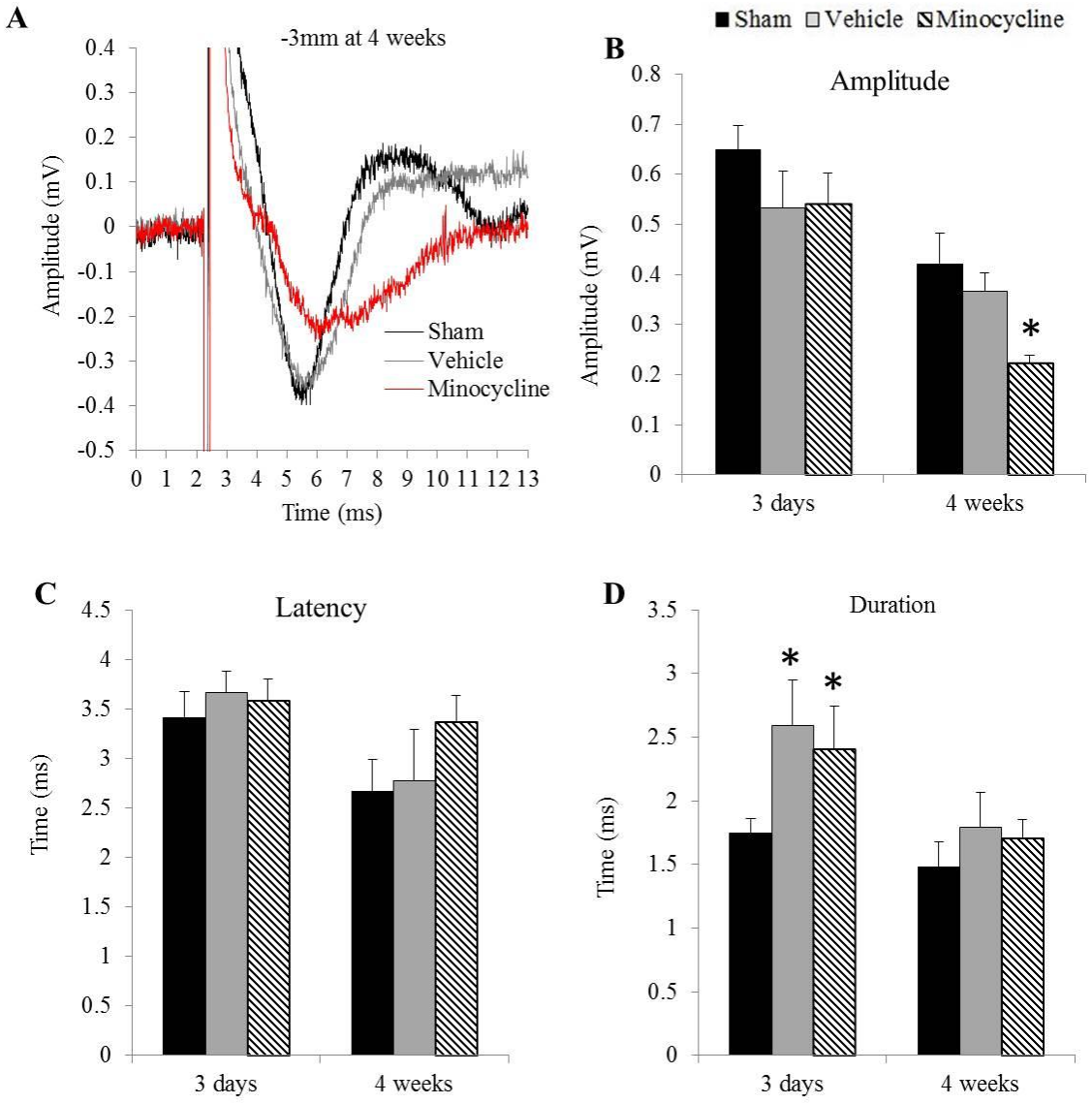

Figure 4.8 Acute histological outcomes in the injured subiculum following minocycline treatment.

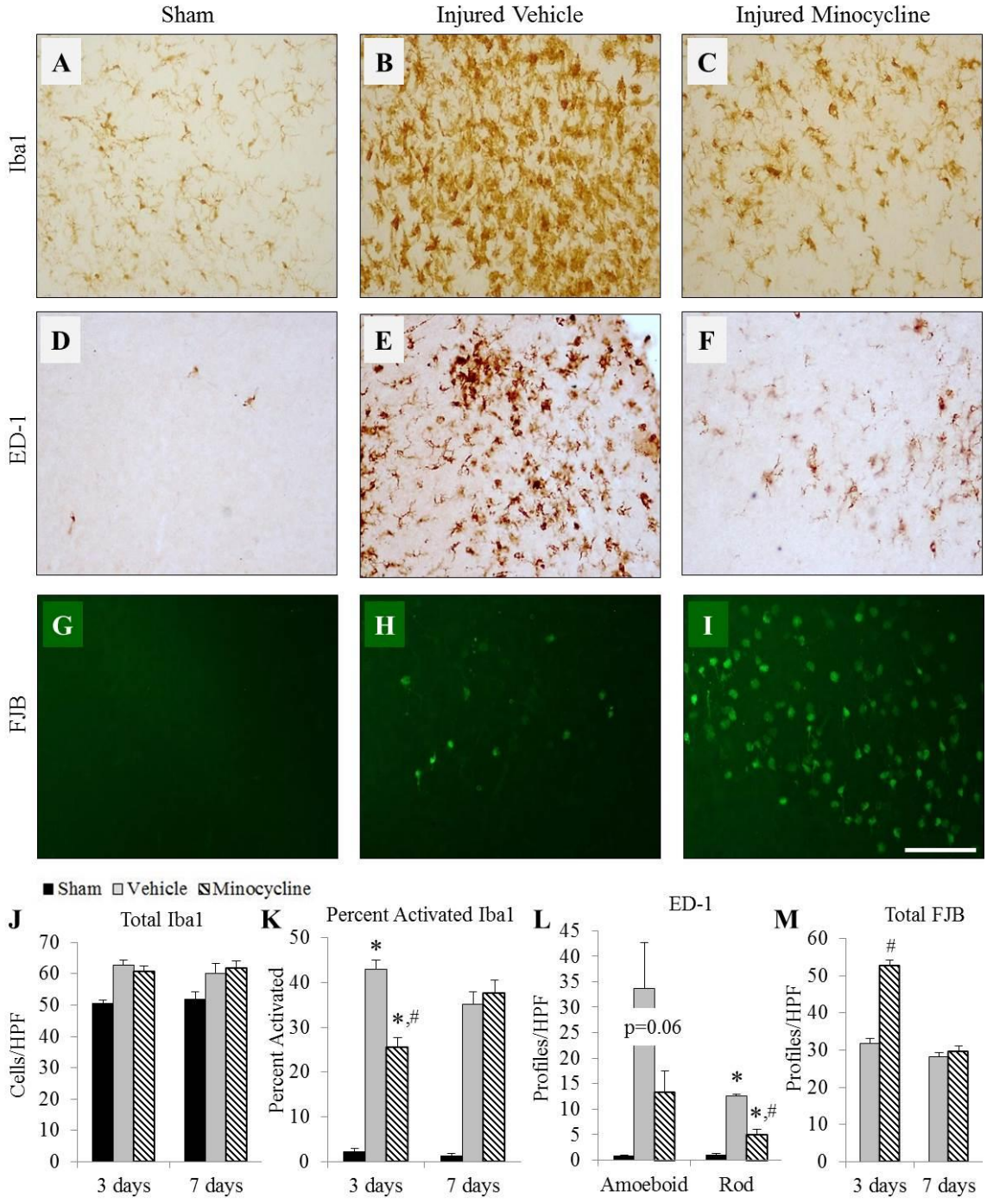

Figure 4.9 Microglial/macrophage reactivity and neurodegeneration in the injured subiculum at 15 days post-injury following acute minocycline treatment.

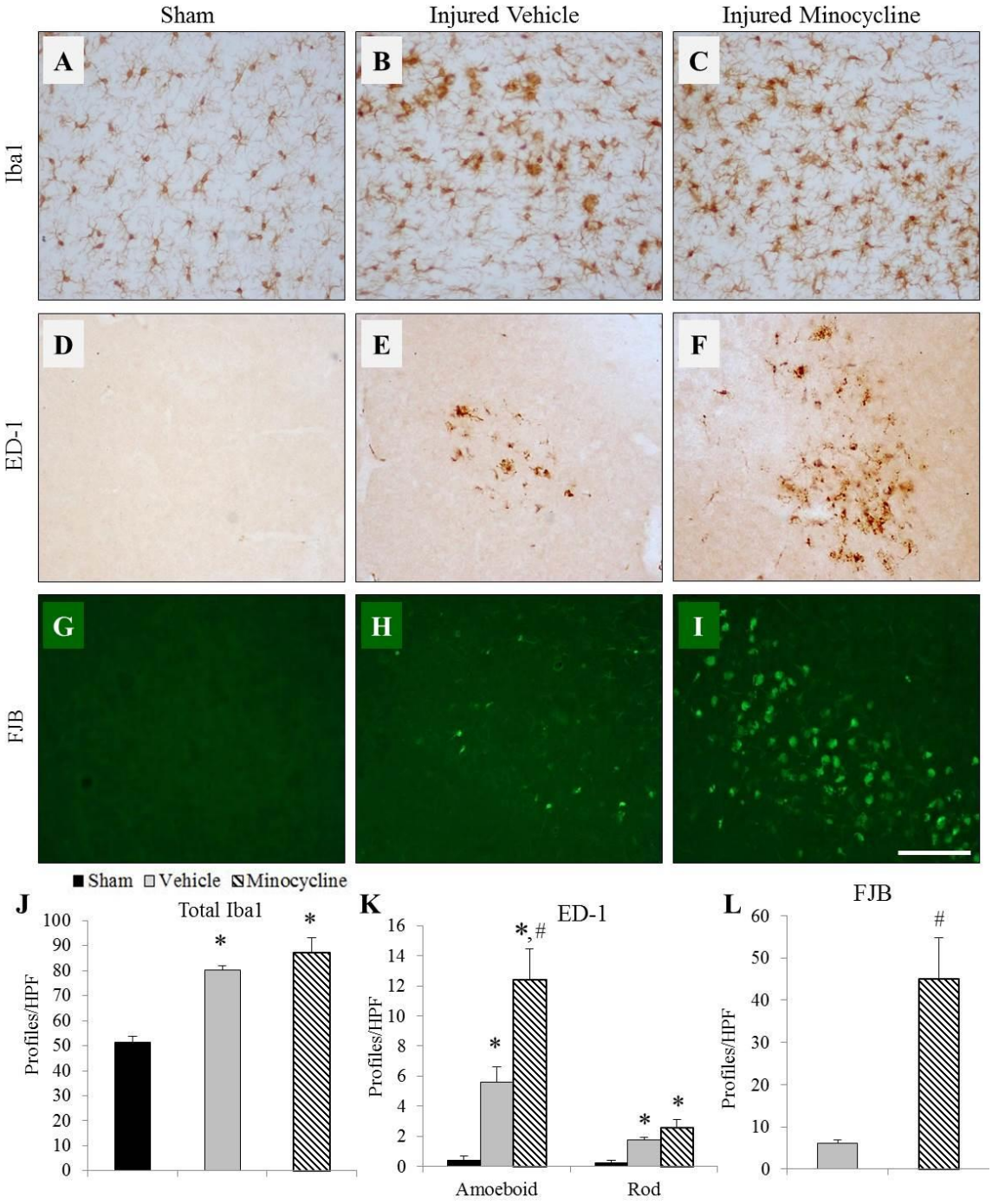

Figure 4.10 Microglial/macrophage reactivity in the injured thalamus following minocycline treatment at 3 and 7 days post-injury.

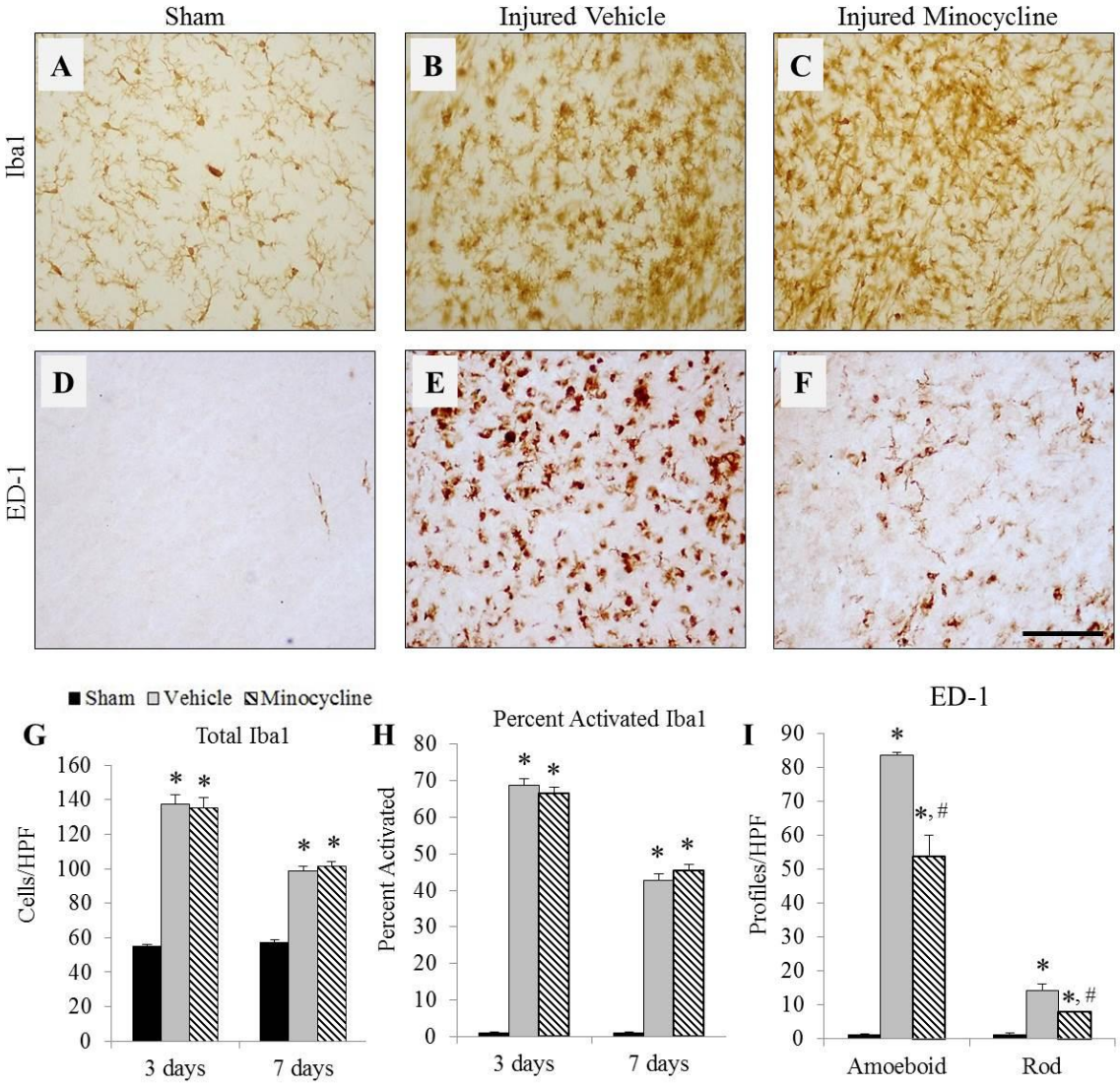

Figure 4.11 Degeneration and axonal injury in the injured thalamus at 3 and 7 days post-injury following acute minocycline treatment.

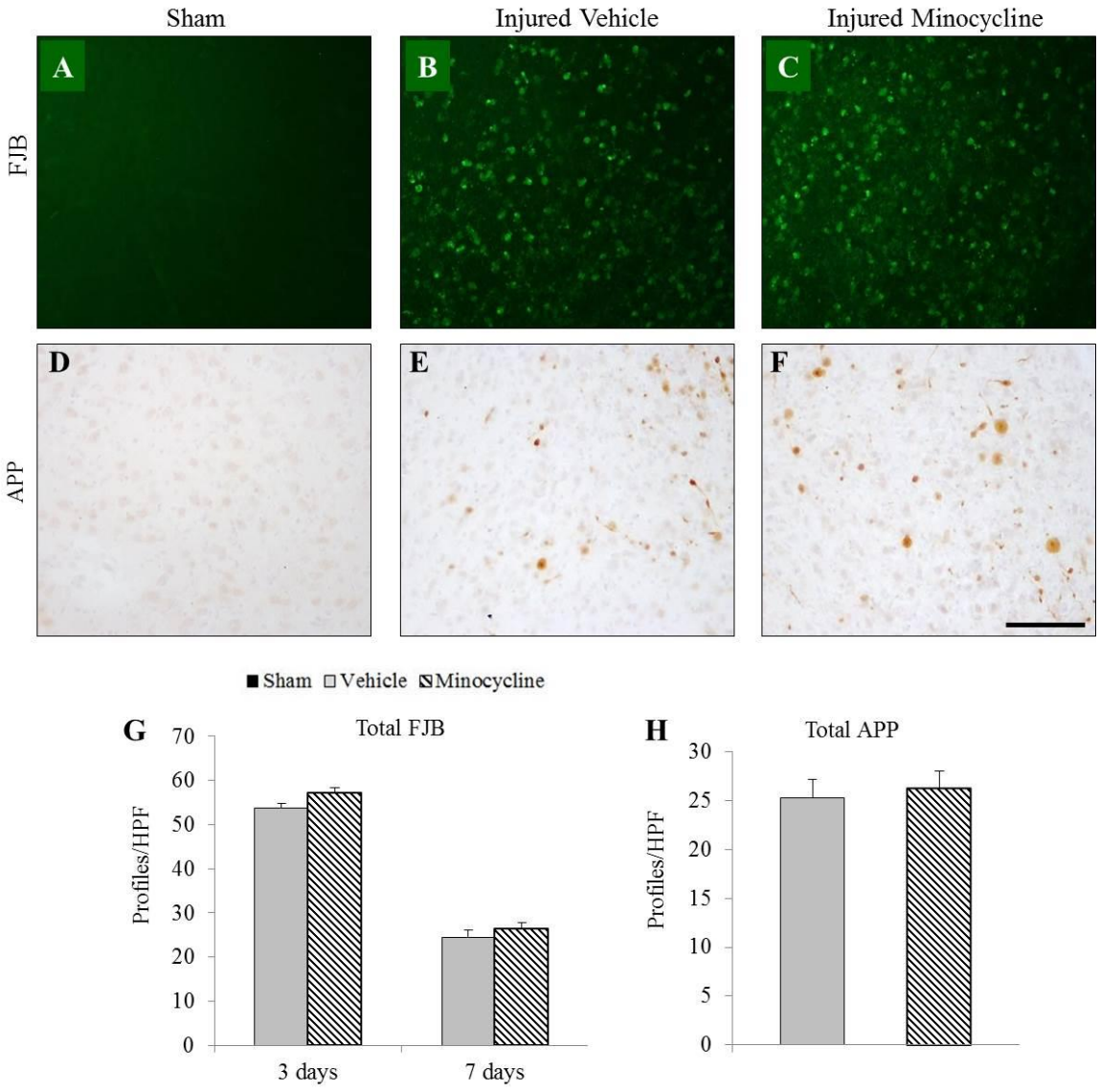

Figure 4.12 Microglial/macrophage reactivity and degeneration in the injured thalamus at 15 days post-injury following acute minocycline treatment.

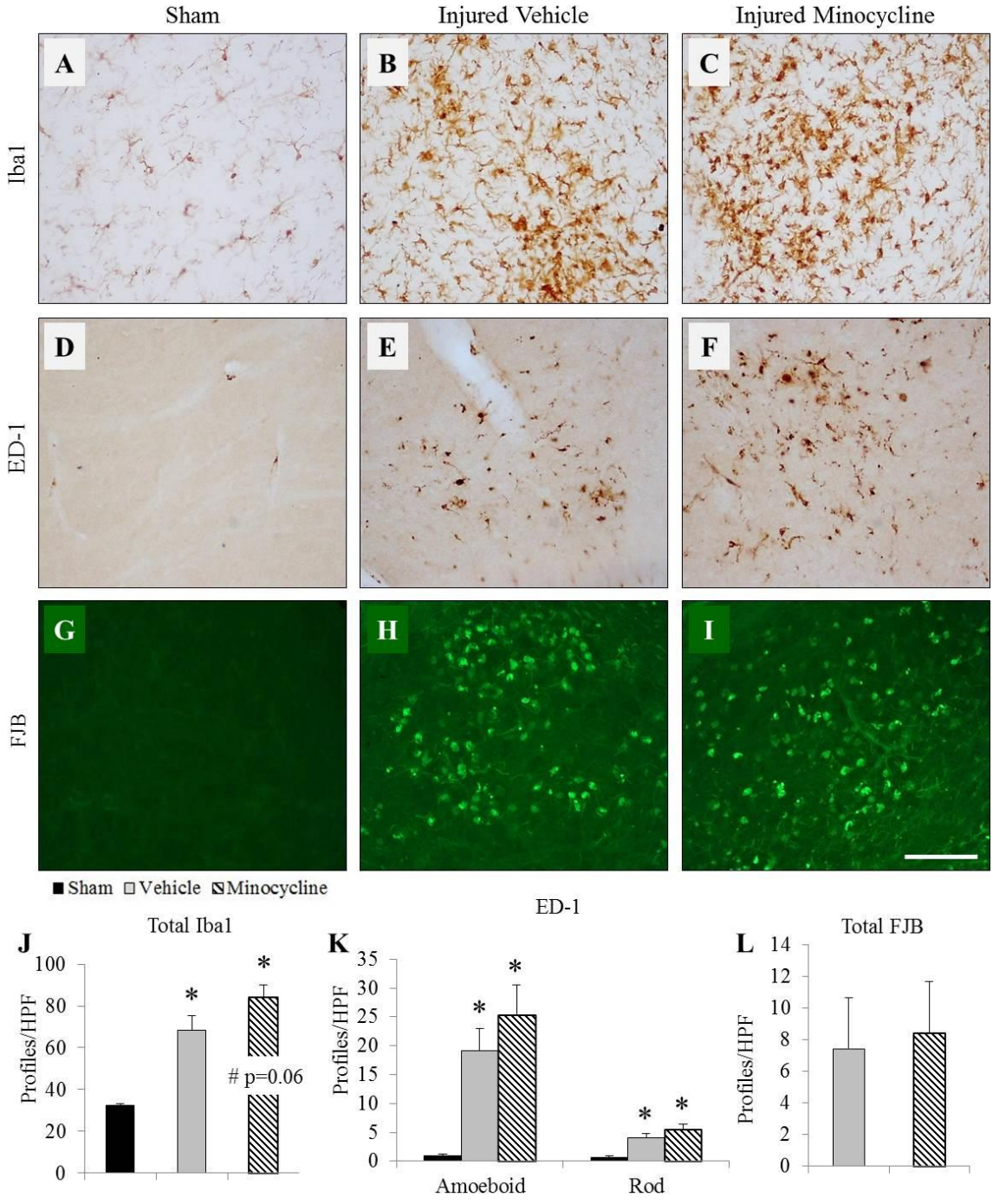

Figure 4.13 Microglial/macrophage reactivity and degeneration in the injured thalamus 4 weeks post-injury following acute minocycline treatment.

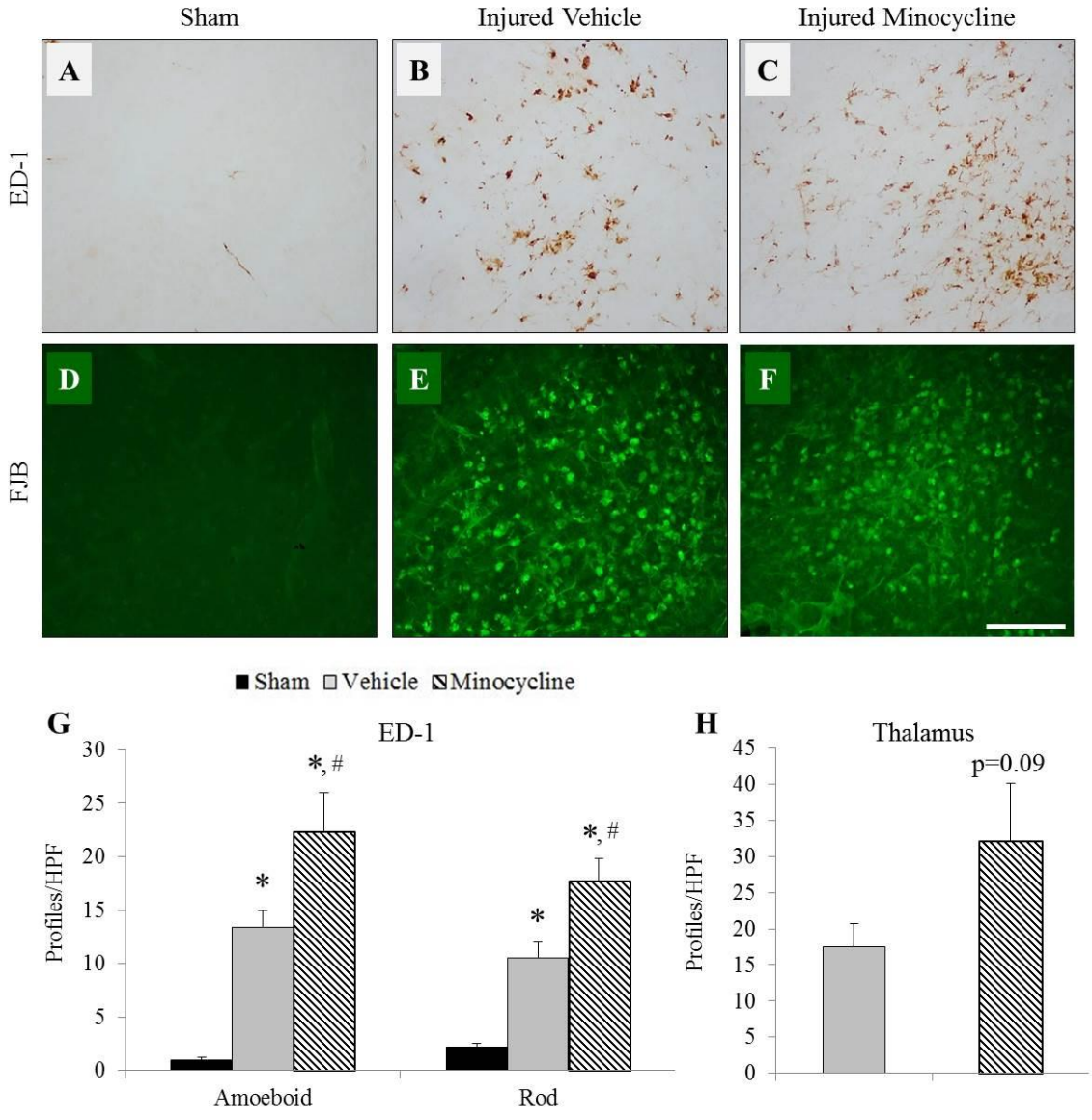

Figure 4.14 Effect of acute minocycline treatment on microglial/macrophage reactivity in the white matter at 3 and 7 days post-injury.

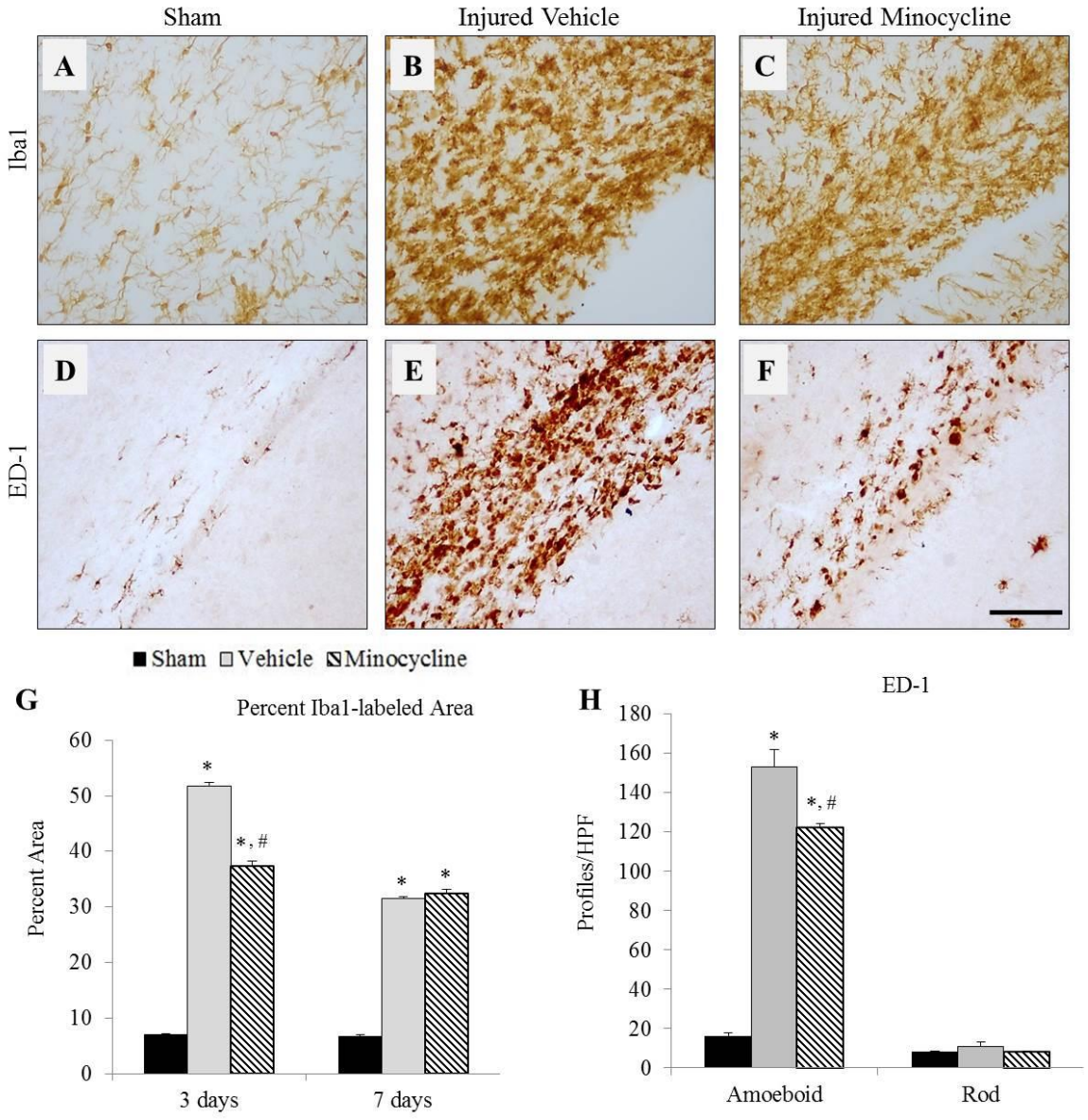

Figure 4.15 Effect of acute minocycline treatment on degeneration and axonal injury in the white matter at 3 and 7 days post-injury.

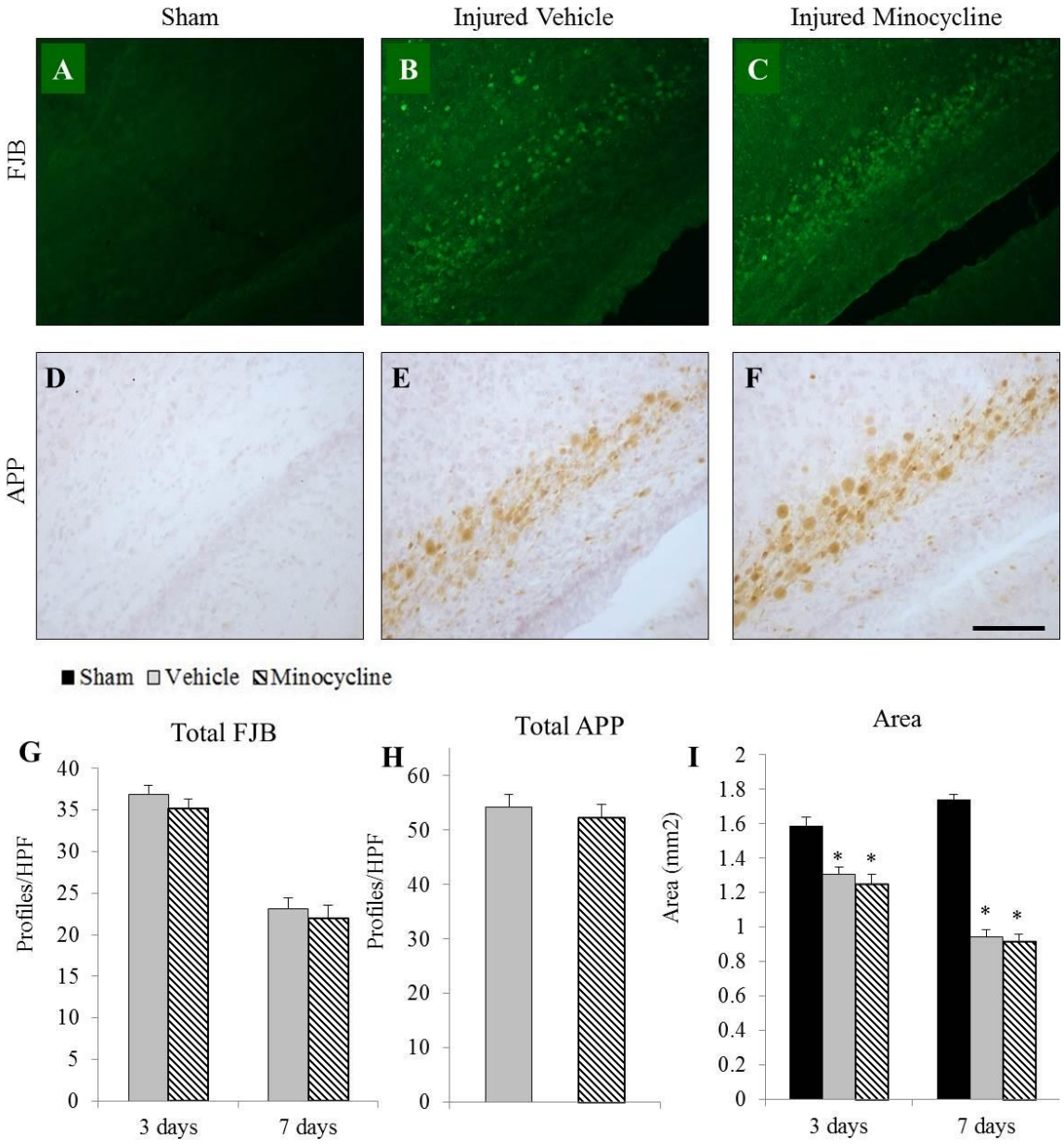

Figure 4.16 Microglial/macrophage reactivity and degeneration in the injured white matter at 15 days post-injury following acute minocycline treatment.

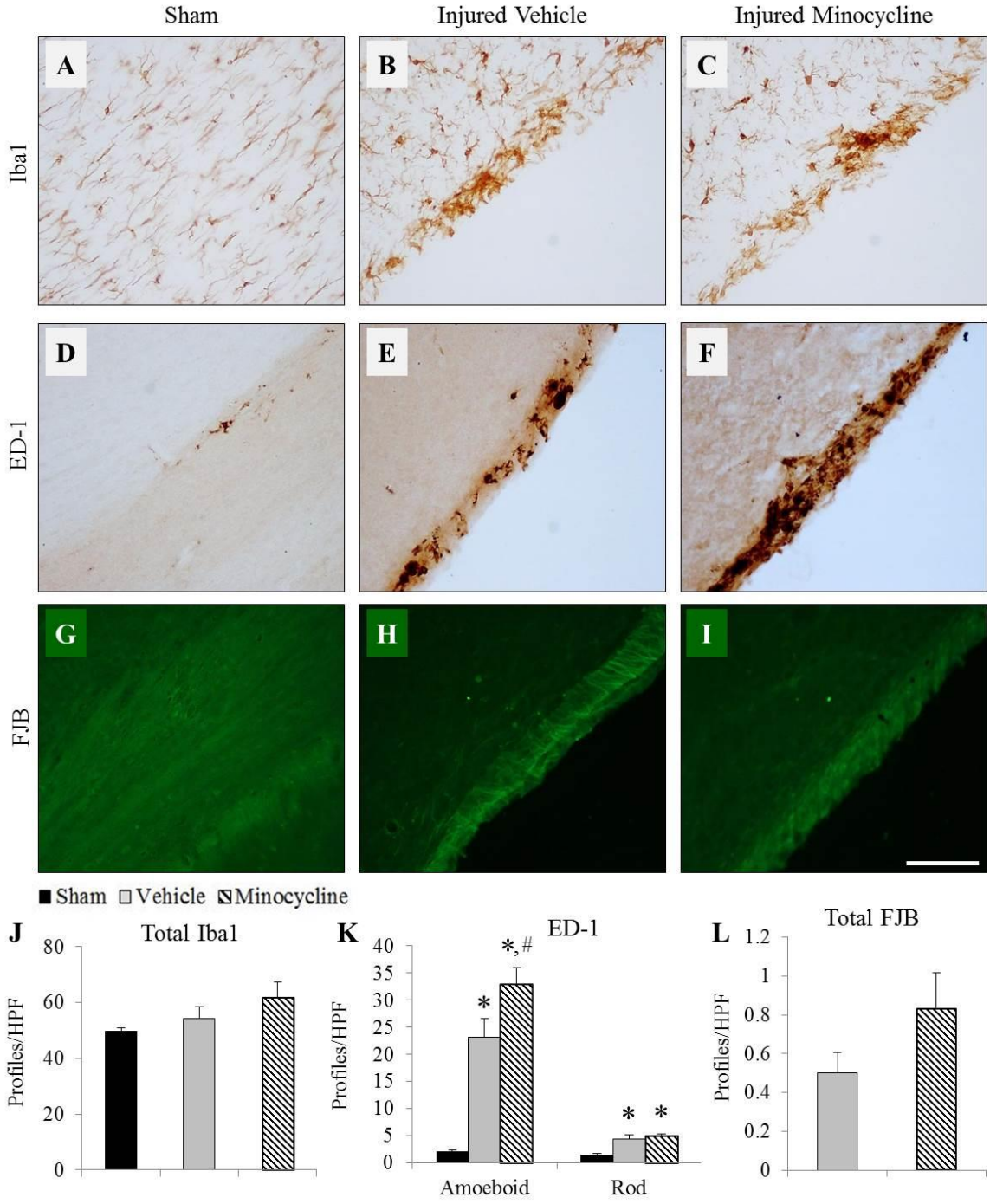

Figure 4.17 Effect of minocycline treatment on axonal transport in the third week post-injury.

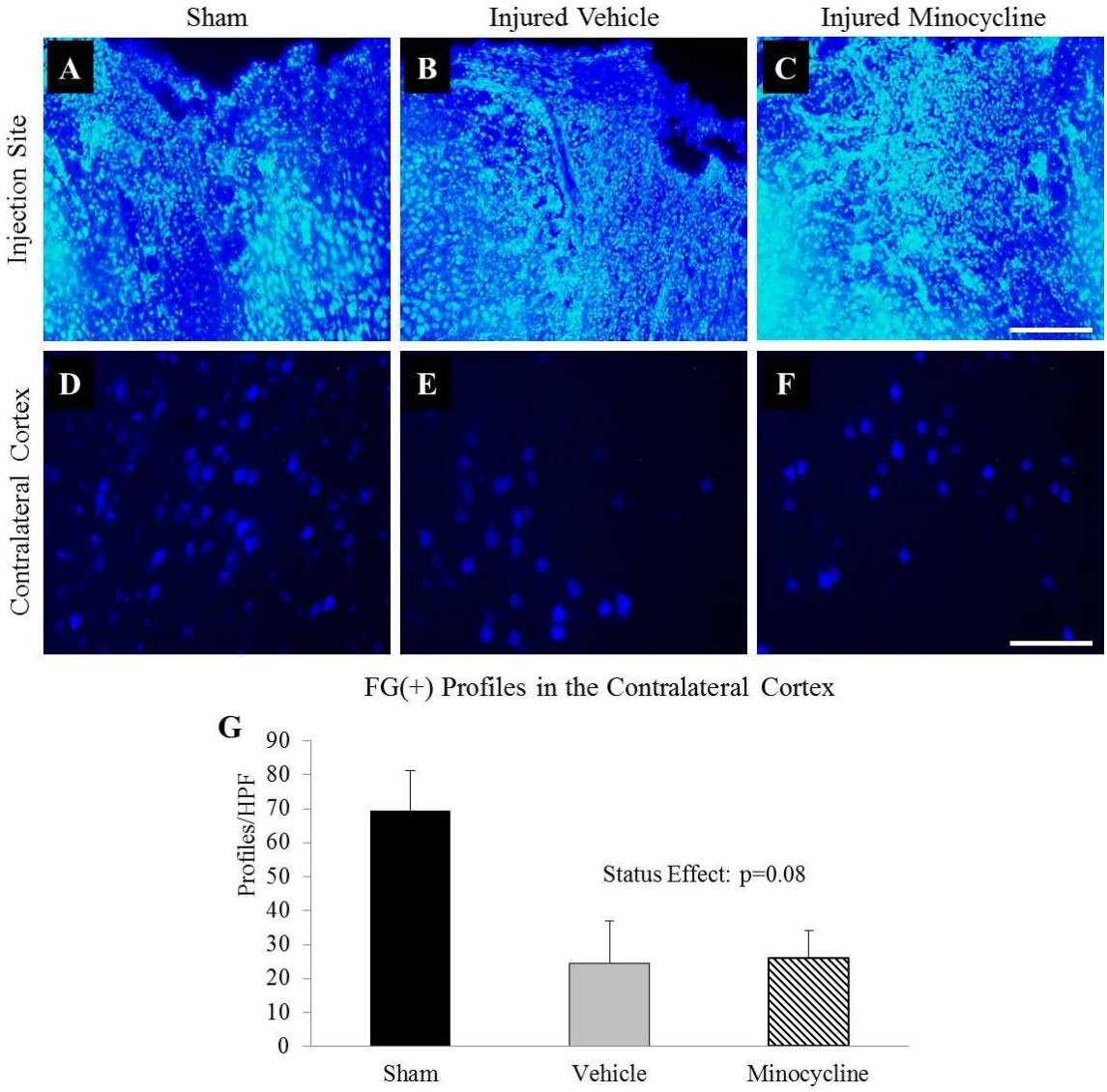

Figure 4.18 Microglial/macrophage reactivity and degeneration in the injured white matter at 4 weeks post-injury following acute minocycline treatment.

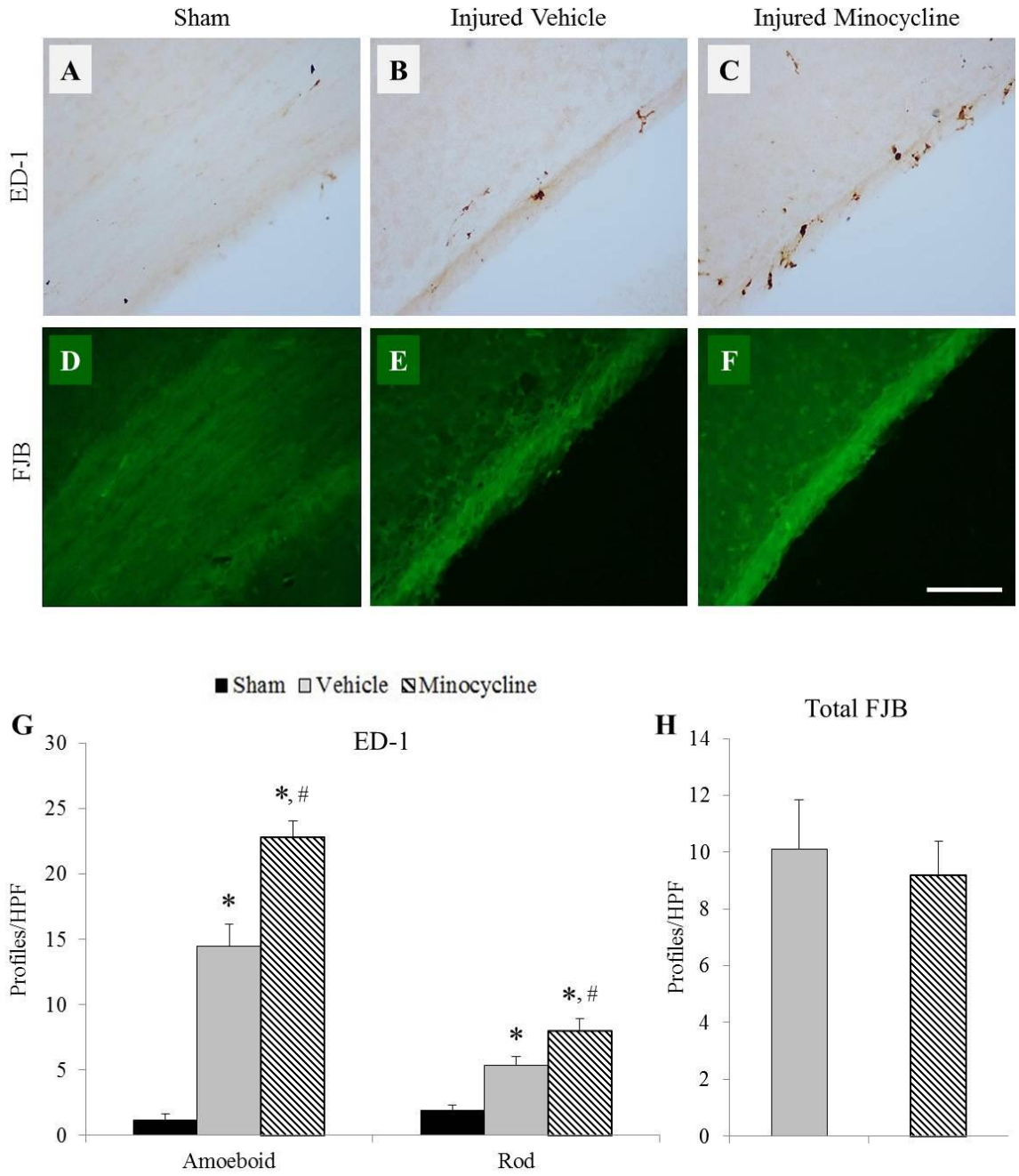

Figure 4.19 Spatial learning and memory assessment following acute minocycline treatment.

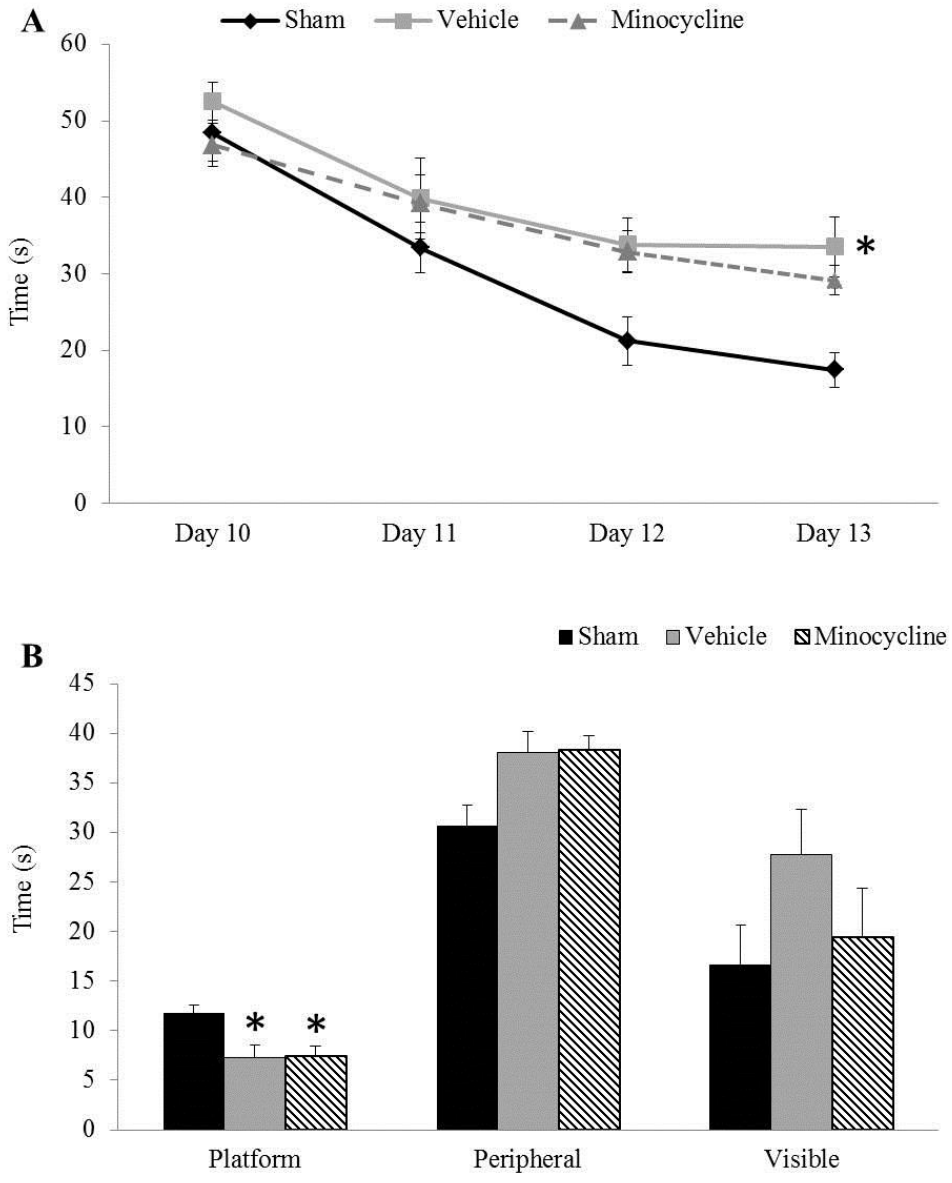

CHAPTER 5: LONG-TERM FUNCTIONAL DEFICITS FOLLOWING TBI IN THE NEONATE RAT

5.1 ABSTRACT

Children that survive traumatic brain injury can face life-long functional deficits in the form of cognitive impairments, motor deficits, alterations in mood-related behavior, and the development of seizure disorder. The anatomical regions associated with certain functional changes may not exhibit cellular pathology in the form of microglial/macrophage reactivity or neurodegeneration, but that is not to say that neuronal physiology is not altered in these regions. In the 4th post-injury week, brain-injured animals demonstrated mild anxiety-like behavior in the elevated plus maze (EPM), a deficit in short-term working memory in a novel object recognition (NOR) assessment, increased seizure susceptibility, increased fine locomotion, and a deficit in forelimb motor control compared to sham-injured animals. Additionally, neuronal activity was altered in the frontal motor cortex- a region that is outside of the impact site and demonstrates no cellular pathology. At 3 days post-injury, brain-injured animals exhibited evidence of hypoactivity in this region while at 21 days post-injury, brain-injured animals demonstrated hyperactivity. Systemic administration of the antibiotic minocycline reduced the working memory deficit, completely reversed the forelimb motor control deficit, and completely reversed the injury-induced hypoactivity at 3 days and the injury-induced hyperactivity at 4 weeks post-injury. Depletion of microglia/macrophages within the impact site, however, had no effect on forelimb motor control or neuronal activity in the forelimb region of the motor cortex. These results indicate that the systemic minocycline administration had whole-brain effects beyond just cellular pathology while the localized microglial/macrophage depletion was unable to affect pathology outside the impact site.

5.2 INTRODUCTION

Traumatic brain injury (TBI) sustained by young children has been shown to result in long-term behavioral disability. Brain-injured children exhibit cognitive deficits in measures of working memory post-injury as well as demonstrate evidence of anxiety disorder (Treble et al., 2013; Max et al., 2015). Children that sustained brain injuries between the ages of 0 and 15 years performed poorly in a task of visuospatial working memory when compared to age-matched uninjured controls (Treble et al., 2013). Additionally, research has indicated that children are at risk for the development of novel psychiatric disorders within the first year post-injury including severe personality changes and anxiety disorder (Max et al., 2015). Motor deficits have also been identified as a long-term consequence of early childhood TBI as 25% of brain-injured children demonstrated deficient motor abilities in a longitudinal prospective study (Ewing-Cobbs et al., 1998). Specifically, children that sustained brain injuries had difficulty completing an assessment of manual dexterity that involved placing pegs in the correct orientation in a peg board (Ewing-Cobbs et al., 2008). Along with these alterations in functionality, children that sustain TBIs have an increased risk for developing post traumatic epilepsy (PTE) and seizure activity. Approximately 40% of children that sustained a TBI developed PTE and this was most strongly correlated to severe injuries in younger children (Arndt et al., 2013).

In pre-clinical models, injury-induced alterations in neuronal activity may manifest as functional changes. Prince & Tseng (1993) demonstrated that an undercut cortical injury to the developing rat brain within the first 4 weeks of life resulted in hyperactivity 3 weeks following the injury and evidence of post-traumatic epileptic

activity. Later, this group demonstrated that an undercut injury to the cortex of postnatal day (PND) 21 rats resulted in an epileptogenic phenotype in which there was increased neuronal firing in layer V of the affected cortex (Jin et al., 2006) and a deficit in inhibitory GABAergic signaling within the same area (Ma & Prince, 2012). While this undercut model is a severe penetrating form of brain injury, evidence has emerged that impact-based brain trauma can result in alterations in neuronal activity leading to epileptogenesis. Nichols et al. (2015) showed that CCI injury to the PND17 rat produced epileptoform discharges in the first two weeks following injury as measured by continuous EEG monitoring. Additionally, neurons within the impact site (in the peri-injury region around the site of lesion) demonstrated increased bursting activity during slice recording within the 3rd week post-injury. These studies, however, did not assess the animal's susceptibility to behavioral seizure and it is unclear if our injury to PND11 rats creates vulnerability for altered activity that may lead to an increased susceptibility to seize.

Injury-induced lesion or cavitation makes recording within the direct impact site difficult and in one such model using PND17 rats, alterations in neuronal activity in the cortex contralateral to the impact site were observed, indicating that regions outside of the impact site that are devoid of cellular pathology (in this case lesion) can be affected by the injury (Li et al., 2014). Due to the fact that our PND11 closed head injury model does not result in a lesion or cavitation (Raghupathi & Huh, 2007), we were previously able to determine that the injury only resulted in a transient deficit in neuronal activity in the motor cortex at bregma level and not deeper within the impact site (Chapter 3). It is

unclear, however, whether our injury induces alterations in activity outside of our impact site in regions that may be crucial for functional alterations.

Working memory deficits observed in the clinical population have also been recapitulated in pre-clinical animal models of pediatric TBI. Rat pups that sustained an open controlled cortical impact injury on PND 17 demonstrated deficits in novel object recognition (NOR) memory 2 weeks post-injury (Schober et al., 2014). A different laboratory observed similar results using open CCI injury in PND21 rat pups in which brain-injured animals explored the novel object significantly less than sham-injured animals 1 week post-injury (Scafidi et al., 2010). Novel object recognition has been shown to be heavily dependent on the perirhinal cortex and the medial prefrontal cortex (short-term) or the hippocampus (long-term) (Barker et al., 2007; Antunes & Biala, 2012). In our injury model, there is no evidence of cellular pathology in the prefrontal or perirhinal cortices so the short-term NOR assessment will allow for further investigation into the diffuse nature of our injury.

Investigation into anxiety-like behavior following TBI to the immature brain has produced conflicting results. Mice injured on PND21 demonstrated an increase in time spent in the open areas in the elevated zero maze compared to sham-injured mice 2 weeks post-injury indicating a decrease in anxiety-like behavior (Pullela et al., 2006). This same group, however, later observed that their brain-injured mice demonstrated a form of social anxiety in adulthood as evidenced by decreased sociability in a resident-intruder and three-chamber test indicating that general anxiety and social anxiety may be affected differently after injury (Semple et al., 2012). In a model of mild TBI in PND30 rats, brain-injured male rats demonstrated decreased anxiety-like behaviors as evident by a

decrease in closed arm time in the elevated plus maze and an increase in the percent time spent in in the middle of an open field arena while female brain-injured rats showed no differences from sham-injured animals in measures of anxiety-like behavior (Mychasiuk et al., 2014). Rats that were injured via CCI on PND17, however, showed an increase in time spent in the dark portion of the elevated zero maze in adulthood indicating an anxious phenotype (Ajao et al., 2012). Additionally, brain injury induced by controlled weight drop in a PND7 rat resulted in an anxiety-like phenotype as evidenced by a decrease in exploratory behavior in the center of an open field arena compared to sham-injured animals 2 weeks after injury (Sonmez et al., 2007). These mixed results may indicate that there is an age at injury effect with regards to the manifestation of anxiety-like behaviors following injury to the immature brain and it is unknown whether our injury to PND11 rats will produce an increase or decrease in anxiety-like behavior.

Locomotor difficulties have been identified in both the acute and chronic post-injury periods. Adelson et al. (1997) observed motor deficits in rats that were injured on PND17 that were dependent on injury severity. The severely injured group (100g weight drop) showed deficits on the balance beam and inclined plane task that persisted for 4 days post-injury while the "ultra-severe" injury group (150g weight drop) demonstrated sustained deficits out to 10 days post-injury. Focal injury to the frontal lobe in PND21 mice resulted in long-term impairment in rotarod performance and open field rearing behavior at 2 months post-injury (Chen et al., 2013). When PND21 mice were injured laterally over the parietal cortex, however, there was no difference between brain-injured and sham-injured animals in terms of rotarod and balance beam performance, but researchers observed a general hyperactivity as brain-injured animals demonstrated more

exploratory behavior in the open field task compared to sham-injured animals (Pullela et al., 2006). We have previously demonstrated that our brain-injured animals do not exhibit a deficit in swim speed as measured in a Morris water maze (MWM) spatial learning task (Raghupathi & Huh, 2007), but have no information on terrestrial locomotion or limb dexterity in our animals.

While we previously demonstrated that anti-microglial/macrophage therapeutics (clodronate and minocycline) had no effect on injury-induced spatial learning and memory impairment (Chapters 3 & 4), other studies have shown positive effects of anti-microglial/macrophage treatments, specifically minocycline, in other functional tasks. Minocycline administration has been particularly effective in reducing locomotion-based impairments following brain injury. In a model of adult brain-injury, minocycline-treated mice showed marked improvement on the rotarod task 1-4 days after injury compared to brain-injured animals that received the saline vehicle (Sanchez-Mejia et al., 2001). A similar model using adult mice also found that minocycline treatment improved performance on a ledged beam task 1-2 days after injury (Bye et al., 2007). In a model of hypoxic-ischemia in rats on PND4, minocycline treatment immediately before injury and once a day for 3 days after the injury significantly reduced impairment in the wire hanging task starting at 1 week post-injury (Fan et al., 2006). Modulation of microglial activation through CX3CR1 knockout, however, caused an exacerbation of injury-induced locomotor deficits in the rotarod task in adult mice (Febinger et al., 2015) and microglial depletion in uninjured neonate rats (PND1 and PND4) can increase baseline locomotor activity (Nelson & Lenz, 2017). It is unclear, however, whether acute anti-

microglial/macrophage treatment can positively affect functional outcome in the chronic post-injury period following impact-based trauma to the neonatal rat brain.

In the current study, we aimed to expand the functional profile of our injury model to include assessments that are clinically relevant to the human brain-injured population and addressed the possibility that there may be alterations in neuronal activity outside of our direct impact site that could affect functional outcome. Additionally, the current study investigated the use of acute anti-microglial/macrophage therapeutics in ameliorating long-term functional outcomes.

5.3 MATERIALS AND METHODS

5.3.1 Brain Injuries

On postnatal day 11, male and female Sprague Dawley rat pups were randomly assigned to injury and treatment conditions. Procedure was followed as described in section 3.3.1. Animals for the characterization study (Part A) are listed in table 5.1 and animals for the minocycline and clodronate studies (Part B) are listed in table 5.2.)

5.3.2 Minocycline Treatment Paradigm

Sham- and brain-injured animals were administered minocycline hydrochloride (45mg/kg/injection, Sigma, St. Louis, MO) or phosphate buffered saline vehicle (PBS, 0.2 ml/kg/injection) immediately following the injury via intraperitoneal injection. Animals received subsequent injections every 12 hours for 3 days for a total of 6 injections (Chapter 4.3.1, Fig. 5.1 B).

5.3.3 Clodronate Administration Paradigm

Sham- and brain-injured animals were randomly assigned to receive the liposome-encapsulated clodronate or the empty liposomes and the previously stated procedure was followed (Chapter 3.3.3, Fig. 5.1 C).

5.3.4 Cortical evoked field potential (EFP) electrophysiology and quantification

Evoked field potential recordings were taken from layer 5 of the motor cortex 1mm anterior to bregma (forelimb region of the motor cortex) at 3, 7, and 21 days post-injury (characterization) , 3 days and 4 weeks (minocycline), or 4 weeks (clodronate) and quantified as previously described (Chapter 3.3.7).

5.3.5 Behavior testing and analyses

Behavior assessments for the characterization study, the minocycline study, and the clodronate study were performed within the 4th post-injury week (Fig. 5.1).

Elevated Plus Maze

Animals were assessed for the presence of anxiety-like behaviors using the elevated plus maze (EPM). This plus maze sits approximately 3-ft off the ground and contains two enclosed arms and two completely open arms (Fig. 5.2 A). Animals were placed in the neutral zone (intersect of the 4 arms) facing an open arm and left to explore the maze without distraction for 5 minutes. The maze was cleaned with 70% ethanol in between animals. Trials were videotaped and later analyzed for the time spent in the open arms (including both 2-paw and 4-paw entry), 4-paw open arm time, time spent in the closed arms, number of head dips, number of 2-paw entries into the open arms, number of 4-paw entries into the open arms, and the number of entries into the closed arms. The idea behind this task is that animals that demonstrate a more anxious phenotype will more likely remain in the closed arms for a prolonged period of time and will not partake in risk-taking behaviors such as open arm entries and head dips (Walf and Frye, 2007).

Novel Object Recognition

Both sham-injured and brain-injured animals were tested for short-term working memory using a novel object recognition (NOR) paradigm. The test was performed in an open-top plastic enclosure and video recorded from above in order to visualize the entire field. Animals were subjected to two separate 10-minute habituation trials on the two days prior to testing in which the animals were left to explore the empty chamber (Fig. 5.3 A). On the day of testing, two identical objects (glass bottles) were placed at opposing diagonal corners of the chamber and animals spent 5 minutes exploring the objects in a pre-test trial (Fig. 5.3 B). The time spent exploring both objects was quantified in order to confirm that the animals spent an equal amount of time with the identical objects. An hour after the pre-test trial, one of the glass bottles was replaced with a metal cylinder and the animals were allowed to once again explore the objects for 5 minutes (Fig. 5.3 C). Again, the time spent exploring each object was quantified and presented as the percent time spent exploring either the original or novel object (object exploration time/total exploration time). One sham-injured animal and one brain-injured animal had to be excluded from analyses because they did not reach the criterion for total exploration (15 seconds) in the test trial.

Seizure Susceptibility

Seizures were induced using the $GABA_A$ antagonist flurothyl (bis[2,2,2-trifluoroethyl] ether, Sigma-Aldrich, St. Louis, MO) (Wakamori et al., 1991; Krasowski, 2000). Animals were placed in a plexiglass chamber and flurothyl was dripped

(30µl/minute) onto a piece of filter paper within the chamber via a tube attached to a 1-ml syringe on a syringe pump (syringe pump model) (Fig. 5.4 A). Sessions were videotaped and the flurothyl was dripped into the chamber until the animal went into full tonic-clonic seizure. At that point, the chamber was opened, the ether dissipated, and the seizure was halted naturally. The videos were analyzed and the time to the first mycolonic jerk (latency to seize) and the timed length of the seizure were recorded. Seizure length was characterized as the time from the beginning of full tonic clonic seizure until the animal stilled and regained awareness of surroundings (reaction to sound or movement outside the chamber).

Activity Monitoring

Sham-injured and brain-injured animals were monitored for locomotor activity using the SmartFrame Open Field Station monitoring system (Kinder Scientific, Poway, CA). Animals were placed in chambers measuring 41cm x 41cm x 38cm equipped with a 16x16 photobeam grid that recorded both lateral (ambulatory movement) and vertical (rearing) beam breaks. Additionally, this system characterized any movement that did not qualify as a complete ambulatory beam break as a fine movement. These movements can include twitches, grooming behavior, and tail flicks. Data was collected and condensed using MotorMonitor software (manufacturer and version) and presented as the number of beam breaks meeting the basic locomotion, fine locomotion, and rearing criteria during the entire 5-minute collection trial.

Straight-path Swim Task

Both sham-injured and brain-injured animals were trained to swim the length of the 48” aquarium in a straight path as previously described (Stoltz et al., 1999). The water in the tank was 18-20°C and to make sure the test rats could see the platform, a cue rat was placed on the platform and a flag was adhered to the side of the platform. During training the tank was separated into quarters to form the 4 training release points at varying distances from the platform (Fig. 5.6 A, dashed grey lines). The animals were released from these points in order until they could swim the length of the tank in a straight path without turning or running into the sides. On the day of the test (24 hours after training), animals were subjected to one acclimation trial released from the back of the tank in order to familiarize them with the task. In all subsequent trials, animals were released from the back of the tank and recorded for quantification. Animals were tested by cage and allowed to rest for 2 minutes in between trials. When animals completed 3 straight-path runs without turning or running into the walls of the tank, they were considered finished and returned to their home cage. Videos had to be slowed down to 0.125x normal speed in order to accurately count both forelimb and hindlimb strokes. Data is presented as the average number of strokes across 3 runs.

5.3.6 Statistical analyses

All statistical analyses were performed using Statistica software (Version 7.0, Tulsa, OK). For the NOR pre-test, a 3-way ANOVA was run using status (sham/injured or sham/injured vehicle/injured minocycline), sex, and object number as independent variables to ascertain whether the animals had a preference for the placement of the objects. All other measures (NOR test, swim test, activity monitoring, EPM, seizure, and

cortical EFPs) were analyzed using two separate 2-way ANOVAs using status (status (sham/injured, sham/injured vehicle/injured minocycline, sham empty-lip/injured empty-lip/sham clod-lip/injured clod-lip) and sex as independent variables. When animal numbers did not allow for an adequate comparison of the sexes, one-way ANOVAs using status as the categorical predictor were used. When appropriate, Newman-Keuls posthoc tests were performed with $p \leq 0.05$ being considered significant.

5.4 RESULTS

5.4.1. Brain-injured animals exhibit a wide range of behavioral deficits in the chronic post-injury period.

Brain-injured animals exhibited a mild increase in anxiety-like behavior

Brain-injured animals spent significantly more time (219 ± 7s) in the closed arm portions of the maze compared to sham-injured animals (184 ± 9s) ($F_{1,19}$=9.32, p<0.01) indicative of anxiety-like behavior (Fig. 5.2 B). This corresponded to a mild, but insignificant decrease in the number of entries the brain-injured animals made into the closed arms indicating that brain-injured animals may have been staying longer in the closed arms per entry (brain-injured: 11 ± 0.8 entries, sham-injured: 13 ± 0.9 entries, $F_{1,19}$=3.46, p=0.08, Fig. 5.2 C). Brain-injured animals demonstrated a decrease in both total open arm time and 4-paw open arm time, but these differences did not reach significance when compared to sham-injured animals (total open arm: brain-injured: 32 ± 4s, sham: 45 ± 7s; $F_{1,19}$=2.38, p=0.14; 4-paw open: brain-injured: 5 ± 2s, sham: 15 ± 5s: $F_{1,19}$=3.08, p=0.10) (Fig. 5.2 D,E). Brain-injured animals also demonstrated a decrease in the amount of times they made entries into the open arms with 4 paws that did not reach significance when compared to sham-injured animals (brain-injured: 0.9 ± 0.2 entries, sham-injured: 2 ± 0.5 entries; $F_{1,19}$=4.17, p=0.06, Fig. 5.2 F). Additionally, there was a mild, but insignificant decrease in the number of times brain-injured animals looked over the edge of the maze (head dips) (brain-injured: 8 ± 0.6 dips, sham-injured: 10 ± 1 dip, $F_{1,19}$=2.58, p=0.12, Fig. 5.2 G). Finally, there was no difference between brain-injured and sham-injured animals in the number of entries they made into the open arms with only 2 paws (brain-injured: 6 ± 0.8 entries, sham-injured: 7 ± 1 entry; $F_{1,19}$=0.22, p=0.64,

Fig. 5.2 H). There was no interaction between status and sex for any outcome measure (total closed arm time: $F_{1,19}$=1.06, p=0.32; closed arm entries: $F_{1,19}$=0.04, p=0.85, total open arm time: $F_{1,19}$=0.09, p=0.76, 4-paw open arm time: $F_{1,19}$=0.01, p=0.92, 4-paw entries: $F_{1,19}$=0.05, p=0.82, head dips: $F_{1,19}$=0.92, p=0.35, 2-paw entries: $F_{1,19}$=2.14, p=0.16). While the behaviors that demonstrate a lack of anxiety (open arm times and head dips) were not significantly different between groups, there were mild decreases in these behaviors in the brain-injured group and paired with the significant increase in closed-arm time, the brain-injured animals may exhibit a mildly anxious phenotype.

Brain-injured animals demonstrated short-term working memory deficits at 4 weeks post-injury.

In the pre-test trial for novel object recognition both sham-injured and brain-injured animals spent similar amounts of time with both of the identical glass bottles ($F_{1,34}$=0.55; p=0.46) indicating that the animals did not have a preference for a specific corner of the chamber (Fig. 5.3 D). There was no interaction between injury status, sex, and bottle in the amount of exploratory time in the pre-test ($F_{1,34}$=0.55; p=0.46). In the test trial, brain-injured animals spent significantly less time exploring the novel object and significantly more time exploring the original object compared to sham-injured animals ($F_{1,17}$=20.57; p<0.001; Fig. 5.3 E). This indicated that the brain-injured animals did not retain the information learned from the pre-test trial and gave the original object a similar amount of attention as the novel object. There was no interaction between injury status and sex in the amount of time spent exploring either the novel or original object ($F_{1,17}$=0.94; p=0.35).

Brain-injured animals demonstrated an increased vulnerability to seizure activity.

When subjected to vaporized flurothyl, both sham-inured and brain-injured animals seized (Fig. 5.4). The first myoclonic jerk was defined as the first involuntary whole-body twitch in which the limbs splayed outward and was closely followed by full status seizure. Brain-injured animals demonstrated an increased vulnerability to seizure activity as indicated by a significantly decreased latency to the myoclonic jerk compared to sham-injured animals (Brain-injured: 223 ± 8s, sham-injured: 259 ± 6s, $F_{1,19}$=11.70, $p<0.01$, Fig. 5.4 B). Despite this increase in seizure susceptibility, the length of the seizure did not differ between brain-injured (154 ± 12s) and sham-injured (156 ± 12s) animals ($F_{1,19}$=0.25, p=0.63, Fig. 5.4 C). There was no interaction between injury status and sex in either the latency to seize ($F_{1,19}$=0.33; p=0.57) or the length of seizure ($F_{1,19}$=0.25; p=0.63). These data indicate that there may be an injury-induced alteration in brain circuitry that makes the initiation of seizure activity more likely, but does not affect the propagation and cessation of the seizure activity.

Brain-injured animals exhibited an increase in fine locomotion at 4 weeks post-injury.

Brain-injured animals broke a similar amount of beams that qualified for basic ambulatory locomotion compared to sham-injured animals (brain-injured: 889 ± 53, sham-injured: 948 ± 33; $F_{1,19}$=1.89; p=0.19) indicating that injury did not cause a deficit in basic locomotion at 4 weeks post-injury (Fig. 5.5 A). Similarly, brain-injured animals and sham-injured animals did not differ in the amount of vertical beam breaks indicative of rearing behavior (brain-injured: 23 ± 5, sham-injured: 32 ± 3; $F_{1,19}$=1.86, p=0.19, Fig.

5.5 B). Analysis of the fine locomotor beam breaks, however, revealed an overall effect of injury status that indicated that brain-injured animals performed more fine motor beam breaks compared to sham-injured animals (brain-injured: 444 ± 22, sham-injured: 395 ± 10; $F_{1,19}$=4.24, p=0.05, Fig. 5.5 C). This may be due to an increase in involuntary twitching or anxious grooming behavior at 4 weeks post-injury. There was no interaction between injury status and sex in basic movement ($F_{1,19}$=1.89; p=0.19), rearing behavior ($F_{1,19}$=1.86; p=0.19), and fine movement ($F_{1,19}$=2.62; p=0.12).

Brain-injured animals demonstrated a deficit in forelimb motor control at 4 weeks post-injury.

When swimming in a straight path, rats will typically keep their forelimbs immobile and use their hindlimbs to propel them forward (Stoltz et al., 1999). This behavior was observed in our sham-injured animals (Fig. 5.6 B). Animals that sustained a brain injury, however, used their forelimbs when swimming and this forelimb use was preferential to the limb contralateral (right forelimb) to the injury site (left hemisphere) (Fig. 5.6 C). When this limb use was quantified and analyzed, a two-way ANOVA (injury status x sex) revealed an effect of injury status that showed that brain-injured animals used their right forelimb significantly more than sham-injured animals (brain-injured: 2.63 ± 0.52, sham-injured: 0.39 ± 0.16; $F_{1,19}$=10.77, p<0.01, Fig. 5.6 D). There was no interaction between sex and injury status ($F_{1,19}$=1.53, p=0.23). The use of the forelimb ipsilateral to the injury site (left forelimb), however, did not differ between brain-injured animals and sham-injured animals (brain-injured: 1.26 ± 0.49, sham-injured: 0.52 ± 0.17; $F_{1,19}$=1.56, p=0.30, Fig. 5.6 D) further supporting the preferential

use of the forelimb contralateral to the injury. Additionally, the use of the right forelimb in the brain-injured animals did not seem to be a compensatory mechanism for any type of hindlimb deficit as there were no differences in hindlimb use between brain-injured and sham-injured animals (right hindlimb, brain-injured: 11.16 ± 0.56, sham-injured: 11.19 ± 0.30, $F_{1,19}$=0.004, p=0.95; left hindlimb, brain-injured: 11.00 ± 0.61, sham-injured: 10.96 ± 0.44, $F_{1,19}$=0.28, p=0.61, Fig. 5.6 E).

5.4.2 Brain-injured animals demonstrated alterations in neuronal activity in the forelimb region of the frontal motor cortex.

In light of behavioral changes that implicate frontal cortex circuitry (NOR and forelimb motor deficits) evoked field potentials (EFPs) were recorded a millimeter anterior to bregma in the forelimb region of the motor cortex (Fig. 5.7 A). This region is outside of the direct impact site and does not show any cellular pathology such as activated microglia/macrophages or degenerating FJB-labeled cells. The amplitude, latency, and duration was quantified for each signal, averaged according to injury condition, and presented at a stimulus intensity of 800 μA (Fig. 5.7 D-F). Brain-injured animals demonstrated altered activity in the forelimb region of the motor cortex that was indicative of hypoactivity at 3 days post-injury (Fig. 5.7 B) and hyperactivity at 21 days post-injury (Fig. 5.7 C). A 3-way ANOVA (status, sex, and time) analyzing the amplitudes of the signals revealed a significant interaction between status and time ($F_{2,27}$=17.73; p<0.001), but no interaction between status, time, and sex ($F_{2,27}$=1.35; p=0.28). Post-hoc analysis of the interaction between status and time indicated that signals from brain-injured animals were significantly smaller in amplitude than signals

from sham-injured animals at 3 days post-injury (sham-injured, 0.55 ± 0.07mV; brain-injured, 0.20 ± 0.02mV; $p<0.01$, Fig. 5.7 B,D). There was no difference in the amplitude of the signals from sham-injured and brain-injured animals at 7 days post-injury (sham-injured, 0.30 ± 0.07mV; brain-injured, 0.33 ± 0.05mV; $p=0.71$, Fig. 5.7 D), but at 21 days post-injury, the signals from brain-injured animals were significantly larger than those from sham-injured animals (sham-injured, 0.24 ± 0.04mV; brain-injured, 0.49 ± 0.08mV; $p<0.05$, Fig. 5.7 C,D). Also, there was a developmental decrease observed in sham-injured animals in which the signal amplitude at 3 days was significantly larger than at 7 days ($p<0.05$) and 21 days post-injury ($p<0.01$).

Altered activity can also manifest as a difference in the time it takes the signal to arrive at the recording electrode after stimulation (latency, Fig. 5.7 E). A 3-way ANOVA analyzing signal latencies revealed a significant interaction between status and time ($F_{2,27}=10.91$; $p<0.001$). Post-hoc analysis revealed that, at 3 days post-injury, the signals from brain-injured animals arrived much slower than the signals from sham-injured animals (sham-injured, 2.63 ± 0.34s; brain-injured, 4.46 ± 0.20s; $p<0.05$, Fig. 5.7 B,E). There was no difference in latency of signal between sham- and brain-injured animals at 7 days (sham-injured, 3.93 ± 0.67s; brain-injured, 3.55 ± 0.23s; $p=0.74$, Fig. 5.7 E). At 21 days post-injury, the signals from brain-injured animals arrived faster than those from sham-injured animals, but this difference did not reach significance (sham-injured, 3.62 ± 0.20s; brain-injured, 2.3 ± 0.50s; $p=0.07$, Fig. 5.7 C,E). There was no interaction between status, time, and sex in the latency of the signal ($F_{2,27}=0.71$; $p=0.50$). Differences in the width of signal can also be indicative of altered activity in the region of interest. Analysis of the width of the signal showed no significant differences between

sham-injured and brain-injured animals at 3 days (sham-injured, 2.31 ± 0.45s; brain-injured, 2.03 ± 0.32s), 7 days (sham-injured, 2.02 ± 0.19s; brain-injured, 2.17 ± 0.56s), or 21 days post-injury (sham-injured, 1.80 ± 0.23s; brain-injured, 1.94 ± 0.21s; $F_{2,27}$=0.17; p=0.84, Fig. 5.7 F). There was also no significant interaction between status, time, and sex ($F_{2,27}$=0.21; p=0.81).

5.4.3 Systemic minocycline administration influenced functional outcomes at 4 weeks post-injury.

Treatment with minocycline improved the injury-induced working memory deficit

In the pre-test, sham-injured and brain-injured (irrespective of treatment) animals spent similar percentages of time with both objects and there was no interaction effect between status (sham-injured, brain-injured vehicle, brain-injured minocycline), sex, and bottle ($F_{2,54}$=0.85; p=0.43, Fig. 5.8 A). A 2-way ANOVA of the percent time spent with the novel and original object in the test trial revealed a significant effect of status ($F_{2,27}$=16.98; p<0.001) and post-hoc testing indicated that sham-injured animals spent significantly more time with the novel object than both brain-injured groups (sham-injured: 78 ± 2; brain-injured vehicle: 60 ± 1, p<0.001; brain-injured minocycline: 68 ± 3, p<0.01, Fig. 5.8 B). The minocycline-treated brain-injured group, however, spent a significantly higher percentage of time with the novel object compared to the brain-injured animals that received the vehicle (p<0.01) indicating that minocycline treatment had a positive effect on working memory in the 4th post-injury week (Fig. 5.8 B). There was no significant interaction between status and sex in the percent of time spent with the novel object ($F_{2,27}$=2.04; p=0.15).

Minocycline treatment did not affect seizure activity

When exposed to flurothyl gas, 100% of animals seized. Due to a low number of animals in this seizure study (Table 5.2), sex was not used as an independent variable for analysis. A one-way ANOVA analyzing the latency to the first myoclonic jerk revealed a significant effect of injury status ($F_{2,8}$=10.31; p<0.01) in which sham-injured animals (283 ± 8s) had significantly longer latencies than both brain-injured groups irrespective of treatment status (brain-injured vehicle: 230 ± 5s, p<0.01; brain-injured minocycline: 225 ± 12s, p<0.01, Fig. 5.9 A) replicating the increased susceptibility observed in the brain-injured animals in the characterization study (Fig. 5.4 B). Minocycline-treated brain-injured animals, however, did not differ from the brain-injured animals that received the vehicle (p=0.72) in terms of latency to seize. Similar to the characterization study, the length of the seizure did not differ between sham-injured animals and either brain-injured group ($F_{2,8}$=0.26; p=0.78).

Minocycline treatment exacerbated the mild injury-induced increase in fine movement.

Similar to the characterization study, brain-injured animals did not show any differences in basic locomotion compared to sham-injured animals (sham-injured: 857 ± 38 beam breaks, brain-injured vehicle: 892 ± 52 beam breaks, brain-injured minocycline: 889 ± 42 beam breaks) and there was no significant interaction between status and sex ($F_{2,42}$=1.58; p=0.22, Fig. 5.10 A). Analysis of the fine movement revealed a significant effect of status ($F_{2,42}$=5.27; p<0.01), but no interaction between status and sex ($F_{2,42}$=2.93; p=0.06, Fig. 5.10 B). Post-hoc analysis of the status effect indicated that

sham-injured animals made significantly fewer fine movement beam breaks (368 ± 11 beam breaks) than minocycline-treated brain-injured animals (435 ±15 beam breaks, $p<0.01$), but did not differ from the brain-injured animals that received the vehicle (395 ± 16 beam breaks, $p=0.18$). Minocycline-treated brain-injured animals also made significantly more fine movement beam breaks compared to the brain-injured animals that received the vehicle ($p<0.05$, Fig. 5.10 B). The effect on fine movement originally observed in the characterization study (Fig. 5.5 C) was very mild and was not repeated in the brain-injured animals that received the vehicle in this study. This may be due to an increase in the number of animals in each group and the introduction of a third status group. This increase in animals also revealed an injury-induced decrease in rearing behavior. A 2-way ANOVA revealed a significant effect of status ($F_{2,42}=7.62$; $p<0.01$) that showed that sham-injured animals made significantly more rearing beam breaks (29 ± 4 beam breaks) compared to brain-injured animals that received the vehicle (19 ± 3 beam breaks, $p<0.01$) and brain-injured minocycline-treated animals (17 ± 2 beam breaks, $p<0.01$). There was, however, a significant interaction between status and sex ($F_{2,42}=4.55$; $p<0.05$) that indicated that sham-injured females made significantly more rearing beam breaks than any other group ($p<0.01$).

Treatment with minocycline reversed injury-induced deficits in forelimb motor control

Forelimb motor control was quantified for all groups by counting the number of strokes taken with both of the forelimbs (contralateral to the injury = right forelimb, ipsilateral to the injury = left forelimb). A 2-way ANOVA analyzing the number of strokes taken with the forelimb contralateral to the injury revealed a significant effect of

status ($F_{2,18}$=9.65; p<0.01) and no interaction between status and sex ($F_{2,18}$=0.46; p=0.64, Fig. 5.11). Post-hoc analysis of the status effect showed that brain-injured animals that received the vehicle took significantly more strokes with the forelimb contralateral to the injury (4 ± 0.65 strokes) compared to both sham-injured animals (0.62 ± 0.41 strokes, p<0.01) and brain-injured animals treated with minocycline (0.93 ± 0.37 strokes, p<0.01). Brain-injured animals treated with minocycline showed no difference in the number of strokes taken compared to sham-injured animals (p=0.68) indicating a treatment-induced rescue of the forelimb motor control deficit. Similar to the characterization study, there was no difference in the number of strokes taken with the forelimb ipsilateral to the injury for any group (sham-injured: 0.62 ± 0.27 strokes, brain-injured vehicle: 1.54 ± 0.26 strokes, brain-injured minocycline: 1.20 ± 0.27 strokes, $F_{2,18}$=0.17; p=0.84).

Minocycline treatment reversed injury-induced hypoactivity at 3 days post-injury and injury-induced hyperactivity at 4 weeks post-injury

At 3 days post-injury, analysis of the signal amplitude revealed a significant effect of status ($F_{2,13}$=8.38; p<0.01) and no interaction effect between status and sex ($F_{2,13}$=0.27; p=0.77). Post-hoc analysis revealed that the previously-observed hypoactivity in brain-injured animals in the characterization study (Fig. 5.7) was also observed in the brain-injured animals that received the vehicle as their signals were significantly smaller than those from sham-injured animals (sham-injured: 0.48 ± 0.04 mV, brain-injured vehicle: 0.23 ± 0.03 mV, p<0.01, Fig. 5.12 A, C). Minocycline-treated brain-injured animals, however, had significantly larger signals compared to brain-injured animals that received the vehicle (0.44 ± 0.06 mV, p<0.01). Additionally, their signals do not differ from sham-

injured animals (p=0.55), indicating a rescue of the injury-induced decrease in signal amplitude. Analysis of signal latency at 3 days revealed a significant effect of status ($F_{2,13}$=7.28; p<0.01) that indicated that brain-injured animals, irrespective of treatment, demonstrated increased latencies compared to sham-injured animals (sham-injured: 3.12 ± 0.23s; brain-injured vehicle: 3.97 ± 0.20s, p<0.05; brain-injured minocycline: 3.95 ± 0.36s, p<0.05, Fig. 5.12 D). While minocycline treatment appeared to rescue the injury-induced deficit in signal amplitude, brain-injured minocycline-treated animals did not show a recovery in injury-induced deficits in signal latency as the latencies of their signals did not differ from the latencies of the signals from brain-injured animals that received the vehicle (p=0.95). There was an interaction between status and sex ($F_{2,13}$=4.33; p<0.05) that indicated that male brain-injured minocycline-treated animals had significantly longer latencies compared to female brain-injured minocycline-treated animals (p<0.05). Similar to the characterization study, there was no significant effect of status ($F_{2,13}$=0.86; p=0.44) and no significant interaction between status and sex ($F_{2,13}$=2.77; p=0.10) in terms of the signal duration (Fig. 5.12 E).

At 4 weeks post-injury, analysis of the signal amplitude showed a significant effect of status ($F_{2,10}$=5.75; p<0.05) and no interaction between status and sex ($F_{2,10}$=0.08; p=0.93). Brain-injured animals that received the vehicle had significantly larger signals than sham-injured animals (sham-injured: 0.22 ± 0.02mV, brain-injured vehicle: 0.39 ± 0.08mV, p<0.05), indicative of hyperactivity. Signals from brain-injured minocycline-treated animals (0.19 ± 0.02mV) were significantly smaller than those from brain-injured animals that received the vehicle (p<0.05) and did not differ from sham-injured animals (p=0.67), indicating that minocycline treatment rescued the injury-induced hyperactivity

observed in the chronic post-injury period (Fig. 5.12 B,C). Interestingly, there was no significant effect of status or significant interaction between status and sex in the latency of the signals indicating that any altered activity did not manifest in a change in signal latency (Fig. 5.12 D). There was also no significant effect of status ($F_{2,10}$=0.18; p=0.84) or significant interaction between status and sex in the duration of the signals ($F_{2,10}$=3.86; p=0.06).

5.4.7 Acute microglial/macrophage depletion does not alter injury-induced deficits

Clodronate administration does not alter forelimb motor control in the forelimb contralateral to the injury site but increased use in the forelimb ipsilateral to the impact

Both sham-injured and brain-injured animals treated with clodronate liposomes or empty liposomes were subjected to the straight path swim task in the 4th week post-injury when an injury-induced deficit in forelimb motor control was previously observed (Fig. 5.6). Analysis revealed an effect of status ($F_{3,27}$=11.12; p<0.001) but no interaction between status and sex ($F_{3,27}$=0.42; p=0.74, Fig. 5.13). Post hoc analysis indicated that brain-injured animals that received the empty liposomes used the forelimb contralateral to the injury significantly more than the sham-injured group that received the empty liposomes (sham-injured empty-lip: 0.44 ± 0.21 strokes; brain-injured empty-lip: 5.04 ± 1.27 strokes, p<0.01). Similarly, brain-injured animals that received the clodronate liposomes used the forelimb contralateral to the injury site significantly more than sham-injured animals that received the clodronate liposomes (sham-injured clod-lip: 0.26 ± 0.12 strokes; brain-injured clod-lip: 6.11 ± 1.28 strokes, p<0.001). The number of strokes with the contralateral forelimb, however, did not differ between brain-injured

animals that received the empty liposomes and those that received the clodronate liposome treatment (p=0.41). Also, the strokes taken by sham-injured animals did not differ between treatment conditions (empty-lip vs. clod-lip, p=0.89, Fig. 5.13). Interestingly, there was a significant effect of status in the use of the forelimb ipsilateral to the injury ($F_{3,27}$=3.95; p<0.05). Post-hoc assessment revealed that brain-injured animals that received clodronate liposomes took significantly more strokes with the forelimb ipsilateral to the injury (2.07 ± 0.22 strokes) compared to the sham-injured clodronate liposome group (1.04 ± 0.64 strokes, p=0.05) and the brain-injured animals that received the empty liposomes (2.07 ± 0.22 strokes, p<0.05). There was no significant interaction between status and sex for use of the forelimb ipsilateral to the injury ($F_{3,27}$=2.06; p=0.13).

Clodronate administration does not alter injury-induced hyperactivity in the forelimb region of the motor cortex at 4 weeks post-injury

Evoked field potentials in the clodronate study were only recorded in the chronic post-injury period after evidence of microglial/macrophage repopulation (Fig. 5.1). Signals from the forelimb region of the motor cortex of brain-injured animals were large compared to sham-injured animals irrespective of treatment (Fig. 5.14 A). Analysis of signal amplitude revealed a significant effect of status ($F_{3,25}$=17.46; p<0.001) and no interaction between status and sex ($F_{3,25}$=0.15; p=0.93). Brain-injured animals that received the empty liposomes and brain-injured animals that received the clodronate liposomes had significantly larger signals than the corresponding sham-injured animals (sham-injured empty-lip: 0.21 ± 0.02 mV, brain-injured empty-lip: 0.40 ± 0.04 mV,

$p<0.001$; sham-injured clod-lip: 0.19 ± 0.02 mV, brain-injured clod-lip: 0.45 ± 0.04 mV, $p<0.001$; Fig. 5.14 B). Signals from sham-injured animals that received the empty liposomes were similar in magnitude to the signals from sham-injured animals that received the clodronate liposomes ($p=0.57$). Also, signals from brain-injured animals that received the empty liposomes did not differ in magnitude from the signals from brain-injured animals that received the clodronate liposomes ($p=0.26$). Interestingly, there was no significant effect of status (latency: $F_{3,25}=0.49$; $p=0.69$; duration: $F_{3,25}=0.27$; $p=0.85$) or interaction between status and sex for the latency of the signal ($F_{3,25}=0.81$; $p=0.50$, Fig. 5.14 C) or the duration of the signal ($F_{3,25}=0.37$; $p=0.77$, Fig. 5.14 D). Together, these data indicate that the acute microglial/macrophage depletion within the impact site had no effect on neuronal activity in the forelimb motor cortex- a region that is anterior to the impact site.

5.5 DISCUSSION

The current study illustrated a wide range of behavioral deficits in the chronic post-injury period and demonstrated alterations in neuronal activity not related to cellular pathology. Previous to this set of experiments, the only functional outcome assessed in our injury model was spatial learning and memory in the Morris water maze (Raghupathi & Huh, 2007). In this study, brain-injured animals demonstrated mild increases in anxiety-like behavior in the elevated plus maze, an impairment in short-term novel object recognition memory, an increased susceptibility to seize, increased fine locomotion, and impairment in forelimb motor control. Brain-injured animals also demonstrated hypoactivity in the forelimb region of the motor cortex at 3 days post-injury that later evolved into a hyperactivity at 21 days post-injury. Acute treatment with minocycline reduced the NOR impairment, reversed the deficit in forelimb motor function, and completely rescued the alterations in neuronal activity in the forelimb region of the motor cortex at both 3 days and 4 weeks post-injury. This treatment, however, did not have any effect on seizure susceptibility. Similarly, acute clodronate administration to the impact site did not affect the forelimb motor control deficit or the hyperactivity at 4 weeks post-injury.

In our animals, we observed a mild increase in anxiety-like behavior as evidenced by an increase in the time spent in the closed arms of the EPM. The mild, but insignificant, decrease observed in the closed arm entries may indicate that our animals were spending more time in the closed arms simply due to a decrease in overall locomotion. This, however, is not true as brain-injured and sham-injured animals performed similarly in measures of basic locomotion in the open field activity monitoring

chamber. Our results are in line with the previous observation that brain injury in young rats (PND7 & PND17) resulted in increased anxiety-like behavior in the open field or elevated zero maze (Sonmez et al., 2007, Ajao et al., 2012). Groups using older animals (PND21-PND30), however, observed a decrease in anxiety-like behavior (Pullela et al., 2006; Mychasiuk et al., 2014) that may point to an age-at-injury effect indicating that impact to a younger brain may result in a different manifestation of anxiety-like behaviors. There is also evidence in both humans and animals that injury to the developing brain may have profound effects on social behavior and result in a form of social anxiety (Yeates et al., 2004; Max et al., 2011; Semple et al. 2012). Semple et al. (2012) demonstrated an increase in social anxiety behavior in an animal model using PND21 mice that had previously shown a decrease in general anxiety behavior. Studies such as this indicate that assessment of social anxiety after injury may yield very different results from the assessment of general anxiety (or novel environment anxiety as the case may be for tests utilizing open fields and elevated mazes) and this may be a worthwhile avenue of investigation in our injury model.

We have previously shown that our animals (injured on PND11) demonstrate cognitive impairment in the form of spatial learning and memory deficits in the Morris water maze at 4 weeks post-injury (Raghupathi & Huh, 2007). Interestingly, when the same injury was performed on slightly older rat pups (PND17), these animals did not demonstrate any deficit in this same spatial learning and memory task at 4 weeks. Anatomical structures that have implications for this task include the retrosplenial cortex, the subiculum of the hippocampus, and the laterodorsal thalamus (Vann et al., 2009; O'Mara et al., 2009; van Groen et al., 2002)- all of which demonstrate some degree of

cellular pathology (neurodegeneration and microglial/macrophage reactivity) in our injury model (Chapter 3, Hanlon et al., 2016b). Working memory tasks that involve long intervals between training and assessment have been found to involve hippocampal connections, but short-term working memory, especially object recognition based memory, involves the prefrontal cortex and the perirhinal cortex (Barker et al., 2007). While these regions did not demonstrate any cellular pathology after our CCI injury, other injury models using young animals have demonstrated novel object recognition memory deficits (Scafidi et al., 2010; Schober et al., 2012). The fact that our injury produced deficits in this assessment illustrates the diffuse nature of our impact-based model as it is possible that there are alterations in activity in the circuitry responsible for novel object recognition.

The forelimb deficit that was observed in the straight path swim task may be directly related to the alteration in neuronal activity in the forelimb region of the motor cortex. This task is dependent on the animal's ability to exert inhibitory control over excitatory processes that contribute to forelimb locomotion as rats typically swim in a straight path using only their hindlimbs for propulsion. Stoltz et al. (1999) showed that a lesion in this region of the motor cortex resulted in a sustained deficit in forelimb inhibitory motor control. Adult rats that underwent lesion injury to the forelimb region of the motor cortex exhibited increased use of the forelimb contralateral to the lesion in the straight-path swim task out to 8 weeks post-lesion. Our animals also showed increased utilization of the forelimb contralateral to the injury that coincided with increased EFP signal amplitudes and decreased signal latencies in the forelimb region of the motor cortex. This hyperactivity may be indicative of a loss of inhibitory control in this region

thus resulting in the observed behavioral alteration. This evidence of hyperactivity within the brain may also contribute to the observed increase in seizure susceptibility at 4 weeks post-injury. With these results, investigation into the integrity of the inhibitory signaling in the brain may provide new mechanistic insight into the observed alterations.

We have demonstrated that systemic minocycline administration can reduce injury-induced microglial/macrophage reactivity at 3 days post-injury within the impact site, but does not affect spatial learning and memory impairment (Chapter 4, Hanlon et al., 2016b). It is unclear, however, whether minocycline treatment can alter microglial/macrophage function in regions without cellular pathology thereby altering functional outcomes as well. In this study, treating brain-injured animals with minocycline for only the first 3 days post-injury resulted in functional recovery at 4 weeks post-injury. This treatment reduced the NOR deficit, reversed the deficit in forelimb inhibitory motor control, and also reversed both the acute and chronic alterations in neuronal activity in the forelimb region of the motor cortex. Minocycline has previously been effective in reversing novel object recognition deficits in the chronic post-injury period following brain-injury in adult mice (Siopi et al., 2012). Our similar results indicate that minocycline may have effects on the circuitry behind NOR memory.

The fact that the reversal of the injury-induced hyperactivity in the forelimb region of the motor cortex also coincided with a complete rescue of the deficit in forelimb inhibitory motor control supports the hypothesis that the behavior is directly related to the alteration in activity in this region. Despite a reduction in this hyperactivity, however, minocycline treatment did not affect seizure susceptibility indicating that the hyperactivity in the forelimb region of the motor cortex and the

increased vulnerability to seizure may be unrelated. Minocycline administration, however, may have direct effects on neuronal activity as it has been shown that one week of daily minocycline treatment decreased hyperactivity in dorsal root neurons in a model of burn-induced pain 4 weeks after the burn injury (Chang & Waxman, 2010). Additionally, when minocycline is directly applied to hippocampal neurons, the treatment can decrease glutamate-induced hyperactivity and intracellular calcium increases (Gonzalez et al., 2007).

Together with our data, this indicates that minocycline may have effects that are unrelated to its ability to alter the microglial/macrophage activation state. This is further supported by the fact that clodronate-mediated microglial/macrophage depletion within the impact site did not alter the neuronal hyperactivity at 4 weeks or the deficit in forelimb motor control. If the minocycline-mediated effects were related to the decrease in microglial/macrophage reactivity in the impact site, the results of the clodronate study would have mirrored the results of the minocycline study. It is also possible that microglia/macrophages in the regions anterior to the impact site that are implicated in these behaviors (PFC, forelimb motor cortex) are still releasing mediators that could affect neuronal activity. For example, high levels of the pro-inflammatory mediator, IL-1beta, have been shown to decrease the amplitude of extracellular signals in hippocampal slices (Bellinger et al., 1993). As the minocycline treatment is systemic (instead of local such as the clodronate administration), it is possible that the drug is having an effect on soluble mediators in this region. Determining the concentrations of inflammatory mediators in these frontal regions may reveal an additional mechanism behind minocycline's beneficial effects.

5.6 FIGURE LEGENDS

Figure 5.1 Experimental timelines. (A) Schematic representing the order of the behavioral assessments that occurred in the 4th week post-injury (days 20-28) of the characterization study. **(B)** Schematic representing the treatment paradigm and the functional outcomes for the minocycline study. **(C)** Schematic representing the treatment paradigm and functional outcomes for the clodronate study.

Figure 5.2 Assessment of anxiety behavior using the elevated plus maze (EPM). (A) Diagram of the EPM apparatus. **(B)** Quantified closed arm time. **(C)** Number of entries into the closed arms. **(D)** Total time spent in the open arms (includes 2-paw and 4-paw entires). **(E)** Total time spent in the open arm with a complete 4-paw entry. **(F)** Number of entries into the open arm with all 4 paws. **(G)** Number of times animals looked over the edge of the open arms. **(H)** Number of entries into the open arm with only 2 paws. *$p \leq 0.05$ compared to sham-injured group. Error bars represent the standard error of the mean.

Figure 5.3. Assessment of short-term working memory using novel object recognition (NOR) (A) Schematic representing the habituation to the NOR chamber in which the animals were left to explore the empty chamber for two 10-minute sessions in the 2 days prior to testing. **(B)** Schematic representing the pre-test trial in which animals were left to explore two identical objects for a 5-minute period. **(C)** Schematic representing the test trial in which one of the original objects was replaced with a novel

object and animals were left to explore the objects for a 5-minute period. **(D)** Quantification of exploratory behavior during the pre-test trial. **(E)** Quantification of exploratory behavior during the test trial. Quantitative data **(D,E)** presented as the proportion of time spent with the objects over the total exploratory time. *p≤0.05 compared to sham-injured animals. Error bars represent the standard error of the mean.

Figure 5.4. Assessment of flurothyl-induced seizure susceptibility. (A) Schematic of the seizure induction chamber. **(B)** Quantification of the latency to the first myoclonic jerk. **(C)** Quantification of the length of seizure. Quantitative data **(B,C)** presented as time in seconds. *p≤0.05 compared to sham-injured animals. Error bars represent the standard error of the mean.

Figure 5.5. Assessment of open field locomotion. (A) Quantification of the number of beam breaks that qualified for basic ambulatory locomotion. **(B)** Quantification of the beam breaks that did not meet criterion for ambulatory or rearing motion and were thus characterized as fine locomotion. **(C)** Vertical beam breaks that qualified as rearing behavior. Data presented as number of beam breaks. *p≤0.05 compared to sham-injured animals. Error bars represent the standard error of the mean.

Figure 5.6. Assessment of forelimb motor function using the straight-path swim task. (A) Schematic of the swim test aquarium and experimental set-up. **(B)** Still image depicting the swimming form of a sham-injured animal. **(C)** Still image depicting the swimming form of a brain-injured animal. Note the use of the forelimb (red circle). **(D)**

Quantification of right (contralateral to impact) and left (ipsilateral to impact) forelimb use. **(E)** Quantification of right (contralateral to impact) and left (ipsilateral to impact) hindlimb use. Quantitative data **(D,E)** presented as the average number of strokes. *p≤0.05 compared to sham-injured animals. Error bars represent the standard error of the mean.

Figure 5.7. Assessment of neuronal activity in the forelimb region of the motor cortex. (A) Diagram representing electrode placement and recording location relative to the impact site. **(B)** Representative evoked field potentials (EFPs) from sham-injured and brain-injured animals at 3 days post-injury. **(C)** Representative EFPs from sham-injured and brain-injured animals at 21 days post-injury. **(D)** Quantification of the signal amplitude (mV) for sham-injured and brain-injured animals at 3, 7 and 21 days post-injury. **(E)** Quantification of the signal latency (s) for sham-injured and brain-injured animals at 3, 7, and 21 days post-injury. **(F)** Duration/signal width (s) for sham-injured and brain-injured animals at 3, 7, and 21 days post-injury. Quantitative data **(D,E,F)** presented at 800 μA stimulus intensity. *p≤0.05 compared to corresponding sham-injured group. Error bars represent the standard error of the mean.

Figure 5.8 Assessment of working memory following acute minocycline treatment. (A) Percent time spent with the identical objects in the pre-test. **(B)** Percent time spent with the novel and original objects in the test. *p≤0.05 compared to corresponding sham-injured group. #p≤0.05 compared to the brain-injured vehicle group. Error bars represent the standard error of the mean.

Figure 5.9 Assessment of seizure susceptibility following acute minocycline treatment. (A) Latency to the first myoclonic jerk measured in seconds. **(B)** Length of the seizure measured in seconds. *p≤0.05 compared to corresponding sham-injured group. Error bars represent the standard error of the mean.

Figure 5.10 Assessment of open field locomotion after acute minocycline treatment. (A) Number of basic movement beam breaks. **(B)** Number of fine movement beam breaks. **(C)** Number of rearing beam breaks. *p≤0.05 compared to corresponding sham-injured group. #p≤0.05 compared to the brain-injured vehicle group. Error bars represent the standard error of the mean.

Figure 5.11 Assessment of forelimb use after acute minocycline treatment. Number of strokes by the forelimbs contralateral (right) or ipsilateral (left) to the injury. *p≤0.05 compared to corresponding sham-injured group. #p≤0.05 compared to the brain-injured vehicle group. Error bars represent the standard error of the mean.

Figure 5.12 Assessment of evoked field potentials in the forelimb region of the motor cortex after acute minocycline treatment. (A) Representative traces from sham-injured, brain-injured vehicle, and brain-injured minocycline animals at 3 days post-injury. **(B)** Representative traces from sham-injured, brain-injured vehicle, and brain-injured minocycline animals at 4 weeks post-injury. **(C)** Quantification of signal amplitude for sham-injured, brain-injured vehicle, and brain-injured minocycline animals at 3 days and

4 weeks post-injury. **(D)** Quantification of signal latency for sham-injured, brain-injured vehicle, and brain-injured minocycline animals at 3 days and 4 weeks post-injury. **(E)** Quantification of the duration/width of the signal from sham-injured, brain-injured vehicle, and brain-injured minocycline animals at 3 days and 4 weeks post-injury. *p≤0.05 compared to corresponding sham-injured group. #p≤0.05 compared to the brain-injured vehicle group. Error bars represent the standard error of the mean.

Figure 5.13 Assessment of forelimb use following acute microglial/macrophage depletion. Number of strokes by the forelimbs contralateral (right) or ipsilateral (left) to the injury. *p≤0.05 compared to corresponding sham-injured group. #p≤0.05 compared to the brain-injured empty-lip group. Error bars represent the standard error of the mean.

Figure 5.14 Assessment of evoked field potential in the forelimb region of the motor cortex following acute microglial/macrophage depletion. (A) Representative traces from sham-injured empty-lip, brain-injured empty-lip, sham-injured clod-lip and brain-injured clod-lip animals at 4 weeks post-injury. **(B)** Quantification of signal amplitude for sham-injured empty-lip, brain-injured empty-lip, sham-injured clod-lip and brain-injured clod-lip animals at 4 weeks post-injury. **(C)** Quantification of signal latency for sham-injured empty-lip, brain-injured empty-lip, sham-injured clod-lip and brain-injured clod-lip animals at 4 weeks post-injury. **(D)** Quantification of the duration/width of the signal from sham-injured empty-lip, brain-injured empty-lip, sham-injured clod-lip and brain-injured clod-lip animals at 4 weeks post-injury. *p≤0.05 compared to corresponding sham-injured group. Error bars represent the standard error of the mean.

5.7 TABLES and FIGURES

Table 5.1 Listing of characterization animals for Part A

*The same animals were used for EPM, NOR, Seizure, Activity Monitoring, and Swim Test

Outcome	Experiment	Time Point (days)	Group	N
Elevated Plus Maze	Characterization	24	Sham	11
			Injured	12
Novel Object Recognition	Characterization	27	Sham	11
			Injured	12
Seizure	Characterization	28	Sham	11
			Injured	12
Activity Monitoring	Characterization	20	Sham	11
			Injured	12
Swim Test	Characterization	22	Sham	11
			Injured	12
+1mm E-phys	Characterization	3	Sham	6
			Injured	6
		7	Sham	6
			Injured	6
		21	Sham	6
			Injured	6
Total*	**Characterization**		**Sham**	**29**
			Injured	**30**

Table 5.2 Listing of minocycline and clodronate study animals for Part B

*Overlap in some behavioral animals

**Overlap in some behavioral and E-phys animals

Outcome	Experiment	Time Point (days)	Group	N
Novel Object Recognition	Minocycline	27	Sham	11
			Injured Vehicle	12
			Injured Minocycline	12
Activity Monitoring	Minocycline	20	Sham	15
			Injured Vehicle	16
			Injured Minocycline	17
Seizure	Minocycline	28	Sham	3
			Injured Vehicle	4
			Injured Minocycline	4
Swim Test	Minocycline	22	Sham	7
			Injured Vehicle	8
			Injured Minocycline	9
+1 mm E-phys	Minocycline	3	Sham	7
			Injured Vehicle	6
			Injured Minocycline	6
		21-28 (4 weeks)	Sham	4
			Injured Vehicle	4
			Injured Minocycline	8
Total*	**Minocycline**		**Sham**	**22**
			Injured Vehicle	**22**
			Injured Minocycline	**26**
Swim Test	Clodronate	24	Sham Empty-Lip	9
			Injured Empty-Lip	8
			Sham Clod-Lip	9
			Injured Clod-Lip	9
+1mm E-phys	Clodronate	25-30 (4 weeks)	Sham Empty-Lip	8
			Injured Empty-Lip	8
			Sham Clod-Lip	9
			Injured Clod-Lip	8
Total**	**Clodronate**		**Sham Empty-Lip**	**9**
			Injured Empty-Lip	**8**
			Sham Clod-Lip	**9**
			Injured Clod-Lip	**9**

Figure 5.1 Experimental Timelines

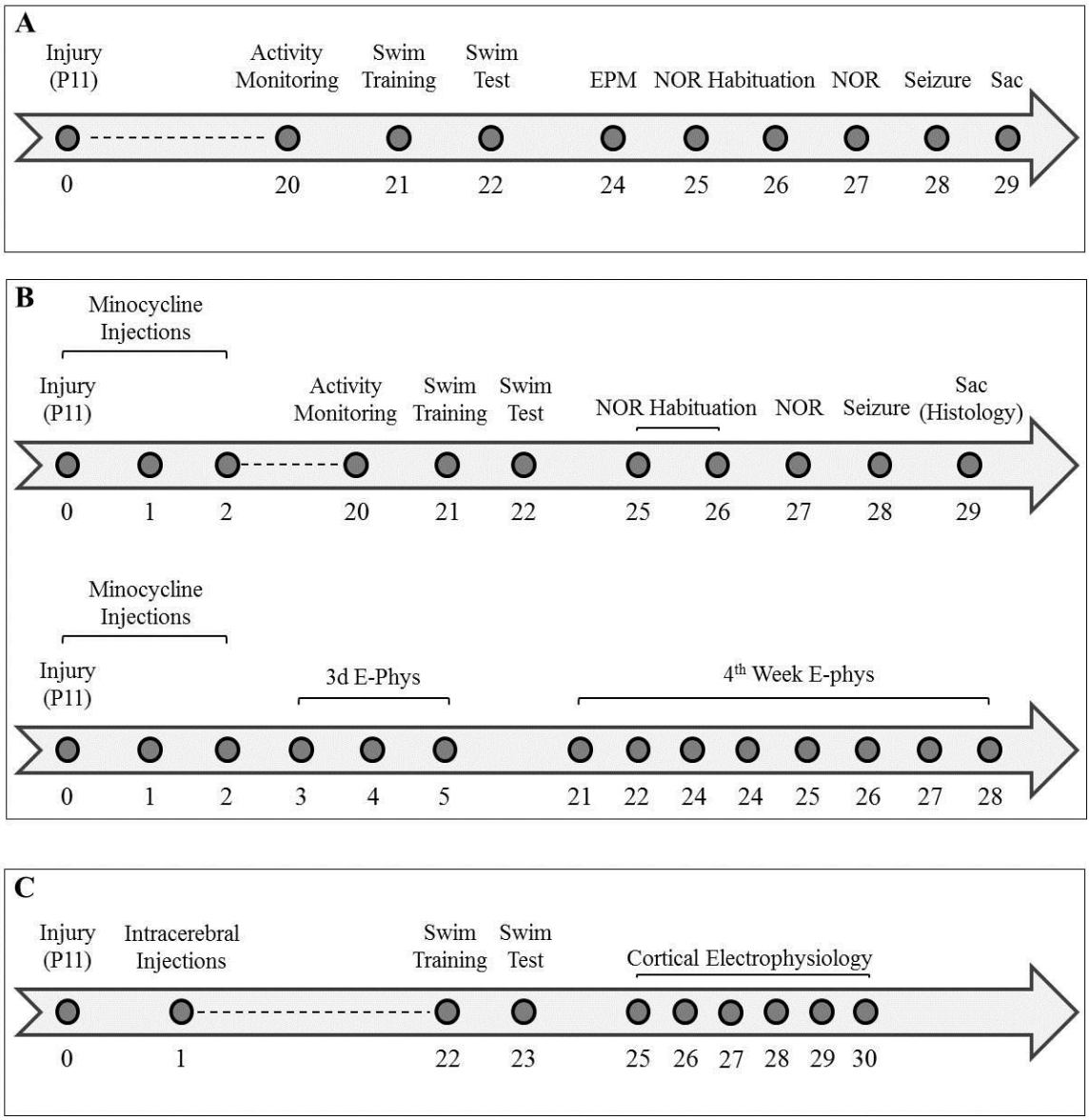

Figure 5.2 Assessment of anxiety behavior using the elevated plus maze (EPM).

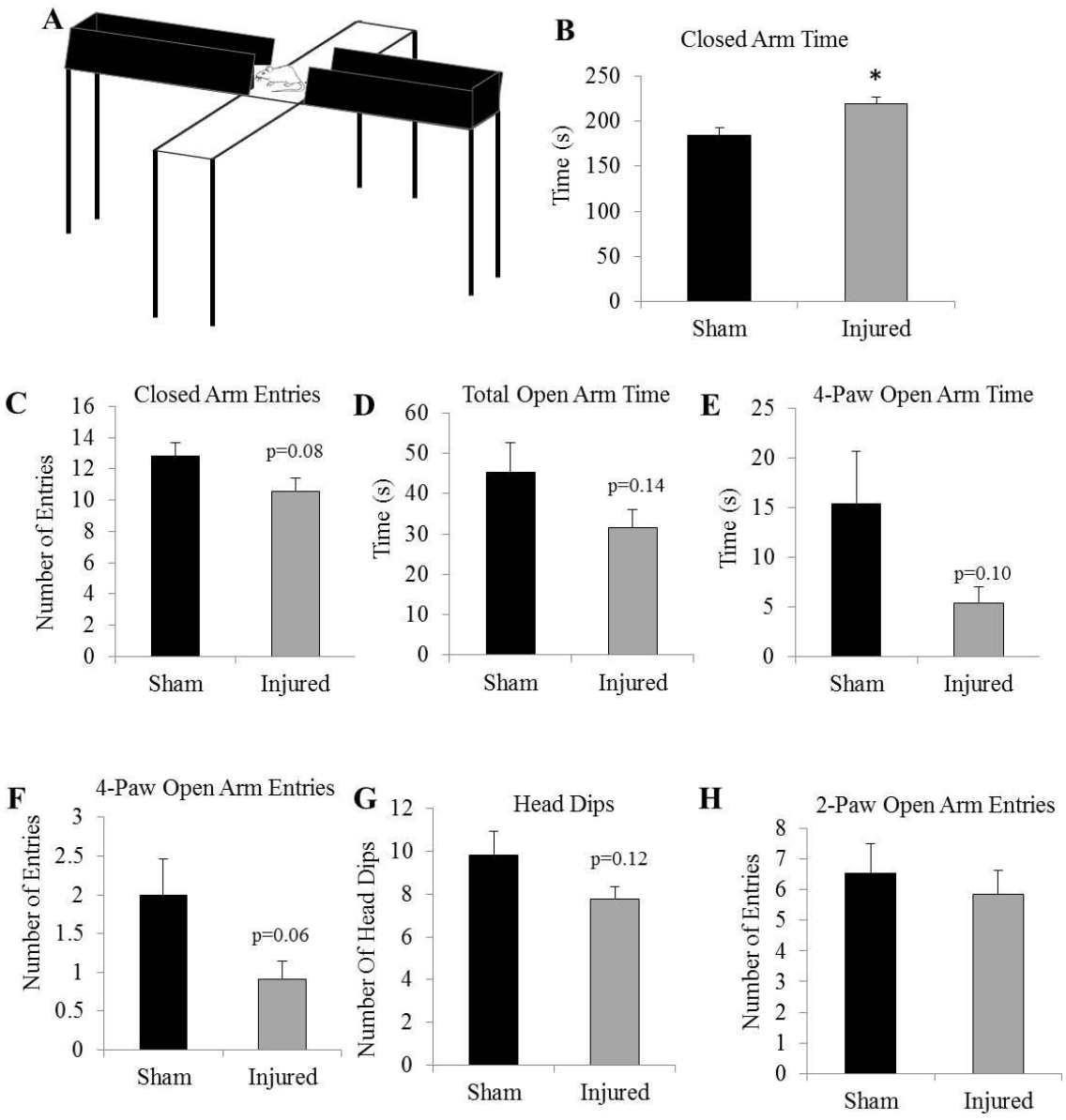

Figure 5.3 Assessment of short-term working memory using novel object recognition (NOR)

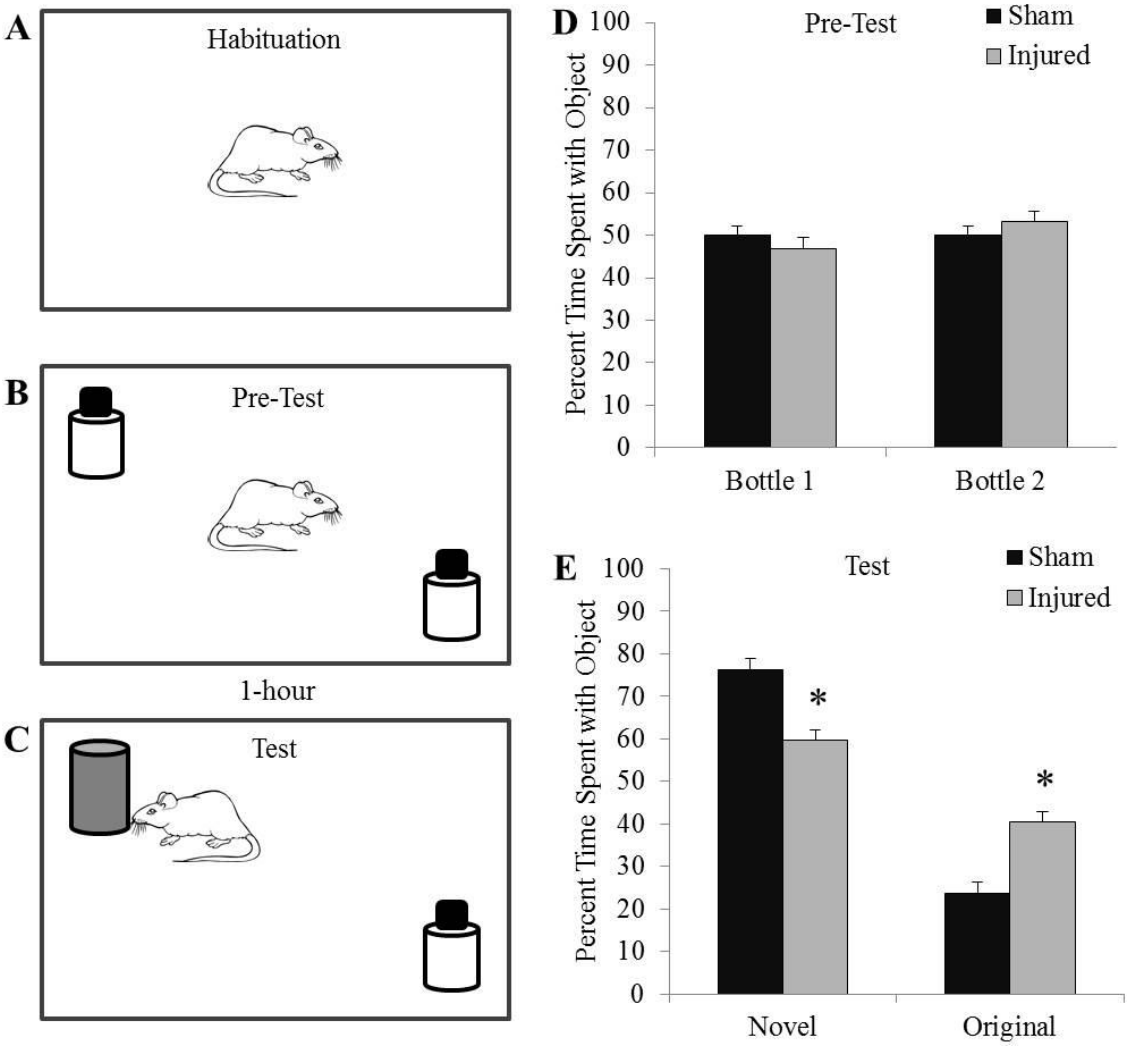

Figure 5.4 Assessment of flurothyl-induced seizure susceptibility

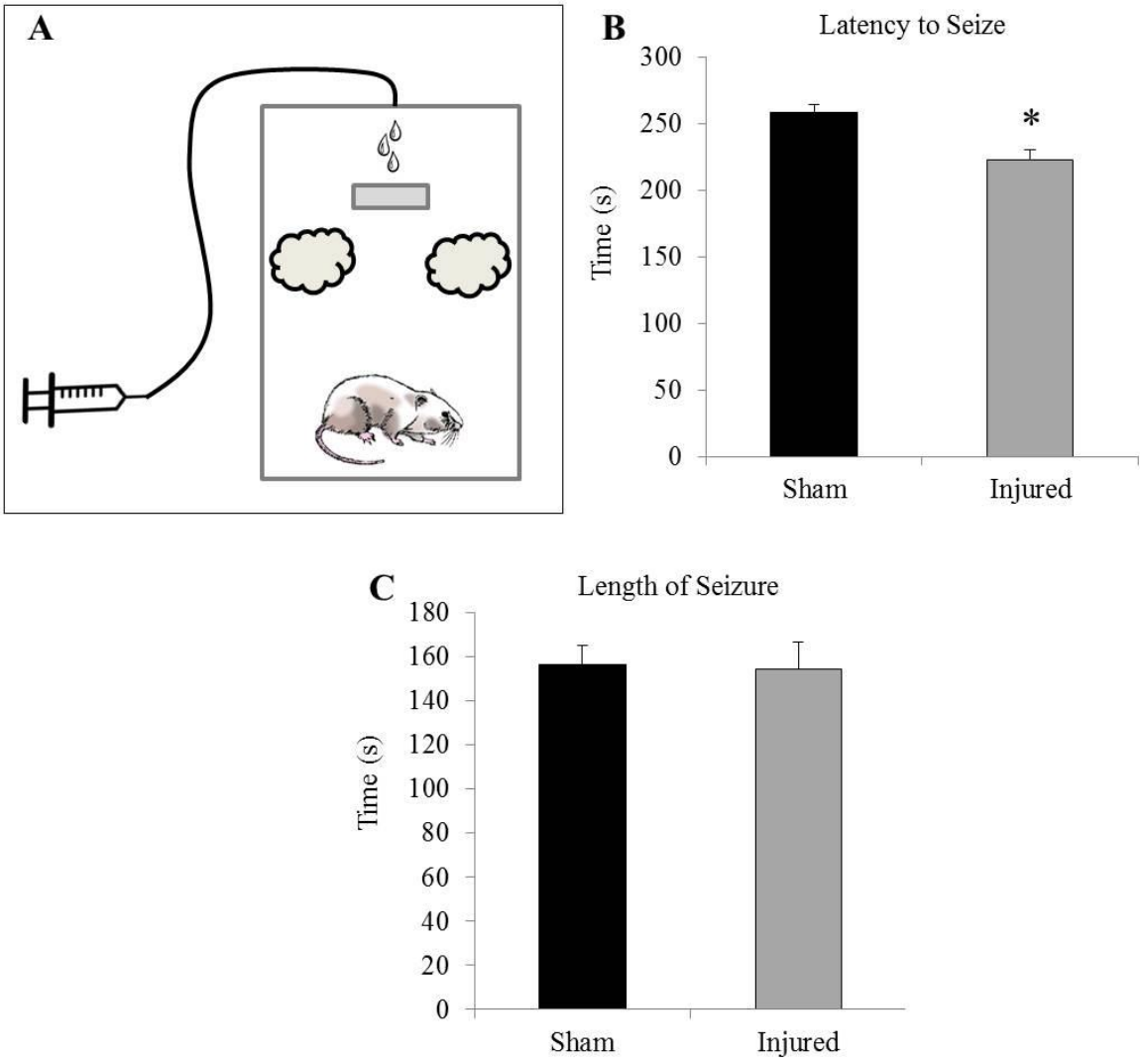

Figure 5.5 Assessment of open field locomotion

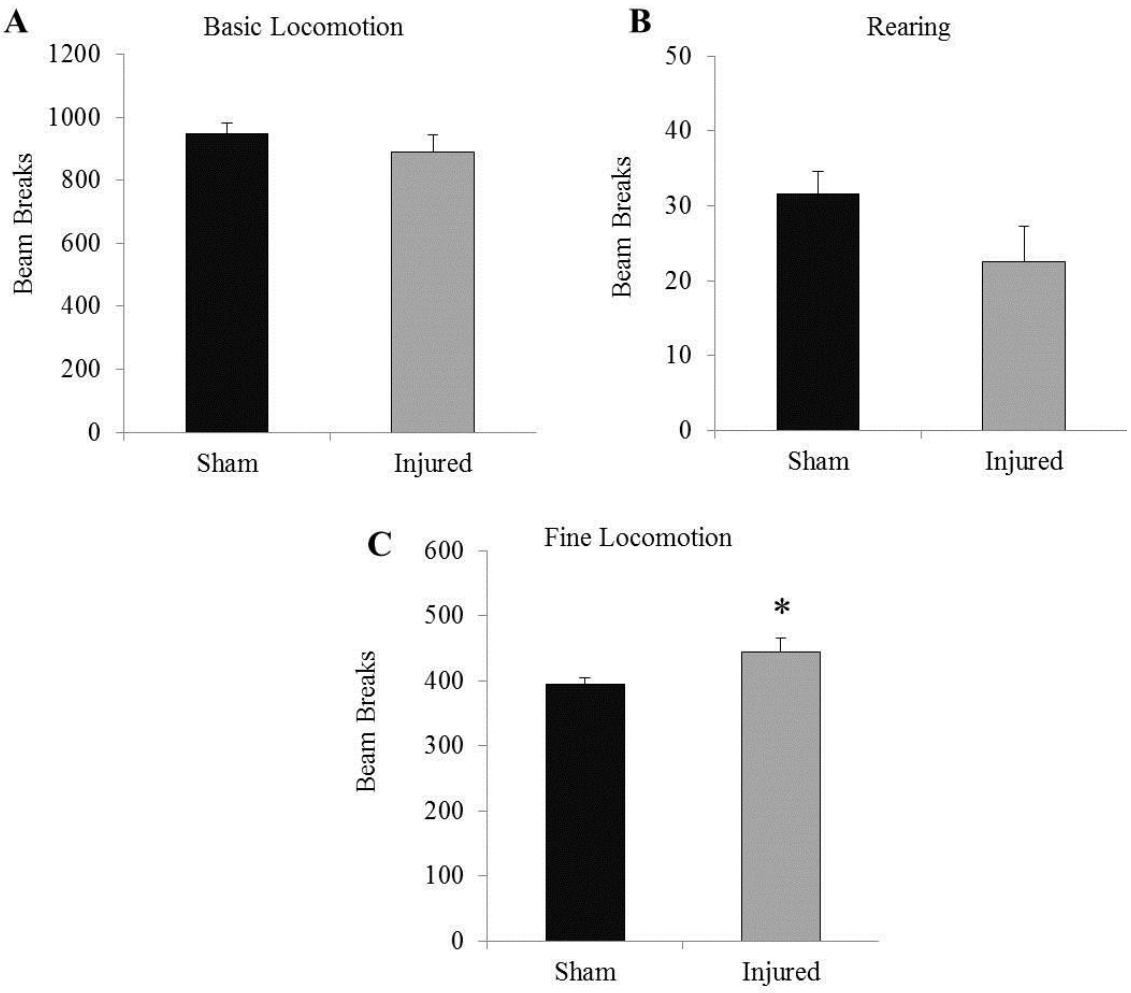

Figure 5.6 Assessment of forelimb motor function using the straight-path swim task

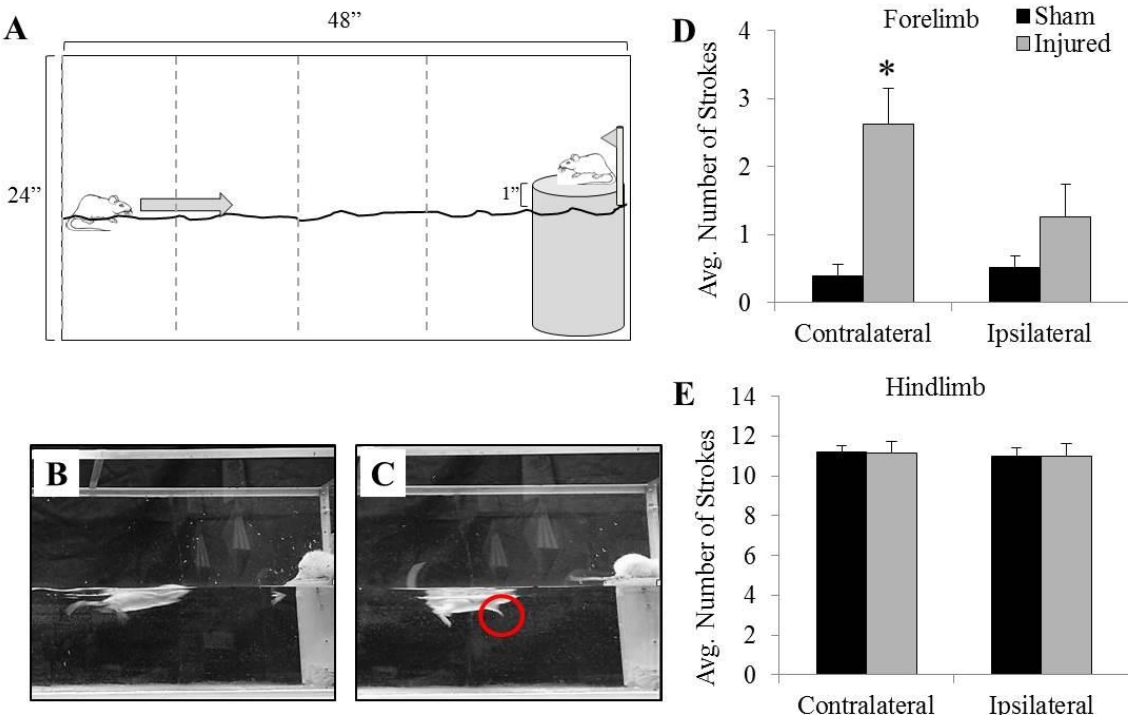

Figure 5.7 Assessment of neuronal activity in the forelimb region of the motor cortex

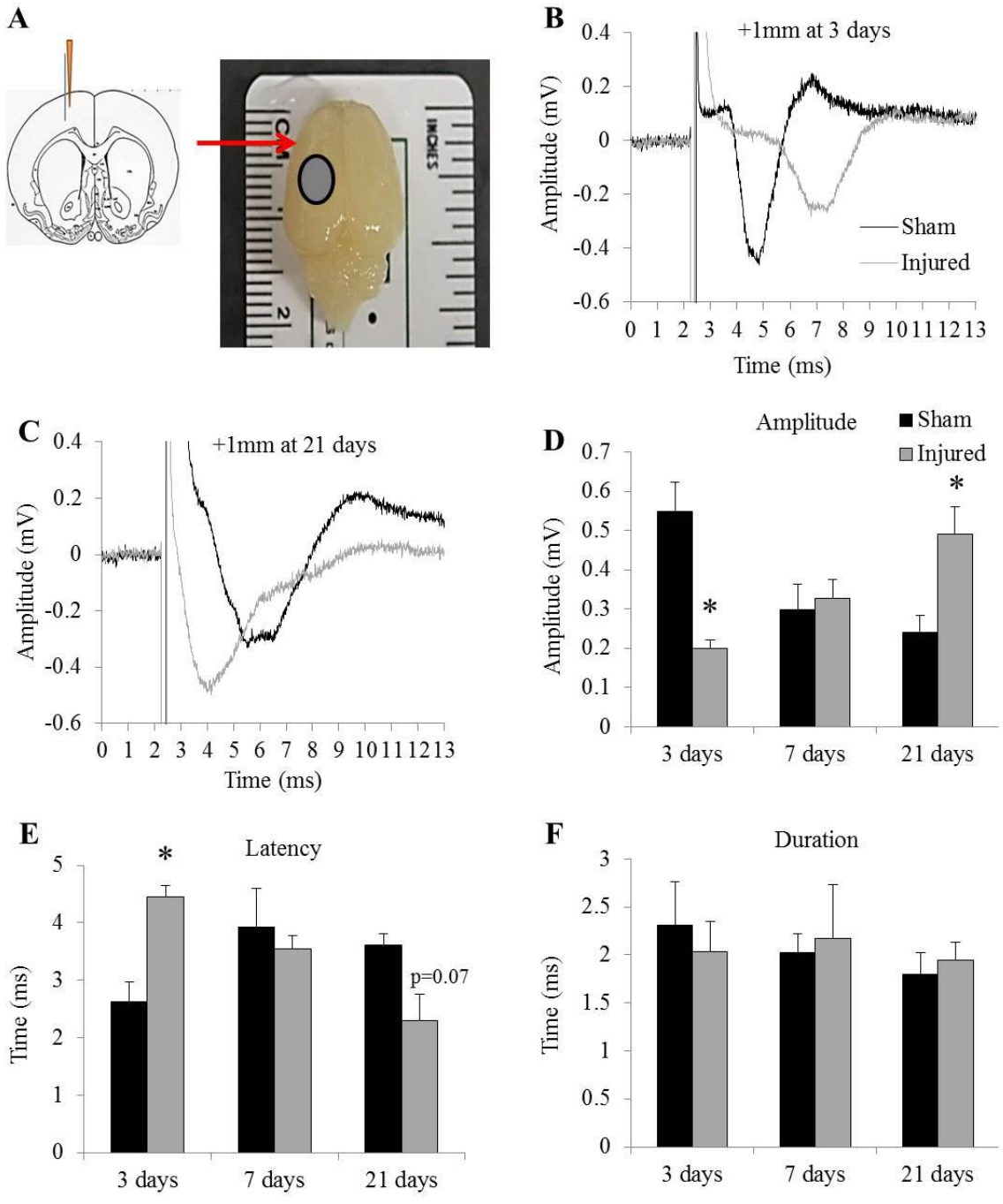

Figure 5.8 Assessment of working memory following acute minocycline treatment

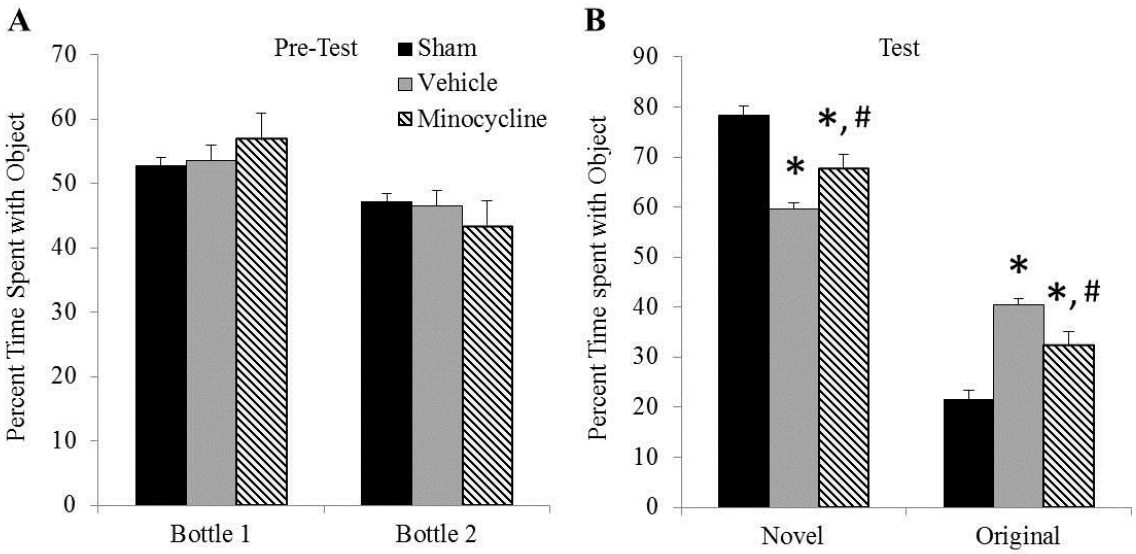

Figure 5.9 Assessment of seizure susceptibility following acute minocycline treatment

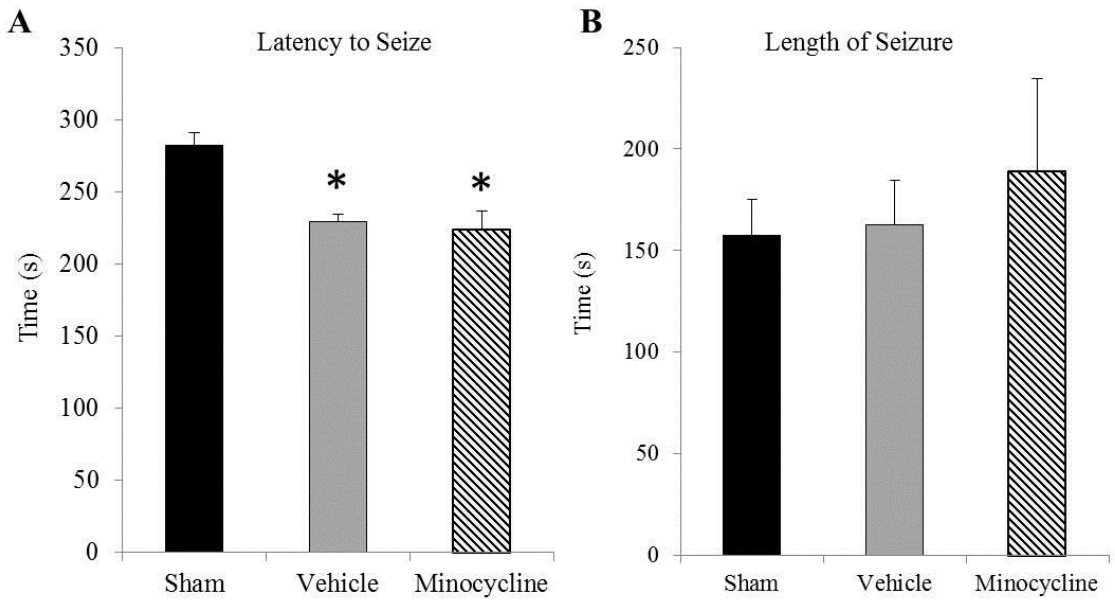

Figure 5.10 Assessment of open field locomotion after acute minocycline treatment

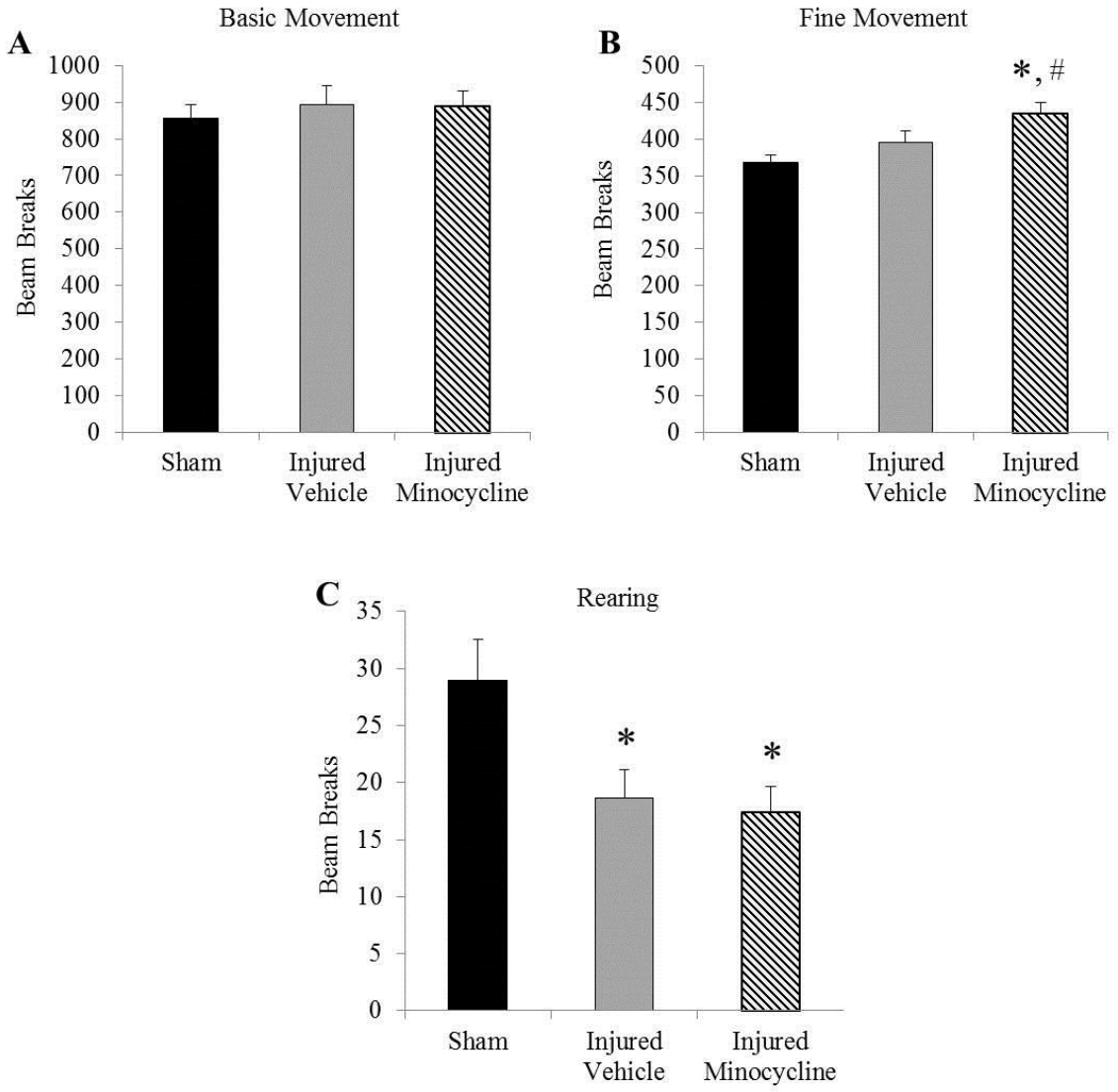

Figure 5.11 Assessment of forelimb use after acute minocycline treatment

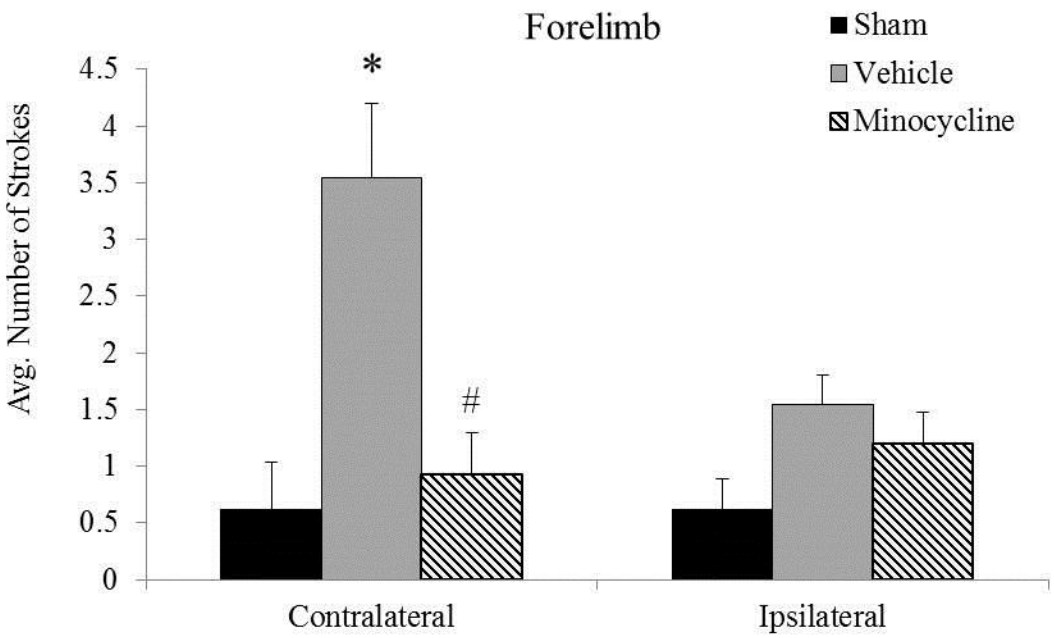

5.12 Assessment of evoked field potentials in the forelimb region of the motor cortex after acute minocycline treatment

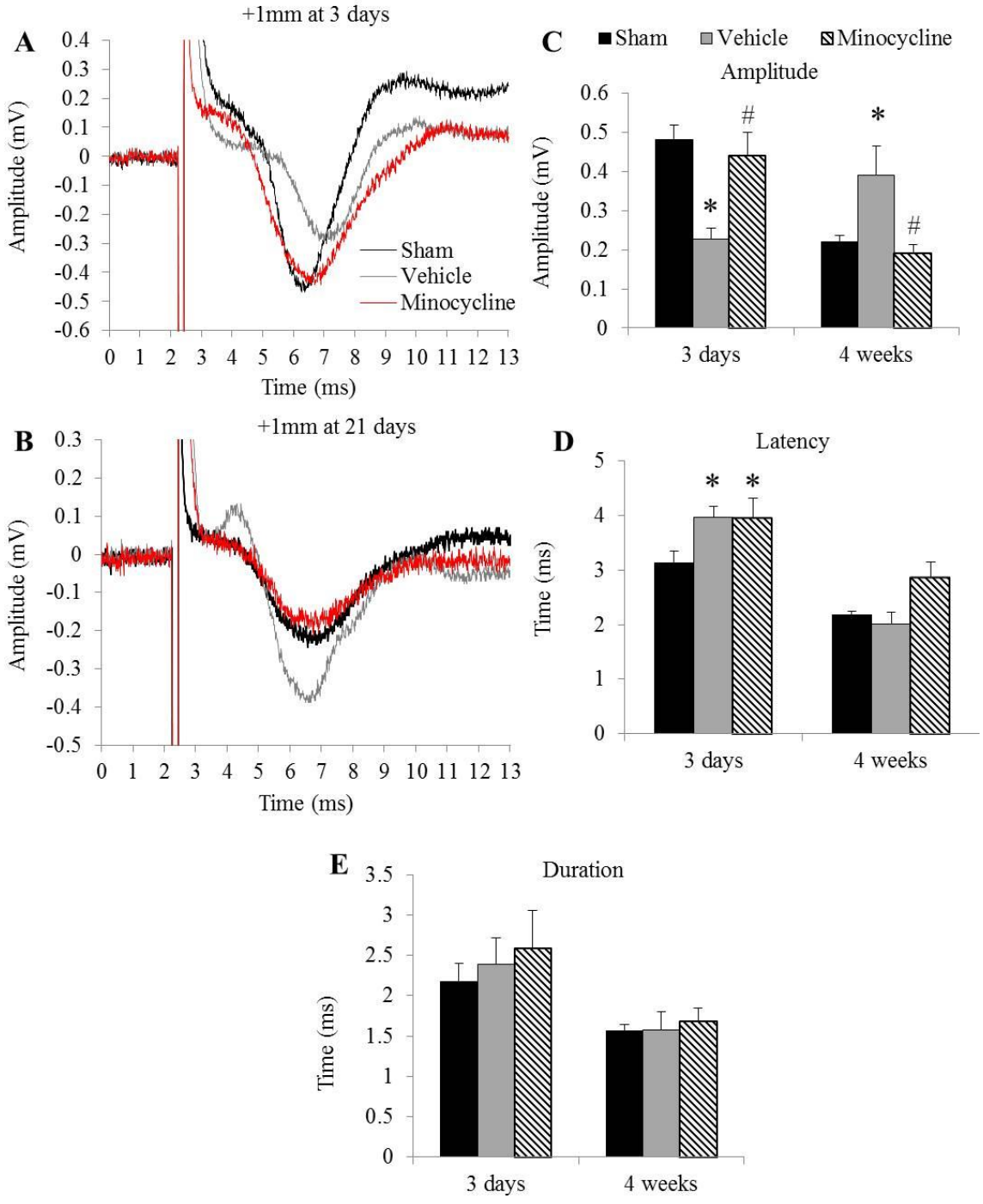

5.13 Assessment of forelimb use following acute microglial/macrophage depletion

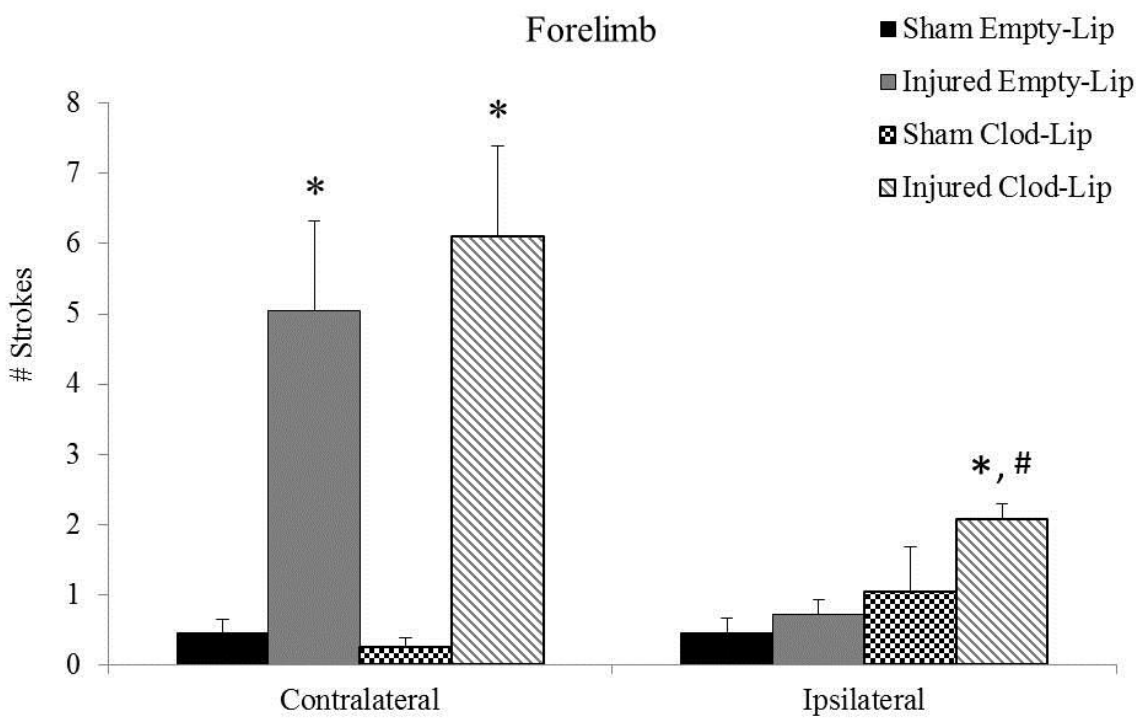

Fig. 5.14 Assessment of evoked field potential in the forelimb region of the motor cortex following acute microglial/macrophage depletion

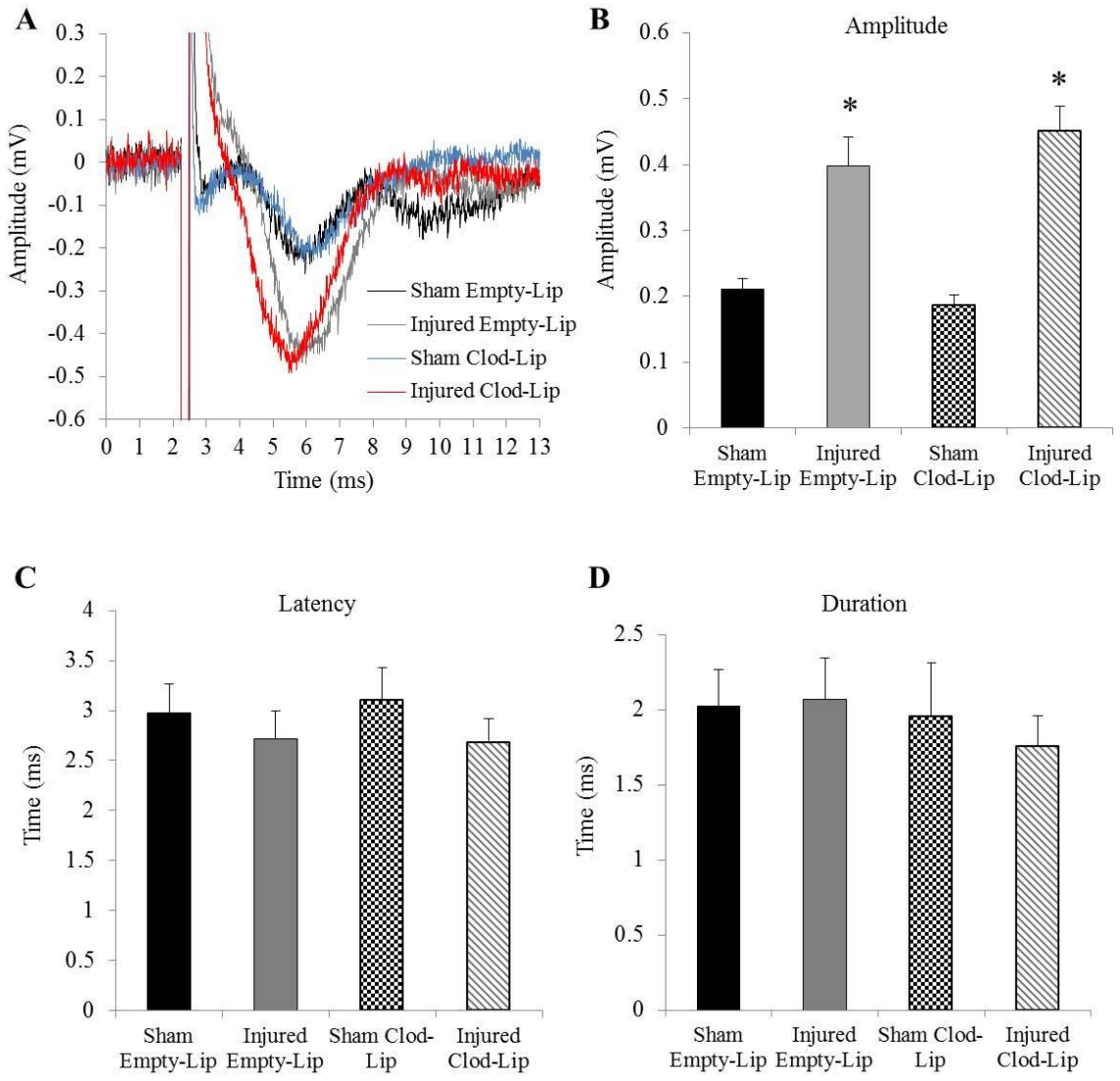

CHAPTER 6: GENERAL DISCUSSION

6.1 SIGNIFIGANCE OF FINDINGS

The current set of studies is the first to take a multi-faceted approach in investigating microglial/macrophage reactivity following impact-based trauma in the immature brain. Through the use of clodronate-mediated microglial/macrophage depletion and minocycline-mediated reduction in microglial/macrophage activation, these experiments emphasize the crucial role that microglia/macrophages play in the acute post-injury period. Despite the fact that these interventions are very different in their mechanisms of action, treatment resulted in similar exacerbations of injury-induced neuropathology. These results challenge the dogma that acute microglial/macrophage activation following traumatic brain injury perpetuates neuronal damage (Loane, 2010). They also suggest that the microglial/macrophage response following injury to the immature brain is not only different from the response following injury to the adult brain, but that it is necessary to contain the spread of neuropathology. With these results, how should a physician treat a brain-injured infant? This project indicates that acute pharmacologic intervention beyond vital stabilization may not be appropriate for treatment of traumatic brain injury in the infant.

This project also emphasizes the complexities of injuring a developing brain. Brain development in the rat continues through the first 7 weeks of life with full adult maturation evident at PND60 (Semple et al., 2013). Injuring the animal at postnatal day 11 can impact not only the processes happening around that time, but everything that occurs after the time of injury. On postnatal day 11, the rat pup is equivalent to a newborn infant in terms of scaled brain weight and developmental benchmarks (Clancy et al., 2007; Semple et al., 2013). Right around this time there is immense brain growth,

gliogenesis, increases in axonal and dendritic densities, maturation of the immune system, and an increase in immature oligodendrocytes in the white matter (Semple et al., 2013). The diagram below adapted from Semple et al., 2013 identifies processes that are altered by insult to the developing brain thus leading to functional impairments.

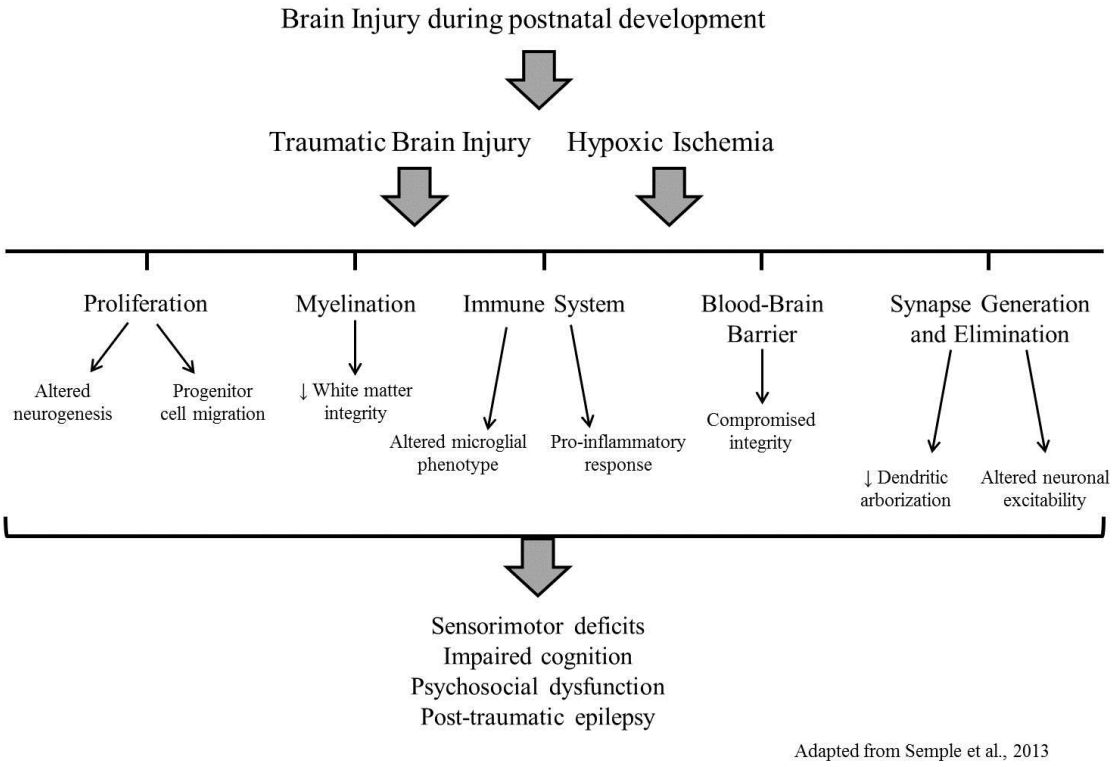

Adapted from Semple et al., 2013

These processes include cell proliferation, myelination, immune system maturation, blood brain barrier (BBB) formation, and synapse generation and elimination. All of these processes have implications for this project. Disruption of myelination may factor into the alterations we observed in compound action potential electrophysiology in addition to the observed increase in white matter damage that was unaffected by the treatments. The concurrent development of the BBB and maturation of the immune system around the time of injury may play a role in the differential effects observed in

targeting microglial/macrophage activation following injury to the adult and developing brain (Chapter 1.4). Affecting the developmental processes of cell proliferation, synapse generation, and synapse elimination with an injury may have profound effects on the formation of proper circuitry and may therefore result in alterations in neuronal activity. More specifically during this time, the GABAergic system in the cortex is still maturing and only approximately 50% of mature GABAergic synapses have formed by 11 days after birth. Importantly, at 11 days old, the alterations that allow for GABA to switch from acting as an excitatory neurotransmitter to an inhibitory neurotransmitter are still underway (Le Magueresse and Monyer, 2013). This interplay with developmental processes has significant implications for the electrophysiological results observed in this set of studies. We observed a developmental decrease in the amplitude of signal from sham-injured animals that may correspond with the maturation of the GABAergic system and a disruption in this maturation may explain the alterations in cortical activity that were observed in our studies. It is, therefore, important to consider any effects on developmental processes that may contribute to the post-injury pathology when interpreting experimental results. Further research into the interplay between development and injury in this model of TBI in the neonate rat is necessary.

In this thesis, minocycline was used as a tool to reduce microglial/macrophage activation, but this FDA-approved antibiotic has real potential for being used as a post-injury therapeutic intervention (Potts et al., 2006, Plane et al., 2010). The results of this study suggest that minocycline may not be safe to use in the acute post-injury period in brain-injured children. Minocycline administration did not ameliorate white matter damage, resulted in prolonged exacerbation of injury-induced grey matter pathology, and

caused a deficit in neuronal activity within the impact site. This treatment did, however, ameliorate working memory deficits, rescue deficits in forelimb motor control, and reverse changes in neuronal activity in the forelimb region of the motor cortex. These conflicting results emphasize the need for further investigation into this drug and its potential off-target effects in the developing brain.

These studies also lend support for the idea that microglial/macrophage reactivity is not associated with axonal pathology in the injured or diseased brain (Bennett and Brody, 2014; de Monasterio-Schrader et al., 2013, Hanlon et al., 2016a). In the grey matter, acute microglial/macrophage manipulation resulted in a potential rebound effect in which activated microglia/macrophages were increased in chronic post-injury period and this was associated with an increase in neurodegeneration. While clodronate-mediated microglial/macrophage depletion was associated with increased neurodegeneration, it did not coincide with an increase in microglial/macrophage reactivity. Conversely, minocycline treatment resulted in an increase in microglial/macrophage reactivity in the chronic post-injury period that was not associated with an increase in axonal degeneration. Additionally, neither intervention affected APP accumulation in the acute post-injury period and minocycline had no effect on the transport of Fluoro-gold two weeks following the injury. Also, microglial/macrophage depletion in the white matter had no effect on axonal conductance as measured by compound action potential electrophysiology and minoncycline treatment had no effect on atrophy in the white matter. Taken together, these results may indicate that function of activated microglia/macrophages in the white matter may be very different from the function of activated microglia/macrophages in the grey matter and, therefore, may

respond to treatment differently. More specific investigation into white matter pathology, such as myelination and oligodendrocyte damage, may be necessary to accurately understand the interactions between microglia and white matter pathology following injury.

This thesis also expands our knowledge of neuronal activity following injury to the immature brain. A large body of evidence from the undercut model of brain injury in the PND21 rat implicates a role for excitatory/inhibitory imbalance in the brain following injury (Prince, 2009, more detail in Chapter 5.2). Modulation of post-injury excitation using a positive modulator of the $GABA_A$ receptor (Diazepam) rescued injury-induced spatial learning and memory deficits while blocking this receptor exacerbated deficits in adult rats (O'Dell et al., 2000). Also, in a model of TBI in the adult mouse, hypoactivity was evident in the first day post-injury and hyperactivity was observed at 2 weeks post-injury (Ping and Jin, 2015). The work in my dissertation demonstrates a similar hypoactivity-to-hyperactivity phenotypic switch suggesting that closed head injury to the PND11 rat may have an effect on the inhibitory/excitatory balance required for proper maintenance of neuronal circuitry. Evoked field potential recording, however, may not be sensitive enough to make accurate statements regarding the effect of injury on the excitatory/inhibitory balance in the cortex and whole-cell patch clamp recording in the cortex may be necessary. These studies open the door for further investigation into this phenomenon and its implications for post-injury functional deficits.

Finally, characterization of the microglial/macrophage response and assessment of functional impairments in the chronic post-injury period greatly emphasized the relevance of this PND11 injury as a preclinical model of pediatric TBI. Previously, the

only functional deficit reported in our animals was a prolonged spatial learning and memory deficit (Raghupathi and Huh, 2007). Demonstrating the working memory impairments, increases in anxiety, vulnerability to seizure activity, and locomotor impairment in addition to prolonged microglial/macrophage responses and alterations in neuronal activity not only lends support for the relevance of this model but also provides new avenues of investigation into the mechanisms behind injury-induced functional impairment.

6.2 FUTURE DIRECTIONS

This thesis provides support for the notion that the microglial/macrophage response following injury to the developing brain is distinct from the response following injury to the adult brain. In the developing brain, eliminating microglia/macrophages or reducing the microglial/macrophage activation state resulted in an exacerbation of pathology at the doses used in this study. This is in contrast to what has been reported in the adult brain and has vast implications for post-injury therapeutics based on the age-dependent efficacy of the drug. From characterization of the microglial/macrophage response, we now know that the microglial/macrophage reactivity is sustained out to 4 weeks after injury. It raises the question as to whether delayed treatment has any effect on injury-induced pathology. In a preliminary study, we administered our same minocycline treatment paradigm (Chapter 4; 45 mg/kg every 12 hours for 3 days) beginning on day 12 after injury and euthanized the animals for histology on post-injury day 15 to assess microglial/macrophage reactivity and neurodegeneration. With very few animals per group (N = 3 animals/group), we observed a decrease in microglial/macrophage reactivity and a decrease in neurodegeneration in the cortex of brain-injured animals treated with the delayed minocycline paradigm (Fig. 6.2.1). Quantification of ED-1-labeled activated microglia/macrophages in the cortex (Fig. 6.2.1 A,B) revealed a significant effect of status for both amoeboid- ($F_{2,6}$=82.52, $p<0.001$) and rod-shaped cells ($F_{2,6}$=9.04, $p<0.05$, Fig. 6.2.1 E); and post-hoc analysis revealed that both brain-injured groups had significantly more amoeboid microglia/macrophages compared to sham-injured animals ($p<0.05$) and that minocycline-treated brain-injured animals had significantly fewer amoeboid microglia/macrophages compared to brain-

injured animals that received the vehicle ($p<0.001$). Brain-injured animals that received the vehicle also had more rod-shaped ED-1(+) microglia/macrophages compared to both sham-injured and brain-injured minocycline-treated animals ($p<0.05$). Sham-injured animals and brain-injured animals treated with minocycline did not differ in the number of rod-shaped microglia/macrophages in the cortex ($p=0.49$). Similar decreases in ED-1 labeling were also observed in the thalamus and subiculum, but not in the white matter. FJB(+) profiles were also decreased in the cortex following delayed minocycline treatment (Fig. 6.2.1 C,D), but this result failed to reach significance potentially due to a small sample size ($t(4)=-2.05$, $p=0.11$, Fig. 6.2.1 F). Despite no difference in ED-1 labeling between brain-injured minocycline-treated animals and those that received the vehicle in the white matter, there was a mild reduction in FJB(+) profiles in the white matter ($t(4)=-2.97$, $p=0.04$). Additionally, there was a significant reduction of FJB(+) profiles in the thalamus and the reduction in the subiculum was trending on significant. More animals are needed to complete this study, but these preliminary results indicate that delayed targeting of the microglial/macrophage response may be more effective in treating injury-induced neuropathology. Additionally, animals that receive this paradigm will have to be tested for injury-induced behavioral deficits to see if the delayed treatment can also ameliorate long-term functional deficits.

The results stated in this thesis project raise questions about the activation state of microglia/macrophages and the mediators that these cells release. While previous attempts at ELISA-mediated assessment of pro- and anti-inflammatory mediators have been unsuccessful in our lab, we recently conducted a set of experiments to evaluate the mRNA expression of different mediators in the cortex of sham- and brain-injured

animals. In light of the interesting electrophysiological results observed in the forelimb region of the motor cortex and minocycline's effects on this measure (Chapter 5), I collected tissue from this region and the -3mm cortical region for QPCR evaluation at 3 days post-injury (Fig. 6.2.2). With small sample sizes (N=3/group), there appeared to be an injury-induced increase in cytokine expression in the +1mm section anterior to the impact site where we did not observe cellular microglial/macrophage activation (Fig. 6.2.2 A-C). Brain-injured animals demonstrate approximately a 75% increase in TNFα mRNA expression (Fig. 6.2.2 A), a 300% increase in IL-1β mRNA expression (Fig. 6.2.2 B), and a 66% increase in IL-10 mRNA expression (Fig. 6.2.2 C) compared to sham-injured animals. Interestingly, in the -3mm section where we observed dense cellular pathology, there did not seem to be an injury-induced increase in TNFα mRNA expression (Fig. 6.2.2 D), but there was a 475% increase in IL-1β mRNA expression (Fig. 6.2.2 E) and an almost 300% increase in IL-10 mRNA expression (Fig. 6.2.2F) compared to sham-injured animals. In the +1mm section, minocycline administration seemed to decrease mRNA expression of both IL-1β and IL-10 without affecting TNFα expression levels (Fig. 6.2.2 A-C). The modulation of IL-1β by minocycline may explain the ability of minocycline to reverse injury-induced hypoactivity in this region at this time point (Chapter 5) as it has been demonstrated that exposure to high levels of IL-1β can decrease extracellular field potentials (Ross et al., 2003, Fig. 6.2.2 B). Minocycline treatment also decreased IL-1β and IL-10 mRNA expression in the impact site (-3mm) indicating that the minocycline-induced decrease in microglial/macrophage activation observed at 3 days was associated with a decrease in both pro- and anti-inflammatory cytokines (Fig. 6.2.2 E,F). It has been shown that TNFα can modulate α-amino-3-

hydroxy-5-methyl-4-isoxazoleproprionic acid (AMPA) and gamma-aminobutyric acid (GABA) receptor membrane trafficking to affect both excitatory and inhibitory neurotransmission (Stellwagen et al., 2005). Additionally, IL-1β has been shown to affect neuronal activity through the modulation of NMDA-mediated currents (Yang et al., 2005). While our extracellular field potential data indicated that there were injury-induced alterations in neuronal activity, it is unclear what is happening at the single cell level and further investigation is needed to tie these changes in population activity to the observed changes in cytokine mRNA expression. It is also unclear how these manipulations factor into the observed prolonged neuropathology and further QPCR studies at chronic time points are needed.

The results from these studies indicate a role for peripheral cell infiltration following injury. The markers used (Iba1 and ED-1) have been shown to label both endogenous microglia and infiltrating peripheral macrophages that can enter the brain following injury (Jeong et al., 2013). Separating infiltrating cells from resident microglia would allow for more specific characterization and targeting of the endogenous response. Infiltration also becomes very relevant in experiments dealing with microglial/macrophage depletion. There is some evidence that speaks to repopulation through peripheral cells in the absence of microglia in the aging brain (Varvel et al., 2012), but it is possible that peripheral infiltration in the developing brain is different, especially in the context of injury. In comparing the microglia/macrophage response following a lesion to the visual cortex, peripheral macrophages were the predominant responder cell in the lesioned neonatal cortex whereas microglia were the main responder following lesion to the adult cortex (Milligan et al., 1991). After stroke in the neonate

rat, peripheral infiltration was assessed and it was determined that the cells responding around the infarct were endogenous microglia despite high increases in monocyte chemoattractant protein-1 (MCP-1) (Denker et al., 2007). One way to separate the endogenous microglia from peripheral macrophages would be to use flow cytometry to separate cells based on specific markers. The most common way of doing this is to use a non-specific microglia/macrophage marker such as Iba1 to distinguish microglia/macrophages from neutrophils and then to use CD45 expression levels to differentiate between peripheral macrophages (CD45 high) and endogenous microglia (CD45 low) (Jeong et al., 2013). A working flow cytometry protocol would also answer the question of repopulation following clodronate-mediated microglial/macrophage depletion. In the absence of a working protocol, however, we may be able to answer these questions by using clodronate to deplete peripheral macrophages prior to injury and prior to the depletion of endogenous microglia.

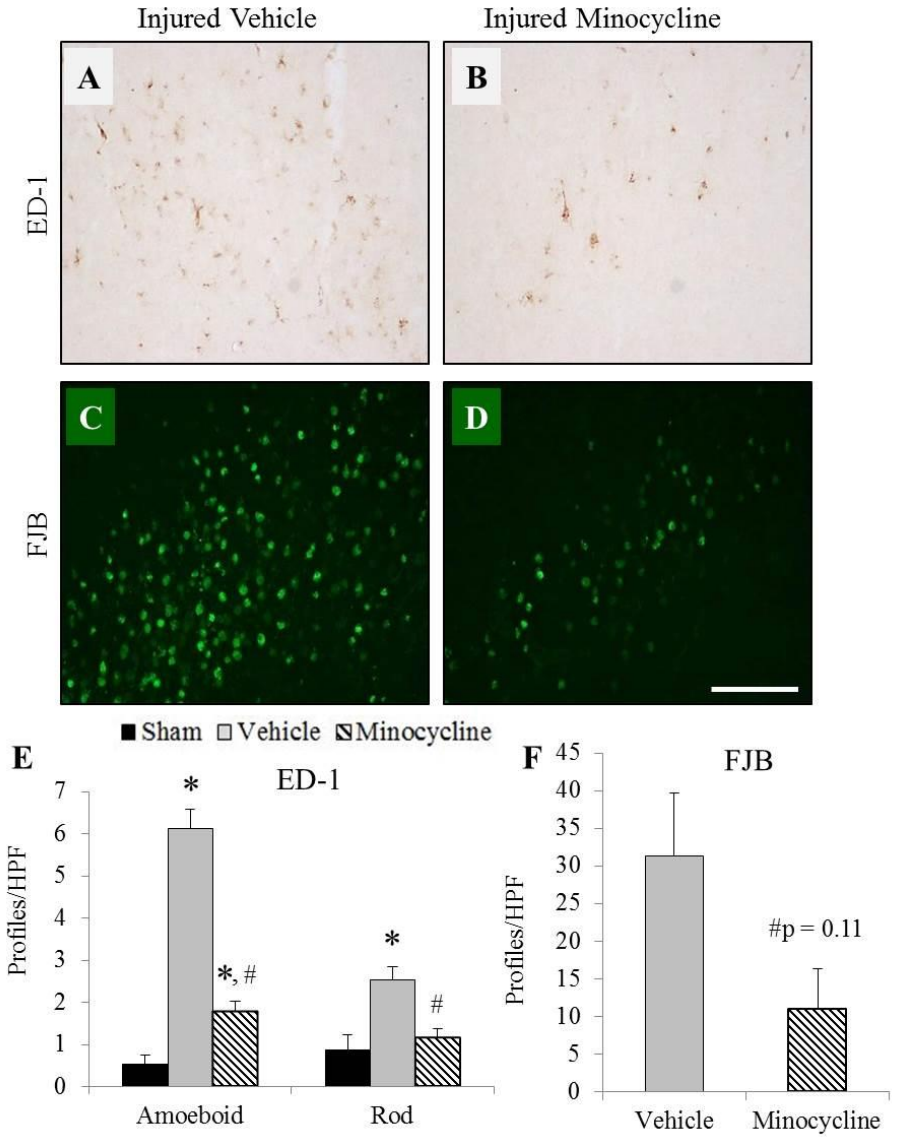

Fig. 6.2.1 Effect of delayed minocycline treatment in the cortex. Representative photomicrographs of ED-1(+) microglia **(A,B)** and FJB(+) profiles **(C,D)** in the cortex of brain-injured animals that received the vehicle **(A,C)** and those that received minocycline **(B,D)**. Quantification of amoeboid and rod microglia **(E)** and FJB(+) profiles **(F)** in the cortex at 15 days post-injury. Error bars represent the standard error of the mean. *p≤0.05 compared to the sham-injured group, #p≤0.05 compared to the brain-injured vehicle group.

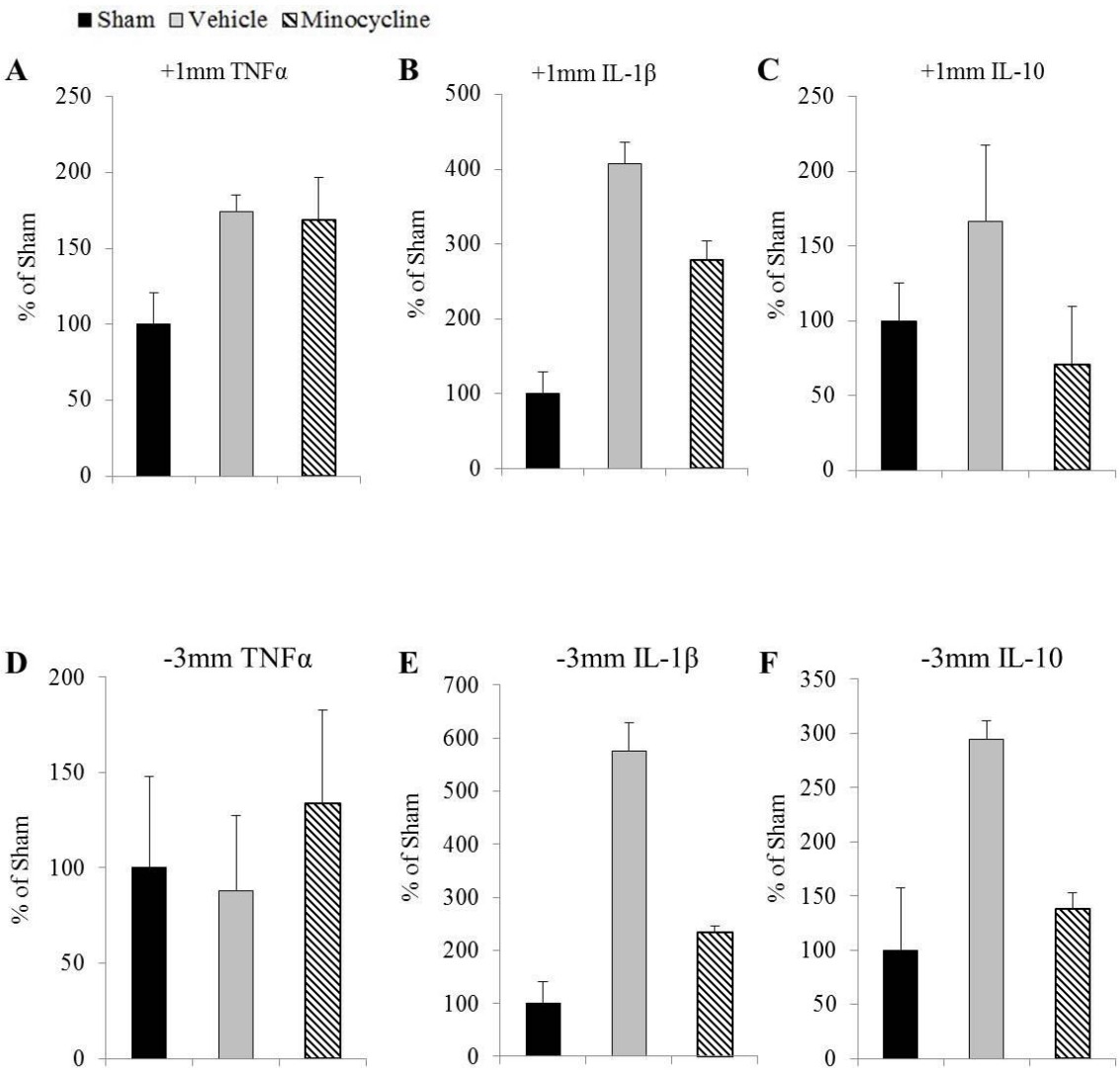

Fig. 6.2.2 Effect of acute minocycline administration on mRNA expression of pro- and anti-inflammatory cytokines in specific cortical regions. Quantification of cytokines at +1mm (A-C) and -3mm (D-F). Error bars represent the standard error of the mean.

REFERENCES

Abdel Baki SG, Schwab B, Haber M, Fenton AA, Bergold PJ (2010) Minocycline synergizes with N-acetylcysteine and improves cognition and memory following traumatic brain injury in rats. PloS one 5:e12490.

Adelson PD, Dixon CE, Kochanek PM (2000) Long-term dysfunction following diffuse traumatic brain injury in the immature rat. Journal of neurotrauma 17:273-282.

Adelson PD, Dixon CE, Robichaud P, Kochanek PM (1997) Motor and cognitive functional deficits following diffuse traumatic brain injury in the immature rat. Journal of neurotrauma 14:99-108.

Adelson PD, Jenkins LW, Hamilton RL, Robichaud P, Tran MP, Kochanek PM (2001) Histopathologic response of the immature rat to diffuse traumatic brain injury. Journal of neurotrauma 18:967-976.

Adelson PD, Ragheb J, Kanev P, Brockmeyer D, Beers SR, Brown SD, Cassidy LD, Chang Y, Levin H (2005) Phase II clinical trial of moderate hypothermia after severe traumatic brain injury in children. Neurosurgery 56:740-754; discussion 740-754.

Adelson PD, Robichaud P, Hamilton RL, Kochanek PM (1996) A model of diffuse traumatic brain injury in the immature rat. Journal of neurosurgery 85:877-884.

Alhelali I, Stewart TC, Foster J, Alharfi IM, Ranger A, Daoud H, Fraser DD (2015) Basal skull fractures are associated with mortality in pediatric severe traumatic brain injury. The journal of trauma and acute care surgery 78:1155-1161.

Ajao DO, Pop V, Kamper JE, Adami A, Rudobeck E, Huang L, Vlkolinsky R, Hartman RE, Ashwal S, Obenaus A, Badaut J (2012) Traumatic brain injury in young rats

leads to progressive behavioral deficits coincident with altered tissue properties in adulthood. Journal of neurotrauma 29:2060-2074.

Amick JE, Yandora KA, Bell MJ, Wisniewski SR, Adelson PD, Carcillo JA, Janesko KL, DeKosky ST, Carlos TM, Clark RS, Kochanek PM (2001) The Th1 versus Th2 cytokine profile in cerebrospinal fluid after severe traumatic brain injury in infants and children. Pediatric critical care medicine : a journal of the Society of Critical Care Medicine and the World Federation of Pediatric Intensive and Critical Care Societies 2:260-264.

Anderson V, Catroppa C, Morse S, Haritou F, Rosenfeld J (2005) Functional plasticity or vulnerability after early brain injury? Pediatrics 116:1374-1382.

Anderson V, Catroppa C, Morse S, Haritou F, Rosenfeld JV (2009) Intellectual outcome from preschool traumatic brain injury: a 5-year prospective, longitudinal study. Pediatrics 124:e1064-1071.

Andes D, Craig WA (2002) Animal model pharmacokinetics and pharmacodynamics: a critical review. International journal of antimicrobial agents 19:261-268.

Andriessen TM, Jacobs B, Vos PE (2010) Clinical characteristics and pathophysiological mechanisms of focal and diffuse traumatic brain injury. Journal of cellular and molecular medicine 14:2381-2392.

Annegers JF, Hauser WA, Coan SP, Rocca WA (1998) A population-based study of seizures after traumatic brain injuries. The New England journal of medicine 338:20-24.

Antunes M, Biala G (2012) The novel object recognition memory: neurobiology, test procedure, and its modifications. Cognitive processing 13:93-110.

Armstead WM, Kurth CD (1994) Different cerebral hemodynamic responses following fluid percussion brain injury in the newborn and juvenile pig. Journal of neurotrauma 11:487-497.

Arndt DH, Lerner JT, Matsumoto JH, Madikians A, Yudovin S, Valino H, McArthur DL, Wu JY, Leung M, Buxey F, Szeliga C, Van Hirtum-Das M, Sankar R, Brooks-Kayal A, Giza CC (2013) Subclinical early posttraumatic seizures detected by continuous EEG monitoring in a consecutive pediatric cohort. Epilepsia 54:1780-1788.

Arvin KL, Han BH, Du Y, Lin SZ, Paul SM, Holtzman DM (2002) Minocycline markedly protects the neonatal brain against hypoxic-ischemic injury. Annals of neurology 52:54-61.

Asai H, Ikezu S, Tsunoda S, Medalla M, Luebke J, Haydar T, Wolozin B, Butovsky O, Kugler S, Ikezu T (2015) Depletion of microglia and inhibition of exosome synthesis halt tau propagation. Nature neuroscience 18:1584-1593.

Azevedo FA, Carvalho LR, Grinberg LT, Farfel JM, Ferretti RE, Leite RE, Jacob Filho W, Lent R, Herculano-Houzel S (2009) Equal numbers of neuronal and nonneuronal cells make the human brain an isometrically scaled-up primate brain. The Journal of comparative neurology 513:532-541.

Babikian T, Merkley T, Savage RC, Giza CC, Levin H (2015) Chronic Aspects of Pediatric Traumatic Brain Injury: Review of the Literature. Journal of neurotrauma 32:1849-1860.

Bal-Price A, Brown GC (2001) Inflammatory neurodegeneration mediated by nitric oxide from activated glia-inhibiting neuronal respiration, causing glutamate release and excitotoxicity. The Journal of neuroscience : the official journal of the Society for Neuroscience 21:6480-6491.

Barker GR, Bird F, Alexander V, Warburton EC (2007) Recognition memory for objects, place, and temporal order: a disconnection analysis of the role of the medial prefrontal cortex and perirhinal cortex. The Journal of neuroscience : the official journal of the Society for Neuroscience 27:2948-2957.

Barlow KM, Thomson E, Johnson D, Minns RA (2005) Late neurologic and cognitive sequelae of inflicted traumatic brain injury in infancy. Pediatrics 116:e174-185.

Battista D, Ferrari CC, Gage FH, Pitossi FJ (2006) Neurogenic niche modulation by activated microglia: transforming growth factor beta increases neurogenesis in the adult dentate gyrus. The European journal of neuroscience 23:83-93.

Belayev L, Alonso OF, Liu Y, Chappell AS, Zhao W, Ginsberg MD, Busto R (2001) Talampanel, a novel noncompetitive AMPA antagonist, is neuroprotective after traumatic brain injury in rats. Journal of neurotrauma 18:1031-1038.

Bell MJ, Kochanek PM, Doughty LA, Carcillo JA, Adelson PD, Clark RS, Wisniewski SR, Whalen MJ, DeKosky ST (1997) Interleukin-6 and interleukin-10 in cerebrospinal fluid after severe traumatic brain injury in children. Journal of neurotrauma 14:451-457.

Bellinger FP, Madamba S, Siggins GR (1993) Interleukin 1 beta inhibits synaptic strength and long-term potentiation in the rat CA1 hippocampus. Brain research 628:227-234.

Bennett RE, Brody DL (2014) Acute reduction of microglia does not alter axonal injury in a mouse model of repetitive concussive traumatic brain injury. Journal of neurotrauma 31:1647-1663.

Berger RP, Heyes MP, Wisniewski SR, Adelson PD, Thomas N, Kochanek PM (2004) Assessment of the macrophage marker quinolinic acid in cerebrospinal fluid after pediatric traumatic brain injury: insight into the timing and severity of injury in child abuse. Journal of neurotrauma 21:1123-1130.

Berger RP, Ta'asan S, Rand A, Lokshin A, Kochanek P (2009) Multiplex assessment of serum biomarker concentrations in well-appearing children with inflicted traumatic brain injury. Pediatric research 65:97-102.

Beynon SB, Walker FR (2012) Microglial activation in the injured and healthy brain: what are we really talking about? Practical and theoretical issues associated with the measurement of changes in microglial morphology. Neuroscience 225:162-171.

Biber K, Neumann H, Inoue K, Boddeke HW (2007) Neuronal 'On' and 'Off' signals control microglia. Trends in neurosciences 30:596-602.

Bittigau P, Sifringer M, Pohl D, Stadthaus D, Ishimaru M, Shimizu H, Ikeda M, Lang D, Speer A, Olney JW, Ikonomidou C (1999) Apoptotic neurodegeneration following trauma is markedly enhanced in the immature brain. Annals of neurology 45:724-735.

Boje KM, Arora PK (1992) Microglial-produced nitric oxide and reactive nitrogen oxides mediate neuronal cell death. Brain research 587:250-256.

Bona E, Andersson AL, Blomgren K, Gilland E, Puka-Sundvall M, Gustafson K, Hagberg H (1999) Chemokine and inflammatory cell response to hypoxia-ischemia in immature rats. Pediatric research 45:500-509.

Buki A, Siman R, Trojanowski JQ, Povlishock JT (1999) The role of calpain-mediated spectrin proteolysis in traumatically induced axonal injury. Journal of neuropathology and experimental neurology 58:365-375.

Buller KM, Carty ML, Reinebrant HE, Wixey JA (2009) Minocycline: a neuroprotective agent for hypoxic-ischemic brain injury in the neonate? Journal of neuroscience research 87:599-608.

Buttram SD, Wisniewski SR, Jackson EK, Adelson PD, Feldman K, Bayir H, Berger RP, Clark RS, Kochanek PM (2007) Multiplex assessment of cytokine and chemokine levels in cerebrospinal fluid following severe pediatric traumatic brain injury: effects of moderate hypothermia. Journal of neurotrauma 24:1707-1717.

Bye N, Habgood MD, Callaway JK, Malakooti N, Potter A, Kossmann T, Morganti-Kossmann MC (2007) Transient neuroprotection by minocycline following traumatic brain injury is associated with attenuated microglial activation but no changes in cell apoptosis or neutrophil infiltration. Experimental neurology 204:220-233.

Cai Z, Lin S, Fan LW, Pang Y, Rhodes PG (2006) Minocycline alleviates hypoxic-ischemic injury to developing oligodendrocytes in the neonatal rat brain. Neuroscience 137:425-435.

Carbonell WS, Maris DO, McCall T, Grady MS (1998) Adaptation of the fluid percussion injury model to the mouse. Journal of neurotrauma 15:217-229.

Carty ML, Wixey JA, Colditz PB, Buller KM (2008) Post-insult minocycline treatment attenuates hypoxia-ischemia-induced neuroinflammation and white matter injury in the neonatal rat: a comparison of two different dose regimens. International journal of developmental neuroscience : the official journal of the International Society for Developmental Neuroscience 26:477-485.

Catroppa C, Anderson V (2005) A prospective study of the recovery of attention from acute to 2 years following pediatric traumatic brain injury. Journal of the International Neuropsychological Society : JINS 11:84-98.

Catroppa C, Anderson V, Ditchfield M, Coleman L (2008) Using magnetic resonance imaging to predict new learning outcome at 5 years after childhood traumatic brain injury. Journal of child neurology 23:486-496.

Catroppa C, Anderson VA, Morse SA, Haritou F, Rosenfeld JV (2007) Children's attentional skills 5 years post-TBI. Journal of pediatric psychology 32:354-369.

Chang YW, Waxman SG (2010) Minocycline attenuates mechanical allodynia and central sensitization following peripheral second-degree burn injury. The journal of pain : official journal of the American Pain Society 11:1146-1154.

Chen CY, Noble-Haeusslein LJ, Ferriero D, Semple BD (2013) Traumatic injury to the immature frontal lobe: a new murine model of long-term motor impairment in the absence of psychosocial or cognitive deficits. Developmental neuroscience 35:474-490.

Chen Z, Jalabi W, Shpargel KB, Farabaugh KT, Dutta R, Yin X, Kidd GJ, Bergmann CC, Stohlman SA, Trapp BD (2012) Lipopolysaccharide-induced microglial activation and neuroprotection against experimental brain injury is independent of

hematogenous TLR4. The Journal of neuroscience : the official journal of the Society for Neuroscience 32:11706-11715.

Cherry JD, Olschowka JA, O'Banion MK (2014) Neuroinflammation and M2 microglia: the good, the bad, and the inflamed. Journal of neuroinflammation 11:98.

Chhor V, Moretti R, Le Charpentier T, Sigaut S, Lebon S, Schwendimann L, Ore MV, Zuiani C, Milan V, Josserand J, Vontell R, Pansiot J, Degos V, Ikonomidou C, Titomanlio L, Hagberg H, Gressens P, Fleiss B (2016) Role of microglia in a mouse model of paediatric traumatic brain injury. Brain, behavior, and immunity.

Choi DW (1987) Ionic dependence of glutamate neurotoxicity. The Journal of neuroscience : the official journal of the Society for Neuroscience 7:369-379.

Cikla U, Chanana V, Kintner DB, Covert L, Dewall T, Waldman A, Rowley P, Cengiz P, Ferrazzano P (2016) Suppression of microglia activation after hypoxia-ischemia results in age-dependent improvements in neurologic injury. Journal of neuroimmunology 291:18-27.

Clancy B, Finlay BL, Darlington RB, Anand KJ (2007) Extrapolating brain development from experimental species to humans. Neurotoxicology 28:931-937.

Claus CP, Tsuru-Aoyagi K, Adwanikar H, Walker B, Manvelyan H, Whetstone W, Noble-Haeusslein LJ (2010) Age is a determinant of leukocyte infiltration and loss of cortical volume after traumatic brain injury. Developmental neuroscience 32:454-465.

Coats B, Binenbaum G, Smith C, Peiffer RL, Christian CW, Duhaime AC, Margulies SS (2017) Cyclic Head Rotations Produce Modest Brain Injury in Infant Piglets. Journal of neurotrauma 34:235-247.

Coronado VG, Xu L, Basavaraju SV, McGuire LC, Wald MM, Faul MD, Guzman BR, Hemphill JD, Centers for Disease C, Prevention (2011) Surveillance for traumatic brain injury-related deaths--United States, 1997-2007. Morbidity and mortality weekly report Surveillance summaries 60:1-32.

Cowell RM, Xu H, Galasso JM, Silverstein FS (2002) Hypoxic-ischemic injury induces macrophage inflammatory protein-1alpha expression in immature rat brain. Stroke; a journal of cerebral circulation 33:795-801.

Csuka E, Hans VH, Ammann E, Trentz O, Kossmann T, Morganti-Kossmann MC (2000) Cell activation and inflammatory response following traumatic axonal injury in the rat. Neuroreport 11:2587-2590.

Culotta PA, Crowe JE, Tran QA, Jones JY, Mehollin-Ray AR, Tran HB, Donaruma-Kwoh M, Dodge CT, Camp EA, Cruz AT (2017) Performance of computed tomography of the head to evaluate for skull fractures in infants with suspected non-accidental trauma. Pediatric radiology 47:74-81.

Damoiseaux JG, Dopp EA, Calame W, Chao D, MacPherson GG, Dijkstra CD (1994) Rat macrophage lysosomal membrane antigen recognized by monoclonal antibody ED1. Immunology 83:140-147.

de Monasterio-Schrader P, Patzig J, Mobius W, Barrette B, Wagner TL, Kusch K, Edgar JM, Brophy PJ, Werner HB (2013) Uncoupling of neuroinflammation from axonal degeneration in mice lacking the myelin protein tetraspanin-2. Glia 61:1832-1847.

Denker SP, Ji S, Dingman A, Lee SY, Derugin N, Wendland MF, Vexler ZS (2007) Macrophages are comprised of resident brain microglia not infiltrating peripheral monocytes acutely after neonatal stroke. Journal of neurochemistry 100:893-904.

DiLeonardi AM, Huh JW, Raghupathi R (2009) Impaired axonal transport and neurofilament compaction occur in separate populations of injured axons following diffuse brain injury in the immature rat. Brain research 1263:174-182.

Dileonardi AM, Huh JW, Raghupathi R (2012) Differential effects of FK506 on structural and functional axonal deficits after diffuse brain injury in the immature rat. Journal of neuropathology and experimental neurology 71:959-972.

Dixon CE, Clifton GL, Lighthall JW, Yaghmai AA, Hayes RL (1991) A controlled cortical impact model of traumatic brain injury in the rat. Journal of neuroscience methods 39:253-262.

Dixon CE, Lyeth BG, Povlishock JT, Findling RL, Hamm RJ, Marmarou A, Young HF, Hayes RL (1987) A fluid percussion model of experimental brain injury in the rat. Journal of neurosurgery 67:110-119.

Djebaili M, Guo Q, Pettus EH, Hoffman SW, Stein DG (2005) The neurosteroids progesterone and allopregnanolone reduce cell death, gliosis, and functional deficits after traumatic brain injury in rats. Journal of neurotrauma 22:106-118.

Domingues HS, Portugal CC, Socodato R, Relvas JB (2016) Oligodendrocyte, Astrocyte, and Microglia Crosstalk in Myelin Development, Damage, and Repair. Frontiers in cell and developmental biology 4:71.

Douglas AC (1963) The deposition of tetracycline in human nails and teeth: A

complication of long-term treatment. British journal of diseases of the chest 57 (1): 44.

Drabek T, Janata A, Jackson EK, End B, Stezoski J, Vagni VA, Janesko-Feldman K, Wilson CD, van Rooijen N, Tisherman SA, Kochanek PM (2012) Microglial depletion using intrahippocampal injection of liposome-encapsulated clodronate in prolonged hypothermic cardiac arrest in rats. Resuscitation 83:517-526.

Duhaime AC, Christian CW, Rorke LB, Zimmerman RA (1998) Nonaccidental head injury in infants--the "shaken-baby syndrome". The New England journal of medicine 338:1822-1829.

Duhaime AC, Gennarelli TA, Thibault LE, Bruce DA, Margulies SS, Wiser R (1987) The shaken baby syndrome. A clinical, pathological, and biomechanical study. Journal of neurosurgery 66:409-415.

Duhaime AC, Margulies SS, Durham SR, O'Rourke MM, Golden JA, Marwaha S, Raghupathi R (2000) Maturation-dependent response of the piglet brain to scaled cortical impact. Journal of neurosurgery 93:455-462.

Duhaime AC, Raghupathi R (1999) Age-specific therapy for traumatic injury of the immature brain: experimental approaches. Experimental and toxicologic pathology : official journal of the Gesellschaft fur Toxikologische Pathologie 51:172-177.

Durham SR, Clancy RR, Leuthardt E, Sun P, Kamerling S, Dominguez T, Duhaime AC (2000) CHOP Infant Coma Scale ("Infant Face Scale"): a novel coma scale for children less than two years of age. Journal of neurotrauma 17:729-737.

Eglitis MA, Mezey E (1997) Hematopoietic cells differentiate into both microglia and macroglia in the brains of adult mice. Proceedings of the National Academy of Sciences of the United States of America 94:4080-4085.

Eklind S, Mallard C, Arvidsson P, Hagberg H (2005) Lipopolysaccharide induces both a primary and a secondary phase of sensitization in the developing rat brain. Pediatric research 58:112-116.

Elewa HF, Hilali H, Hess DC, Machado LS, Fagan SC (2006) Minocycline for short-term neuroprotection. Pharmacotherapy 26:515-521.

Eucker SA, Smith C, Ralston J, Friess SH, Margulies SS (2011) Physiological and histopathological responses following closed rotational head injury depend on direction of head motion. Experimental neurology 227:79-88.

Ewing-Cobbs L, Barnes M (2002) Linguistic outcomes following traumatic brain injury in children. Seminars in pediatric neurology 9:209-217.

Ewing-Cobbs L, Fletcher JM, Levin HS, Francis DJ, Davidson K, Miner ME (1997) Longitudinal neuropsychological outcome in infants and preschoolers with traumatic brain injury. Journal of the International Neuropsychological Society : JINS 3:581-591.

Ewing-Cobbs L, Johnson CP, Juranek J, DeMaster D, Prasad M, Duque G, Kramer L, Cox CS, Swank PR (2016) Longitudinal diffusion tensor imaging after pediatric traumatic brain injury: Impact of age at injury and time since injury on pathway integrity. Human brain mapping 37:3929-3945.

Ewing-Cobbs L, Kramer L, Prasad M, Canales DN, Louis PT, Fletcher JM, Vollero H, Landry SH, Cheung K (1998) Neuroimaging, physical, and developmental

findings after inflicted and noninflicted traumatic brain injury in young children. Pediatrics 102:300-307.

Ewing-Cobbs L, Miner ME, Fletcher JM, Levin HS (1989) Intellectual, motor, and language sequelae following closed head injury in infants and preschoolers. Journal of pediatric psychology 14:531-547.

Ewing-Cobbs L, Prasad M, Kramer L, Landry S (1999) Inflicted traumatic brain injury: relationship of developmental outcome to severity of injury. Pediatric neurosurgery 31:251-258.

Ewing-Cobbs L, Prasad M, Kramer L, Louis PT, Baumgartner J, Fletcher JM, Alpert B (2000) Acute neuroradiologic findings in young children with inflicted or noninflicted traumatic brain injury. Child's nervous system : ChNS : official journal of the International Society for Pediatric Neurosurgery 16:25-33; discussion 34.

Ewing-Cobbs L, Prasad MR, Kramer L, Cox CS, Jr., Baumgartner J, Fletcher S, Mendez D, Barnes M, Zhang X, Swank P (2006) Late intellectual and academic outcomes following traumatic brain injury sustained during early childhood. Journal of neurosurgery 105:287-296.

Ewing-Cobbs L, Prasad MR, Landry SH, Kramer L, DeLeon R (2004) Executive functions following traumatic brain injury in young children: a preliminary analysis. Developmental neuropsychology 26:487-512.

Ewing-Cobbs L, Prasad MR, Mendez D, Barnes MA, Swank P (2013) Social interaction in young children with inflicted and accidental traumatic brain injury: relations

with family resources and social outcomes. Journal of the International Neuropsychological Society : JINS 19:497-507.

Ewing-Cobbs L, Prasad MR, Swank P, Kramer L, Cox CS, Jr., Fletcher JM, Barnes M, Zhang X, Hasan KM (2008) Arrested development and disrupted callosal microstructure following pediatric traumatic brain injury: relation to neurobehavioral outcomes. NeuroImage 42:1305-1315.

Ewing-Cobbs L, Prasad MR, Swank P, Kramer L, Mendez D, Treble A, Payne C, Bachevalier J (2012) Social communication in young children with traumatic brain injury: relations with corpus callosum morphometry. International journal of developmental neuroscience : the official journal of the International Society for Developmental Neuroscience 30:247-254.

Fan L, Young PR, Barone FC, Feuerstein GZ, Smith DH, McIntosh TK (1995) Experimental brain injury induces expression of interleukin-1 beta mRNA in the rat brain. Brain research Molecular brain research 30:125-130.

Fan L, Young PR, Barone FC, Feuerstein GZ, Smith DH, McIntosh TK (1996) Experimental brain injury induces differential expression of tumor necrosis factor-alpha mRNA in the CNS. Brain research Molecular brain research 36:287-291.

Fan LW, Lin S, Pang Y, Rhodes PG, Cai Z (2006) Minocycline attenuates hypoxia-ischemia-induced neurological dysfunction and brain injury in the juvenile rat. The European journal of neuroscience 24:341-350.

Faul M, Xu, L., Wald, M.M., Coronado, V.G. (2010) Traumatic brain injury in the United States: Emergency Department Visits, Hospitalizations, and Deaths.

Atlanta, GA: Centers for Disease Control and Prevention, National Center for Injury Prevention and Control.

Faustino JV, Wang X, Johnson CE, Klibanov A, Derugin N, Wendland MF, Vexler ZS (2011) Microglial cells contribute to endogenous brain defenses after acute neonatal focal stroke. The Journal of neuroscience : the official journal of the Society for Neuroscience 31:12992-13001.

Febinger HY, Thomasy HE, Pavlova MN, Ringgold KM, Barf PR, George AM, Grillo JN, Bachstetter AD, Garcia JA, Cardona AE, Opp MR, Gemma C (2015) Time-dependent effects of CX3CR1 in a mouse model of mild traumatic brain injury. Journal of neuroinflammation 12:154.

Feeney DM, Boyeson MG, Linn RT, Murray HM, Dail WG (1981) Responses to cortical injury: I. Methodology and local effects of contusions in the rat. Brain research 211:67-77.

Ferrazzano P, Chanana V, Uluc K, Fidan E, Akture E, Kintner DB, Cengiz P, Sun D (2013) Age-dependent microglial activation in immature brains after hypoxia-ischemia. CNS & neurological disorders drug targets 12:338-349.

Fineman I, Giza CC, Nahed BV, Lee SM, Hovda DA (2000) Inhibition of neocortical plasticity during development by a moderate concussive brain injury. Journal of neurotrauma 17:739-749.

Fox C, Dingman A, Derugin N, Wendland MF, Manabat C, Ji S, Ferriero DM, Vexler ZS (2005) Minocycline confers early but transient protection in the immature brain following focal cerebral ischemia-reperfusion. Journal of cerebral blood flow and

metabolism : official journal of the International Society of Cerebral Blood Flow and Metabolism 25:1138-1149.

Friess SH, Ichord RN, Owens K, Ralston J, Rizol R, Overall KL, Smith C, Helfaer MA, Margulies SS (2007) Neurobehavioral functional deficits following closed head injury in the neonatal pig. Experimental neurology 204:234-243.

Galland L (2014) The gut microbiome and the brain. Journal of medicinal food 17:1261-1272.

Ganesalingam K, Yeates KO, Taylor HG, Walz NC, Stancin T, Wade S (2011) Executive functions and social competence in young children 6 months following traumatic brain injury. Neuropsychology 25:466-476.

Garrido-Mesa N, Zarzuelo A, Galvez J (2013) Minocycline: far beyond an antibiotic. British journal of pharmacology 169:337-352.

Garwood CJ, Pooler AM, Atherton J, Hanger DP, Noble W (2011) Astrocytes are important mediators of Abeta-induced neurotoxicity and tau phosphorylation in primary culture. Cell death & disease 2:e167.

Geddes JF, Hackshaw AK, Vowles GH, Nickols CD, Whitwell HL (2001a) Neuropathology of inflicted head injury in children. I. Patterns of brain damage. Brain : a journal of neurology 124:1290-1298.

Geddes JF, Vowles GH, Hackshaw AK, Nickols CD, Scott IS, Whitwell HL (2001b) Neuropathology of inflicted head injury in children. II. Microscopic brain injury in infants. Brain : a journal of neurology 124:1299-1306.

Ghosh A, Wilde EA, Hunter JV, Bigler ED, Chu Z, Li X, Vasquez AC, Menefee D, Yallampalli R, Levin HS (2009) The relation between Glasgow Coma Scale score

and later cerebral atrophy in paediatric traumatic brain injury. Brain injury 23:228-233.

Ginhoux F, Greter M, Leboeuf M, Nandi S, See P, Gokhan S, Mehler MF, Conway SJ, Ng LG, Stanley ER, Samokhvalov IM, Merad M (2010) Fate mapping analysis reveals that adult microglia derive from primitive macrophages. Science 330:841-845.

Girard S, Sebire H, Brochu ME, Briota S, Sarret P, Sebire G (2012) Postnatal administration of IL-1Ra exerts neuroprotective effects following perinatal inflammation and/or hypoxic-ischemic injuries. Brain, behavior, and immunity 26:1331-1339.

Giza CC, Mink RB, Madikians A (2007) Pediatric traumatic brain injury: not just little adults. Current opinion in critical care 13:143-152.

Glang A, Tyler J, Pearson S, Todis B, Morvant M (2004) Improving educational services for students with TBI through statewide consulting teams. NeuroRehabilitation 19:219-231.

Gleckman AM, Bell MD, Evans RJ, Smith TW (1999) Diffuse axonal injury in infants with nonaccidental craniocerebral trauma: enhanced detection by beta-amyloid precursor protein immunohistochemical staining. Archives of pathology & laboratory medicine 123:146-151.

Gomes-Leal W (2012) Microglial physiopathology: how to explain the dual role of microglia after acute neural disorders? Brain and behavior 2:345-356.

Gonzalez JC, Egea J, Del Carmen Godino M, Fernandez-Gomez FJ, Sanchez-Prieto J, Gandia L, Garcia AG, Jordan J, Hernandez-Guijo JM (2007) Neuroprotectant

minocycline depresses glutamatergic neurotransmission and Ca(2+) signalling in hippocampal neurons. The European journal of neuroscience 26:2481-2495.

Goshen I, Kreisel T, Ounallah-Saad H, Renbaum P, Zalzstein Y, Ben-Hur T, Levy-Lahad E, Yirmiya R (2007) A dual role for interleukin-1 in hippocampal-dependent memory processes. Psychoneuroendocrinology 32:1106-1115.

Goulden V, Glass D, Cunliffe WJ (1996) Safety of long-term high-dose minocycline in the treatment of acne. The British journal of dermatology 134:693-695.

Graeber MB, Streit WJ (2010) Microglia: biology and pathology. Acta neuropathologica 119:89-105.

Greve MW, Zink BJ (2009) Pathophysiology of traumatic brain injury. The Mount Sinai journal of medicine, New York 76:97-104.

Grundl PD, Biagas KV, Kochanek PM, Schiding JK, Barmada MA, Nemoto EM (1994) Early cerebrovascular response to head injury in immature and mature rats. Journal of neurotrauma 11:135-148.

Guillemin GJ (2012) Quinolinic acid, the inescapable neurotoxin. The FEBS journal 279:1356-1365.

Hamm RJ, O'Dell DM, Pike BR, Lyeth BG (1993) Cognitive impairment following traumatic brain injury: the effect of pre- and post-injury administration of scopolamine and MK-801. Brain research Cognitive brain research 1:223-226.

Hanisch UK (2002) Microglia as a source and target of cytokines. Glia 40:140-155.

Hanisch UK, Kettenmann H (2007) Microglia: active sensor and versatile effector cells in the normal and pathologic brain. Nature neuroscience 10:1387-1394.

Hanlon LA, Huh JW, Raghupathi R (2016a) Minocycline Transiently Reduces Microglia/Macrophage Activation but Exacerbates Cognitive Deficits Following Repetitive Traumatic Brain Injury in the Neonatal Rat. Journal of neuropathology and experimental neurology 75:214-226.

Hanlon LA, Raghupathi R, Huh JW (2016b) Differential effects of minocycline on microglial activation and neurodegeneration following closed head injury in the neonate rat. Experimental neurology 290:1-14.

Hardcastle N, Benzon HA, Vavilala MS (2014) Update on the 2012 guidelines for the management of pediatric traumatic brain injury - information for the anesthesiologist. Paediatric anaesthesia 24:703-710.

Harwood SM, Yaqoob MM, Allen DA (2005) Caspase and calpain function in cell death: bridging the gap between apoptosis and necrosis. Annals of clinical biochemistry 42:415-431.

He J, Evans CO, Hoffman SW, Oyesiku NM, Stein DG (2004) Progesterone and allopregnanolone reduce inflammatory cytokines after traumatic brain injury. Experimental neurology 189:404-412.

Heneka MT, Kummer MP, Latz E (2014) Innate immune activation in neurodegenerative disease. Nature reviews Immunology 14:463-477.

Hickey WF, Kimura H (1988) Perivascular microglial cells of the CNS are bone marrow-derived and present antigen in vivo. Science 239:290-292.

Hoek RM, Ruuls SR, Murphy CA, Wright GJ, Goddard R, Zurawski SM, Blom B, Homola ME, Streit WJ, Brown MH, Barclay AN, Sedgwick JD (2000) Down-

regulation of the macrophage lineage through interaction with OX2 (CD200). Science 290:1768-1771.

Homsi S, Federico F, Croci N, Palmier B, Plotkine M, Marchand-Leroux C, Jafarian-Tehrani M (2009) Minocycline effects on cerebral edema: relations with inflammatory and oxidative stress markers following traumatic brain injury in mice. Brain research 1291:122-132.

Homsi S, Piaggio T, Croci N, Noble F, Plotkine M, Marchand-Leroux C, Jafarian-Tehrani M (2010) Blockade of acute microglial activation by minocycline promotes neuroprotection and reduces locomotor hyperactivity after closed head injury in mice: a twelve-week follow-up study. Journal of neurotrauma 27:911-921.

Hoogland IC, Houbolt C, van Westerloo DJ, van Gool WA, van de Beek D (2015) Systemic inflammation and microglial activation: systematic review of animal experiments. Journal of neuroinflammation 12:114.

Huh JW, Franklin MA, Widing AG, Raghupathi R (2006) Regionally distinct patterns of calpain activation and traumatic axonal injury following contusive brain injury in immature rats. Developmental neuroscience 28:466-476.

Huh JW, Raghupathi R (2007) Chronic cognitive deficits and long-term histopathological alterations following contusive brain injury in the immature rat. Journal of neurotrauma 24:1460-1474.

Huh JW, Raghupathi R (2009) New concepts in treatment of pediatric traumatic brain injury. Anesthesiology clinics 27:213-240.

Huh JW, Widing AG, Raghupathi R (2008) Midline brain injury in the immature rat induces sustained cognitive deficits, bihemispheric axonal injury and neurodegeneration. Experimental neurology 213:84-92.

Huh JW, Widing AG, Raghupathi R (2011) Differential effects of injury severity on cognition and cellular pathology after contusive brain trauma in the immature rat. Journal of neurotrauma 28:245-257.

Ibrahim NG, Ralston J, Smith C, Margulies SS (2010) Physiological and pathological responses to head rotations in toddler piglets. Journal of neurotrauma 27:1021-1035.

Igarashi T, Potts MB, Noble-Haeusslein LJ (2007) Injury severity determines Purkinje cell loss and microglial activation in the cerebellum after cortical contusion injury. Experimental neurology 203:258-268.

Inta I, Vogt MA, Vogel AS, Bettendorf M, Gass P, Inta D (2016) Minocycline exacerbates apoptotic neurodegeneration induced by the NMDA receptor antagonist MK-801 in the early postnatal mouse brain. European archives of psychiatry and clinical neuroscience 266:673-677.

Ip EY, Giza CC, Griesbach GS, Hovda DA (2002) Effects of enriched environment and fluid percussion injury on dendritic arborization within the cerebral cortex of the developing rat. Journal of neurotrauma 19:573-585.

Israelsson C, Bengtsson H, Kylberg A, Kullander K, Lewen A, Hillered L, Ebendal T (2008) Distinct cellular patterns of upregulated chemokine expression supporting a prominent inflammatory role in traumatic brain injury. Journal of neurotrauma 25:959-974.

Ivacko JA, Sun R, Silverstein FS (1996) Hypoxic-ischemic brain injury induces an acute microglial reaction in perinatal rats. Pediatric research 39:39-47.

Jantzie LL, Cheung PY, Todd KG (2005) Doxycycline reduces cleaved caspase-3 and microglial activation in an animal model of neonatal hypoxia-ischemia. Journal of cerebral blood flow and metabolism : official journal of the International Society of Cerebral Blood Flow and Metabolism 25:314-324.

Jenny C, Hymel KP, Ritzen A, Reinert SE, Hay TC (1999) Analysis of missed cases of abusive head trauma. Jama 281:621-626.

Jeong HK, Ji K, Min K, Joe EH (2013) Brain inflammation and microglia: facts and misconceptions. Experimental neurobiology 22:59-67.

Jin X, Prince DA, Huguenard JR (2006) Enhanced excitatory synaptic connectivity in layer v pyramidal neurons of chronically injured epileptogenic neocortex in rats. The Journal of neuroscience : the official journal of the Society for Neuroscience 26:4891-4900.

Johnson CP, Juranek J, Swank PR, Kramer L, Cox CS, Jr., Ewing-Cobbs L (2015) White matter and reading deficits after pediatric traumatic brain injury: A diffusion tensor imaging study. NeuroImage Clinical 9:668-677.

Kampfl A, Posmantur RM, Zhao X, Schmutzhard E, Clifton GL, Hayes RL (1997) Mechanisms of calpain proteolysis following traumatic brain injury: implications for pathology and therapy: implications for pathology and therapy: a review and update. Journal of neurotrauma 14:121-134.

Kan P, Amini A, Hansen K, White GL, Jr., Brockmeyer DL, Walker ML, Kestle JR (2006) Outcomes after decompressive craniectomy for severe traumatic brain injury in children. Journal of neurosurgery 105:337-342.

Krasowski MD (2000) Differential modulatory actions of the volatile convulsant flurothyl and its anesthetic isomer at inhibitory ligand-gated ion channels. Neuropharmacology 39:1168-1183.

Keenan HT, Bratton SL (2006) Epidemiology and outcomes of pediatric traumatic brain injury. Developmental neuroscience 28:256-263.

Keenan HT, Runyan DK, Marshall SW, Nocera MA, Merten DF (2004) A population-based comparison of clinical and outcome characteristics of young children with serious inflicted and noninflicted traumatic brain injury. Pediatrics 114:633-639.

Keenan HT, Runyan DK, Marshall SW, Nocera MA, Merten DF, Sinal SH (2003) A population-based study of inflicted traumatic brain injury in young children. Jama 290:621-626.

Kelly P, John S, Vincent AL, Reed P (2015) Abusive head trauma and accidental head injury: a 20-year comparative study of referrals to a hospital child protection team. Archives of disease in childhood 100:1123-1130.

Kelso ML, Scheff NN, Scheff SW, Pauly JR (2011) Melatonin and minocycline for combinatorial therapy to improve functional and histopathological deficits following traumatic brain injury. Neuroscience letters 488:60-64.

Kettenmann H, Hanisch UK, Noda M, Verkhratsky A (2011) Physiology of microglia. Physiological reviews 91:461-553.

Kierdorf K, Prinz M (2013) Factors regulating microglia activation. Frontiers in cellular neuroscience 7:44.

Kim HS, Suh YH (2009) Minocycline and neurodegenerative diseases. Behavioural brain research 196:168-179.

Kobayashi K, Imagama S, Ohgomori T, Hirano K, Uchimura K, Sakamoto K, Hirakawa A, Takeuchi H, Suzumura A, Ishiguro N, Kadomatsu K (2013) Minocycline selectively inhibits M1 polarization of microglia. Cell death & disease 4:e525.

Kobayashi Y (2008) The role of chemokines in neutrophil biology. Frontiers in bioscience : a journal and virtual library 13:2400-2407.

Kovesdi E, Kamnaksh A, Wingo D, Ahmed F, Grunberg NE, Long JB, Kasper CE, Agoston DV (2012) Acute minocycline treatment mitigates the symptoms of mild blast-induced traumatic brain injury. Frontiers in neurology 3:111.

Kreutzberg GW (1996) Microglia: a sensor for pathological events in the CNS. Trends in neurosciences 19:312-318.

Kumamaru H, Saiwai H, Kobayakawa K, Kubota K, van Rooijen N, Inoue K, Iwamoto Y, Okada S (2012) Liposomal clodronate selectively eliminates microglia from primary astrocyte cultures. Journal of neuroinflammation 9:116.

Lam TI, Bingham D, Chang TJ, Lee CC, Shi J, Wang D, Massa S, Swanson RA, Liu J (2013) Beneficial effects of minocycline and botulinum toxin-induced constraint physical therapy following experimental traumatic brain injury. Neurorehabilitation and neural repair 27:889-899.

Langlois JA, Rutland-Brown W, Thomas KE (2005) The incidence of traumatic brain injury among children in the United States: differences by race. The Journal of head trauma rehabilitation 20:229-238.

Lawson LJ, Perry VH, Dri P, Gordon S (1990) Heterogeneity in the distribution and morphology of microglia in the normal adult mouse brain. Neuroscience 39:151-170.

Lechpammer M, Manning SM, Samonte F, Nelligan J, Sabo E, Talos DM, Volpe JJ, Jensen FE (2008) Minocycline treatment following hypoxic/ischaemic injury attenuates white matter injury in a rodent model of periventricular leucomalacia. Neuropathology and applied neurobiology 34:379-393.

Lehenkari PP, Kellinsalmi M, Napankangas JP, Ylitalo KV, Monkkonen J, Rogers MJ, Azhayev A, Vaananen HK, Hassinen IE (2002) Further insight into mechanism of action of clodronate: inhibition of mitochondrial ADP/ATP translocase by a nonhydrolyzable, adenine-containing metabolite. Molecular pharmacology 61:1255-1262.

Le Magueresse C, Monyer H (2013) GABAergic interneurons shape the functional maturation of the cortex. Neuron 77:388-405.

Levin HS, Song J, Ewing-Cobbs L, Chapman SB, Mendelsohn D (2001) Word fluency in relation to severity of closed head injury, associated frontal brain lesions, and age at injury in children. Neuropsychologia 39:122-131.

Li N, Yang Y, Glover DP, Zhang J, Saraswati M, Robertson C, Pelled G (2014) Evidence for impaired plasticity after traumatic brain injury in the developing brain. Journal of neurotrauma 31:395-403.

Liesemer K, Bratton SL, Zebrack CM, Brockmeyer D, Statler KD (2011) Early post-traumatic seizures in moderate to severe pediatric traumatic brain injury: rates, risk factors, and clinical features. Journal of neurotrauma 28:755-762.

Lighthall JW (1988) Controlled cortical impact: a new experimental brain injury model. Journal of neurotrauma 5:1-15.

Lima A, Sardinha VM, Oliveira AF, Reis M, Mota C, Silva MA, Marques F, Cerqueira JJ, Pinto L, Sousa N, Oliveira JF (2014) Astrocyte pathology in the prefrontal cortex impairs the cognitive function of rats. Molecular psychiatry 19:834-841.

Lin HY, Huang CC, Chang KF (2009) Lipopolysaccharide preconditioning reduces neuroinflammation against hypoxic ischemia and provides long-term outcome of neuroprotection in neonatal rat. Pediatric research 66:254-259.

Liu Y, Silverstein FS, Skoff R, Barks JD (2002) Hypoxic-ischemic oligodendroglial injury in neonatal rat brain. Pediatric research 51:25-33.

Loane DJ, Byrnes KR (2010) Role of microglia in neurotrauma. Neurotherapeutics : the journal of the American Society for Experimental NeuroTherapeutics 7:366-377.

Loane DJ, Kumar A (2016) Microglia in the TBI brain: The good, the bad, and the dysregulated. Experimental neurology 275 Pt 3:316-327.

London A, Cohen M, Schwartz M (2013) Microglia and monocyte-derived macrophages: functionally distinct populations that act in concert in CNS plasticity and repair. Frontiers in cellular neuroscience 7:34.

Longhi L, Gesuete R, Perego C, Ortolano F, Sacchi N, Villa P, Stocchetti N, De Simoni MG (2011) Long-lasting protection in brain trauma by endotoxin preconditioning. Journal of cerebral blood flow and metabolism : official journal of the International Society of Cerebral Blood Flow and Metabolism 31:1919-1929.

Lotocki G, de Rivero Vaccari J, Alonso O, Molano JS, Nixon R, Dietrich WD, Bramlett HM (2011) Oligodendrocyte Vulnerability Following Traumatic Brain Injury in

Rats: Effect of Moderate Hypothermia. Therapeutic hypothermia and temperature management 1:43-51.

Margulies SS, Thibault KL (2000) Infant skull and suture properties: measurements and implications for mechanisms of pediatric brain injury. Journal of biomechanical engineering 122:364-371.

Ma Y, Prince DA (2012) Functional alterations in GABAergic fast-spiking interneurons in chronically injured epileptogenic neocortex. Neurobiology of disease 47:102-113.

Marmarou A, Foda MA, van den Brink W, Campbell J, Kita H, Demetriadou K (1994) A new model of diffuse brain injury in rats. Part I: Pathophysiology and biomechanics. Journal of neurosurgery 80:291-300.

Martens PR (1993) Coma scales in paediatric resuscitation. Resuscitation 25:285-288.

Matis G, Birbilis T (2008) The Glasgow Coma Scale--a brief review. Past, present, future. Acta neurologica Belgica 108:75-89.

Max JE, Keatley E, Wilde EA, Bigler ED, Schachar RJ, Saunders AE, Ewing-Cobbs L, Chapman SB, Dennis M, Yang TT, Levin HS (2012) Depression in children and adolescents in the first 6 months after traumatic brain injury. International journal of developmental neuroscience : the official journal of the International Society for Developmental Neuroscience 30:239-245.

Max JE, Lopez A, Wilde EA, Bigler ED, Schachar RJ, Saunders A, Ewing-Cobbs L, Chapman SB, Yang TT, Levin HS (2015) Anxiety disorders in children and adolescents in the second six months after traumatic brain injury. Journal of pediatric rehabilitation medicine 8:345-355.

Max JE, Robertson BA, Lansing AE (2001) The phenomenology of personality change due to traumatic brain injury in children and adolescents. The Journal of neuropsychiatry and clinical neurosciences 13:161-170.

McAfoose J, Baune BT (2009) Evidence for a cytokine model of cognitive function. Neuroscience and biobehavioral reviews 33:355-366.

McCleskey PE, Littleton KH (2004) Minocycline-induced blue-green discoloration of bone. A case report. The Journal of bone and joint surgery American volume 86-A:146-148.

McIntosh TK, Vink R, Noble L, Yamakami I, Fernyak S, Soares H, Faden AL (1989) Traumatic brain injury in the rat: characterization of a lateral fluid-percussion model. Neuroscience 28:233-244.

McRae A, Gilland E, Bona E, Hagberg H (1995) Microglia activation after neonatal hypoxic-ischemia. Brain research Developmental brain research 84:245-252.

Meehan WP, 3rd, Zhang J, Mannix R, Whalen MJ (2012) Increasing recovery time between injuries improves cognitive outcome after repetitive mild concussive brain injuries in mice. Neurosurgery 71:885-891.

Milligan CE, Levitt P, Cunningham TJ (1991) Brain macrophages and microglia respond differently to lesions of the developing and adult visual system. The Journal of comparative neurology 314:136-146.

Morganti JM, Riparip LK, Rosi S (2016) Call Off the Dog(ma): M1/M2 Polarization Is Concurrent following Traumatic Brain Injury. PloS one 11:e0148001.

Mychasiuk R, Farran A, Esser MJ (2014) Assessment of an experimental rodent model of pediatric mild traumatic brain injury. Journal of neurotrauma 31:749-757.

Narang SK, Estrada C, Greenberg S, Lindberg D (2016) Acceptance of Shaken Baby Syndrome and Abusive Head Trauma as Medical Diagnoses. The Journal of pediatrics 177:273-278.

Natale JE, Ahmed F, Cernak I, Stoica B, Faden AI (2003) Gene expression profile changes are commonly modulated across models and species after traumatic brain injury. Journal of neurotrauma 20:907-927.

Nayak D, Roth TL, McGavern DB (2014) Microglia development and function. Annual review of immunology 32:367-402.

Nelson LH, Lenz KM (2017) Microglia depletion in early life programs persistent changes in social, mood-related, and locomotor behavior in male and female rats. Behavioural brain research 316:279-293.

Neumann H, Takahashi K (2007) Essential role of the microglial triggering receptor expressed on myeloid cells-2 (TREM2) for central nervous tissue immune homeostasis. Journal of neuroimmunology 184:92-99.

Newell E, Shellington DK, Simon DW, Bell MJ, Kochanek PM, Feldman K, Bayir H, Aneja RK, Carcillo JA, Clark RS (2015) Cerebrospinal Fluid Markers of Macrophage and Lymphocyte Activation After Traumatic Brain Injury in Children. Pediatric critical care medicine : a journal of the Society of Critical Care Medicine and the World Federation of Pediatric Intensive and Critical Care Societies 16:549-557.

Nichols J, Perez R, Wu C, Adelson PD, Anderson T (2015) Traumatic brain injury induces rapid enhancement of cortical excitability in juvenile rats. CNS neuroscience & therapeutics 21:193-203.

Nimmerjahn A, Kirchhoff F, Helmchen F (2005) Resting microglial cells are highly dynamic surveillants of brain parenchyma in vivo. Science 308:1314-1318.

O'Dell DM, Gibson CJ, Wilson MS, DeFord SM, Hamm RJ (2000) Positive and negative modulation of the GABA(A) receptor and outcome after traumatic brain injury in rats. Brain research 861:325-332.

Okonkwo DO, Pettus EH, Moroi J, Povlishock JT (1998) Alteration of the neurofilament sidearm and its relation to neurofilament compaction occurring with traumatic axonal injury. Brain research 784:1-6.

O'Mara SM, Sanchez-Vives MV, Brotons-Mas JR, O'Hare E (2009) Roles for the subiculum in spatial information processing, memory, motivation and the temporal control of behaviour. Progress in neuro-psychopharmacology & biological psychiatry 33:782-790.

Ornstein TJ, Max JE, Schachar R, Dennis M, Barnes M, Ewing-Cobbs L, Levin HS (2013) Response inhibition in children with and without ADHD after traumatic brain injury. Journal of neuropsychology 7:1-11.

Ornstein TJ, Sagar S, Schachar RJ, Ewing-Cobbs L, Chapman SB, Dennis M, Saunders AE, Yang TT, Levin HS, Max JE (2014) Neuropsychological performance of youth with secondary attention-deficit/hyperactivity disorder 6- and 12-months after traumatic brain injury. Journal of the International Neuropsychological Society : JINS 20:971-981.

Paolicelli RC, Bolasco G, Pagani F, Maggi L, Scianni M, Panzanelli P, Giustetto M, Ferreira TA, Guiducci E, Dumas L, Ragozzino D, Gross CT (2011) Synaptic

pruning by microglia is necessary for normal brain development. Science 333:1456-1458.

Parks SE, Annest JL, Hill HA, Karch DL (2012) Pediatric Abusive Head Trauma: Recommended Definitions for Public Health Surveillance and Research. Atlanta, GA: Centers for Disease Control and Prevention, National Center for Injury Prevention and Control, Division of Violence Prevention.

Peferoen L, Kipp M, van der Valk P, van Noort JM, Amor S (2014) Oligodendrocyte-microglia cross-talk in the central nervous system. Immunology 141:302-313.

Pettus EH, Christman CW, Giebel ML, Povlishock JT (1994) Traumatically induced altered membrane permeability: its relationship to traumatically induced reactive axonal change. Journal of neurotrauma 11:507-522.

Pettus EH, Povlishock JT (1996) Characterization of a distinct set of intra-axonal ultrastructural changes associated with traumatically induced alteration in axolemmal permeability. Brain research 722:1-11.

Plane JM, Shen Y, Pleasure DE, Deng W (2010) Prospects for minocycline neuroprotection. Archives of neurology 67:1442-1448.

Pohl D, Bittigau P, Ishimaru MJ, Stadthaus D, Hubner C, Olney JW, Turski L, Ikonomidou C (1999) N-Methyl-D-aspartate antagonists and apoptotic cell death triggered by head trauma in developing rat brain. Proceedings of the National Academy of Sciences of the United States of America 96:2508-2513.

Poliak SC, DiGiovanna JJ, Gross EG, Gantt G, Peck GL (1985) Minocycline-associated tooth discoloration in young adults. Jama 254:2930-2932.

Pont-Lezica L, Bechade C, Belarif-Cantaut Y, Pascual O, Bessis A (2011) Physiological roles of microglia during development. Journal of neurochemistry 119:901-908.

Portera-Cailliau C, Price DL, Martin LJ (1997) Excitotoxic neuronal death in the immature brain is an apoptosis-necrosis morphological continuum. The Journal of comparative neurology 378:70-87.

Potter EG, Cheng Y, Natale JE (2009) Deleterious effects of minocycline after in vivo target deprivation of thalamocortical neurons in the immature, metallothionein-deficient mouse brain. Journal of neuroscience research 87:1356-1368.

Potts MB, Koh SE, Whetstone WD, Walker BA, Yoneyama T, Claus CP, Manvelyan HM, Noble-Haeusslein LJ (2006) Traumatic injury to the immature brain: inflammation, oxidative injury, and iron-mediated damage as potential therapeutic targets. NeuroRx : the journal of the American Society for Experimental NeuroTherapeutics 3:143-153.

Prasad M, Sobhan S, Ewing-Cobbs L (2008) Home-based caregiver-centered cognitive intervention for very young children with traumatic brain injury [Abstract]. In: North American Brain Injury Society's Sixth Annual Conference on Brain Injury. Journal of head trauma rehabilitation 23(5): 339-355.

Prasad MR, Swank PR, Ewing-Cobbs L (2017) Long-Term School Outcomes of Children and Adolescents With Traumatic Brain Injury. The Journal of head trauma rehabilitation 32:E24-E32.

Prince DA, Parada I, Scalise K, Graber K, Jin X, Shen F (2009) Epilepsy following cortical injury: cellular and molecular mechanisms as targets for potential prophylaxis. Epilepsia 50 Suppl 2:30-40.

Prince DA, Tseng GF (1993) Epileptogenesis in chronically injured cortex: in vitro studies. Journal of neurophysiology 69:1276-1291.

Prins ML, Hovda DA (1998) Traumatic brain injury in the developing rat: effects of maturation on Morris water maze acquisition. Journal of neurotrauma 15:799-811.

Prins ML, Hovda DA (2001) Mapping cerebral glucose metabolism during spatial learning: interactions of development and traumatic brain injury. Journal of neurotrauma 18:31-46.

Pullela R, Raber J, Pfankuch T, Ferriero DM, Claus CP, Koh SE, Yamauchi T, Rola R, Fike JR, Noble-Haeusslein LJ (2006) Traumatic injury to the immature brain results in progressive neuronal loss, hyperactivity and delayed cognitive impairments. Developmental neuroscience 28:396-409.

Raghavendra Rao VL, Dogan A, Bowen KK, Dempsey RJ (2000) Traumatic brain injury leads to increased expression of peripheral-type benzodiazepine receptors, neuronal death, and activation of astrocytes and microglia in rat thalamus. Experimental neurology 161:102-114.

Raghubar KP, Barnes MA, Prasad M, Johnson CP, Ewing-Cobbs L (2013) Mathematical outcomes and working memory in children with TBI and orthopedic injury. Journal of the International Neuropsychological Society : JINS 19:254-263.

Raghupathi R, Huh JW (2007) Diffuse brain injury in the immature rat: evidence for an age-at-injury effect on cognitive function and histopathologic damage. Journal of neurotrauma 24:1596-1608.

Raghupathi R, Margulies SS (2002) Traumatic axonal injury after closed head injury in the neonatal pig. Journal of neurotrauma 19:843-853.

Ramesh G, MacLean AG, Philipp MT (2013) Cytokines and chemokines at the crossroads of neuroinflammation, neurodegeneration, and neuropathic pain. Mediators of inflammation 2013:480739.

Ransohoff RM (2016) A polarizing question: do M1 and M2 microglia exist? Nature neuroscience 19:987-991.

Ransohoff RM, Perry VH (2009) Microglial physiology: unique stimuli, specialized responses. Annual review of immunology 27:119-145.

Rao VL, Dogan A, Todd KG, Bowen KK, Dempsey RJ (2001) Neuroprotection by memantine, a non-competitive NMDA receptor antagonist after traumatic brain injury in rats. Brain research 911:96-100.

Rea K, Dinan TG, Cryan JF (2016) The microbiome: A key regulator of stress and neuroinflammation. Neurobiology of stress 4:23-33.

Reeves TM, Phillips LL, Povlishock JT (2005) Myelinated and unmyelinated axons of the corpus callosum differ in vulnerability and functional recovery following traumatic brain injury. Experimental neurology 196:126-137.

Reilly PL, Simpson DA, Sprod R, Thomas L (1988) Assessing the conscious level in infants and young children: a paediatric version of the Glasgow Coma Scale. Child's nervous system : ChNS : official journal of the International Society for Pediatric Neurosurgery 4:30-33.

Rosenzweig HL, Minami M, Lessov NS, Coste SC, Stevens SL, Henshall DC, Meller R, Simon RP, Stenzel-Poore MP (2007) Endotoxin preconditioning protects against the cytotoxic effects of TNFalpha after stroke: a novel role for TNFalpha in LPS-ischemic tolerance. Journal of cerebral blood flow and metabolism : official

journal of the International Society of Cerebral Blood Flow and Metabolism 27:1663-1674.

Ross DT, Meaney DF, Sabol MK, Smith DH, Gennarelli TA (1994) Distribution of forebrain diffuse axonal injury following inertial closed head injury in miniature swine. Experimental neurology 126:291-299.

Ruppel RA, Kochanek PM, Adelson PD, Rose ME, Wisniewski SR, Bell MJ, Clark RS, Marion DW, Graham SH (2001) Excitatory amino acid concentrations in ventricular cerebrospinal fluid after severe traumatic brain injury in infants and children: the role of child abuse. The Journal of pediatrics 138:18-25.

Saatman KE, Bozyczko-Coyne D, Marcy V, Siman R, McIntosh TK (1996) Prolonged calpain-mediated spectrin breakdown occurs regionally following experimental brain injury in the rat. Journal of neuropathology and experimental neurology 55:850-860.

Sanchez AR, Rogers RS, 3rd, Sheridan PJ (2004) Tetracycline and other tetracycline-derivative staining of the teeth and oral cavity. International journal of dermatology 43:709-715.

Sanchez Mejia RO, Ona VO, Li M, Friedlander RM (2001) Minocycline reduces traumatic brain injury-mediated caspase-1 activation, tissue damage, and neurological dysfunction. Neurosurgery 48:1393-1399; discussion 1399-1401.

Sanderson KL, Raghupathi R, Saatman KE, Martin D, Miller G, McIntosh TK (1999) Interleukin-1 receptor antagonist attenuates regional neuronal cell death and cognitive dysfunction after experimental brain injury. Journal of cerebral blood

flow and metabolism : official journal of the International Society of Cerebral Blood Flow and Metabolism 19:1118-1125.

Scafidi S, Racz J, Hazelton J, McKenna MC, Fiskum G (2010) Neuroprotection by acetyl-L-carnitine after traumatic injury to the immature rat brain. Developmental neuroscience 32:480-487.

Schlienger RG, Bircher AJ, Meier CR (2000) Minocycline-induced lupus. A systematic review. Dermatology 200:223-231.

Schober ME, Requena DF, Block B, Davis LJ, Rodesch C, Casper TC, Juul SE, Kesner RP, Lane RH (2014) Erythropoietin improved cognitive function and decreased hippocampal caspase activity in rat pups after traumatic brain injury. Journal of neurotrauma 31:358-369.

Schulz C, Gomez Perdiguero E, Chorro L, Szabo-Rogers H, Cagnard N, Kierdorf K, Prinz M, Wu B, Jacobsen SE, Pollard JW, Frampton J, Liu KJ, Geissmann F (2012) A lineage of myeloid cells independent of Myb and hematopoietic stem cells. Science 336:86-90.

Schwartz L, Taylor HG, Drotar D, Yeates KO, Wade SL, Stancin T (2003) Long-term behavior problems following pediatric traumatic brain injury: prevalence, predictors, and correlates. Journal of pediatric psychology 28:251-263.

Semple BD, Blomgren K, Gimlin K, Ferriero DM, Noble-Haeusslein LJ (2013) Brain development in rodents and humans: Identifying benchmarks of maturation and vulnerability to injury across species. Progress in neurobiology 106-107:1-16.

Semple BD, Canchola SA, Noble-Haeusslein LJ (2012) Deficits in social behavior emerge during development after pediatric traumatic brain injury in mice. Journal of neurotrauma 29:2672-2683.

Semple BD, Sadjadi R, Carlson J, Chen Y, Xu D, Ferriero DM, Noble-Haeusslein LJ (2016) Long-Term Anesthetic-Dependent Hypoactivity after Repetitive Mild Traumatic Brain Injuries in Adolescent Mice. Developmental neuroscience 38:220-238.

Semple BD, Trivedi A, Gimlin K, Noble-Haeusslein LJ (2015) Neutrophil elastase mediates acute pathogenesis and is a determinant of long-term behavioral recovery after traumatic injury to the immature brain. Neurobiology of disease 74:263-280.

Shannon P, Smith CR, Deck J, Ang LC, Ho M, Becker L (1998) Axonal injury and the neuropathology of shaken baby syndrome. Acta neuropathologica 95:625-631.

Shohami E, Novikov M, Bass R, Yamin A, Gallily R (1994) Closed head injury triggers early production of TNF alpha and IL-6 by brain tissue. Journal of cerebral blood flow and metabolism : official journal of the International Society of Cerebral Blood Flow and Metabolism 14:615-619.

Siopi E, Cho AH, Homsi S, Croci N, Plotkine M, Marchand-Leroux C, Jafarian-Tehrani M (2011) Minocycline restores sAPPalpha levels and reduces the late histopathological consequences of traumatic brain injury in mice. Journal of neurotrauma 28:2135-2143.

Siopi E, Llufriu-Daben G, Fanucchi F, Plotkine M, Marchand-Leroux C, Jafarian-Tehrani M (2012) Evaluation of late cognitive impairment and anxiety states following

traumatic brain injury in mice: the effect of minocycline. Neuroscience letters 511:110-115.

Smith DH, Chen XH, Xu BN, McIntosh TK, Gennarelli TA, Meaney DF (1997) Characterization of diffuse axonal pathology and selective hippocampal damage following inertial brain trauma in the pig. Journal of neuropathology and experimental neurology 56:822-834.

Smith JA, Das A, Ray SK, Banik NL (2012) Role of pro-inflammatory cytokines released from microglia in neurodegenerative diseases. Brain research bulletin 87:10-20.

Smith K, Leyden JJ (2005) Safety of doxycycline and minocycline: a systematic review. Clinical therapeutics 27:1329-1342.

Song G, Dhodda VK, Blei AT, Dempsey RJ, Rao VL (2002) GeneChip analysis shows altered mRNA expression of transcripts of neurotransmitter and signal transduction pathways in the cerebral cortex of portacaval shunted rats. Journal of neuroscience research 68:730-737.

Sonmez U, Sonmez A, Erbil G, Tekmen I, Baykara B (2007) Neuroprotective effects of resveratrol against traumatic brain injury in immature rats. Neuroscience letters 420:133-137.

Spain A, Daumas S, Lifshitz J, Rhodes J, Andrews PJ, Horsburgh K, Fowler JH (2010) Mild fluid percussion injury in mice produces evolving selective axonal pathology and cognitive deficits relevant to human brain injury. Journal of neurotrauma 27:1429-1438.

Stein SC, Spettell C (1995) The Head Injury Severity Scale (HISS): a practical classification of closed-head injury. Brain injury 9:437-444.

Stellwagen D, Beattie EC, Seo JY, Malenka RC (2005) Differential regulation of AMPA receptor and GABA receptor trafficking by tumor necrosis factor-alpha. The Journal of neuroscience : the official journal of the Society for Neuroscience 25:3219-3228.

Sternbach GL (2000) The Glasgow coma scale. The Journal of emergency medicine 19:67-71.

Stoltz S, Humm JL, Schallert T (1999) Cortical injury impairs contralateral forelimb immobility during swimming: a simple test for loss of inhibitory motor control. Behavioural brain research 106:127-132.

Stone JR, Singleton RH, Povlishock JT (2001) Intra-axonal neurofilament compaction does not evoke local axonal swelling in all traumatically injured axons. Experimental neurology 172:320-331.

Stover JF, Schoning B, Beyer TF, Woiciechowsky C, Unterberg AW (2000) Temporal profile of cerebrospinal fluid glutamate, interleukin-6, and tumor necrosis factor-alpha in relation to brain edema and contusion following controlled cortical impact injury in rats. Neuroscience letters 288:25-28.

Sullivan HG, Martinez J, Becker DP, Miller JD, Griffith R, Wist AO (1976) Fluid-percussion model of mechanical brain injury in the cat. Journal of neurosurgery 45:521-534.

Suskauer SJ, Huisman TA (2009) Neuroimaging in pediatric traumatic brain injury: current and future predictors of functional outcome. Developmental disabilities research reviews 15:117-123.

Tam WY, Ma CH (2014) Bipolar/rod-shaped microglia are proliferating microglia with distinct M1/M2 phenotypes. Scientific reports 4:7279.

Tang M, Alexander H, Clark RS, Kochanek PM, Kagan VE, Bayir H (2010) Minocycline reduces neuronal death and attenuates microglial response after pediatric asphyxial cardiac arrest. Journal of cerebral blood flow and metabolism : official journal of the International Society of Cerebral Blood Flow and Metabolism 30:119-129.

Tang Y, Le W (2016) Differential Roles of M1 and M2 Microglia in Neurodegenerative Diseases. Molecular neurobiology 53:1181-1194.

Taylor SE, Morganti-Kossmann C, Lifshitz J, Ziebell JM (2014) Rod microglia: a morphological definition. PloS one 9:e97096.

Teasdale G, Jennett B (1974) Assessment of coma and impaired consciousness. A practical scale. Lancet 2:81-84.

Tong KA, Ashwal S, Holshouser BA, Nickerson JP, Wall CJ, Shutter LA, Osterdock RJ, Haacke EM, Kido D (2004) Diffuse axonal injury in children: clinical correlation with hemorrhagic lesions. Annals of neurology 56:36-50.

Tong W, Igarashi T, Ferriero DM, Noble LJ (2002) Traumatic brain injury in the immature mouse brain: characterization of regional vulnerability. Experimental neurology 176:105-116.

Toulmond S, Rothwell NJ (1995) Interleukin-1 receptor antagonist inhibits neuronal damage caused by fluid percussion injury in the rat. Brain research 671:261-266.

Treble A, Hasan KM, Iftikhar A, Stuebing KK, Kramer LA, Cox CS, Jr., Swank PR, Ewing-Cobbs L (2013) Working memory and corpus callosum microstructural

integrity after pediatric traumatic brain injury: a diffusion tensor tractography study. Journal of neurotrauma 30:1609-1619.

Tsuji M, Taguchi A, Ohshima M, Kasahara Y, Ikeda T (2012) Progesterone and allopregnanolone exacerbate hypoxic-ischemic brain injury in immature rats. Experimental neurology 233:214-220.

Tsuji M, Wilson MA, Lange MS, Johnston MV (2004) Minocycline worsens hypoxic-ischemic brain injury in a neonatal mouse model. Experimental neurology 189:58-65.

Tung GA, Kumar M, Richardson RC, Jenny C, Brown WD (2006) Comparison of accidental and nonaccidental traumatic head injury in children on noncontrast computed tomography. Pediatrics 118:626-633.

Turner RC, Naser ZJ, Lucke-Wold BP, Logsdon AF, Vangilder RL, Matsumoto RR, Huber JD, Rosen CL (2017) Single low-dose lipopolysaccharide preconditioning: neuroprotective against axonal injury and modulates glial cells. Neuroimmunology and neuroinflammation 4:6-15.

van Beek EM, Cochrane F, Barclay AN, van den Berg TK (2005) Signal regulatory proteins in the immune system. Journal of immunology 175:7781-7787.

van Groen T, Kadish I, Wyss JM (2002) The role of the laterodorsal nucleus of the thalamus in spatial learning and memory in the rat. Behavioural brain research 136:329-337.

van Rooijen N, van Kesteren-Hendrikx E (2003) "In vivo" depletion of macrophages by liposome-mediated "suicide". Methods in enzymology 373:3-16.

Vann SD, Aggleton JP, Maguire EA (2009) What does the retrosplenial cortex do? Nature reviews Neuroscience 10:792-802.

Varvel NH, Grathwohl SA, Baumann F, Liebig C, Bosch A, Brawek B, Thal DR, Charo IF, Heppner FL, Aguzzi A, Garaschuk O, Ransohoff RM, Jucker M (2012) Microglial repopulation model reveals a robust homeostatic process for replacing CNS myeloid cells. Proceedings of the National Academy of Sciences of the United States of America 109:18150-18155.

Venkatesan C, Chrzaszcz M, Choi N, Wainwright MS (2010) Chronic upregulation of activated microglia immunoreactive for galectin-3/Mac-2 and nerve growth factor following diffuse axonal injury. Journal of neuroinflammation 7:32.

Verger K, Junque C, Levin HS, Jurado MA, Perez-Gomez M, Bartres-Faz D, Barrios M, Alvarez A, Bartumeus F, Mercader JM (2001) Correlation of atrophy measures on MRI with neuropsychological sequelae in children and adolescents with traumatic brain injury. Brain injury 15:211-221.

Vexler ZS, Yenari MA (2009) Does inflammation after stroke affect the developing brain differently than adult brain? Developmental neuroscience 31:378-393.

Vowles GH, Scholtz CL, Cameron JM (1987) Diffuse axonal injury in early infancy. Journal of clinical pathology 40:185-189.

Walf AA, Frye CA (2007) The use of the elevated plus maze as an assay of anxiety-related behavior in rodents. Nature protocols 2:322-328.

Wakamori M, Ikemoto Y, Akaike N (1991) Effects of two volatile anesthetics and a volatile convulsant on the excitatory and inhibitory amino acid responses in dissociated CNS neurons of the rat. Journal of neurophysiology 66:2014-2021.

Wake H, Moorhouse AJ, Jinno S, Kohsaka S, Nabekura J (2009) Resting microglia directly monitor the functional state of synapses in vivo and determine the fate of ischemic terminals. The Journal of neuroscience : the official journal of the Society for Neuroscience 29:3974-3980.

Wakselman S, Bechade C, Roumier A, Bernard D, Triller A, Bessis A (2008) Developmental neuronal death in hippocampus requires the microglial CD11b integrin and DAP12 immunoreceptor. The Journal of neuroscience : the official journal of the Society for Neuroscience 28:8138-8143.

Wang AL, Yu AC, Lau LT, Lee C, Wu le M, Zhu X, Tso MO (2005) Minocycline inhibits LPS-induced retinal microglia activation. Neurochemistry international 47:152-158.

Wang X, Hagberg H, Nie C, Zhu C, Ikeda T, Mallard C (2007) Dual role of intrauterine immune challenge on neonatal and adult brain vulnerability to hypoxia-ischemia. Journal of neuropathology and experimental neurology 66:552-561.

Wang Y, Yue X, Kiesewetter DO, Niu G, Teng G, Chen X (2014) PET imaging of neuroinflammation in a rat traumatic brain injury model with radiolabeled TSPO ligand DPA-714. European journal of nuclear medicine and molecular imaging 41:1440-1449.

Wasserman JK, Schlichter LC (2007) Minocycline protects the blood-brain barrier and reduces edema following intracerebral hemorrhage in the rat. Experimental neurology 207:227-237.

Whalen MJ, Carlos TM, Kochanek PM, Wisniewski SR, Bell MJ, Clark RS, DeKosky ST, Marion DW, Adelson PD (2000) Interleukin-8 is increased in cerebrospinal fluid of children with severe head injury. Critical care medicine 28:929-934.

Wilde EA, Hunter JV, Newsome MR, Scheibel RS, Bigler ED, Johnson JL, Fearing MA, Cleavinger HB, Li X, Swank PR, Pedroza C, Roberson GS, Bachevalier J, Levin HS (2005) Frontal and temporal morphometric findings on MRI in children after moderate to severe traumatic brain injury. Journal of neurotrauma 22:333-344.

Williams DN, Laughlin LW, Lee YH (1974) Minocycline: Possible vestibular side-effects. Lancet 2:744-746.

Woodcock T, Morganti-Kossmann MC (2013) The role of markers of inflammation in traumatic brain injury. Frontiers in neurology 4:18.

Yang S, Liu ZW, Wen L, Qiao HF, Zhou WX, Zhang YX (2005) Interleukin-1beta enhances NMDA receptor-mediated current but inhibits excitatory synaptic transmission. Brain research 1034:172-179.

Yeates KO, Swift E, Taylor HG, Wade SL, Drotar D, Stancin T, Minich N (2004) Short- and long-term social outcomes following pediatric traumatic brain injury. Journal of the International Neuropsychological Society : JINS 10:412-426.

Ylvisaker M, Adelson PD, Braga LW, Burnett SM, Glang A, Feeney T, Moore W, Rumney P, Todis B (2005) Rehabilitation and ongoing support after pediatric TBI: twenty years of progress. The Journal of head trauma rehabilitation 20:95-109.

Ylvisaker M, Todis B, Glang A, Urbanczyk B, Franklin C, DePompei R, Feeney T, Maxwell NM, Pearson S, Tyler JS (2001) Educating students with TBI: themes and recommendations. The Journal of head trauma rehabilitation 16:76-93.

Yoon SY, Patel D, Dougherty PM (2012) Minocycline blocks lipopolysaccharide induced hyperalgesia by suppression of microglia but not astrocytes. Neuroscience 221:214-224.

Yrjanheikki J, Tikka T, Keinanen R, Goldsteins G, Chan PH, Koistinaho J (1999) A tetracycline derivative, minocycline, reduces inflammation and protects against focal cerebral ischemia with a wide therapeutic window. Proceedings of the National Academy of Sciences of the United States of America 96:13496-13500.

Yuan W, Holland SK, Schmithorst VJ, Walz NC, Cecil KM, Jones BV, Karunanayaka P, Michaud L, Wade SL (2007) Diffusion tensor MR imaging reveals persistent white matter alteration after traumatic brain injury experienced during early childhood. AJNR American journal of neuroradiology 28:1919-1925.

Zhang Z, Saraswati M, Koehler RC, Robertson C, Kannan S (2015) A New Rabbit Model of Pediatric Traumatic Brain Injury. Journal of neurotrauma 32:1369-1379.

APPENDIX 1:

Differential effects of minocycline on microglial activation and neurodegeneration following closed head injury in the neonate rat

Hanlon L.A., Raghupathi R., Huh J.W. (2016)

Experimental Neurology 290:1-14.

The following is work that, in conjunction with a portion of the data from chapter 4, was published by Experimental Neurology in 2016 (Print in 2017).

This work explores the effect of a prolonged minocycline dosing paradigm (9 days) on sustained microglial/macrophage activation, neurodegeneration, axonal degeneration, and spatial learning and memory deficits.

A1.1 ABSTRACT

Microglial/macrophage activation can be a chronic phenomenon that may require prolonged treatment. The antibiotic minocycline has been effective in decreasing microglial/macrophage activation and ameliorating neuronal damage, but some of these studies indicate that the effects of minocycline are transient. The half-life of the drug in rodents (2-3 hours) is much shorter than the half-life in humans (Up to 16 hours). To test whether extended dosing of minocycline may be necessary to reduce ongoing pathologic alterations, a group of animals received minocycline for 9 days. Immediately following termination of treatment, microglial/macrophage reactivity and neurodegeneration in all regions examined were exacerbated in minocycline-treated brain-injured animals compared to brain-injured animals that received vehicle ($p<0.001$), an effect that was only sustained in the cortex and hippocampus up to 15 days post-injury ($p<0.001$). Whereas injury-induced spatial learning deficits remained unaffected by minocycline treatment, memory deficits appeared to be significantly worse ($p<0.05$). These results indicate that supressing the microglial/macrophage response following injury to the developing brain may be detrimental to long-term pathological alterations and cogntive function.

A1.2 INTRODUCTION

The acute response to injury in the developing brain includes a robust neuroinflammatory cascade evident by the presence of pro- and anti-inflammatory mediators in the cerebrospinal fluid of brain-injured children (Amick et al., 2001, Buttram et al., 2007, Berger et al., 2009). Additionally, increased levels of quinolinic acid (a marker of microglial/macrophage activation) were also discovered in the CSF of brain-injured children indicating a role for microglia/macrophages in perpetuating this immune response (Berger et al., 2004). Work in pre-clinical animal models of pediatric TBI suggest that microglial/macrophage activation is a sustained phenomenon that lasts well into the chronic post-injury period and may be associated with long-term functional impairment. Microglial activation was evident out to 3 weeks post-injury in the cortex and subcortical white matter of brain-injured neonatal rabbits and these animals also demonstrated cognitive impairments in novel object recognition memory (Zhang et al., 2015). Minocycline is an antibiotic that has anti-inflammatory properties and has been shown to decrease microglial/macrophage activation (Garrido-Mesa et al., 2013). While minocycline treatment has resulted in lasting neuroprotective and beneficial effects following brain injury (Homsi et al., 2010, Siopi et al., 2012), there is also some evidence that suggests that the effects of minocycline are transient (Bye et al., 2007, Chhor et al., 2016, Hanlon et al., 2016). Minocycline treatment reduced microglial activation, cell death, and injury severity at 1 day post-injury in brain-injured neonatal mice, but this effect was lost by 5 days post-injury (Chhor et al., 2016). In a model of repetitive brain injury in the neonatal rat, minocycline administration only decreased microglial/macrophage activation in the white matter at 3 days post-injury- an effect that

was not replicated in other brain regions, had no effect on injury-induced degeneration, and was not sustained out to 7 days (Hanlon et al., 2016). We've also demonstrated that minocycline administration following a single injury to the immature brain only decreased microglial/macrophage activation the day after ending the treatment (3 days post-injury) and that this had no effect on spatial learning and memory impairment (See Chapter 4). With these results and the knowledge that minocycline has an extremely short half-life in rodents (Andes and Craig, 2002), we hypothesized that an extended minocycline dosing paradigm may be necessary to produce prolonged neuroprotection and ameliorate cognitive impairment after injury to the developing brain.

A1.3 MATERIALS AND METHODS

A1.3.1 Brain Injuries and Minocycline Administration

Brain injuries were conducted as described in Chapter 3. Immediately after injury, animals were randomly assigned to receive intraperitoneal injections of either minocycline (45mg/Kg) or PBS vehicle (0.2mL/Kg); following a second injection of minocycline or vehicle 12 hours later, animals received once daily intraperitoneal injections of minocycline or vehicle (45mg/Kg/injection or 0.2mL/Kg/injection) for 9 days for a total of 11 injections. Sham-injured animals were also randomly assigned to receive either vehicle or minocycline. Similar extended dosing paradigms have been successful in reducing microglial activation in the chronic post-injury period following HI in neonate rats (Carty et al., 2008, Wixey et al., 2011), diffuse TBI in the adult mouse (Ng et al., 2012) and contusive TBI in the adult rat (Lam et al., 2013).

A1.3.2 Histology, Immunohistochemistry, and Quantification

Tissue processing and immunohistochemistry were conducted according to the procedures outlined in Chapter 3.3.4 with the exception that activated microglia/macrophages were only evaluated using Iba1 and not CD68/ED-1. Additionally, astrocytic reactivity (GFAP) and axonal injury (APP) were not evaluated in this study. Quantification was conducted as previously described (Chapter 3.3.4). Briefly, total and activated Iba1(+) microglia/macrophages were counted in 20x HPF images in the cortex, subiculum, and thalamus. Quantification of Iba1 immunoreactivity in the white matter was conducted by a thresholded area analysis as previously described

(Hanlon et al., 2016). FJB(+) profiles were counted in 20x HPF images in the cortex, white matter, subiculum, and thalamus. Areas of the cortex and white matter were measured using manual tracing of 1x (cortex) or 4x (white matter) images in the program Image J.

A1.3.3 Spatial learning and Memory

Animals were assessed using a Morris water maze spatial learning paradigm on post-injury days 10-13 and subjected to 2 probe retention trials and a visible platform trial to assess potential vision deficits on post-injury day 14. See Chapter 3.3.8 for full procedure.

A1.4 RESULTS

A1.4.1 Effect of minocycline in the cortex and white matter tracts

At 10 and 15 days post-injury, brain-injured animals demonstrated evidence of microglial/macrophage activation and FJB reactivity in the same areas of the cortex and white matter tracts (Fig. A1.1) as those observed at 3 and 7 days post-injury. In sham-injured animals, resting Iba1 (+) microglia/macrophages with elongated cell bodies and long processes predominated (Fig. A1.1A inset), whereas Iba1(+) microglia/macrophages in brain-injured animals, were amoeboid in appearance (Fig. A1.1B inset). The effects of extending minocycline administration to 9 days following brain injury (study 2) on microglial/macrophage reactivity and neurodegeneration were different from the effects of the short duration treatment paradigm used in study 1. In the cortex, a 3-way ANOVA revealed an interaction effect only between group and time ($F_{2,23}$=32.13, $p<0.001$; Fig. A1.1A), and not between group, time and sex ($F_{2,23}$=0.05, $p=0.96$); post-hoc analysis indicated that at 10 days post-injury, minocycline-treated, brain-injured animals had significantly fewer microglia/macrophages compared to vehicle-treated brain-injured animals ($p<0.01$; Fig. A1.1A). In contrast, at the 15-day time point, the number of Iba1(+) cells in the minocycline group was significantly greater than that in the vehicle group ($p<0.001$; Fig. A1.1A). Analysis of the proportion of activated microglia/macrophages also demonstrated an interaction effect between group and time ($F_{2,23}$=10.11, $p<0.001$) with minocycline-treated, brain-injured animals exhibiting a significantly greater proportion compared to their counterparts that received vehicle at both 10 ($p<0.001$; Fig. A1.1B) and 15 days ($p<0.001$, Fig. A1.1B). Again, sex of the

animal had no interaction effect with group or time ($F_{2,23}$=0.15, p=0.87). Minocycline-treated, brain-injured animals contained significantly more FJB(+) profiles compared to brain-injured animals that received vehicle ($F_{1,15}$=76.78, p<0.001; Fig. A1.1C). There was an interaction effect between group, sex and time ($F_{1,15}$=10.29, p<0.01) that indicated that at 10 days post-injury, male minocycline-treated, brain-injured animals had significantly more FJB(+) profiles in the cortex compared to male brain-injured animals that received the vehicle (p<0.001; Fig. A1.1C). FJB reactivity was greater in the cortex of brain-injured females that received the vehicle compared to their male counterparts at 10 days (p<0.01), but female brain-injured minocycline-treated animals had significantly fewer FJB(+) profiles in the cortex compared to their male counterparts at 10 days (p<0.05). Female brain-injured animals demonstrated similar FJB reactivity irrespective of treatment at 10 days post-injury (p=0.24). At 15 days, however, both male and female brain-injured minocycline-treated animals had significantly more FJB(+) profiles than their brain-injured counterparts that received the vehicle (p<0.05).

In the white matter tracts below the site of impact, area analysis of Iba1 labeling revealed an interaction effect between group and time ($F_{2,23}$=71.6, p<0.001) with a post-hoc analysis indicating that minocycline-treated, brain-injured animals had significantly greater labeled area at 10 days post-injury (p<0.001), but not at 15 days (p=0.30), than brain-injured animals that received vehicle (Fig. A1.1D). There was an interaction effect between sex and condition that indicated that male brain-injured animals that received the vehicle had significantly decreased labeled white matter area compared to female brain-injured animals that received the vehicle (p<0.001) while brain-injured minocycline-treated males had significantly increased labeled white matter area compared to brain-

injured minocycline-treated females ($p<0.01$). Furthermore, both brain-injured minocycline-treated males and females demonstrated increased white matter area compared to their counterparts that received the vehicle (males, $p<0.001$; females, $p<0.01$). Minocycline-treated, brain-injured animals had significantly more FJB+ profiles at 10 days ($p<0.001$), but not at 15 days ($p=0.91$) post-injury, than their counterparts that received vehicle (Fig. A1.1E) and this was not affected by the sex of the animals.

Compared to sham-injured animals (Fig. A1.1F), brain-injured animals exhibited a substantially enlarged lateral ventricle in the hemisphere ipsilateral to the impact site at 10 (Fig. A1.1G and A1.1H) and 15 days post-injury (not shown). Moreover, both the cortex and the underlying white matter tracts were visibly thinner in the brain-injured animals. Quantitative analysis of the area of the cortex revealed an interaction effect between group and time post-injury ($F_{2,22}=4.70$, $p<0.05$; Fig. A1.1I); post-hoc analysis indicated that at 10 days post-injury both brain-injured groups exhibited smaller cortical areas compared to the sham-injured group ($p<0.01$). Importantly, the area of the cortex in the brain-injured group that was treated with minocycline was significantly less than that in brain-injured animals that received vehicle ($p<0.001$; Fig. A1.1I). At 15 days post-injury, the cortical areas in both brain-injured groups were significantly less than in sham-injured animals ($p<0.001$; Fig. A1.1I) but the minocycline-treated group was not different from the group that received vehicle ($p=0.31$). An interaction effect between group, sex, and time was observed ($F_{2,22}=3.42$, $p=0.05$) that indicated that sham-injured males had significantly increased cortical area compared to sham-injured females ($p<0.05$) at 15 days post-injury. In sham-injured animals and in the hemisphere contralateral to the impact site in brain-injured animals, robust myelin labeling in the

corpus callosum and lateral white matter was observed (Figures A1.1F-H). In brain-injured animals the white matter atrophy that was observed at both 3 and 7 days post-injury (vide supra) persisted to the 10 and 15 day time points. Quantitative analyses revealed an interaction effect between group and time ($F_{2,23}$=57.23, $p<0.001$; Fig. A1.1J) and the post-hoc analysis indicated that brain-injured animals exhibited a significantly smaller area compared to sham-injured animals at both 10 and 15 days post-injury ($p<0.001$); importantly, minocycline-treated brain-injured animals had significantly smaller white matter areas than the brain-injured animals that received the vehicle at 10 days post-injury ($p<0.05$), but not at 15 days post-injury ($p=0.93$; Fig. A1.1J). An interaction effect between group, sex and time ($F_{2,23}$=5.19, $p<0.05$) indicated that sham-injured males had significantly greater white matter areas than sham-injured females ($p<0.001$) at 15 days post-injury.

A1.4.2 Effect of minocycline in the hippocampus and thalamus

At 10 and 15 days post-injury, brain-injured animals demonstrated increased numbers of microglia/macrophages and FJB reactivity in the hippocampus and thalamus compared to their sham-injured counterparts (Fig. A1.2). In the hippocampus, these alterations continued to be restricted to the dorsal aspect of the subiculum wherein a 3-way ANOVA revealed an interaction effect between group and time ($F_{2,23}$=23.01, $p<0.001$; Fig. A1.2A), but no effect of sex ($F_{2,23}$=0.01, $p=0.99$); post-hoc analysis indicated that at 10 days post-injury, minocycline-treated, brain-injured animals had significantly fewer microglia/macrophages compared to their counterparts that received vehicle ($p=0.05$; Fig. A1.2A). At 15 days post-injury, however, minocycline-treated

brain-injured animals had significantly more microglia/macrophages than brain-injured animals that received vehicle ($p<0.001$). The proportion of activated microglia/macrophages in the subiculum also demonstrated an interaction effect between group and time ($F_{2,23}=3.93$, $p<0.05$; Fig. A1.2B) with no effect of sex ($F_{2,23}=2.59$, $p=0.10$). There was, however, an increase in the proportion of activated microglia/macrophages in minocycline-treated, brain-injured animals compared to those that received vehicle animals at both times post-injury ($p<0.001$; Fig. A1.2B). Minocycline-treated animals also contained greater numbers of FJB(+) profiles at both time points post-injury compared to brain-injured animals that received vehicle ($F_{1,15}=18.15$, $p<0.001$; Fig. A1.2C). Similarly, there was no effect of sex with regards to FJB in the subiculum ($F_{1,15}=0.57$, $p=0.46$).

In the thalamus, the regional distribution of activated microglia/macrophages and FJB reactive profiles at 10 and 15 days post-injury was similar to that observed at 3 and 7 days post-injury (not shown). Analysis of the number of microglia/macrophages revealed an interaction effect between group and time ($F_{2,23}=16.26$, $p<0.001$; Fig. A1.2D) with the post-hoc test indicating that brain-injured animals had significantly more microglia/macrophages compared to sham-injured animals at 10 days post-injury ($p<0.001$), but not at 15 days post-injury (vehicle group, $p=0.48$; minocycline group, $p=0.59$). Sex did not influence the interaction between group and time ($F_{2,23}=1.05$, $p=0.37$). When the population of activated microglia/macrophages was analyzed, an interaction effect between group and time ($F_{2,23}=53.46$, $p<0.001$; Fig. A1.2E) was observed with a subsequent post-hoc analysis revealing that at 10 days post-injury, minocycline-treated, brain-injured animals had a higher percentage of activated cells

compared to brain-injured animals that received vehicle ($p<0.001$), and that this effect was lost at 15 days post-injury ($p=0.39$); there was no effect of sex ($F_{2,23}=2.50$, $p=0.10$). Minocycline-treated, brain-injured animals exhibited significantly more FJB+ profiles in the thalamus at 10 days post-injury ($p<0.001$), but not at 15 days post-injury ($p=0.88$), compared to brain-injured animals that received vehicle (Fig. A1.2F) and this was unaffected by sex ($F_{1,15}=0.79$, $p=0.39$).

A1.4.3 Effect of minocycline on spatial learning and memory

As observed in study 1, brain-injured animals in study 2 were also impaired in their ability to learn and remember the location of the submerged platform (Fig. A1.3). Analysis of spatial learning patterns illustrated in Figure A1.3A revealed main effects of group ($F_{2,105}=9.16$, $p<0.001$) and training day ($F_{3,105}=44.72$, $p<0.001$), but no interaction ($F_{6,105}=1.41$, $p=0.22$; Fig. A1.3A). Post-hoc analysis demonstrated that brain-injured animals took significantly longer to locate the hidden platform compared to sham-injured animals ($p<0.01$), and that there was no difference in latencies between the two brain-injured groups ($p=0.65$) indicating that prolonged minocycline treatment had no effect on injury-induced spatial learning deficits; there was no influence of sex of the animal on these observations ($F_{6,105}=0.62$, $p=0.71$). A 2-way ANOVA for the time spent in the platform zones revealed a main effect of group ($F_{2,35}=7.33$, $p<0.01$) and an interaction effect between group and sex ($F_{2,35}=3.31$, $p<0.05$). Post-hoc analysis indicated that sham-injured animals spent more time in the platform zones than brain-injured animals treated with minocycline ($p<0.01$), but not with vehicle ($p=0.18$); however, brain-injured minocycline-treated animals spent significantly less time in the platform

zone than their counterparts that received vehicle ($p<0.05$). Male sham-injured animals spent more time in the platform zone than their minocycline-treated, brain-injured counterparts ($p=0.10$), but this was not different from either brain-injured counterparts that received vehicle ($p=0.10$) or female sham-injured animals ($p>0.05$). Similarly, analysis of the time spent in the peripheral zone revealed a main effect of group ($F_{2,35}=6.24$, $p<0.01$) and an interaction effect between group and sex ($F_{2,35}=4.15$, $p<0.05$). Post-hoc analyses indicated that sham-injured animals spent significantly less time in the peripheral zone compared to brain-injured animals treated with minocycline ($p<0.01$), but not brain-injured animals that received vehicle ($p=0.15$; Fig. A1.3B); importantly, minocycline-treated brain-injured animals spent more time in the peripheral zones compared to their counterparts that received the vehicle ($p=0.05$). Male sham-injured animals spent less time in the peripheral zone compared to males from both brain-injured groups (vehicle, $p<0.05$; minocycline, $p<0.01$) and female sham-injured animals ($p<0.05$). There was no group or sex effect in the visible platform trial, indicating that observed spatial learning deficits in brain-injured animals were not due to a problem in visual function ($F_{2,35}=0.08$,$p=0.92$; Fig. A1.3B). Additionally, deficits in learning and retention were not due to deficits in motor function as indicated by a lack of differences between groups or sexes in swim speed (sham-injured: 26 ± 0.43 cm/s; brain-injured vehicle: 24 ± 0.81 cm/s; brain-injured minocycline: 24 ± 0.82 cm/s; $F_{2,35}=1.52$, $p=0.23$).

A1.5 DISCUSSION

Because sustained benefits with the short-term administration of minocycline were not observed (Chapter 4), the dosing was extended into the second week post-injury and terminated immediately prior to behavioral analyses. Dosing minocycline for 6 days decreased microglial/macrophage activation while simultaneously reducing the extent of HI-induced oligodendrocyte cell death and myelin loss (Carty et al., 2008, Wixey et al., 2011) and neurodegeneration (Leonardo et al., 2008). In contrast, a 7- or 14-day dosing paradigm that was effective in decreasing the number of activated microglia/macrophages did not affect brain trauma-induced neurogenesis at 2 or 6 weeks post-injury (Ng et al., 2012). In a model of adult TBI, daily administration of minocycline for 7, 12 or 16 days reduced microglial/macrophage activation and reversed spatial learning and memory deficits at 8 weeks post-injury but did not attenuate lesion volume (Lam et al., 2013). In the current study, extended minocycline administration resulted in an increase in the number of activated microglia/macrophages in the multiple brain regions which was accompanied by an increase in the number of FJB(+) profiles. This observation is consistent with that in a mouse model of visual cortex ablation in which minocycline administration to injured metallothionein-deficient immature brain increased the number of activated microglia/macrophages while simultaneously increasing the extent of neuronal loss which was associated with a minocycline-induced upregulation of pro-apoptotic genes (Potter et al., 2009). Moreover, the modest exacerbation of spatial memory deficits observed in the minocycline-treated animals may be related to increased neurodegeneration in the subiculum of the hippocampus, an area that has been implicated in spatial learning and memory function (O'Mara, 2005, O'Mara et al., 2009). In addition,

the increased numbers of activated microglia/macrophages may have led to pathologic increases in pro-inflammatory cytokines such as IL-1β which can inhibit both long-term potentiation and worsen acquisition and retention of a spatial memory task (Ross et al., 2003, Trofimov et al., 2012).

A major limitation to the current set of experiments, and in all of our work with minocycline, is that we've only used one dose- 45mg/kg. This dose has shown efficacy in several models of brain injury (Buller et al., 2009, Hanlon et al., 2016), but it is possible that it is not an appropriate dose for extended use. Neonatal mice that received a lower daily dose (22.5 mg/kg) of minocycline for 6 days showed improvement in white matter pathology following hypoxia-ischemia (Carty et al., 2008), raising the possibility the 45 mg/kg dose for 9 days may be too high. Irrespective of potential dosing confounds, the results of the present study suggest that the use of minocycline and suppression of the acute microglial/macrophage response following injury to the immature brain may not be viable therapeutic strategies.

A1.6 FIGURE LEGENDS

Figure A1.1 Effect of extended minocycline administration in the cortex and subcortical white matter tracts.

Graphs illustrate counts of Iba1(+) cells (A), the proportion of activated Iba1(+) cells (B), and counts of FJB(+) profiles (C) in the cortex, area of Iba1 immunoreactivity (D), and the number of FJB(+) profiles (E) in the subcortical white matter. Inset images in panels A and B are representative of Iba1 (+) cells from sham-injured and brain-injured animals, respectively. Representative photomicrographs of Nissl-myelin stained sections from sham-injured (F), brain-injured injected with vehicle (G), and brain-injured, minocycline-treated animals (H) at 10 days post-injury. Graphs illustrate the area of the cortex (I) and the underlying white matter (J). The sex of the animals affected the values for FJB profile counts (C) but did not affect the quantification in other outcomes and areas. *, $p \leq 0.05$ compared to sham-injured values; #, $p \leq 0.05$ compared to brain-injured animals receiving vehicle; @, $p \leq 0.05$ compared to corresponding males. HPF, high power field. Scale bar for insets in panels A and B in panel A=10μm; scale bar for panels F-H in panel H=500μm.

Figure A1.2 Effect of extended minocycline administration in the hippocampus and thalamus.

Graphs illustrate counts of Iba1(+) (A, D), the proportion of activated Iba1(+) cells (B,E), and counts of FJB(+) profiles (C,F) in the hippocampus (A-C) and the thalamus (D-F). Sex had no influence on outcomes so values for male and female rats

were combined for graphical representation. *, $p \leq 0.05$ compared to sham-injured values; #,$p \leq 0.05$ compared to brain-injured animals injected with vehicle. HPF, high power field.

Figure A1.3 Effect of extended minocycline administration on injury-induced spatial learning and memory deficits.

(A) Latency to the platform on each day represents the average of 4 trials. (B) Average times spent in the area surrounding the platform location and the periphery of the maze during the spatial retention (probe) trial. Also included is the time to the visible platform. Sex had no effect on spatial learning and memory outcomes so values for male and female rats were combined for graphical representation. *, $p \leq 0.05$ compared to sham-injured animals; #, $p \leq 0.05$ compared to brain-injured animals injected with vehicle.

A1.7 FIGURES

Figure A1.1 Effect of extended minocycline administration in the cortex and subcortical white matter tracts.

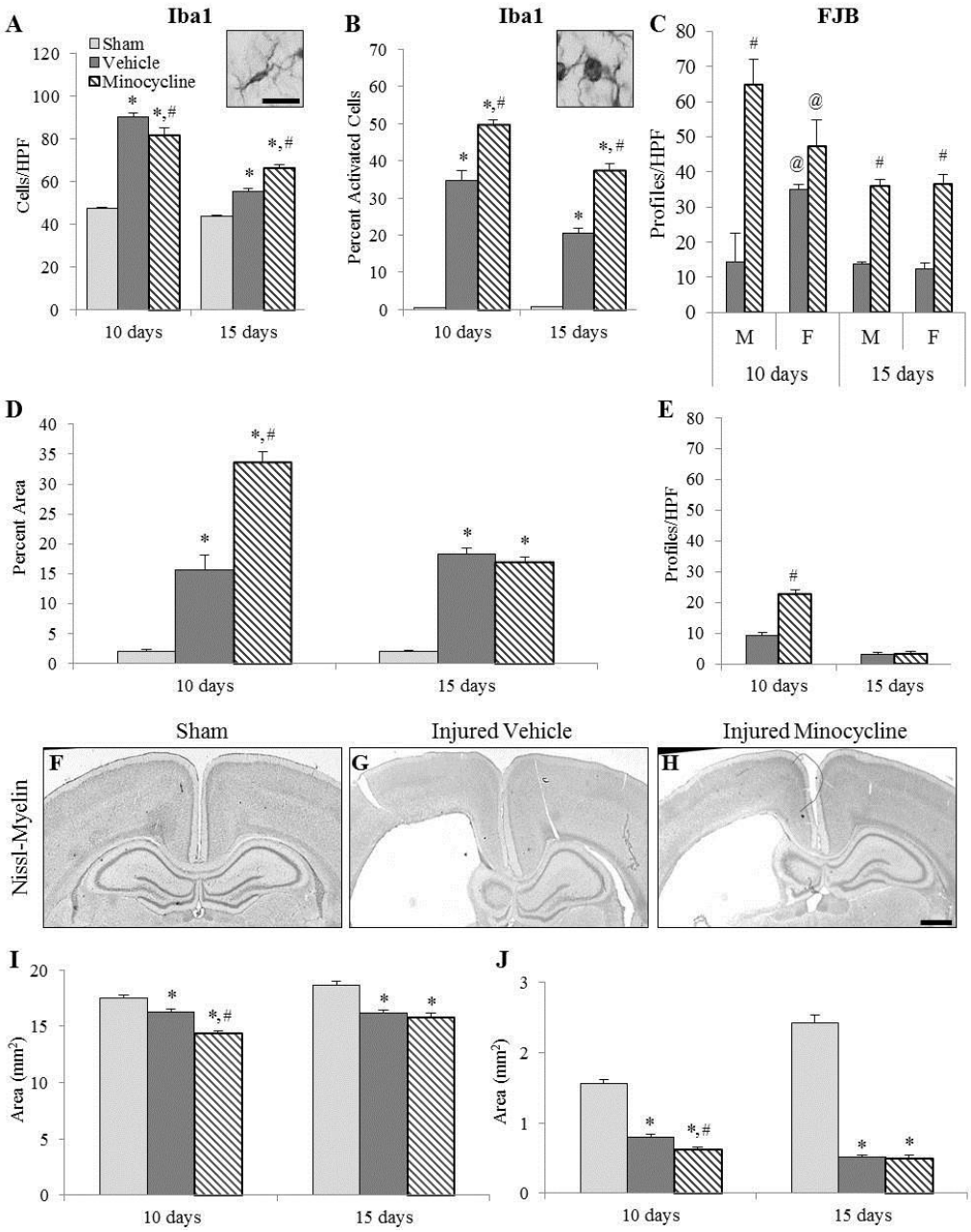

Figure A1.2 Effect of extended minocycline administration in the hippocampus and thalamus.

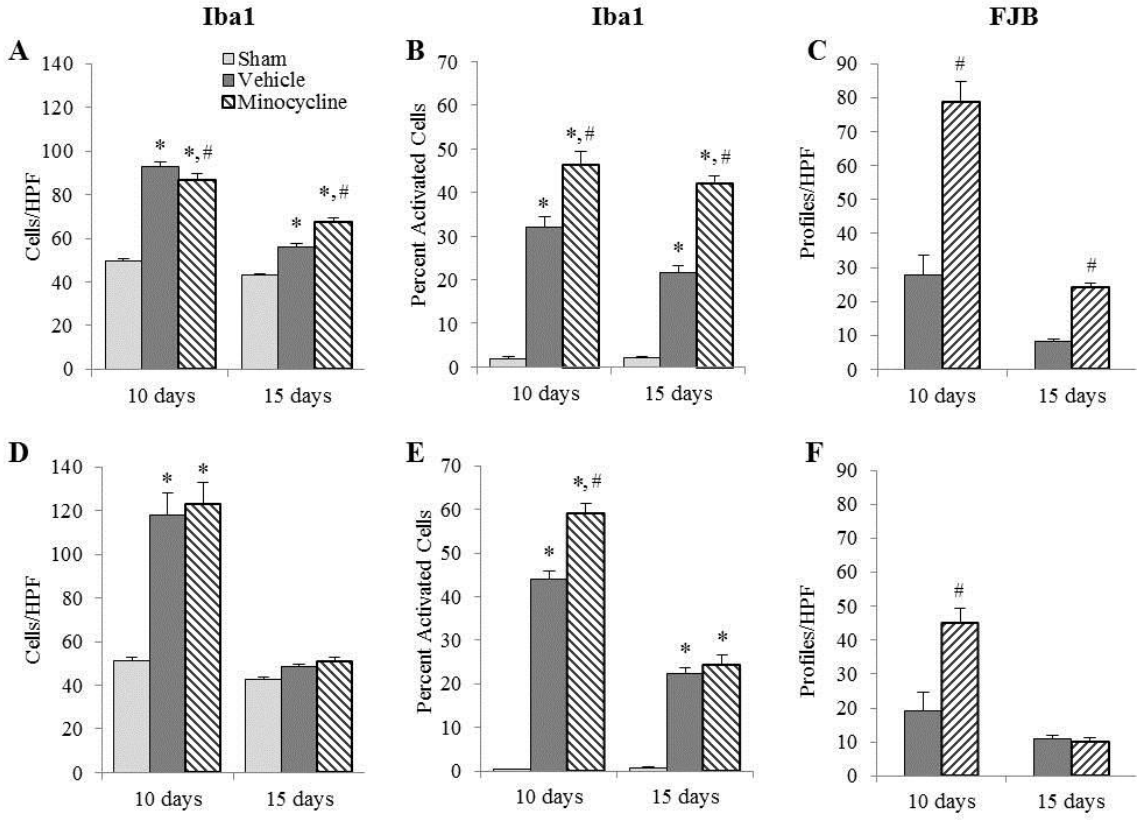

Figure A1.3 Effect of extended minocycline administration on injury-induced spatial learning and memory deficits.

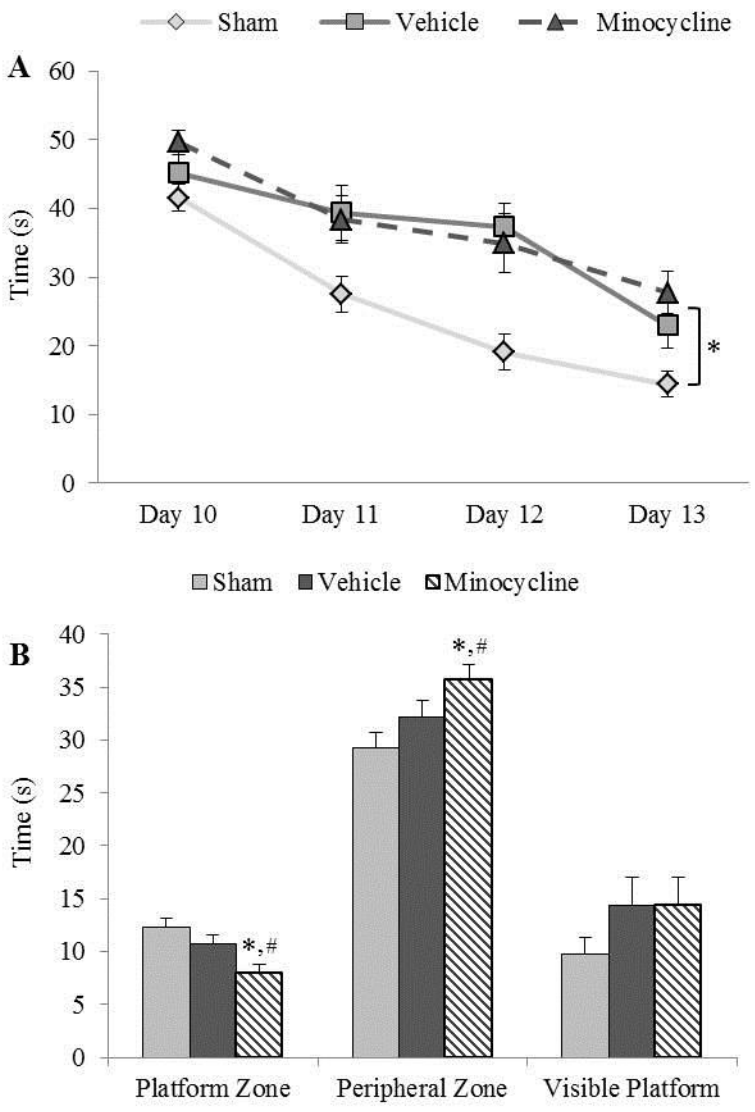

A1.8 REFERENCES

Amick JE, Yandora KA, Bell MJ, Wisniewski SR, Adelson PD, Carcillo JA, Janesko KL, DeKosky ST, Carlos TM, Clark RS, Kochanek PM (2001) The Th1 versus Th2 cytokine profile in cerebrospinal fluid after severe traumatic brain injury in infants and children. Pediatric critical care medicine : a journal of the Society of Critical Care Medicine and the World Federation of Pediatric Intensive and Critical Care Societies 2:260-264.

Andes D, Craig WA (2002) Animal model pharmacokinetics and pharmacodynamics: a critical review. International journal of antimicrobial agents 19:261-268.

Berger RP, Heyes MP, Wisniewski SR, Adelson PD, Thomas N, Kochanek PM (2004) Assessment of the macrophage marker quinolinic acid in cerebrospinal fluid after pediatric traumatic brain injury: insight into the timing and severity of injury in child abuse. Journal of neurotrauma 21:1123-1130.

Berger RP, Ta'asan S, Rand A, Lokshin A, Kochanek P (2009) Multiplex assessment of serum biomarker concentrations in well-appearing children with inflicted traumatic brain injury. Pediatric research 65:97-102.

Buller KM, Carty ML, Reinebrant HE, Wixey JA (2009) Minocycline: a neuroprotective agent for hypoxic-ischemic brain injury in the neonate? Journal of neuroscience research 87:599-608.

Buttram SD, Wisniewski SR, Jackson EK, Adelson PD, Feldman K, Bayir H, Berger RP, Clark RS, Kochanek PM (2007) Multiplex assessment of cytokine and chemokine levels in cerebrospinal fluid following severe pediatric traumatic brain injury: effects of moderate hypothermia. Journal of neurotrauma 24:1707-1717.

Bye N, Habgood MD, Callaway JK, Malakooti N, Potter A, Kossmann T, Morganti-Kossmann MC (2007) Transient neuroprotection by minocycline following traumatic brain injury is associated with attenuated microglial activation but no changes in cell apoptosis or neutrophil infiltration. Experimental neurology 204:220-233.

Carty ML, Wixey JA, Colditz PB, Buller KM (2008) Post-insult minocycline treatment attenuates hypoxia-ischemia-induced neuroinflammation and white matter injury in the neonatal rat: a comparison of two different dose regimens. International journal of developmental neuroscience : the official journal of the International Society for Developmental Neuroscience 26:477-485.

Chhor V, Moretti R, Le Charpentier T, Sigaut S, Lebon S, Schwendimann L, Ore MV, Zuiani C, Milan V, Josserand J, Vontell R, Pansiot J, Degos V, Ikonomidou C, Titomanlio L, Hagberg H, Gressens P, Fleiss B (2016) Role of microglia in a mouse model of paediatric traumatic brain injury. Brain, behavior, and immunity.

Garrido-Mesa N, Zarzuelo A, Galvez J (2013) Minocycline: far beyond an antibiotic. British journal of pharmacology 169:337-352.

Hanlon LA, Huh JW, Raghupathi R (2016) Minocycline Transiently Reduces Microglia/Macrophage Activation but Exacerbates Cognitive Deficits Following Repetitive Traumatic Brain Injury in the Neonatal Rat. Journal of neuropathology and experimental neurology 75:214-226.

Homsi S, Piaggio T, Croci N, Noble F, Plotkine M, Marchand-Leroux C, Jafarian-Tehrani M (2010) Blockade of acute microglial activation by minocycline promotes neuroprotection and reduces locomotor hyperactivity after closed head

injury in mice: a twelve-week follow-up study. Journal of neurotrauma 27:911-921.

Lam TI, Bingham D, Chang TJ, Lee CC, Shi J, Wang D, Massa S, Swanson RA, Liu J (2013) Beneficial effects of minocycline and botulinum toxin-induced constraint physical therapy following experimental traumatic brain injury. Neurorehabilitation and neural repair 27:889-899.

Leonardo CC, Eakin AK, Ajmo JM, Collier LA, Pennypacker KR, Strongin AY, Gottschall PE (2008) Delayed administration of a matrix metalloproteinase inhibitor limits progressive brain injury after hypoxia-ischemia in the neonatal rat. Journal of neuroinflammation 5:34.

Ng SY, Semple BD, Morganti-Kossmann MC, Bye N (2012) Attenuation of microglial activation with minocycline is not associated with changes in neurogenesis after focal traumatic brain injury in adult mice. Journal of neurotrauma 29:1410-1425.

O'Mara S (2005) The subiculum: what it does, what it might do, and what neuroanatomy has yet to tell us. Journal of anatomy 207:271-282.

O'Mara SM, Sanchez-Vives MV, Brotons-Mas JR, O'Hare E (2009) Roles for the subiculum in spatial information processing, memory, motivation and the temporal control of behaviour. Progress in neuro-psychopharmacology & biological psychiatry 33:782-790.

Potter EG, Cheng Y, Natale JE (2009) Deleterious effects of minocycline after in vivo target deprivation of thalamocortical neurons in the immature, metallothionein-deficient mouse brain. Journal of neuroscience research 87:1356-1368.

Ross FM, Allan SM, Rothwell NJ, Verkhratsky A (2003) A dual role for interleukin-1 in LTP in mouse hippocampal slices. Journal of neuroimmunology 144:61-67.

Siopi E, Llufriu-Daben G, Fanucchi F, Plotkine M, Marchand-Leroux C, Jafarian-Tehrani M (2012) Evaluation of late cognitive impairment and anxiety states following traumatic brain injury in mice: the effect of minocycline. Neuroscience letters 511:110-115.

Trofimov AN, Zubareva OE, Simbirtsev AS, Klimenko VM (2012) [The influence of neonatal interleukin-1beta increase on the formation of adult rats' spatial memory]. Rossiiskii fiziologicheskii zhurnal imeni IM Sechenova / Rossiiskaia akademiia nauk 98:782-792.

Wixey JA, Reinebrant HE, Spencer SJ, Buller KM (2011) Efficacy of post-insult minocycline administration to alter long-term hypoxia-ischemia-induced damage to the serotonergic system in the immature rat brain. Neuroscience 182:184-192.

Zhang Z, Saraswati M, Koehler RC, Robertson C, Kannan S (2015) A New Rabbit Model of Pediatric Traumatic Brain Injury. Journal of neurotrauma 32:1369-1379.

APPENDIX 2:

Minocycline transiently reduces microglia/macrophage activation but exacerbates cognitive deficits following repetitive traumatic brain injury in the neonate rat

Hanlon, L.A., Huh, J.W., and Raghupathi, R. (2016)

Journal of neuropathology and experimental neurology 75:214-226.

The following work was conducted as my original rotation project in the Raghupathi lab and describes microglial/macrophage activaiton and the effects of minocycline in a neonatal rat model of repetitive traumatic brain injury. This was published in 2016 in the Journal of Neuropathology and Experimental Neurology.

A2.1 ABSTRACT

Elevated microglial/macrophage-associated biomarkers in the cerebrospinal fluid of infant victims of abusive head trauma (AHT) suggest that these cells play a role in the pathophysiology of the injury. In this model of AHT in the 11-day-old rat, three impacts (24 hours apart) resulted in microglial/macrophage reactivity, traumatic axonal injury, neuronal degeneration, cortical and white matter atrophy, and spatial learning and memory deficits. In models of neonatal hypoxic ischemia, the antibiotic minocycline has been effective in decreasing injury-induced microglial/macrophage activation while simultaneously attenuating cellular and functional deficits, but the potential for this compound to rescue deficits after impact-based trauma to the immature brain remains unexplored. Acute minocycline administration in this model of AHT decreased microglial/macrophage reactivity in the corpus callosum of brain-injured animals at 3 days post-injury, but this effect was lost by 7 days post-injury. Additionally, minocycline treatment had no effect on traumatic axonal injury, neurodegeneration, tissue atrophy, or spatial learning deficits. Interestingly, minocycline-treated animals demonstrated exacerbated injury-induced spatial memory deficits. Our results contradict previous findings in other models of brain injury and suggest that minocycline is ineffective in reducing microglial/macrophage activation and ameliorating injury-induced deficits following repetitive neonatal traumatic brain injury.

A2.2 INTRODUCTION

Inflicted injury or abuse is one of the leading causes of traumatic brain injury (TBI) in infants under 1 year of age (Bishop, 2006). The annual incidence for abusive head trauma (AHT) in this age group is estimated to be in the range of 20-30 cases per every 100,000 patients (SE Parks, 2012) and survivors of early childhood TBI often develop cognitive and behavioral deficits well into adulthood (Bonnier et al., 1995, Duhaime et al., 1996, Barlow et al., 2005, Ewing-Cobbs et al., 2006). Whereas subdural hemorrhages are particularly indicative of AHT (Reece and Sege, 2000, Myhre et al., 2007, Matschke et al., 2009), subarachnoid hemorrhage, epidural hematomas, edema, and contusions are also prevalent in injured infant brains (Dias et al., 1998). Importantly, the presence of chronic subdural hematomas, cerebral atrophy, and *ex vacuo* ventriculomegaly suggests that these children are incurring multiple TBIs as a result of repeated instances of abuse (Dias et al., 1998, Jenny et al., 1999, Ewing-Cobbs et al., 2000).

The initial models of abusive head trauma utilized unrestrained shaking or rapid rotations of the head (Smith et al., 1998, Bonnier et al., 2002, Raghupathi et al., 2004, Friess et al., 2009, Finnie et al., 2012). Repetitive shaking in lambs and neonate rodents resulted in axonal injury, glial reactivity, retinal tearing, and hemorrhage (Smith et al., 1998, Bonnier et al., 2002, Finnie et al., 2012). In piglets, two rotational injuries exacerbated traumatic axonal injury and resulted in cognitive deficits (Raghupathi et al., 2004, Friess et al., 2009). With the recognition of impact as an important component of AHT (Christian et al., 2009), impact-based models of pediatric have been developed. In 11-day-old rat pups, 2 impacts to the intact skull exacerbated traumatic axonal injury, and

astrogliosis compared to a single impact, whereas 3 impacts accelerated traumatic axonal injury and resulted in *ex vacuo* ventriculomegaly (Huh et al., 2007).In the juvenile rat (35-days-old), two impacts exacerbated axonal injury, astrocytic reactivity, and cognitive deficits (Prins et al., 2010). Collectively, these data underscore the importance of the utility of multiple animal models of AHT.

A number of studies have evaluated biomarkers in the cerebrospinal fluid of infants and children subjected to inflicted or accidental TBI (Papa et al., 2013). Compared to accidental TBI, victims of AHT have increased levels of macrophage/microglial-associated proteins and neurochemicals such as interleukins-4 and -12 and quinolinic acid (Amick et al., 2001, Berger et al., 2004). Few studies have evaluated microglia/macrophage activation in pediatric TBI models. In a neonatal mouse model of TBI, microglial reactivity was present in the same areas as degenerating neurons (Tong et al., 2002). In contrast, the microglial/macrophage response has been extensively documented following hypoxic-ischemic brain injury in the neonate rat (McRae et al., 1995, Ivacko et al., 1996, Cowell et al., 2002); importantly, the microglial/macrophage response in 9-day-old animals was increased compared to animals that were injured on post-natal day 30 (Ferrazzano et al., 2013). The neuroinflammatory cascade and microglial reactivity have, therefore, been identified as targets for therapeutic action in both adult and pediatric TBI (Potts et al., 2006, Loane and Byrnes, 2010).During development, microglia play a crucial role in removing apoptotic cells and dysfunctional synapses so it is not uncommon to observe activated microglia/macrophage profiles in an uninjured neonate animal (Paolicelli et al., 2011, Pont-Lezica et al., 2011). Limiting microglial/macrophage activation in a developing injured brain needs to be

carefully evaluated because it may negatively impact the normal developmental functions of microglia.

Minocycline is a broad-spectrum tetracycline antibiotic that is effective in reducing brain damage in multiple models of brain injury across the age spectrum (Elewa et al., 2006, Plane et al., 2010). It reduces microglial activation and proliferation thereby attenuating injury-induced deficits in adult models of TBI (Sanchez Mejia et al., 2001, Homsi et al., 2010, Kovesdi et al., 2012). In rat models of neonatal hypoxic-ischemia (HI), minocycline also decreased microglial activation and subsequently rescued injury-induced tissue atrophy, myelination deficits, oligodendrocyte cell death, and locomotor activity deficits (Arvin et al., 2002, Cai et al., 2006, Fan et al., 2006). However, the efficacy of minocycline in neonate brain injury may be limited. Thus, minocycline administration was not effective in rescuing injury-induced cell death in brains that were more severely injured (Cai et al., 2006). In a model of focal cerebral ischemia in the neonatal rat brain, minocycline was only able to decrease injury volume 24 hours after the insult, but had no effect 7 days after injury, indicative of the transient nature of the neuroprotection (Fox et al., 2005). In a mouse model of neonatal hypoxic-ischemia, minocycline exacerbated injury-induced tissue damage (Tsuji et al., 2004). It must be noted that most of these studies used a single dose and therefore the limited efficacy may be attributed to an incorrect dose/dosing paradigm. To date, there have been no studies specifically evaluating the efficacy of minocycline in a model of pediatric TBI. The present study sought to test the hypothesis that minocycline administration following repetitive TBI in the neonate rat will ameliorate post-traumatic cellular pathology and spatial learning deficits by reducing microglial/macrophage reactivity.

A2.3 MATERIALS AND METHODS

A2.3.1 Brain Injuries and Drug Administration

Eleven-day-old male and female Sprague-Dawley rat pups (Charles River, Wilmington MA) were injured (N=43) using an electrically-driven impact device (eCCI, Custom Design and Fabrication, Richmond VA) as previously described (Huh et al., 2007). Injuries (3 impacts spaced 24 hours apart) were conducted using a metal tip impactor centered over the exposed midline suture at a depth of 2mm and a velocity of 5 m/s. As an analgesic, carprofen (0.1mg/kg, Rimadyl™, Pfizer Animal Health, New York NY) was administered subcutaneously after each impact. Immediately following the third impact, animals received a 45mg/kg dose of minocycline hydrochloride (N=22, Sigma, St. Louis MO) or phosphate buffered saline (N=21, PBS, 0.2ml/kg) vehicle via an intraperitoneal (i.p.) injection. Animals subsequently received injections every 12 hours for 3 days for a total of 6 injections (45 mg/kg/injection or 0.2 ml/kg/injection). This dose was based on the efficacy in models of hypoxic ischemia and stroke in neonate animals (Arvin et al., 2002, Fox et al., 2005, Cai et al., 2006, Fan et al., 2006). The dosing paradigm reflected the short half-life of minocycline in rodents (2-3 hours) (Andes and Craig, 2002) and has been successful in reducing brain damage following trauma and/or stroke (Sanchez Mejia et al., 2001, Bye et al., 2007, Plane et al., 2010, Xue et al., 2010). Sham-injured animals (N=26) received incisions under anesthesia on all 3 days, followed by subcutaneous injections of Rimadyl™. Sham-inujured animals also receivedeither vehicle (N=12) or minocycline (N=14) injections.

A2.3.2 Tissue Collection and Preparation for Immunohistochemistry and Histology

At 3, 7, and 21 days after the third injury, separate groups of brain-injured (3 days: 5 vehicle, 5 minocycline; 7 days: 5 vehicle, 6 minocycline; 21 days: 11 vehicle, 11 minocycline) and sham-injured animals (3 days: 3 vehicle, 4 minocycline; 7 days: 3 vehicle, 4 minocycline; 21 days: 6 vehicle, 6 minocycline) were euthanized and the brains were processed for histology (Huh et al., 2007). Twelve sets of coronal sections (45μm thick, 12-14 sections per set) were collected for each animal. Adjacent sets of sections were mounted on gelatin-coated slides and stained for Fluoro-Jade B (FJB) (Huh et al., 2008) or Nissl-myelin (2% Cresyl Violet and 0.2% Cyanine R). Additional separate sets of sections were evaluated for microglia/macrophages using antibodies for anti-ionized calcium-binding adaptor molecule 1 (Iba1, Wako, Richmond, VA, 1:20,000) and CD68 (Clone ED1, AbD Serotech, Raleigh, NC, 1:500), and traumatic axonal injury using a polyclonal antibody to the C-terminal end of amyloid precursor protein (APP, Zymed, San Francisco, CA, 1:2,000). For anti-APP immunohistochemistry, antigen retrieval was executed by incubation with 10mM sodium citrate (pH 6.5) in a 60ºC water bath for 20 minutes. Primary antibody binding was detected using biotinylated donkey anti-rabbit IgG (Jackson ImmunoResearch, West Grove, PA, 1:1000 for APP and 1:500 for Iba1) or biotinylated donkey anti-mouse IgG (Jackson ImmunoResearch, West Grove, PA, 1:500). Antibody binding was visualized using the ABC Elite System with diaminobenzidine (Vector Laboratories, Burlingame, CA).

All quantifications were performed in 3 non-adjacent sections between 2 and 5 mm posterior to bregma. Quantification of pathology in the cortex and corpus callosum included the area between the cingula and extended to approximately 2mm on either side

of the cingula. Analysis in the thalamus was limited to the regions of staining (dorsolateral thalamus and lateral geniculate nucleus). FJB(+) profiles were manually counted in the cortex (18 high-powered fields, HPF) and thalamus (12 HPF) of brain-injured animals and presented as an average number of profiles per HPF. Analysis of APP-labeled sections was conducted using the grid analysis as previously described (DiLeonardi et al., 2009). Measurements of the areas of the corpus callosum and cortex were taken from Nissl-myelin stained sections as previously described (Creed et al., 2011). Because of the density of Iba1 and ED1 labeling, clear cellular bodies could not be distinguished in order to conduct reliable cell counting. For this reason, we used a thresholding approach from digitized images as described by Donnelly et al. (Donnelly et al., 2009) and the labeled area was divided by the corresponding total area measured in the Nissl-myelin stained sections. For the thalamus, the labeled area was divided by the total area of the analyzed image (10x). The hippocampus was analyzed between 2 and 5mm posterior to bregma.

A2.3.3 Spatial Learning and Memory Assessment

Spatial learning was assessed on days 7-10 after the third injury (N=12 sham-injured, 11 brain-injured vehicle, 11 brain-injured minocycline) as previously described (Huh et al., 2008); the inter-trial interval was 15 minutes for each rat. On day 11 post-injury, animals were tested for retention of the location of the platform (spatial memory) in 2 probe trials of 60 sec duration each and the times spent in the zone closest to the former location of the platform and the periphery of the pool was measured. Following the probe trials, animals were subjected to a visible platform trial in which the top inch of

the platform was exposed and a flag was adhered to the top of the platform. These data were analyzed in terms of latency to the platform in order to detect if the animals had any type of visual deficits. Visual deficits have been observed following focal and diffuse trauma to the neonate animal (Huh and Raghupathi, 2007, Raghupathi and Huh, 2007).

A2.3.4 Statistical Analysis

All data are presented as mean ± standard deviation. Vehicle-treated sham-injured animals and minocycline-treated sham-injured animals showed no differences on any analyses and were therefore combined into one group. All statistics were performed using Statistica 7 (StatSoft, Tulsa OK). Areas of corpus callosum and cortex, and the percent area of Iba1 or ED1 labeling were evaluated using a factorial analysis of variance (ANOVA) with injury status (sham-injured, brain injured vehicle-treated, and brain injured minocycline-treated) and time after injury (3 days, 7 days, and 21 days) used for between-subject comparison. Analysis of APP and FJB labeling were compared using independent samples t-tests. For analyses of the spatial learning, a repeated measures ANOVA was used to compare the latencies to the platform over 4 learning days between the 3 injury groups. A one-way ANOVA was used to compare the times spent in the platform and peripheral zones during the probe trials and the latencies in the visible platform trial. Animals that did not find the visible platform were excluded from all statistical analyses of spatial learning, probe, and visible platform data (1/12 sham-injured, 4/11 brain-injured vehicle, 4/11 brain-injured minocycline). When appropriate, post-hoc analyses were performed using the Newman-Keuls test and a value of $p \leq 0.05$ was considered significant for all analyses.

A2.4 RESULTS

A2.4.1 Minocycline does not affect the extent of Iba1 immunoreactivity

Microglia/macrophages in the corpus callosum of sham-injured animals appeared flat with elongated cell bodies and long processes indicative of a resting phenotype (Fig. A2.1A). Repetitive TBI resulted in activation of microglia/macrophages as evident by an increase in the extent of Iba1 immunoreactivity and an enlargement of the cell bodies (Fig. A2.1B,C). Increased Iba1 labeling was observed between 0.8 and 6 mm posterior to bregma, extended 2 mm lateral to each cingulum, and was present throughout the thickness of the corpus callosum. Quantification of the area of staining revealed an injury effect [$F_{2,42}$=34.66, $p<0.001$], a time effect [$F_{2,42}$=24.63, $p<0.001$], and an interaction effect between time and injury [$F_{4,42}$=5.36, $p<0.01$]. Post hoc analysis revealed that brain-injured animals had significantly increased areas of staining compared to the corresponding sham-injured groups at both 3 and 7 days, but not at 21 days (Fig. A2.1J; $p<0.001$). Additionally, brain-injured vehicle-treated animals demonstrated decreased areas of staining at 7 ($p<0.001$) and 21 days ($p<0.001$) compared to 3 days post-injury, indicating that microglial/macrophage activation in the white matter decreases over time. There was no effect of minocycline treatment at any time post-injury.

Microglia/macrophages in the cortex of sham-injured animals appeared rounded, but still resembled the resting phenotype with clearly visible processes (Fig. A2.1D). In brain-injured animals, regardless of treatment, there was a characteristic pattern of dense immunoreactivity (Fig. A2.1E,F) that extended from the cingulum toward the midline

encompassing the agranular retrosplenial cortex, parts of the frontal cortex (rostral), and parts of the medial occipital cortex (caudal); increased immunoreactivity in the cortex was observed between 2 and 6 mm posterior to bregma. Although quantification of the area of labeling revealed an effect of injury [$F_{2,42}$=4.25, p=0.02], post hoc analysis did not reveal any significant differences between sham- and brain-injured groups (Fig. A2.1K). However, an overall effect of time post-injury was observed [$F_{2,42}$=21.21, p<0.001] and the post hoc analysis revealed that the area of labeling was significantly greater at 3 days compared to 7 (p<0.001) and 21 days post-injury (p<0.001), and at 7 days compared to 21 days following injury (p<0.05). Minocycline treatment had no effect on Iba1 labeling in the cortex at any time post-injury.

Similar to the cortex, microglia/macrophages in the thalamus of sham-injured animals predominantly exhibited a resting phenotype (Fig. A2.1G). Iba1 immunoreactivity was increased in both brain-injured groups compared to the sham-injured group (Fig. A2.1H,I). Microglial/macrophage reactivity was restricted to lateral aspects including the laterodorsal nucleus (rostral) and parts of the lateral geniculate nucleus (caudal) and was only observed up to 7 days post-injury. Quantification revealed an effect of injury [$F_{2,29}$=29.70, p<0.001] and time [$F_{1,29}$=35.25, p<0.001, Fig. A2.1L]. Post hoc analysis of the injury effect revealed that both groups of brain-injured animals showed significantly greater areas of thalamic Iba1 labeling when compared to sham-injured animals (Fig. A2.1L; p<0.001). Minocycline treatment did not affect this injury-induced increase in Iba1 labeling in the thalamus. No increase in Iba1 staining was observed in the hippocampus of brain-injured animals (data not shown).

A2.4.2 Treatment with minocycline decreases ED1 labeling in the corpus callosum.

ED1 labeling was minimally observed in the corpus callosum of sham-injured animals (Fig. A2.2A), but was much more extensive in the brain-injured animals (Fig. A2.2B,C). ED1-positive cells took on a rounded amoeboid morphology with very few, if any, visible processes. The topography and pattern of ED1 immunoreactivity in this region was similar to the pattern previously described for Iba1 staining in the corpus callosum. Quantification of the area of staining (Fig. A2.2G) revealed an injury effect [$F_{2,35}$=24.85, $p<0.001$], a time effect [$F_{2,35}$=17.73, $p<0.001$], and an interaction effect [$F_{4,35}$ =4.98, $p<0.01$]. Post hoc analysis of the injury effect revealed that the ED1 immunoreactivity was significantly increased in both brain-injured groups compared to the sham-injured group ($p<0.001$). Post hoc analysis of the time effect revealed that injured animals had significantly larger areas of staining at both 3 (vehicle, $p<0.001$; minocycline, $p<0.001$) and 7 days (vehicle, $p<0.05$; minocycline, $p<0.01$) post-injury, but this effect was lost at 21 days. Interestingly, a treatment effect was observed at 3 days post-injury with minocycline-treated brain-injured animals exhibiting a mild decrease in the area of ED1 labeling compared to vehicle-treated brain-injured animals ($p=0.05$).

In sham-injured animals, ED1 staining was present in the cortex around what appeared to be blood vessels (Fig. A2.2D). In brain-injured animals, ED1-labeled cells were rounded and had very few visible processes (Fig. A2.2E,F). Quantitative analysis of the area of immunoreactivity (Fig. A2.2H) revealed an injury effect [$F_{2,35}$=8.57, $p<0.001$], a time effect [$F_{2,35}$=16.44, $p<0.001$], and an interaction effect between injury and time [$F_{4,35}$=2.76, $p<0.05$]. Post hoc analysis of the injury effect indicated that brain-injured animals, irrespective of treatment, possessed significantly larger areas of staining

compared to sham-injured animals ($p<0.01$). Post hoc analysis of the time effect revealed that labeling was significantly decreased at 7 ($p<0.001$) and 21 days ($p<0.001$) compared to 3 days post-injury, and an additional significant decrease in area stained was observed between 7 and 21 days post-injury ($p<0.05$). The post hoc analysis for the interaction effect revealed that both groups of injured animals were different from the corresponding sham-injured group at 3 days post-injury (Fig. A2.2H; vehicle, $p<0.01$; minocycline, $p<0.001$), but no such intragroup differences were found at 7 or 21 days post-injury; there was no effect of treatment at any time point. In the thalamus, ED1 labeling was only present in the laterodorsal nucleus 2.0 mm posterior to bregma at 3 days post-injury (data not shown). There was also no discernible ED1 labeling in the hippocampus.

A2.4.3 Minocycline does not affect traumatic axonal injury.

There was no observable APP labeling in sham-injured animals (Fig. A2.3A). Intra-axonal APP labeling in the white matter of brain-injured animals primarily appeared as terminal bulbs, suggesting that the axons had disconnected and/or retracted (Fig. A2.3B,C). These APP-positive profiles were present in the cingulum and dorsal portions of the corpus callosum in rostral sections (0.5 mm to 2 mm posterior to bregma) and through both dorsal and ventral portions of the fiber bundle more caudally (2 mm to 5.5 mm) indicating that APP labeling was increased under the impact site. Axonal APP labeling was present in the corpus callosum at 3 days post-injury and was not visible at 7 days post-injury. Quantitative grid analyses revealed no significant difference in the extent of APP labeling between brain-injured vehicle-treated and minocycline-treated

animals (Fig. A2.3D). No APP-positive profiles were observed in the thalamus at any time post-injury (data not shown).

A2.4.4 Minocycline does not affect neurodegeneration.

In the corpus callosum, FJB(+) profiles were punctate and diffuse, suggestive of axonal degeneration (Fig. A2.4A,B). Labeling in the corpus callosum was extensive at 3 days post-injury (Fig. A2.4A,B) and much less at the 7 and 21 day time points (not shown). Minocycline appeared to have no effect on the extent of labeling when compared to vehicle-treated injured animals (Fig. A2.4A,B). FJB(+) profiles in the cortex exhibited neuronal morphology (Fig. A2.4D,E) and were present in the agranular retrosplenial cortex, the frontal cortex (rostral) and the occipital cortex (caudal). Labeled profiles were visible at 3 days after injury (Fig. A2.4D,E), but not at 7 or 21 days post-injury (data not shown). However, the number of FJB(+) profiles in the cortex did not differ between vehicle- and minocycline-treated brain-treated injured animals (Fig. A2.4I). FJB labeling in the injured thalamus exhibited a mix of diffuse, punctate labeling (axonal) and cellular labeling (Fig. A2.4G,H). FJB(+) profiles were present in the laterodorsal thalamus (rostral) and the lateral geniculate nucleus (caudal) up to 21 days. Treatment with minocycline did not affect the number of FJB(+) profiles at 3 days post-injury (Fig. A2.4I) or at later times (data not shown). Labeled profiles were not present in the hippocampus (data not shown). No FJB(+) profiles were visible in any region of the sham-injured brain (Fig. A2.4C,F).

A2.4.5 Minocycline does not affect tissue loss.

Repeated impacts to the skull of the 11-day-old rat did not result in any overt tears in the white or grey matter and there was no evidence of lesion or cavitation (Fig. A2.5). Area measurement of the subcortical white matter tract between the two cingula revealed an injury effect [$F_{2,47}$=218.04, $p<0.001$] and post hoc analysis indicated that brain-injured animals had significantly decreased white matter areas compared to sham-injured animals ($p<0.001$). There was also an interaction effect between injury and time [$F_{4,47}$=8.88, $p<0.01$] and the post hoc analysis revealed that brain-injured animals within each time point had significantly decreased areas compared to their corresponding sham-injured animals (Fig. A2.5J; $p<0.001$). There was no difference between the vehicle-treated and minocycline-treated brain-injured groups at any time point. Cortical area analysis at 3, 7, and 21 days post-injury revealed a significant effect of injury [$F_{2,47}$=6.20, $p<0.01$] and time [$F_{2,47}$=8.22, $p<0.001$] (Fig. A2.5K). Post hoc analysis of the injury effect revealed that brain-injured animals had significantly lower cortical areas than sham-injured animals (vehicle, $p<0.01$; minocycline, $p<0.05$), but there was no difference between vehicle- and minocycline-treated brain-injured animals. Analysis of the time effect revealed that cortical area was significantly increased at 21 days compared to 3 ($p<0.01$) and 7 ($p<0.05$) days which may be a consequence of age.

A 2.4.6 Minocycline exacerbates spatial retention deficits.

Brain-injured animals had significantly longer latencies to find the hidden platform in the spatial learning task compared to sham-injured animals in the second week following injury (Fig. A2.6A). Analysis of the latencies revealed an injury effect

[$F_{2,66}$=20.13, p<0.001], a time effect (learning days) [$F_{3,66}$=15.24, p<0.001], and an interaction effect [$F_{6,66}$=2.86, p<0.05]. Post hoc analysis of the injury effect revealed that both vehicle- and minocycline-treated brain-injured animals displayed increased escape latencies when compared to the latencies of sham-injured animals (p<0.001). Post hoc analysis of the interaction effect confirmed this injury effect and revealed that the latencies of vehicle-treated brain-injured animals did not differ from the latencies of minocycline-treated brain-injured animals. In the probe trials, brain-injured animals spent significantly more time in the periphery of the maze [$F_{2,22}$=9.83, p<0.001] and significantly less time in the zone corresponding to the platform location [$F_{2,22}$=6.44, p<0.01] (Fig. A2.6B). Post hoc analysis revealed that there was no difference in time spent in either zone between sham-injured animals and vehicle-treated brain-injured animals. In contrast, brain-injured minocycline-treated animals spent significantly more time in the peripheral zone (p<0.001) and less time in the platform zone (p<0.01) than the sham-injured animals. Additionally, brain-injured minocycline-treated animals spent more time in the peripheral zone than brain-injured vehicle-treated animals (p<0.05). During the visible platform trial, an injury effect was observed [$F_{2,22}$=4.01, p<003] and post hoc analysis indicated that both vehicle-treated brain-injured animals (p=0.05) and minocycline-treated brain-injured animals (p=0.06) had difficulty locating the exposed platform compared to the sham-injured animals, suggestive of a visual deficit. Despite this deficit, it must be noted that brain-injured animals were able to find the hidden platform (time effect vide supra) and demonstrated searching behavior through the 4 days of learning and during the probe trial.

A2.5 DISCUSSION

The results of the present study demonstrate that minocycline, administered to neonate rats subjected to repetitive brain trauma, reduced the extent of ED1-labeled microglia/macrophages in the corpus callosum but had no effect on the extent of traumatic axonal injury or axonal degeneration. This effect was observed immediately after the cessation of minocycline treatment and did not extend to the 7 or 21 day time points. Furthermore, the extent of microglia/macrophage activation in the cortex and thalamus and the associated neurodegeneration was unaffected by minocycline treatment. Whereas injury-induced deficits in spatial learning were not reversed, minocycline treatment exacerbated the spatial retention deficits observed in brain-injured animals. Collectively, these data (Table 1) suggest that minocycline may not be an effective therapeutic intervention for neonate animals in the acute period following repetitive TBI.

Whereas minocycline has never been used in a rodent model of neonatal TBI, systemic administration of minocycline has been effective in reducing injury-induced increases in microglial/macrophage activation in models of adult TBI and spinal cord injury (SCI), and neonatal hypoxic-ischemia (HI) (Cai et al., 2006, Fan et al., 2006, Festoff et al., 2006, Bye et al., 2007, Carty et al., 2008, Ng et al., 2012). Using a combination of immunohistochemistry with antibodies to proteins such as Iba1, F4/80 and CD11b or lectin histochemistry and morphology (resting, intermediately-reactive and amoeboid), minocycline administration was observed to reduce the number of activated microglia/macrophages following HI in the neonate rat (Cai et al., 2006, Fan et al., 2006, Carty et al., 2008, Leonardo et al., 2008, Tang et al., 2010) or closed head injury in the adult mouse (Bye et al., 2007, Ng et al., 2012); interestingly, minocycline only decreased

the number of activated cells and did not affect the number of intermediately reactive cells following TBI (Bye et al., 2007). Because of the extensive and robust nature of microglial/macrophage activation observed in the brain-injured animals in the present study, cell counts could not be performed. Instead, an alternate approach based on a threshold of staining intensity was taken which encompasses changes in cell number, morphology (cells becoming larger) and alterations in the expression of the protein/cell surface marker (Donnelly et al., 2009). Whereas this approach has been successful in determining an effect of minocycline on injury-induced microglia/macrophage activation using Iba-1 immunohistochemisty (Ng et al., 2012), the lack of an overall effect using this approach in the present may be indicative of the relative insensitivity of the technique.

Alternatively, the antibody to CD68 (ED1) selectively labels activated (amoeboid) cells by binding to a glycosylated protein that is present in the membranes of phagosomes and lysosomes which are indicative of a phagocytic phenotype (Damoiseaux et al., 1994). Minocycline has been reported to reduce ED1-labeled cells in the cortex and white matter tracts following HI in the neonatal rat (Cai et al., 2006, Lechpammer et al., 2008). Similarly, activated microglia/macrophages labeled with human alveolar macrophage-56 (HAM-56) were reduced following minocycline treatment following SCI in the adult rat (Festoff et al., 2006). In the present study, the decrease in the area of ED1 immunoreactivity following minocycline treatment was limited to the corpus callosum and did not extend to the cortex. Similar regional differences in acute minocycline treatment after neonatal HI were observed wherein the numbers of Iba1-labeled activated microglia/macrophages were decreased in the thalamus and the dorsal raphé, but not the

frontal cortex (Wixey et al., 2011). Although the majority of preclinical studies indicate that acute treatment with minocycline does reduce microglia/macrophage activation, one study did demonstrate that minocycline was ineffective in reducing the number of ED1-labeled activated microglia/macrophages in the cortex after stroke in the neonate rat (Fox et al., 2005).

In the current study, minocycline treatment did not affect injury-induced neurodegeneration and/or tissue atrophy in the cortex or thalamus. In part, this may explain the visual deficit (which was not affected by minocycline treatment) observed in the repetitively brain-injured animals in the current study; FJB(+) neurons were observed in the lateral geniculate nucleus of the thalamus and the occipital cortex, areas that are directly involved in the visual pathway (Peters and Feldman, 1976). In addition, damage to the optic nerve which has been reported following repetitive TBI in adult mice (Tzekov et al., 2014), may underlie the visual deficit and warrants further investigation. In contrast, minocycline has demonstrated success in reducing lesion area in the cortex in models of adult TBI, juvenile asphyxia and neonatal stroke (Sanchez Mejia et al., 2001, Arvin et al., 2002, Bye et al., 2007, Homsi et al., 2009, Tang et al., 2010). The success of minocycline in reducing cellular degeneration is mixed with one study in a model of adult TBI reporting that the effect of minocycline was transient (Bye et al., 2007) and another wherein treatment with minocycline after neonatal HI in the mouse resulted in an increase in tissue loss (Tsuji et al., 2004). Minocycline has been reported to limit apoptotic cell death in animal models of several neurodegenerative diseases (Zhu et al., 2002, Wang et al., 2003), SCI (Teng et al., 2004), cardiac arrest (Tang et al., 2010) and neonatal HI (Cai et al., 2006, Fan et al., 2006, Carty et al., 2008) in addition to decreasing

levels of activated caspase-3 (Arvin et al., 2002). In contrast, minocycline was not effective in reducing the number of apoptotic cells following TBI in the adult mouse (Bye et al., 2007). Despite the attenuation of activated microglial/macrophage reactivity in the corpus callosum, minocycline had no effect on axonal injury and degeneration or white matter tissue loss in the brain-injured animals. By contrast, in neonatal rodent HI brain injury, minocycline attenuated both microglial/macrophage reactivity and the loss of myelin and white matter volume (Cai et al., 2006, Fan et al., 2006, Carty et al., 2008, Lechpammer et al., 2008). Following TBI in adult mice, acute administration of minocycline was associated with a reduction in microglial activation which accompanied an attenuation of tissue loss in the corpus callosum, but had no effect on trauma-induced increase in axonal injury (Homsi et al., 2010, Siopi et al., 2011). Although microglial activation shares a spatiotemporal relationship with axonal injury/degeneration, ultrastructural or functional analyses do not demonstrate a clear cause-and-effect mechanism in adult rodent TBI models (Kelley et al., 2007, Bennett and Brody, 2014).

Given the absence of any overt neuroprotective effects, it is not surprising that post-injury minocycline treatment was ineffective in reducing spatial learning and retention deficits. Brain-injured animals, irrespective of treatment, did not learn the task efficiently and therefore had difficulty in the consolidation phase as reflected in the deficit in the probe trial. In a model of central fluid percussion injury in the adult rat, spatial learning and memory deficits were observed in the absence of overt pathology in the hippocampus (Lyeth et al., 1990). These deficits, however, were associated with alterations in long term potentiation (LTP) in the hippocampus (Miyazaki et al., 1992). While there was no overt pathology present in the hippocampus, other brain regions that

are thought to be involved in spatial learning and memory were affected by the injury. In the present study, brain-injured animals demonstrated neurodegeneration in the retrosplenial cortex (RSC) and the laterodorsal nucleus of the thalamus (LDN); lesions in these areas result in spatial learning deficits in the Morris water maze task (Harker and Whishaw, 2002, van Groen et al., 2002, Vann et al., 2003).

Moreover, the exacerbation of the retention deficit observed in the minocycline-treated animals suggest that minocycline may, by altering microglial-derived soluble mediators such as interleukins-1β, -6, and -18 and tumor necrosis factor-α (TNFα) (Krady et al., 2005, Bye et al., 2007, Wasserman and Schlichter, 2007, Henry et al., 2008), compound injury-induced deficits in synaptic plasticity. It has been demonstrated that these interleukins regulate maintenance of long-term potentiation (LTP) (McAfoose and Baune, 2009, del Rey et al., 2013) while TNFα can upregulate surface expression of α-amino-3-hydorxy-5-methyl-4-isozazoleproprionic (AMPA) receptors and strengthen LTP (Beattie et al., 2002). However, it is unclear if this theory holds true in the injured brain as cytokines levels are significantly increased following injury (Ziebell and Morganti-Kossmann, 2010). For example, pathologic increases in IL-1β can inhibit both LTP and the acquisition and retention of a spatial memory task (Ross et al., 2003, Trofimov et al., 2012). Alternatively, the reduction in the number of phagocytic microglia/macrophages in the corpus callosum may have prevented the removal of cellular debris such as myelin fragments or apoptotic oligodendrocytes, thereby preventing white matter repair (Takahashi et al., 2005, Neumann and Takahashi, 2007). In contrast to our observations in the neonate rat, minocycline treatment in adult brain-injured mice has been observed to reduce impairments in the novel object recognition

task (Siopi et al., 2012). Minocycline treatment has also been effective in reducing injury-induced deficits in non-cognitive behaviors such as locomotion, hyperactivity and anxiety-like behavior following either TBI in adult mice or HI in the neonate rat (Sanchez Mejia et al., 2001, Fan et al., 2006, Homsi et al., 2010).

One potential caveat to the current study is that we only used one dose (45 mg/kg/injection) and one dosing paradigm (every 12 hours for 3 days). The dose and dosing paradigms were chosen based on their efficacy and use in several models of brain injury in both adult and neonatal animals (Sanchez Mejia et al., 2001, Bye et al., 2007, Buller et al., 2009, Plane et al., 2010, Tang et al., 2010). Future efforts will focus on continuing the dosing to the later time points, which has demonstrated success (Carty et al., 2008). Nevertheless, the apparent lack of efficacy of minocycline in neonatal brain trauma raises the possibility that this compound may be acting on anti-inflammatory subsets of microglia/macrophages. Very few studies have investigated the effect of minocycline on microglial/macrophage polarization into M1 (pro-inflammatory) and M2 (anti-inflammatory) phenotypes. Although minocycline was successful in decreasing M1 pro-inflammatory markers while leaving M2 markers unaffected in a mouse model of amyotrophic lateral sclerosis (Kobayashi et al., 2013), it has been reported to increase pro-inflammatory markers in animals that exhibit depressive-like behavior (Burke et al., 2014). Based on the observation that depletion of microglia at the time of injury exacerbated tissue loss following stroke (Faustino et al., 2011), it is tempting to suggest that pro-inflammatory mediators released in acute post-traumatic period may be necessary for neuroprotection after neonatal TBI. Future efforts will be directed at determining the appropriate dosing paradigm and the cellular mechanisms, such as

cytokine synthesis and release and cellular activity, underlying the efficacy of minocycline as an effective intervention for repeated TBI in immature animals.

A2.6 FIGURE LEGENDS

Figure A2.1. Minocycline does not reduce microglia/macrophage activation induced by repeated brain trauma

Representative photomicrographs illustrate Iba1-labeled microglia/macrophages in the corpus callosum (A-C), cortex (D-F), and thalamus (G-I) of sham-injured (A, D, G), brain-injured vehicle-treated (B, E, H), and brain-injured minocycline-treated animals (C, F, I) at 3 days post-injury. Note the increase in Iba1 immunoreactivity and the cell density in the injured brain sections. Quantification of the area labeled with Iba1 above threshold (as described in the Methods) in the corpus callosum (J), cortex (K), and thalamus (L) expressed as a percent of the total area of the corresponding region from Nissl-myelin stained sections. *, $p<0.05$ compared to the sham-injured values at the corresponding time point. Scale bar in panel L = 50μm.

Figure A2.2. Minocycline reduces ED1-labeled microglia/macrophages in the corpus callosum of brain-injured animals.

Representative photomicrographs illustrate ED1-labeled microglia/macrophages in the corpus callosum (A-C) and cortex (D-F) of sham-injured (A, D), brain-injured vehicle-treated (B, E), and brain-injured minocycline-treated animals (C, F) at 3 days post-injury. Note the relative paucity of ED1 labeled cells in sham-injured brains and the robust increase in the cell size and intensity of ED1 immunoreactivity in the brain-injured animals. Quantification of area labeled with ED1 above threshold (as described in the

Methods) in the corpus callosum (G) and cortex (H) expressed as percent of the total area of the corresponding region from Nissl-myelin stained sections. *, $p<0.05$ compared to the sham-injured values at the corresponding time point; #, $p = 0.05$ compared to the brain-injured vehicle-treated group at the corresponding time point. Scale bar in panel F = 25 μm.

Figure A2.3. Minocycline does not reduce the extent of traumatic axonal injury in the corpus callosum of brain-injured animals.

Representative photomicrographs illustrate intra-axonal accumulation of amyloid precursor protein in the corpus callosum of brain-injured vehicle-treated (B), and brain-injured minocycline-treated (C) animals at 3 days post injury; note the absence of immunoreactivity in sham-injured animals (A). Panel D denotes the quantification of APP-labeled profiles using the grid analysis method. Scale bar in panel C = 25μm.

Figure A2.4. Minocycline does not reduce the extent of Fluoro-Jade B labeling in brain-injured animals.

Representative photomicrographs illustrate Fluoro-Jade B labeling in the corpus callosum (A-C), cortex (D-F), and thalamus (G,H) of brain-injured vehicle-treated (A, D, G), brain-injured minocycline-treated (B, E, H) and sham-injured animals (C, F) at 3 days post-injury. Note the absence of Fluoro-Jade B reactivity in sham-injured animals (C, F).

Quantification of FJB(+) profiles in each high power field as described in the Methods (I). Scale bar in panel H = 50μm.

Figure A2.5. **Minocycline does not reverse injury-induced decrease in loss of corpus callosum area.**

Representative Nissl-myelin stained sections from sham-injured (A, D, G), brain-injured vehicle-treated (B, E, H), and brain-injured minocycline-treated animals (C, F, I) at 3 days (A-C), 7 days (D-F), and 21 days post-injury (G-I). Note the appearance of enlarged ventricles at 21 days post-injury in brain-injured animals (panels H and I). Quantification of the area of the corpus callosum (J) and cortex (K). *, $p<0.001$ compared to sham-injured values at the corresponding time point. Scale bar in panel I = 1000μm.

Figure A2.6. **Minocycline does not attenuate injury-induced spatial learning deficits but exacerbates retention deficits.**

(A) Latency to the platform in the spatial learning task using the Morris water maze illustrates the deficit in the time taken to reach the hidden platform in brain-injured animals. (B) Times spent in the periphery of the maze and the area surrounding the platform location during the probe trial. *, $p<0.01$ when compared to the sham-injured animals; #, $p<0.05$ when compared to the brain injured vehicle-treated animals.

A2.7 FIGURES

Figure A2.1. Effect of minocycline on microglia/macrophage activation induced by repeated brain trauma

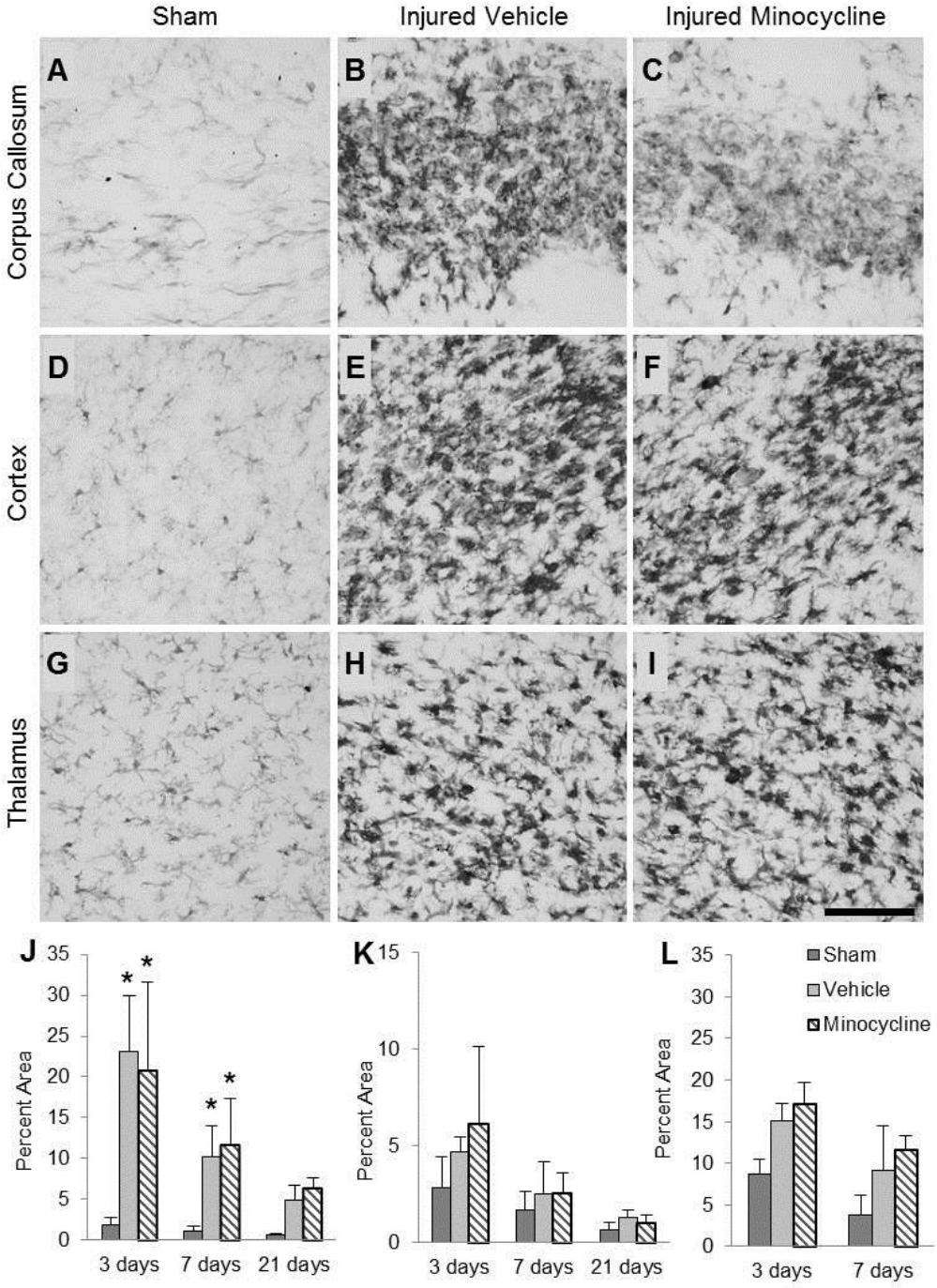

Figure A2.2. Effect of minocycline on microglial/macrophage activation in the corpus callosum of repetitively brain-injured animals.

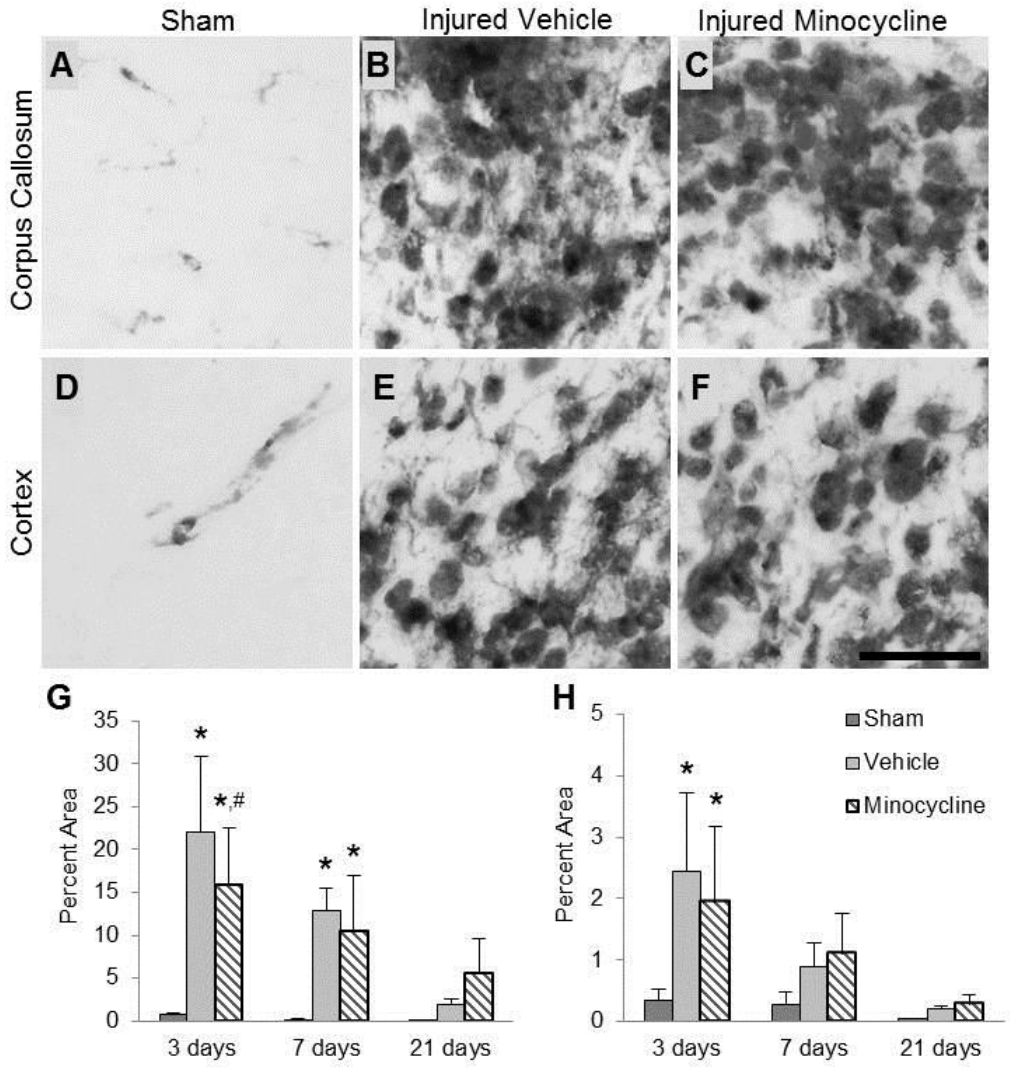

Figure A2.3. Effect of minocycline on traumatic axonal injury in the corpus callosum following repetitive brain injury.

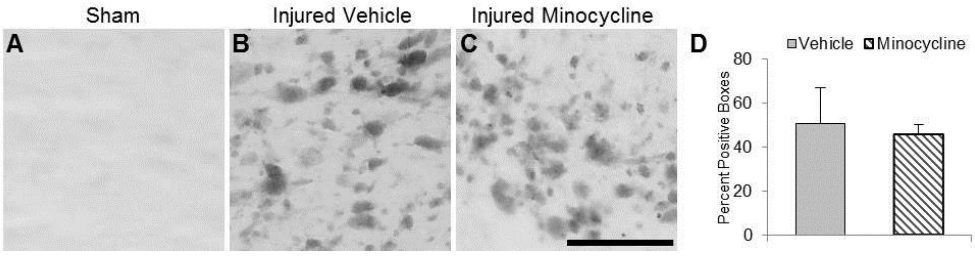

Figure A2.4. Effect of minocycline on Fluoro-Jade B labeling in repetitively brain-injured animals.

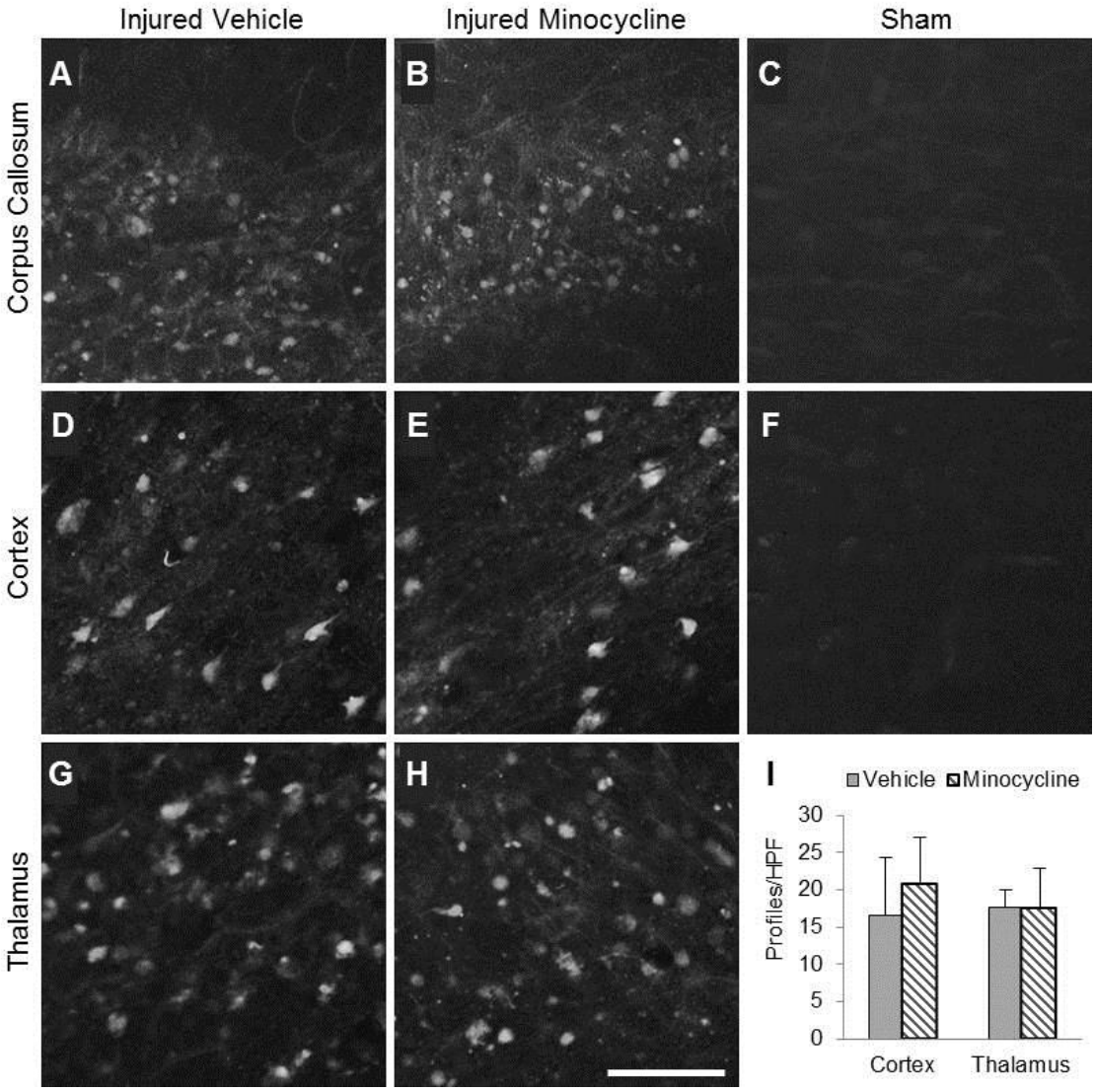

Figure A2.5. Effect of minocycline on tissue atrophy following repetitive brain injury in the neonate rat.

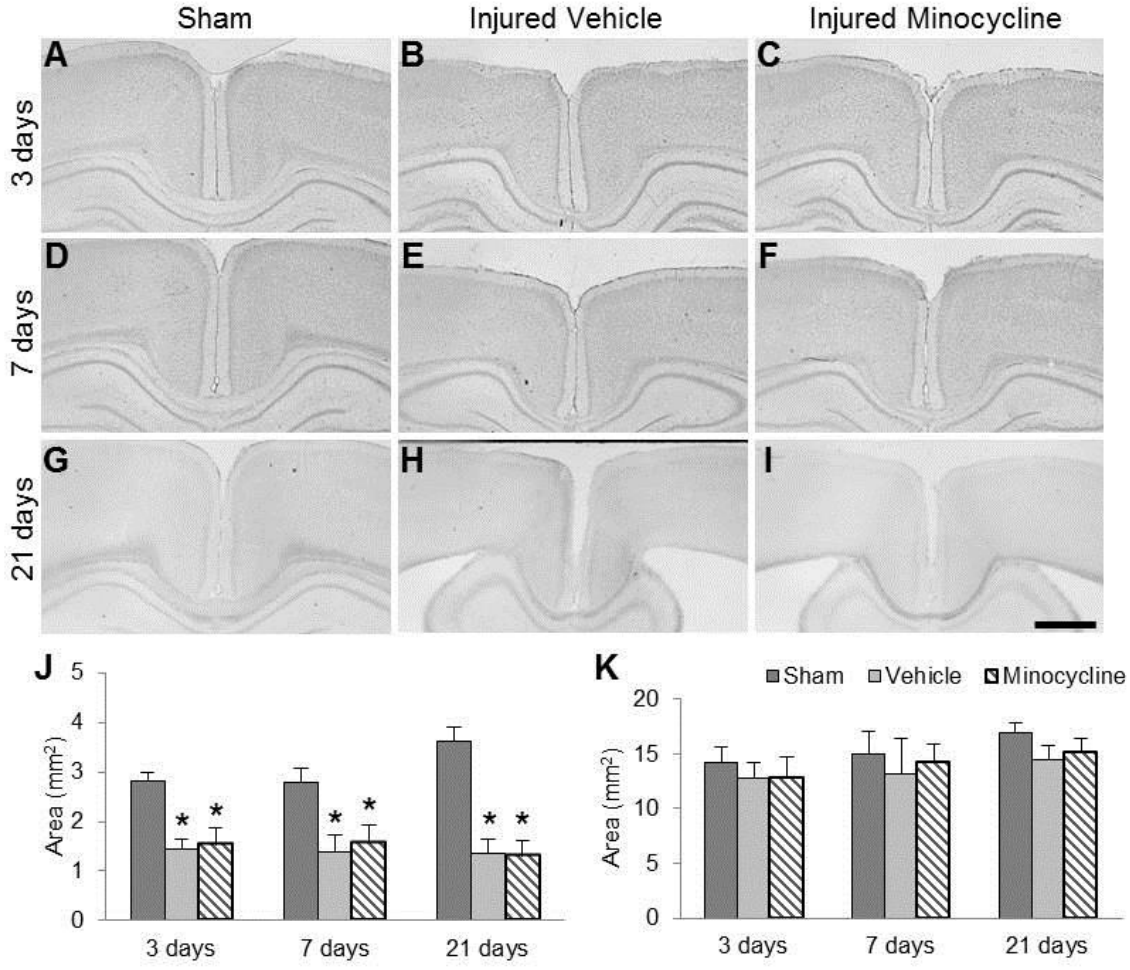

Figure A2.6. **Effect of minocycline on injury-induced spatial learning and memory deficits.**

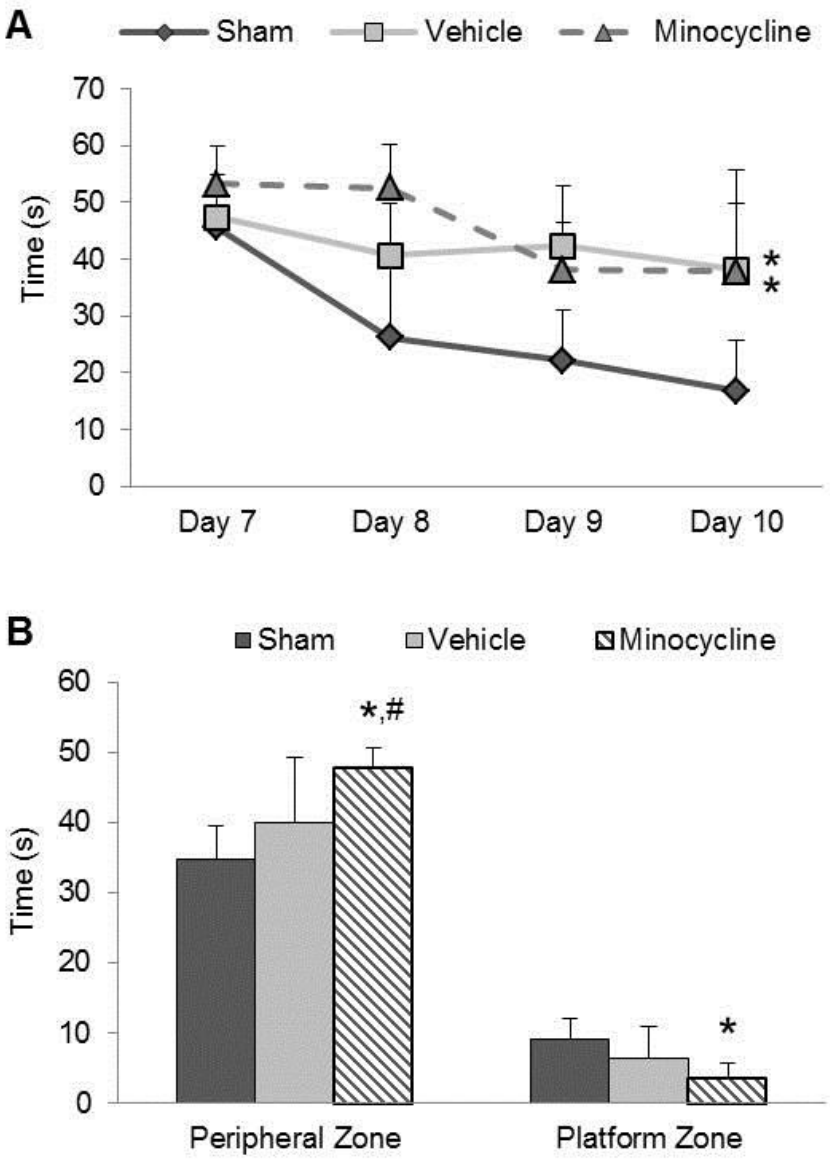

A2.8 References

Amick JE, Yandora KA, Bell MJ, Wisniewski SR, Adelson PD, Carcillo JA, Janesko KL, DeKosky ST, Carlos TM, Clark RS, Kochanek PM (2001) The Th1 versus Th2 cytokine profile in cerebrospinal fluid after severe traumatic brain injury in infants and children. Pediatric critical care medicine : a journal of the Society of Critical Care Medicine and the World Federation of Pediatric Intensive and Critical Care Societies 2:260-264.

Andes D, Craig WA (2002) Animal model pharmacokinetics and pharmacodynamics: a critical review. International journal of antimicrobial agents 19:261-268.

Arvin KL, Han BH, Du Y, Lin SZ, Paul SM, Holtzman DM (2002) Minocycline markedly protects the neonatal brain against hypoxic-ischemic injury. Annals of neurology 52:54-61.

Barlow KM, Thomson E, Johnson D, Minns RA (2005) Late neurologic and cognitive sequelae of inflicted traumatic brain injury in infancy. Pediatrics 116:e174-185.

Beattie EC, Stellwagen D, Morishita W, Bresnahan JC, Ha BK, Von Zastrow M, Beattie MS, Malenka RC (2002) Control of synaptic strength by glial TNFalpha. Science 295:2282-2285.

Bennett RE, Brody DL (2014) Acute reduction of microglia does not alter axonal injury in a mouse model of repetitive concussive traumatic brain injury. Journal of neurotrauma 31:1647-1663.

Berger RP, Heyes MP, Wisniewski SR, Adelson PD, Thomas N, Kochanek PM (2004) Assessment of the macrophage marker quinolinic acid in cerebrospinal fluid after

pediatric traumatic brain injury: insight into the timing and severity of injury in child abuse. Journal of neurotrauma 21:1123-1130.

Bishop NB (2006) Traumatic brain injury: a primer for primary care physicians. Current problems in pediatric and adolescent health care 36:318-331.

Bonnier C, Mesples B, Carpentier S, Henin D, Gressens P (2002) Delayed white matter injury in a murine model of shaken baby syndrome. Brain pathology 12:320-328.

Bonnier C, Nassogne MC, Evrard P (1995) Outcome and prognosis of whiplash shaken infant syndrome; late consequences after a symptom-free interval. Developmental medicine and child neurology 37:943-956.

Buller KM, Carty ML, Reinebrant HE, Wixey JA (2009) Minocycline: a neuroprotective agent for hypoxic-ischemic brain injury in the neonate? Journal of neuroscience research 87:599-608.

Burke NN, Kerr DM, Moriarty O, Finn DP, Roche M (2014) Minocycline modulates neuropathic pain behaviour and cortical M1-M2 microglial gene expression in a rat model of depression. Brain, behavior, and immunity 42:147-156.

Bye N, Habgood MD, Callaway JK, Malakooti N, Potter A, Kossmann T, Morganti-Kossmann MC (2007) Transient neuroprotection by minocycline following traumatic brain injury is associated with attenuated microglial activation but no changes in cell apoptosis or neutrophil infiltration. Experimental neurology 204:220-233.

Cai Z, Lin S, Fan LW, Pang Y, Rhodes PG (2006) Minocycline alleviates hypoxic-ischemic injury to developing oligodendrocytes in the neonatal rat brain. Neuroscience 137:425-435.

Carty ML, Wixey JA, Colditz PB, Buller KM (2008) Post-insult minocycline treatment attenuates hypoxia-ischemia-induced neuroinflammation and white matter injury in the neonatal rat: a comparison of two different dose regimens. International journal of developmental neuroscience : the official journal of the International Society for Developmental Neuroscience 26:477-485.

Christian CW, Block R, Committee on Child A, Neglect, American Academy of P (2009) Abusive head trauma in infants and children. Pediatrics 123:1409-1411.

Cowell RM, Xu H, Galasso JM, Silverstein FS (2002) Hypoxic-ischemic injury induces macrophage inflammatory protein-1alpha expression in immature rat brain. Stroke; a journal of cerebral circulation 33:795-801.

Creed JA, DiLeonardi AM, Fox DP, Tessler AR, Raghupathi R (2011) Concussive brain trauma in the mouse results in acute cognitive deficits and sustained impairment of axonal function. Journal of neurotrauma 28:547-563.

Damoiseaux JG, Dopp EA, Calame W, Chao D, MacPherson GG, Dijkstra CD (1994) Rat macrophage lysosomal membrane antigen recognized by monoclonal antibody ED1. Immunology 83:140-147.

del Rey A, Balschun D, Wetzel W, Randolf A, Besedovsky HO (2013) A cytokine network involving brain-borne IL-1beta, IL-1ra, IL-18, IL-6, and TNFalpha operates during long-term potentiation and learning. Brain, behavior, and immunity 33:15-23.

Dias MS, Backstrom J, Falk M, Li V (1998) Serial radiography in the infant shaken impact syndrome. Pediatric neurosurgery 29:77-85.

DiLeonardi AM, Huh JW, Raghupathi R (2009) Impaired axonal transport and neurofilament compaction occur in separate populations of injured axons following diffuse brain injury in the immature rat. Brain research 1263:174-182.

Donnelly DJ, Gensel JC, Ankeny DP, van Rooijen N, Popovich PG (2009) An efficient and reproducible method for quantifying macrophages in different experimental models of central nervous system pathology. Journal of neuroscience methods 181:36-44.

Duhaime AC, Christian C, Moss E, Seidl T (1996) Long-term outcome in infants with the shaking-impact syndrome. Pediatric neurosurgery 24:292-298.

Elewa HF, Hilali H, Hess DC, Machado LS, Fagan SC (2006) Minocycline for short-term neuroprotection. Pharmacotherapy 26:515-521.

Ewing-Cobbs L, Prasad M, Kramer L, Louis PT, Baumgartner J, Fletcher JM, Alpert B (2000) Acute neuroradiologic findings in young children with inflicted or noninflicted traumatic brain injury. Child's nervous system : ChNS : official journal of the International Society for Pediatric Neurosurgery 16:25-33; discussion 34.

Ewing-Cobbs L, Prasad MR, Kramer L, Cox CS, Jr., Baumgartner J, Fletcher S, Mendez D, Barnes M, Zhang X, Swank P (2006) Late intellectual and academic outcomes following traumatic brain injury sustained during early childhood. Journal of neurosurgery 105:287-296.

Fan LW, Lin S, Pang Y, Rhodes PG, Cai Z (2006) Minocycline attenuates hypoxia-ischemia-induced neurological dysfunction and brain injury in the juvenile rat. The European journal of neuroscience 24:341-350.

Faustino JV, Wang X, Johnson CE, Klibanov A, Derugin N, Wendland MF, Vexler ZS (2011) Microglial cells contribute to endogenous brain defenses after acute neonatal focal stroke. The Journal of neuroscience : the official journal of the Society for Neuroscience 31:12992-13001.

Ferrazzano P, Chanana V, Uluc K, Fidan E, Akture E, Kintner DB, Cengiz P, Sun D (2013) Age-dependent microglial activation in immature brains after hypoxia-ischemia. CNS & neurological disorders drug targets 12:338-349.

Festoff BW, Ameenuddin S, Arnold PM, Wong A, Santacruz KS, Citron BA (2006) Minocycline neuroprotects, reduces microgliosis, and inhibits caspase protease expression early after spinal cord injury. Journal of neurochemistry 97:1314-1326.

Finnie JW, Blumbergs PC, Manavis J, Turner RJ, Helps S, Vink R, Byard RW, Chidlow G, Sandoz B, Dutschke J, Anderson RW (2012) Neuropathological changes in a lamb model of non-accidental head injury (the shaken baby syndrome). Journal of clinical neuroscience : official journal of the Neurosurgical Society of Australasia 19:1159-1164.

Fox C, Dingman A, Derugin N, Wendland MF, Manabat C, Ji S, Ferriero DM, Vexler ZS (2005) Minocycline confers early but transient protection in the immature brain following focal cerebral ischemia-reperfusion. Journal of cerebral blood flow and metabolism : official journal of the International Society of Cerebral Blood Flow and Metabolism 25:1138-1149.

Friess SH, Ichord RN, Ralston J, Ryall K, Helfaer MA, Smith C, Margulies SS (2009) Repeated traumatic brain injury affects composite cognitive function in piglets. Journal of neurotrauma 26:1111-1121.

Harker KT, Whishaw IQ (2002) Impaired spatial performance in rats with retrosplenial lesions: importance of the spatial problem and the rat strain in identifying lesion effects in a swimming pool. The Journal of neuroscience : the official journal of the Society for Neuroscience 22:1155-1164.

Henry CJ, Huang Y, Wynne A, Hanke M, Himler J, Bailey MT, Sheridan JF, Godbout JP (2008) Minocycline attenuates lipopolysaccharide (LPS)-induced neuroinflammation, sickness behavior, and anhedonia. Journal of neuroinflammation 5:15.

Homsi S, Federico F, Croci N, Palmier B, Plotkine M, Marchand-Leroux C, Jafarian-Tehrani M (2009) Minocycline effects on cerebral edema: relations with inflammatory and oxidative stress markers following traumatic brain injury in mice. Brain research 1291:122-132.

Homsi S, Piaggio T, Croci N, Noble F, Plotkine M, Marchand-Leroux C, Jafarian-Tehrani M (2010) Blockade of acute microglial activation by minocycline promotes neuroprotection and reduces locomotor hyperactivity after closed head injury in mice: a twelve-week follow-up study. Journal of neurotrauma 27:911-921.

Huh JW, Raghupathi R (2007) Chronic cognitive deficits and long-term histopathological alterations following contusive brain injury in the immature rat. Journal of neurotrauma 24:1460-1474.

Huh JW, Widing AG, Raghupathi R (2007) Basic science; repetitive mild non-contusive brain trauma in immature rats exacerbates traumatic axonal injury and axonal calpain activation: a preliminary report. Journal of neurotrauma 24:15-27.

Huh JW, Widing AG, Raghupathi R (2008) Midline brain injury in the immature rat induces sustained cognitive deficits, bihemispheric axonal injury and neurodegeneration. Experimental neurology 213:84-92.

Ivacko JA, Sun R, Silverstein FS (1996) Hypoxic-ischemic brain injury induces an acute microglial reaction in perinatal rats. Pediatric research 39:39-47.

Jenny C, Hymel KP, Ritzen A, Reinert SE, Hay TC (1999) Analysis of missed cases of abusive head trauma. Jama 281:621-626.

Kelley BJ, Lifshitz J, Povlishock JT (2007) Neuroinflammatory responses after experimental diffuse traumatic brain injury. Journal of neuropathology and experimental neurology 66:989-1001.

Kobayashi K, Imagama S, Ohgomori T, Hirano K, Uchimura K, Sakamoto K, Hirakawa A, Takeuchi H, Suzumura A, Ishiguro N, Kadomatsu K (2013) Minocycline selectively inhibits M1 polarization of microglia. Cell death & disease 4:e525.

Kovesdi E, Kamnaksh A, Wingo D, Ahmed F, Grunberg NE, Long JB, Kasper CE, Agoston DV (2012) Acute minocycline treatment mitigates the symptoms of mild blast-induced traumatic brain injury. Frontiers in neurology 3:111.

Krady JK, Basu A, Allen CM, Xu Y, LaNoue KF, Gardner TW, Levison SW (2005) Minocycline reduces proinflammatory cytokine expression, microglial activation, and caspase-3 activation in a rodent model of diabetic retinopathy. Diabetes 54:1559-1565.

Lechpammer M, Manning SM, Samonte F, Nelligan J, Sabo E, Talos DM, Volpe JJ, Jensen FE (2008) Minocycline treatment following hypoxic/ischaemic injury attenuates white matter injury in a rodent model of periventricular leucomalacia. Neuropathology and applied neurobiology 34:379-393.

Leonardo CC, Eakin AK, Ajmo JM, Collier LA, Pennypacker KR, Strongin AY, Gottschall PE (2008) Delayed administration of a matrix metalloproteinase inhibitor limits progressive brain injury after hypoxia-ischemia in the neonatal rat. Journal of neuroinflammation 5:34.

Loane DJ, Byrnes KR (2010) Role of microglia in neurotrauma. Neurotherapeutics : the journal of the American Society for Experimental NeuroTherapeutics 7:366-377.

Lyeth BG, Jenkins LW, Hamm RJ, Dixon CE, Phillips LL, Clifton GL, Young HF, Hayes RL (1990) Prolonged memory impairment in the absence of hippocampal cell death following traumatic brain injury in the rat. Brain research 526:249-258.

Matschke J, Voss J, Obi N, Gorndt J, Sperhake JP, Puschel K, Glatzel M (2009) Nonaccidental head injury is the most common cause of subdural bleeding in infants <1 year of age. Pediatrics 124:1587-1594.

McAfoose J, Baune BT (2009) Evidence for a cytokine model of cognitive function. Neuroscience and biobehavioral reviews 33:355-366.

McRae A, Gilland E, Bona E, Hagberg H (1995) Microglia activation after neonatal hypoxic-ischemia. Brain research Developmental brain research 84:245-252.

Miyazaki S, Katayama Y, Lyeth BG, Jenkins LW, DeWitt DS, Goldberg SJ, Newlon PG, Hayes RL (1992) Enduring suppression of hippocampal long-term potentiation following traumatic brain injury in rat. Brain research 585:335-339.

Myhre MC, Grogaard JB, Dyb GA, Sandvik L, Nordhov M (2007) Traumatic head injury in infants and toddlers. Acta paediatrica 96:1159-1163.

Neumann H, Takahashi K (2007) Essential role of the microglial triggering receptor expressed on myeloid cells-2 (TREM2) for central nervous tissue immune homeostasis. Journal of neuroimmunology 184:92-99.

Ng SY, Semple BD, Morganti-Kossmann MC, Bye N (2012) Attenuation of microglial activation with minocycline is not associated with changes in neurogenesis after focal traumatic brain injury in adult mice. Journal of neurotrauma 29:1410-1425.

Paolicelli RC, Bolasco G, Pagani F, Maggi L, Scianni M, Panzanelli P, Giustetto M, Ferreira TA, Guiducci E, Dumas L, Ragozzino D, Gross CT (2011) Synaptic pruning by microglia is necessary for normal brain development. Science 333:1456-1458.

Papa L, Ramia MM, Kelly JM, Burks SS, Pawlowicz A, Berger RP (2013) Systematic review of clinical research on biomarkers for pediatric traumatic brain injury. Journal of neurotrauma 30:324-338.

Peters A, Feldman ML (1976) The projection of the lateral geniculate nucleus to area 17 of the rat cerebral cortex. I. General description. Journal of neurocytology 5:63-84.

Plane JM, Shen Y, Pleasure DE, Deng W (2010) Prospects for minocycline neuroprotection. Archives of neurology 67:1442-1448.

Pont-Lezica L, Bechade C, Belarif-Cantaut Y, Pascual O, Bessis A (2011) Physiological roles of microglia during development. Journal of neurochemistry 119:901-908.

Potts MB, Koh SE, Whetstone WD, Walker BA, Yoneyama T, Claus CP, Manvelyan HM, Noble-Haeusslein LJ (2006) Traumatic injury to the immature brain: inflammation, oxidative injury, and iron-mediated damage as potential therapeutic targets. NeuroRx : the journal of the American Society for Experimental NeuroTherapeutics 3:143-153.

Prins ML, Hales A, Reger M, Giza CC, Hovda DA (2010) Repeat traumatic brain injury in the juvenile rat is associated with increased axonal injury and cognitive impairments. Developmental neuroscience 32:510-518.

Raghupathi R, Huh JW (2007) Diffuse brain injury in the immature rat: evidence for an age-at-injury effect on cognitive function and histopathologic damage. Journal of neurotrauma 24:1596-1608.

Raghupathi R, Mehr MF, Helfaer MA, Margulies SS (2004) Traumatic axonal injury is exacerbated following repetitive closed head injury in the neonatal pig. Journal of neurotrauma 21:307-316.

Reece RM, Sege R (2000) Childhood head injuries: accidental or inflicted? Archives of pediatrics & adolescent medicine 154:11-15.

Ross FM, Allan SM, Rothwell NJ, Verkhratsky A (2003) A dual role for interleukin-1 in LTP in mouse hippocampal slices. Journal of neuroimmunology 144:61-67.

Sanchez Mejia RO, Ona VO, Li M, Friedlander RM (2001) Minocycline reduces traumatic brain injury-mediated caspase-1 activation, tissue damage, and neurological dysfunction. Neurosurgery 48:1393-1399; discussion 1399-1401.

SE Parks JA, HA Hill, DL Karch (2012) Pediatric Abusive Head Trauma: Recommended Definitions for Public Health Surveillance and Research. (Centers for Disease, C., ed) Atlanta GA.

Siopi E, Cho AH, Homsi S, Croci N, Plotkine M, Marchand-Leroux C, Jafarian-Tehrani M (2011) Minocycline restores sAPPalpha levels and reduces the late histopathological consequences of traumatic brain injury in mice. Journal of neurotrauma 28:2135-2143.

Siopi E, Llufriu-Daben G, Fanucchi F, Plotkine M, Marchand-Leroux C, Jafarian-Tehrani M (2012) Evaluation of late cognitive impairment and anxiety states following traumatic brain injury in mice: the effect of minocycline. Neuroscience letters 511:110-115.

Smith SL, Andrus PK, Gleason DD, Hall ED (1998) Infant rat model of the shaken baby syndrome: preliminary characterization and evidence for the role of free radicals in cortical hemorrhaging and progressive neuronal degeneration. Journal of neurotrauma 15:693-705.

Takahashi K, Rochford CD, Neumann H (2005) Clearance of apoptotic neurons without inflammation by microglial triggering receptor expressed on myeloid cells-2. The Journal of experimental medicine 201:647-657.

Tang M, Alexander H, Clark RS, Kochanek PM, Kagan VE, Bayir H (2010) Minocycline reduces neuronal death and attenuates microglial response after pediatric asphyxial cardiac arrest. Journal of cerebral blood flow and metabolism : official journal of the International Society of Cerebral Blood Flow and Metabolism 30:119-129.

Teng YD, Choi H, Onario RC, Zhu S, Desilets FC, Lan S, Woodard EJ, Snyder EY, Eichler ME, Friedlander RM (2004) Minocycline inhibits contusion-triggered mitochondrial cytochrome c release and mitigates functional deficits after spinal cord injury. Proceedings of the National Academy of Sciences of the United States of America 101:3071-3076.

Tong W, Igarashi T, Ferriero DM, Noble LJ (2002) Traumatic brain injury in the immature mouse brain: characterization of regional vulnerability. Experimental neurology 176:105-116.

Trofimov AN, Zubareva OE, Simbirtsev AS, Klimenko VM (2012) [The influence of neonatal interleukin-1beta increase on the formation of adult rats' spatial memory]. Rossiiskii fiziologicheskii zhurnal imeni IM Sechenova / Rossiiskaia akademiia nauk 98:782-792.

Tsuji M, Wilson MA, Lange MS, Johnston MV (2004) Minocycline worsens hypoxic-ischemic brain injury in a neonatal mouse model. Experimental neurology 189:58-65.

Tzekov R, Quezada A, Gautier M, Biggins D, Frances C, Mouzon B, Jamison J, Mullan M, Crawford F (2014) Repetitive mild traumatic brain injury causes optic nerve and retinal damage in a mouse model. Journal of neuropathology and experimental neurology 73:345-361.

van Groen T, Kadish I, Wyss JM (2002) The role of the laterodorsal nucleus of the thalamus in spatial learning and memory in the rat. Behavioural brain research 136:329-337.

Vann SD, Kristina Wilton LA, Muir JL, Aggleton JP (2003) Testing the importance of the caudal retrosplenial cortex for spatial memory in rats. Behavioural brain research 140:107-118.

Wang X, Zhu S, Drozda M, Zhang W, Stavrovskaya IG, Cattaneo E, Ferrante RJ, Kristal BS, Friedlander RM (2003) Minocycline inhibits caspase-independent and -dependent mitochondrial cell death pathways in models of Huntington's disease. Proceedings of the National Academy of Sciences of the United States of America 100:10483-10487.

Wasserman JK, Schlichter LC (2007) Minocycline protects the blood-brain barrier and reduces edema following intracerebral hemorrhage in the rat. Experimental neurology 207:227-237.

Wixey JA, Reinebrant HE, Spencer SJ, Buller KM (2011) Efficacy of post-insult minocycline administration to alter long-term hypoxia-ischemia-induced damage to the serotonergic system in the immature rat brain. Neuroscience 182:184-192.

Xue M, Mikliaeva EI, Casha S, Zygun D, Demchuk A, Yong VW (2010) Improving outcomes of neuroprotection by minocycline: guides from cell culture and intracerebral hemorrhage in mice. The American journal of pathology 176:1193-1202.

Zhu S, Stavrovskaya IG, Drozda M, Kim BY, Ona V, Li M, Sarang S, Liu AS, Hartley DM, Wu DC, Gullans S, Ferrante RJ, Przedborski S, Kristal BS, Friedlander RM (2002) Minocycline inhibits cytochrome c release and delays progression of amyotrophic lateral sclerosis in mice. Nature 417:74-78.

Ziebell JM, Morganti-Kossmann MC (2010) Involvement of pro- and anti-inflammatory cytokines and chemokines in the pathophysiology of traumatic brain injury. Neurotherapeutics : the journal of the American Society for Experimental NeuroTherapeutics 7:22-30.